HEINRICH HEINE
UNIVERSITÄT DÜSSELDORF

Halogenated Tyrosines from Verongid Sponges – A Diverse Class of Marine Metabolites

(Halogenierte Tyrosine aus Verongiden Schwämmen – Eine diverse Klasse mariner Metaboliten)

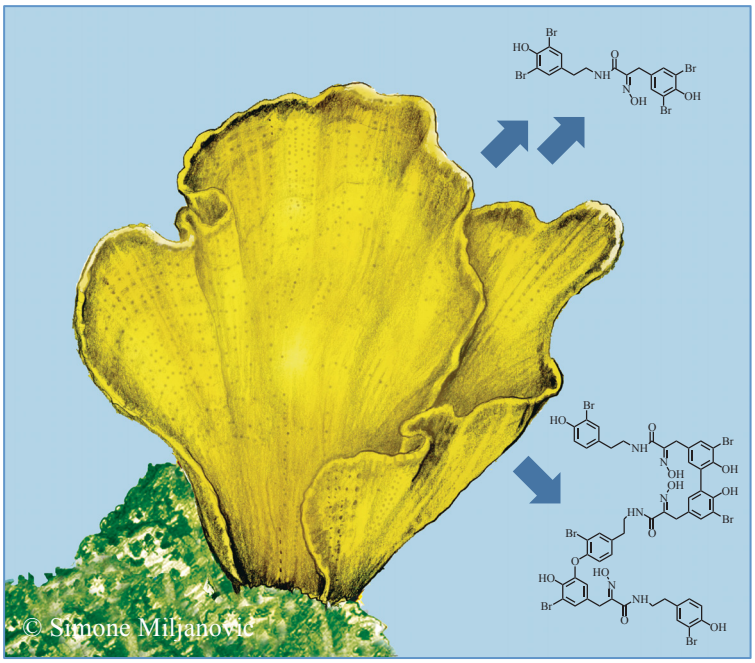

Inaugural-Dissertation

zur Erlangung des Doktorgrades
der Mathematisch-Naturwissenschaftlichen Fakultät
der Heinrich-Heine-Universität Düsseldorf

vorgelegt von

Hendrik Niemann
aus Ahaus

Düsseldorf, Mai 2015

Aus dem Institut für Pharmazeutische Biologie und Biotechnologie
der Heinrich-Heine-Universität Düsseldorf

Gedruckt mit der Genehmigung der
Mathematisch-Naturwissenschaftlichen Fakultät der
Heinrich-Heine-Universität Düsseldorf

Referent: Prof. Dr. Peter Proksch
Koreferent: Prof. Dr. Matthias U. Kassack
Tag der mündlichen Prüfung: _____

Für meine Eltern.

CONTENTS

1 Abstract

The oceans represent by far the largest habitat on earth with an enormous diversity of life. Marine secondary metabolites, that are considered as molecular mediators of these diverse ecosystems, have gathered high interest in recent bioprospecting. The utilization of bioactive compounds derived or inspired from the oceans and especially of those from sessile invertebrates such as sponges is part of numerous modern drug discovery programs. Seven marine derived drugs have so far reached the status of FDA- and/or EMA-approval including the anticancer agent eribulin mesylate (Halaven®), which was developed inspired by the sponge derived macrocyclic polyetherlactone halichondrin B, or vidarabin (Vira-A®), an unusual sponge nucleoside which served as a template for today's first line DNA polymerase antimetabolites such as aciclovir. Apart from a clinical application sponge derived secondary metabolites might fill the gap of worldwide banned organotins to overcome the ecological issue of biofouling, which has a high economical impact on maritime industries including shipping and aquaculture. Among this increasing group of marine derived active principles halogenated tyrosines, which are mainly accumulated by sponges of the order Verongida, exhibit a wide range of bioactivities including anticancer and antifouling effects. Within this study an actual overview on the structural and biological diversity of a small excerpt of halotyrosines was provided. Furthermore, the anticancer and antifouling potential of isolated and synthesized halogenated tyrosine congeners, in particular of the class of bastadins, was investigated. Finally, chemoecological studies on the distribution of halogenated tyrosines in sponges were conducted with emphasis on the presence of such metabolites in sponge skeletons. All obtained results were published in six peer-reviewed publications in four international journals. Detailed abstracts on the four aspects of this thesis are as follows:

Review on Prominent Examples of Brominated Tyrosine Derivatives

To provide an overview on several bioactive and structurally divergent classes of bromotyrosines psammaplin A, *Aplysina* alkaloids featuring aerothionin, aeroplysinin-1 and verongiaquinol (dienone), and the bastadins, including synthetically derived hemibastadin congeners, were selected for a review article. Whereas all of these natural products are believed to be involved in the chemical defense mechanisms of sponges, some of them may also be of particular relevance for drug discovery due to their interaction with specific molecular targets in eukaryotic cells. These targets involve important enzymes and receptors, such as histone deacetylases (HDAC) and DNA methyltransferases (DNMT), which are inhibited by

psammaplin A, as well as ryanodine receptors that are targeted by bastadin type compounds. The hemibastadins such as the synthetically derived 5,5'-dibromohemibastadin-1 (DBHB) are of particular interest due to their antifouling activity. For the latter, a phenoloxidase which catalyzes the bioglue formation needed for firm attachment of fouling organisms to a given substrate was identified as a molecular target. The *Aplysina* alkaloids finally provide a vivid example for dynamic wound induced bioconversions of natural products that generate highly efficient chemical weapons precisely when and where needed.

Anticancer Activities of Several Bastadins

The first naturally occurring trimeric hemibastadin congener, sesquibastadin 1, and the previously reported bastadins 3, 6, 7, 11 and 16 were isolated from the marine sponge *Ianthella basta*. The structure of sesquibastadin 1 was elucidated unambiguously on the basis of 1D and 2D NMR measurements and by HRMS. Among all the isolated compounds, the linear congeners sesquibastadin 1 and bastadin 3 showed the strongest inhibition rates for at least 22 protein kinases (IC_{50} = 0.1−6.5 μM), while the macrocyclic bastadins demonstrated a strong cytotoxic potential against the murine lymphoma cell line L5178Y (IC_{50} = 1.5−5.3 μM). In a further study bastadins 6, 9 and 16 displayed *in vitro* cytostatic and/or cytotoxic effects in six human and murine cancer cell lines. The *in vitro* growth inhibitory effects of these bastadins were similar in cancer cell lines sensitive to pro-apoptotic stimuli *vs.* cancer cell lines displaying various levels of resistance to pro-apoptotic stimuli. While about ten times less toxic than the investigated natural cyclic bastadins, DBHB displayed not only *in vitro* growth inhibitory activity in cancer cells but also anti-angiogenic properties. At a concentration of one tenth of its *in vitro* growth inhibitory concentration, DBHB displayed actual antimigratory effects in mouse B16F10 melanoma cells without any sign of cytotoxicity and/or growth inhibition. The serum concentration used in the cell culture media markedly influenced the DBHB-induced antimigratory effects in the B16F10 melanoma cell population. A binding affinity to albumine was shown for DBHB, which is putatively causative for the treatment failure of the hemibastadin when delivered through the i.v. route in an *in vivo* tumor model.

Antifouling Potential of Hemibastadins Inhibiting Blue Mussel Phenoloxidase

For a systematic investigation of the blue mussel phenoloxidase inhibitory activity of hemibastadin derivatives nine new congeners of DBHB were synthesized, which feature structural variations of the DBHB core structure. These structural modifications include e.g. different halogen substituents present at the aromatic rings, different amine moieties linked to the (E)-2-(hydroxyimino)-3-(4-hydroxyphenyl)propionic acid, the presence of free *vs.*

substituted aromatic hydroxyl groups and a free *vs*. methylated oxime group. All compounds were tested for their inhibitory activity towards the target enzyme *in vitro* and IC_{50} values were calculated. Derivatives, which structurally closely resemble sponge-derived hemibastadins, revealed superior enzyme inhibitory properties *vs*. congeners featuring structural moieties that are absent in the respective natural products. This study suggests that natural selection has yielded structurally optimized antifouling compounds.

Halotyrosines in Verongid Sponge Skeletons

In a final aspect of this thesis sponge skeletons were analyzed with regard to an association or incorporation of halogenated tyrosines. Demosponges such as the investigated *Ianthella basta* and *Aplysina cavernicola* possess a skeleton made up of a composite material with various organic constituents including chitin and/or siliceous spicules. HPLC analysis in combination with NMR and IR spectroscopic measurements revelead that the chitin-based skeletons indeed contain significant amounts of brominated compounds, which are not easily extractable from the skeletons by common solvents, such as methanol. Quantitative potentiometric analyses confirm that the skeleton-associated bromine mainly withstands the methanol-based extraction. This observation suggested that the respective brominated compounds are strongly bound to the sponge skeletons, possibly by covalent bonding. Moreover, gene fragments of halogenases suggested to be responsible for the incorporation of bromine into organic molecules could be amplified from DNA isolated from sponge samples enriched for sponge-associated bacteria. In order to identify the fraction of halogenated metabolites remaining after methanol-extraction further analytical studies on the amino acid composition after basic hydrolysis of *A. cavernicola* skeletons with respect to the presence of halogenated amino acids were performed. Ten halogenated amino acids, of which nine account to the class of tyrosine derivatives such as mono- and dibromotyrosine were identified by GC-MS and LC-MS in $Ba(OH)_2$-dervied skeleton extracts.

2 Zusammenfassung

Die Ozeane stellen den bei Weitem größten Lebensraum der Erde dar mit einer enormen Diversität an Leben. Marine Sekundärmetaboliten, welche als molekulare Mediatoren dieser diversen Ökosysteme verstanden werden, haben großes Interesse im Rahmen aktueller Bioprospektionsstudien erlangt. Die Nutzbarmachung von bioaktiven Verbindungen abgeleitet oder inspiriert von den Ozeanen und im Speziellen von denen aus sessilen Invertebraten wie Schwämmen ist Bestandteil vieler Programme der modernen Wirkstofffindung. Sieben Arzneistoffe marinen Ursprungs haben bis dato den Status einer FDA- und/oder EMA-Zulassung erhalten, darunter das Krebsmedikament Eribulinmesylat (Halaven®), das inspiriert von dem aus Schwämmen isolierten macrozyklischen Polyetherlacton Halichondrin B entwickelt wurde, oder Vidarabin (Vira-A®), ein ungewöhnliches Schwammnukleosid, welches als Vorlage für aktuelle First-Line-DNA-Polymerase-Antimetaboliten wie Aciclovir diente. Neben einer klinischen Anwendung könnten Sekundärmetaboliten aus Schwämmen die durch das weltweite Verbot von Organozinn-Verbindungen entstandene Lücke schließen, um die ökologische Problematik des Biofoulings zu überwinden, welche einen hohen ökonomischen Einfluss auf maritime Industrien wie Schifffahrt und Aquakultur hat. Innerhalb dieser wachsenden Gruppe von aktiven Verbindungen marinen Ursprungs weisen halogenierte Tyrosine, welche vorzugsweise von Schwämmen der Ordnung Verongida akkumuliert werden, eine große Bandbreite an Bioaktivitäten wie Anti-Krebs- und Antifouling-Effekte auf. Im Rahmen dieser Studie wurde ein aktueller Überblick über die strukturelle und biologische Diversität eines kleinen Exzerpts an Halotyrosinen gewährt. Des Weiteren wurde das Anti-Krebs- und Antifouling-Potential von isolierten und synthetisierten halogenierten Tyrosin-Derivaten, im Speziellen von solchen aus der Klasse der Bastadine, untersucht. Abschließend wurden chemoökologische Studien über die Verteilung von halogenierten Tyrosinen in Schwämmen durchgeführt mit Fokus auf die Präsenz derartiger Metaboliten in Schwammskeletten. Alle erhaltenen Ergebnisse wurden in sechs peer-reviewed Publikationen in vier internationalen Fachzeitschriften veröffentlicht. Detailierte Zusammenfassungen der vier Aspekte dieser Dissertation lauten wie folgt:

Übersicht über prominente Beispiele von bromierten Tyrosin-Derivaten

Um einen Überblick über verschiedene bioaktive und strukturell divergente Klassen an Bromtyrosinen zu bieten wurden Psammaplin A, die *Aplysina*-Alkaloide inklusive Aerothionin, Aeroplysinin-1 und Verongiaquinol (Dieonon) und die Bastadine inklusive synthetischer Hemibastadin-Derivate für einen Review-Artikel ausgewählt. Während angenommen wird,

dass all diese Naturstoffe involviert sind in die chemischen Verteidigungsmechanismen von Schwämmen, sind einige von besonderer Bedeutung für die Wirkstofffindung aufgrund ihrer Interaktion mit spezifischen molekularen Zielstrukturen in eukaryotischen Zellen. Zu den Zielstrukturen zählen Enzyme und Rezeptoren wie Histon-Deacetylasen (HDAC) und DNA-Methyltransferasen (DNMT), welche von Psammaplin A inhibiert werden, Ryanodin-Rezeptoren, welche von Verbindungen vom Bastadin-Typ adressiert werden. Die Hemibastadine wie das synthetische 5,5'-Dibromohemibastadin-1 (DBHB) sind aufgrund ihrer Antifouling-Aktivität von gesteigertem Interesse. Für letztgenannte konnte eine Phenoloxidase als molekulare Zielstruktur identifiziert werden, welche die Ausbildung des Bioklebstoffs katalysiert, der die feste Anheftung von Fouling-Organismen an ein gegebenes Substrat ermöglicht. Die *Aplysina* Alkaloide stellen abschließend ein anschauliches Beispiel für dynamische Wund-induzierte Biokonversionen von Naturstoffen dar, welche hoch effiziente chemische Waffen generieren, genau wo und wann diese gebraucht werden.

Antikrebs-Aktivitäten verschiedener Bastadine

Das erste natürlich vorkommende trimere Hemibastadin-Derivat, Sesquibastadin 1, und die zuvor beschriebenden Bastadine 3, 6, 7, 11 und 16 wurden aus dem marinen Schwamm *Ianthella basta* isoliert. Die Struktur von Sesquibastadin 1 wurde eindeutig auf Basis von 1D- und 2D-NMR-Experimenten und HRMS aufgeklärt. Unter allen isolierten Verbindungen zeigten die linearen Kongenere Sesquibastadin 1 und Bastadin 3 die stärksten Inhibitionsraten für mindestens 22 Proteinkinasen (IC_{50} = 0.1-6.5 μM), während die macrozyklischen Bastadine ein starkes zytotoxisches Potenzial gegenüber der murinen Lymphom-Zelllinie L5178Y zeigten (IC_{50} = 1.5-5.3 μM). In einer weiteren Studie demonstrierten Bastadine 6, 9 und 16 *in vitro* zytostatische und/oder zytotoxische Effekte in sechs humanen oder murinen Krebszelllinien. Die *in vitro* wachstumshemmenden Effekte dieser Bastadine waren ähnlich in Krebszelllinien sensitiv für pro-apoptotische Stimuli *vs*. Krebszelllinien, welche verschiedene Resistenzniveaus gegenüber pro-apoptotischen Stimuli aufweisen. Während es ca. zehnfach weniger toxisch als die untersuchten zyklischen Bastadine war, zeigte DBHB *in vitro* nicht nur wachstumshemmende Aktivität gegenüber Krebszellen, sondern auch antiangiogenetische Eigenschaften. Bei einer Konzentration von einem Zehntel gegenüber seiner *in vitro* wachstumshemmenden Konzentration zeigt DBHB wirkliche antimigratorische Effekte in murinen B16F10 Melanomzellen ohne jegliches Anzeichen von Zytotoxizität und/oder Wachstumshemmung. Die Serumkonzentration, welche im Zellkulturmedium eingesetzt wurde, hatte maßgeblichen Einfluss auf die von DBHB induzierten antimigratorischen Effekte in der

Zusammenfassung

B16F10 Melanomzellpopulation. Eine Bindungsaffinität von DBHB zu Albumin konnte gezeigt werden, welche vermutlich ursächlich ist für das Therapieversagen des Hemibastadins bei i.v.-Applikation in einem *in vivo* Tumormodell.

Antifouling-Potential von Hemibastadinen durch Inhibition der Phenoloxidase aus Miesmuscheln

Für eine systematische Untersuchung der inhibitorischen Aktivität von Hemibastadin-Derivaten gegenüber der Phenoloxidase aus Miesmuscheln wurden neun neue Kongenere des DBHB synthesiert, welche strukturelle Variation der DBHB-Kernstruktur bergen. Zu diesen strukturellen Modifikationen zählen beispielsweise andere Halogensubstituenten innerhalb der aromatischen Ringe, weitere Amin-Einheiten verknüpft an die (E)-2-(Hydroxyimino)-3-(4-hydroxyphenyl)propionsäure, das Vorliegen von freien *vs.* substituierten aromatischen Hydroxylgruppen und einer freien *vs.* methylierten Oximfunktion. Alle Verbindungen wurden auf ihre inhibitorische Aktivität gegenüber dem Zielenzym *in vitro* getestet und die IC_{50}-Werte wurden berechnet. Verbindungen, die strukturell den in Schwämmen vorliegenden Hemibastadinen sehr ähnlich sind, zeigten überlegende Enzym-inhibitorische Eigenschaften gegenüber den Derivaten, welche Partialstrukturen tragen, die in den jeweiligen Naturstoffen nicht vorkommen. Diese Studie legt nahe, dass die natürliche Selektion strukturell optimierte Antifouling-Verbindungen hervorgebracht hat.

Halotyrosine in Verongiden Schwammskeletten

In einem abschließenden Aspekt dieser Dissertation wurden Schwammskelette auf eine Assoziation oder Inkorporation von halogenierten Tyrosinen hin untersucht. Hornkieselschwämme wie die untersuchten *Ianthella basta* und *Aplysina cavernicola* besitzen ein Skelett bestehend aus einem komplexen Material mit verschiedenen organischen Bestandteilen wie Chitin und/oder kieselhaltige Spicula. HPLC-Analysen in Kombination mit NMR- und IR-spektroskopischen Messungen konnten zeigen, dass die Chitin-basierten Skelette tatsächlich signifikante Mengen an bromierten Verbindungen tragen, welche sich mittels gängiger Lösungsmittel wie Methanol nicht einfach aus den Skeletten herauslösen lassen. Quantitative Potentiometrie bestätigte, dass das Skelett-assoziierte Brom der Methanol-basierten Extraktion größtenteils standhält. Diese Beobachtung suggerierte, dass die jeweiligen bromierten Metaboliten fest, vermutlich kovalent an die Schwammskelette gebunden sind. Des Weiteren wurden Genfragmente einer Halogenase, welche verantwortlich ist für die Inkorporation von Brom in die organischen Verbindungen, aus einer DNA-Probe amplifiziert werden, welche aus einer Schwamm-Probe mit angereicherter Schwamm-assoziierter

Zusammenfassung

Bakterien-DNA isoliert wurde. Um die Fraktion halogenierter, Methanol unlöslicher Metaboliten zu identifizieren, wurden weitere analytische Studien der Aminosäuren-Zusammensetzung nach basischer Hydrolyse von *A. cavernicola* Skeletten mit Fokus auf das Auftreten halogenierter Aminosäuren durchgeführt. Zehn halogenierte Aminosäuren, von denen neun zur Klasse der Tyrosin-Derivate zählen, wie beispielsweise Mono- und Dibromtyrosin, konnten mittels GC-MS und LC-MS in den $Ba(OH)_2$-Extrakten der Skelette identifiziert werden.

3 Introduction

The sea covers more than 70 % of the earth's surface and represents its most abundant ecosystem. A high biodiversity bearing 34 of the 36 living phyla – of which some are endemic to the oceans – and till now 226,000 described marine eukaryotic species shows the magnitude of this habitat. Within the past decade ~ 20,000 new marine species were described, more than in any previous one (Appeltans *et al.*, 2012; Arrieta *et al.*, 2010). The census of the oceans has not come to an end yet while experts estimate the total number of marine species up to 1 million, indicating that more than two-thirds remain undiscribed till today (Appeltans *et al.*, 2012). Among the marine species sponges have achieved an outstanding story of evolutionary success, lasting for more than 700 million years on our planet (Belarbi *et al.*, 2003). Through this long period of existence these most primitive of the multi-cellular animals (Metazoa) have evolved highly effective chemical defence mechanisms to fight biofouling, predation, neoplastic processes and pathogenic microbial infections (Hertiani *et al.*, 2010; Loh and Pawlik, 2014; Ortlepp *et al.*, 2007; Proksch, 1999; Thoms *et al.*, 2006). These multifaceted sponge derived molecular weapons have gained broad attention to the scientific community of natural product chemists since their enormous potential for modern health sciences was firstly discovered in terms of unusual nucleosides isolated from the marine sponge *Cryptotethiu cryptu* in 1951 (Bergmann and Feeney, 1951). These should later become the first marine derived drugs ara-A (vidarabine) and ara-C (cytarabine) that have been in clinical use against cancer and viral infections for decades (Molinski *et al.*, 2008). The number of newly discovered marine derived molecules is tremendously increasing while modern sample collection, compound isolation and structure elucidation techniques are advancing. More than 1,000 novel metabolites with a diverse panel of bioactivities have been reported annualy for the past couple of years replenishing the (pre)clinical pipelines with complex chemical leads (Montaser and Luesch, 2011). In addition, the chemistry of sponges may not only contribute to the struggle against life threatening diseases like cancer or microbial infections, but will also have a great potential for biotechnological applications, e.g. as biomimetic antifouling leads for maritime industries (Bayer *et al.*, 2011; Ortlepp *et al.*, 2007) as effective current approaches such as organotins have been banned from the worldwide markets due to their adverse toxicity profiles. Among the sponge derived isolates the class of halogenated tyrosine congeners, secondary metabolites typically occurring in the order of Verongida, are prominent examples with an outstanding activity profile.

Introduction

3.1 Significance of the study

As severe clinically issues including drug resistance endanger success rates of current anticancer therapy potent new drug candidates are urgently needed. Similarly eco-friendly alternatives to the worldwide banned organotins in the sector of antifouling must be discovered as biofouling has a high ecological as well as economical impact. The biochemistry of sessile marine invertebrates such as sponges provides solutions for these challenges as demonstrated by the recent success story of eribulin mesylate (Halaven®) approved for metastatic breast cancer. In order to yield more structurally unique metabolites that address novel molecular targets and fill pipelines of each respective sector an intensified marine bioprospecting is believed to play a crucial role within the next decades. To accomplish such ambitious undertakings chemoecological studies on sponges are likewise needed as a better understanding of respective compounds and their significance for the host organism in the individual natural habitat might provoke novel approaches of a putative utilization.

3.2 Marine Sponges

3.2.1 Overview

Marine sponges represent the oldest, multi-cellular animals on earth with an estimated existence of more than 700 million years (Belarbi *et al.*, 2003; Müller, 1998). Among the marine invertebrates they form the phylum Porifera, with the primary characteristic of being mostly sessile metazoans (Hooper and Van Soest, 2002). Two exceptions from this definition are the mobile red sea species *Tethya seychellensis* and *T. aurantium* (Fishelson, 1981). Porifera are simple pore (lat. „porus“) bearing (lat. „ferre“) animals that have asserted themselves in nearly all marine habitats ranging from diverse tropical coral reefs to polar seas. Only a minority of sponges like several species of the genus *Spongilla* inhabit fresh water habitats (Hogg, 1860). The antarctic sponge *Scolymastra joubini*, occuring in the Antarctic Weddell Sea, was found to be the oldest living animal ever discovered on earth with an estimated maximum lifespan (MLSP) of 15,000 years (Philipp and Abele, 2010). Till today 8,382 species account the phylum Porifera (WoRMS, 2015). Current marine census studies and resulting estimations report, that one third of the sponge diversity has been discovered so far, while advancing molecular methods have highly accelerated discovery rates of cryptic species within the past decades (Appeltans *et al.*, 2012). Based on morphological as well as phylogenetic parameters the phylum Porifera can be divided into four classes (figure 1), the Calcarea, the Demospongiae, the Hexactinellida and the Homoscleromorpha (WoRMS, 2015), the latter being just recently separated as ist own class from the Demospongiae (Gazave *et al.*, 2012). Applied morphological distinguishing features between the four classes are different

types of cells and spicules, presence of spongin fibres as well as their body form (Bergquist, 1998). With almost 7,000 described species the Demosponges constitute more than 80 % of all known sponge species. Sponges of this class are characterized by cells bearing a single nucleus and a single external membrane, skeletons bearing spicules consisting of silica and in the majority of cases proteinous spongin fibers and a leuconoid body form (figure 2). Demosponges are typically found in inter-tidal to abyssal depth (Bergquist, 1998).

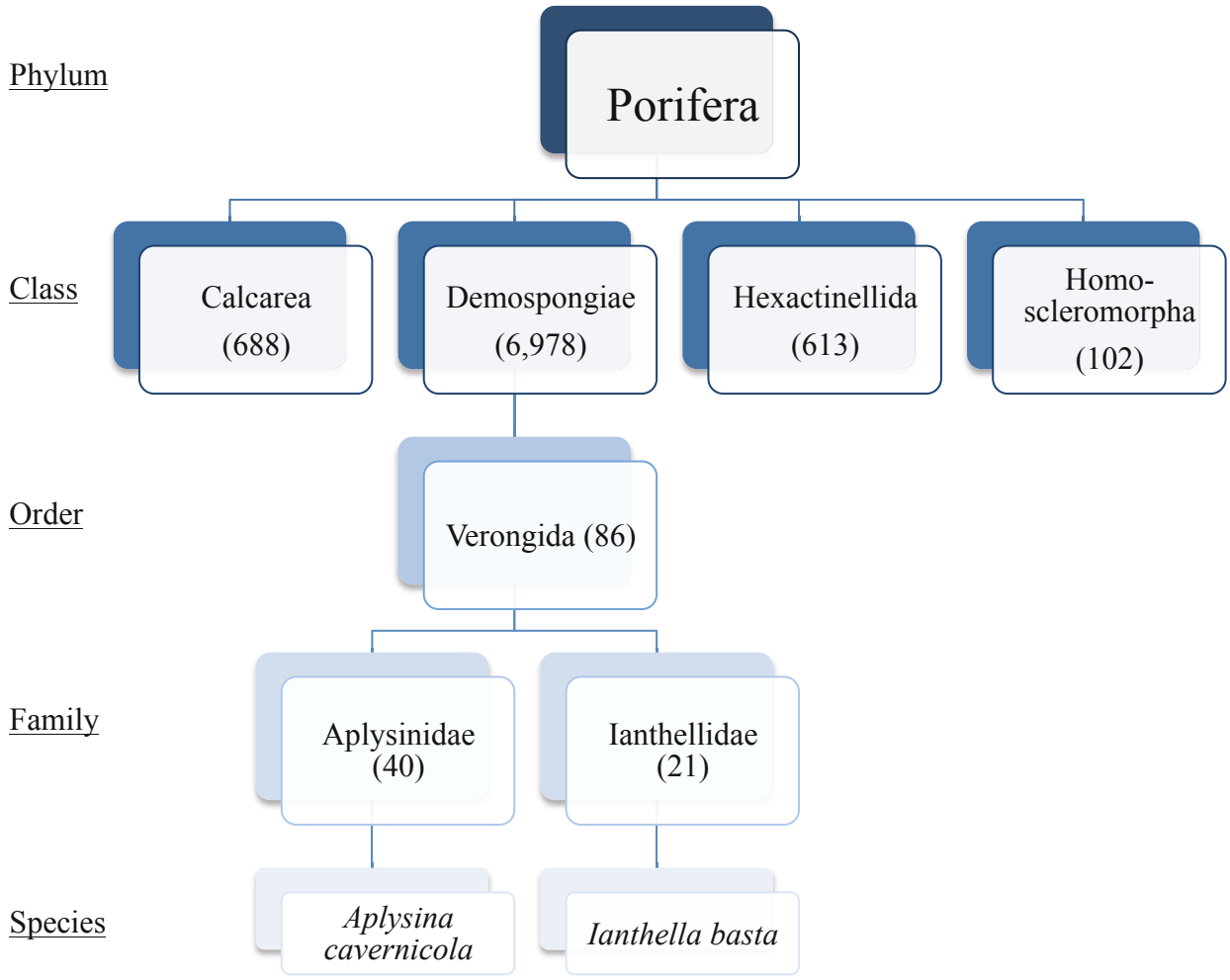

Figure 1. Taxon tree of the phylum Porifera with focus on investigated species *Aplysina cavernicola* and *Ianthella basta*. Numbers of accepted marine extant species within the specific taxon were added in brackets (WoRMS, 2015).

3.2.2 Basic Structure

Among the Metazoa sponges exclusively belong to the subkingdom of Parazoa. In contrast to the true Eumetazoa members of this taxon are characterized by a lack of higher organized tissue and organs such as gonades, a nerval system or muscle cells (Storch and Welsch, 2014). The organisation of sponges is rather characterized by the purpose of being so-called filter feeders (Van Soest *et al.*, 2012). The outer sponge layer (pinacoderm) is formed by pinacocytes. This plate-like type of cells forms a single-layered external skin that maintains

body integrity. Furthermore pinacocytes contribute to the digestion of larger food particles and at the the animal's base this cell type is responsible for the establishment of an anchoring foot to the settled substrate (Bergquist, 1998). Small pores within the pinacoderm, so-called ostia, are the outer entrance of water and nutrition channels, that lead to one or more flagellated chambers. The number of chambers depends on the level of organization of the sponge and can be distinguished in the ascon-, sycon- or leucon-type (figure 2). The interior layer of flagellated chambers (choanoderm) is lined with a specialised type of cells, the choanocytes. With their lumen orientated flagella choanocytes produce an inward stream of water, from which plankton, bacteria and floating particles, are phagocytised and digested intracellularly. The filtered water is then released by a larger channel, the osculum. Sandwiched within the pinacoderm and the choanoderm is a hardly differentiated and jelly-like mesohyl, which is typical for all kinds of sponges (Bergquist, 1998). Within its collagen-like structure the mesohyl additionally bears stromal cells and totipotent archaeocytes (Rieger, 1996; Van Soest *et al.*, 2012).

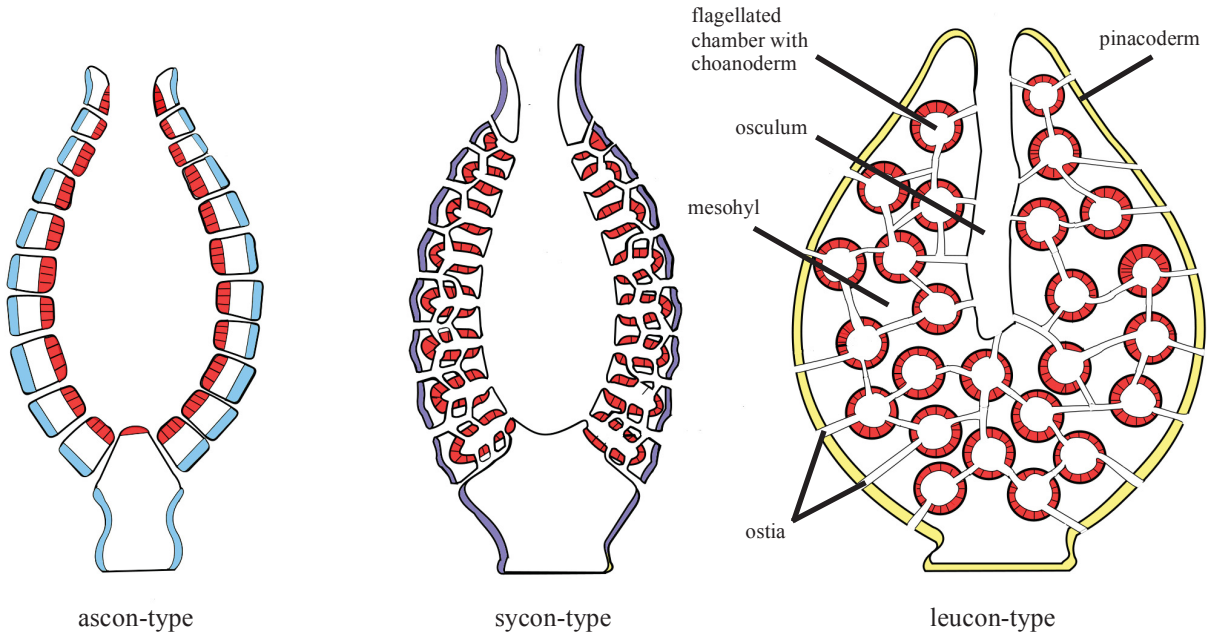

Figure 2. Organisation types of sponges. Ascon-type: primitive sponges < 2mm; sycon-type: sponges with several cm in size; leucon-type: all larger and higher developed sponges like the vast majority of demosponges. Modified from http://www.wikipedia.org.

Besides the cellular components anorganic needles, so-called spicules, are typically present in the mesohyl (De Vos *et al.*, 1991). These diverse structures (figure 3) serve taxonomists as important interspecial differentiation markers. Spicules in calcareous sponges are mainly

composed of calcite while silica is typical for the spicules found in the other three classes (Bergquist, 1998). Spicules are considered as the structural elements that have a major influence on the tissue consistence, which can vary from soft over fragile till very hard (Van Soest *et al.*, 2012). In the sponge *Anthosigmella varians* an induction of spicule formation was observed as a response on tissue predation indicating their contribution to an activated mechanical defense mechanism (Hill and Hill, 2002; Hill *et al.*, 2005).

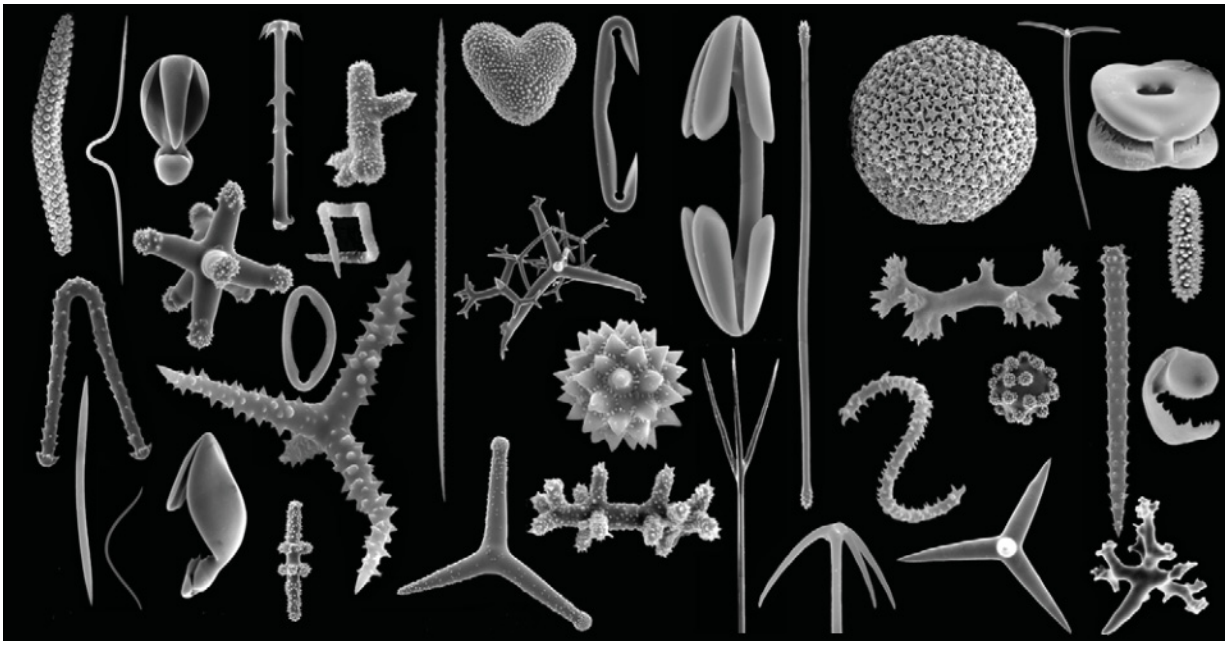

Figure 3. SEM images of sponge spicula (Van Soest *et al.*, 2012).

3.2.3 Sponge Skeletons Composed of Spongin

The composite material of sponge skeletons consists of various organic constituents, in particular the collagenous protein spongin (Hooper and Van Soest, 2002), polysaccharides such as chitin (Brunner *et al.*, 2009; Ehrlich *et al.*, 2007) and above mentioned siliceous spicules (Uriz *et al.*, 2003). Within the class of demosponges three orders, namely the Dendroceratida, the Dictyoceratida and the Verongida totally lack siliceous spicules (Ehrlich, 2010). In these orders, which are also known as the „keratose“ demosponges, the organic skeletons are exclusively made of one or more collagen derivatives, i.e. collagen fibrils, spongin filaments, and/or spongin fibres (Maldonado, 2009). The structure of spongin is until now not fully understood. Back in 1956 Gross *et al.* categorized collagenous fibres of the marine sponge *Spongia graminea* as „spongin A“ and „spongin B“ according to different structural parameters resulted from x-ray diffraction and electron microscopy analyses. In the same study the affiliation to the class of collagen-like proteins was established by the chemical evidence of a high content of hydroxyproline (Gross *et al.*, 1956). Providing a further hint on its chemical

nature spongin was recently defined as a halogenated protein (Ehrlich, 2010). Presumably spongin fibres in sponge skeletons are closely associated or even covalently bond to chitin as it is known for other structural proteins in insects or crustacea (Hackman, 1960). The association of non polymeric small molecules with spongin skeletons has so far only been studied to a minor extent and was therefore chosen for investigation on the example of brominated tyrosines during this study (publication 5).

3.2.4 Verongid Sponges: *Ianthella basta* and *Aplysina cavernicola*

A comparatively small order among marine demosponges bearing actually only 86 species categorized within four families is the order of the Verongida (WoRMS, 2015). Among this order the sponge species *Ianthella basta* (figure 4A) and *Aplysina cavernicola* (figure 4B), both investigated in this thesis are affiliated to the two numerically largest families of Ianthellidae and Aplysinidae (figure 1).

Figure 4. Verongid sponges in their natural habitats. A: *Ianthella basta* in the Pacific ocean (© Bernard Dupont). B: *Aplysina cavernicola* in the Mediterranean Sea at the coast of Sveta Marina, Istria, Croatia.

The elephant-ear sponge (*I. basta*) was originally described as *Spongia basta* back in 1766 by Pallas in his zoophytes (Pallas, 1766). One century later in 1869 Gray described it as a broad fan-like or funnel-shaped sponge with sides folded together, leaving an open space below near the „root“, forming an incomplete funnel, which is more or less distorted and divided (Gray, 1869). Gray continues his description by some morphological aspects such as the skeleton, formed by a substance, that is so dense that it does not, as in the generality of demosponges, become softened and more flexible by being soaked in water. As already mentioned above (section 3.2.3) he furthermore reports that his investigated specimen lacks any traces of siliceous or calcareous spicules and that it can be dissolved in acid (Gray, 1869). With regard to

its natural habitat *I. basta* shows a wide distribution (figure 5) while it typically occurs in the marine waters of the Indian and the Central Indo-Pacific Ocean in the central and southern Great Barrier Reef, at the Indonesian or also along the African coast, e.g. in Kenya or the Mozambique Channel (WoRMS, 2015). Specimen investigated during this study were obtained from Indonesia and Guam, USA, the largest and most southern of the Mariana Islands in the western pacific.

Figure 5. Typical distribution area (red) of *Ianthella basta* within the Indo-Pacific Ocean (yellow) including Guam, USA, as the sampling location of the here investigated specimen. Modified from http://www.wikipedia.org.

The yellow cave-sponge (*A. cavernicola*) received the species status only half a century ago (Vacelet, 1959). Together with the closely related *Aplysina aerophoba* it represents the majority of the Mediterranean sponge population. In contrast to *A. aerophoba*, which can typically be found in shallow waters (up to 15 m), *A. cavernicola* prefers darker locations such as ledges or caverns in depth up to 40 m, which is reflected in its name (Thoms *et al.*, 2003; Wilkinson and Vacelet, 1979). The body shape of *A. cavernicola* is constantly digitate (1-2 cm in diameter and 5-10 cm in height) bearing an oscule (1-3 mm in diameter) at the center of an evident apical depression. These digitations are regularly arranged on a basal encrusting plate attending over 50 cm in diameter. The typical pale yellow colour of *A. cavernicola* changes into medium violet after death and air exposure (Manconi *et al.*, 2013). This sponge species inhabits caves and ledges at various locations among the Mediterranean Sea, such as those

along the French and Croation coastline or in Elba, IT, where the here investigated specimen was collected (figure 6).

Figure 6. Mediterranean Sea and examples of locations typical for the distribution of *Aplysina cavernicola* including Elba, IT, as the sampling location of the here investigated specimen. Modified from http://www.wikipedia.org.

3.3 Marine Natural Products

3.3.1 Marine Pharmaceuticals: from the Oceans to the Clinics

The marine clinical pipeline (table 1) annualy published by the Department of Pharmacology at the Chicago College of Osteopathic Medicine, Midwestern University in Illinois, USA, actually lists seven marine derived compounds approved either by the American Food and Drug Administration (FDA) or European Medicines Agency (EMA) or both. Three out of these seven drugs used for various indications are inspired by sponge metabolites, highlighting especially theses invertebrates as rich sources for unique and highly bioactive leads.

Table 1. Marine clinical pipeline published by the Department of Pharmacology at the Chicago College of Osteopathic Medicine, Midwestern University in Illinois, USA in June 2014 indicating the high relevance of sponge inspired compounds among the marine derived drugs.

Approved by		Compound Name	Trademark	Marine Organism	Chemical Class	Molecular Target	Disease
FDA	EMA						
X	X	Brentuximab vedotin (SGN-35)	Adcetris®	Mollusk/ cyano-bacterium	ADC(MMAE)	CD30 & microtubules	Anaplastic large T-cell systemic malignant lymphoma, Hodgkin's disease
X	X	Cytarabine (Ara-C)	Cytosar-U®	Sponge	Nucleoside	DNA polymerase	Leukemia
X	X	Eribulin mesylate (E7389)	Halaven®	Sponge	Macrolide	Microtubules	Metastatic breast cancer
X	-	Omega-3-acid ethyl esters	Lovaza®	Fish	Omega-3 fatty acids	Trygliceride-synthesizing enzymes	Hypertriglyceridemia
X	X	Ziconotide	Prialt®	Cone snail	Peptide	N-Type Ca Channel	Severe chronic pain
X (discontinued)	-	Vidarabine (Ara-A)	Vira-A®	Sponge	Nucleoside	Viral DNA polymerase	Herpes simplex virus
-	X	Trabectedin (ET-743)	Yondelis®	Tunicate	Alkaloid	Minor groove of DNA	Soft tissue sarcoma and ovarian cancer

The success story of sponge bioprospecting started back in 1951 when Bergmann and Feeney discovered the two unusual nucleosides spongothymidine and spongouridine in some specimen of the marine sponge *Tethya crypta* (syn. *Tectitethya crypta*), which they had collected from the shallow waters of Elliot Key, Florida, USA (Bergmann and Feeney, 1951). The structural uniqueness of the reported nucleosides lays in their D-arabinose-sugar moiety replacing the usual D-ribose. Due to the latter both compounds share the property of being antimetabolites of DNA polymerases with a difference only in specificity of the target enzyme. After a three step phosphorylation to the corresponding triphosphats by kinases the sponge nucleosides act as substrates of either the human or the viral DNA polymerase, which incorporates them into the growing DNA strand leading to a chain determination due to the lack of phosphodiester bridge formation. In 1969 the synthetic sponge nucleoside analogue cytarabin (Ara-C, figure 7A), used for the treatment of acute lymphatic and myeloic leucemia, should become the first marine derived drug introduced to the market (Absalon and Smith, 2009; Thomas, 2009). Several years later in 1976 vidarabin (Ara-A, figure 7A), a further analogue of Bergmann's nucleosides, was approved for the treatment of viral infections such as *Herpes simplex*. Since 2001 the marketing of Ara-A was discontinued due to new drug alternatives. Remarkably, todays first line viral DNA polymerase antimetabolites such as aciclovir, which is even listed in the WHO Model List of Essential Medicines, can be considered as direct advancements of the sponge derived nucleosides (King, 1988; Laport *et al.*, 2009).

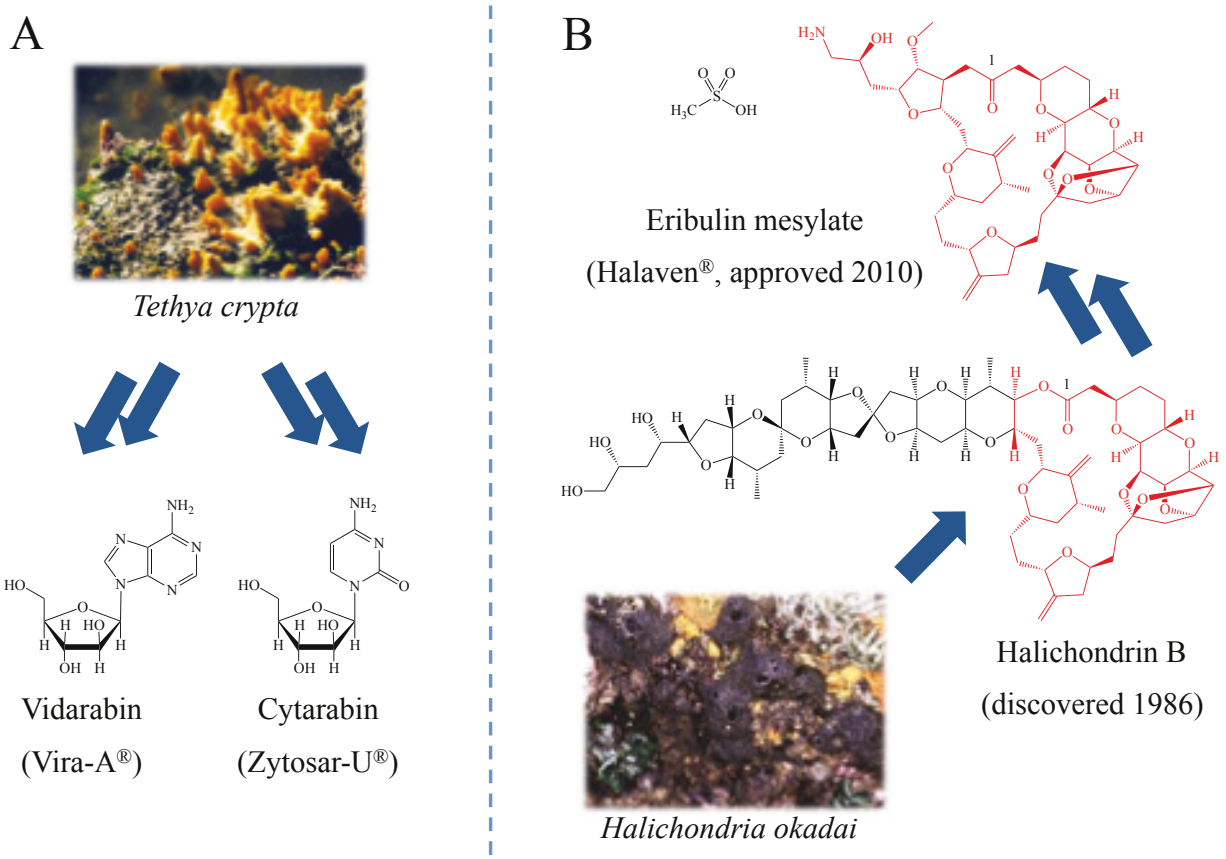

Figure 7. Sponge inspired approved drugs. A: Vidarabin and cytarabin as synthetic analogues of unusual sponge nucleosides from *Tethya crypta*. B: Development of eribulin from the discovery of halichondrin B from *Halichondria okadai* till approval of the structurally altered pharmacophoric warhead as its mesylate salt in 2010.

The third sponge inspired drug on the market is eribulin mesylate (Halaven®), a synthetic analogue of the cytotoxic macrocyclic polyetherlactone halichondrin B typically occuring in the marine sponge *Halichondria okadai* (Hirata and Uemura, 1986). The cytotoxic mode of action is based on a binding to tubulin similar to the vinca-alkaloids (Bai *et al.*, 1991; Dabydeen *et al.*, 2006), leading to a suppression of microtubuli polymerization. In consequence the mitotic cell is arrested in G_2-M phase, which initiates the apoptotic cascade (Smith *et al.*, 2010). Structural alterations in eribulin in comparison to the parent compound (figure 7B) pursue two strategies: firstly, substitution of the ester function (position 1) by a true keto group to obtain hydrolytic stability in consequence with oral bioavailability and secondly a simplification of the highly complex spirocyclic sidechain (13 chiral carbons) to obtain a higher realisability of multigram synthesis. Nevertheless the actual synthesis protocol for eribulin developed and applied by Eisai involves 67 steps. In 2010 this undertaken effort resulted in an approval of eribulin by the FDA (2011 by EMA) for the treatment of metastatic breast cancer (Huyck *et al.*, 2011).

In addition the polyketide PM060184 (figure 8), another tubulin-binding agent with potent anticancer activity which occurrs in the marine sponge *Lithoplocamia lithistoides* (Martínez-Díez *et al.*, 2014), has recently reached clinical phase I.

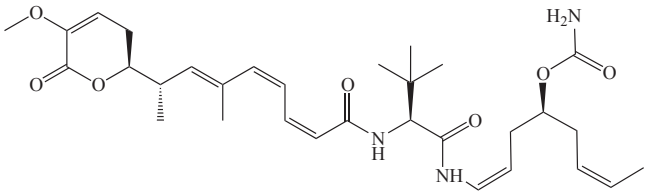

Figure 8. Structure of PM060184 actually listed in clinical phase I.

3.3.2 Chemistry of Verongid Sponges

3.3.2.1 Overview and Biosynthesis

Halogenated derivatives of the aromatic amino acid tyrosine are by far the most common secondary metabolites in many Verongid sponges. According to the marine natural products database MarinLit (03/2015) 97 % of the compounds described from *I. basta* and 94 % from those of the other here investigated species *A. cavernicola* are affiliated with this class of secondary metabolites. The putative biosynthetic pathway towards halogenated *Aplysina* alkaloids and bastadins as well as a hypothesis for the incorporation of halogenated tyrosine into macromolecular spongin of *A. cavernicola* skeletons are shown in figure 9. Starting from phenylalanine the introduction of a *para* phenolic hydroxyl into the aromatic core catalyzed by a hydroxylase is considered as the biosynthetic starting point that forms tyrosine. Subsequently tyrosine is halogenated probably under catalysis of a flavin dependent halogenase. Interestingly, from the genus *Aplysina* brominated (Ciminiello *et al.*, 1997; Fattorusso *et al.*, 1970) as well as chlorinated (D'Ambrosio *et al.*, 1983) and even mixed halogenated (D'Ambrosio *et al.*, 1984) tyrosine derivatives are known while bastadins exclusively occur as brominated congeners in nature. This picture of a diverse halogenation pattern among tyrosine in *Aplysina* can also be drawn with regard to the occurence in macromolecular spongin, whose amino acid analysis resulted in the identification of bromo-, chloro and even iodotyrosine (publication 6). Halogenated tyrosines do not exclusively occur in sponges, but can rather also be found in other marine organisms such as 3,5-diiodotyrosine (iodogorgoic acid) from the coral *Gorgonia cavolinii* (Drechsel, 1896) and brominated and chlorinated derivatives from the cuticle of *Limulus polyphemus* (Welinder, 1972).

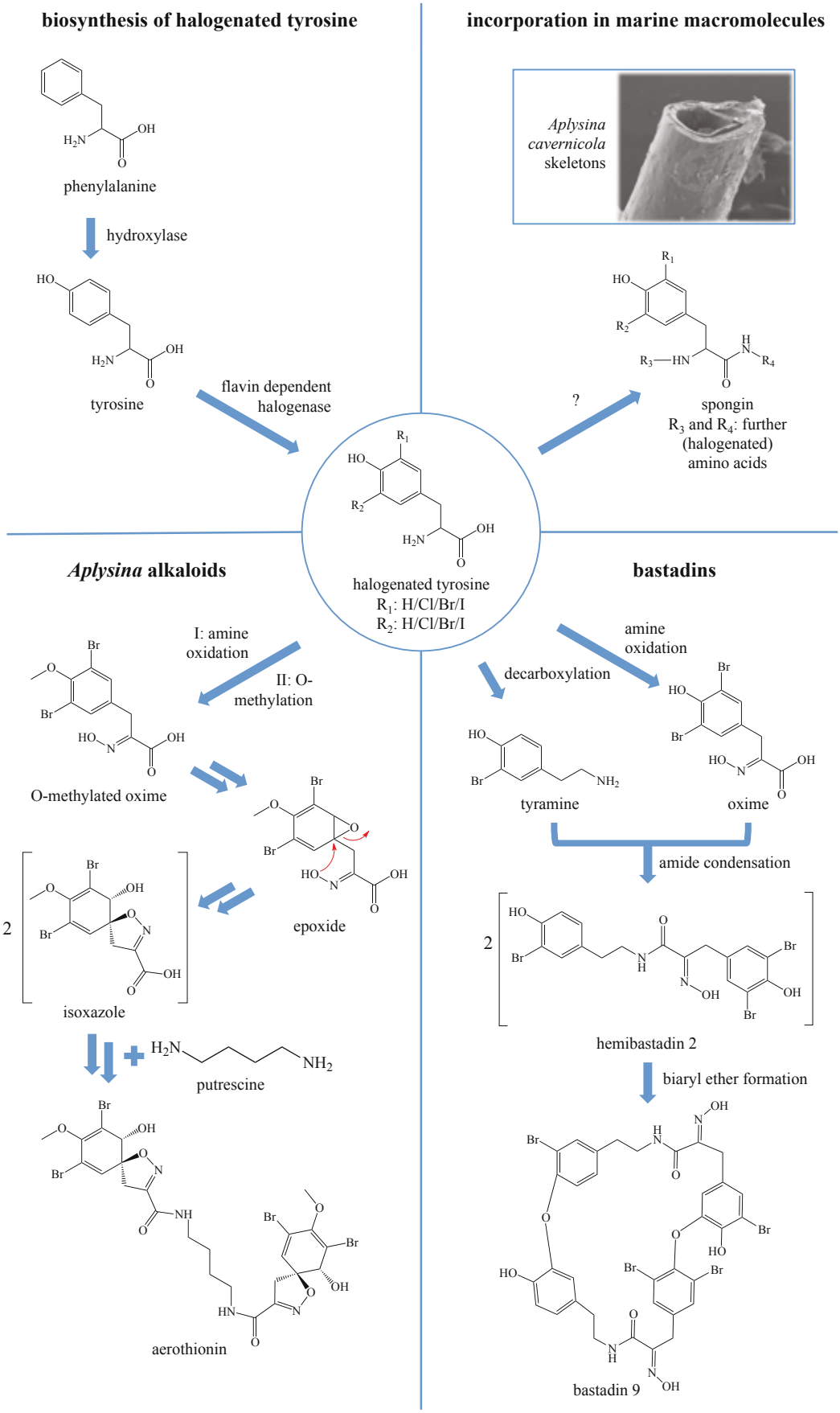

Figure 9. Examples of plausible biosynthetic pathways of halogenated tyrosines in Verongid sponges leading either to proteinous spongin (involved enzyme unknown), isoxazole-bearing *Aplysina* alkaloids or bastadins.

3.3.2.2 *Aplysina* Alkaloids

Several halogenated tyrosines isolated from the genus *Aplysina* such as the investigated species *A. cavernicola* and the closely related *A. aerophoba* have been shwon to contribute to a unique and unusual wound-induced bioconversion mechanism (Ebel *et al.*, 1997; Teeyapant *et al.*, 1993). Typically, bromoisoxazoline alkaloids such as isofistularin-3 aerophobin-2 and aerothionin accumulate as protoxins in the intact sponge tissue (figure 10). The latter was proven to act as a fish deterrent against *Blennius sphinx* and the pufferfish *Canthigaster rostrata* (Thoms *et al.*, 2004). External cues such as mechanical disruption trigger the conversion of the isoxazolines to the nitrile aeroplysinin-1, which is subsequently transformed into verongiaquinol, a corresponding dienone. These bioconversion products have been shown to possess a pronounced cytotoxic (aeroplysinin-1) and growth inhibitory effect towards several marine bacteria and microalgae (dienone) but no fish deterrent effect, whereas precursors like aerothionin were found to be inactive against microbes viceversa (Gochfeld *et al.*, 2012; Teeyapant *et al.*, 1993; Weiss *et al.*, 1996). Hence, the formation of aeroplysinin-1 and the dienone has been proposed to be involved in an activated antibiotic defense of sponges against invading pathogenic bacteria and algae. First indications in favor of an enzymatically catalyzed conversion of aerothionin to the corresponding low molecular weight products were given by Teeyapant *et al.* when observing high amounts of aerothionin when freeze dried sponge samples were extracted in non-aqueous solvents, whereas sponges that were extracted in aqueous solvents yielded large quantities of aeroplysinin-1 and of the dienone instead (Teeyapant *et al.*, 1993). Recently, the enzyme involved for the conversion of aeroplysinin-1 to the dienone was characterized as a unique, manganese-dependent and highly substrate sepcific nitrile hydratase (Lipowicz *et al.*, 2013). Apart from these bioactivities, which obviously contribute to the evolutionary fitness of the sponge in its natural habitat a diverse biological picture of the *Aplysina* alkaloids with regard to a feasible clinical application has been drawn in the past decades. For example the cytotoxic/-static potential of aeroplysinin-1 has been investigated in several studies and strong growth inhibitory effects have been shown on several cell lines such as mouse lymphoma (L5178Y) (Kreuter *et al.*, 1992), human lymphoma (U-937) (Galeano *et al.*, 2011), Ehrlichs ascites tumor (EAT) and HeLa cells (Koulman *et al.*, 1996). For more detailed biological aspects of *Aplysina* alkaloids see publication 1.

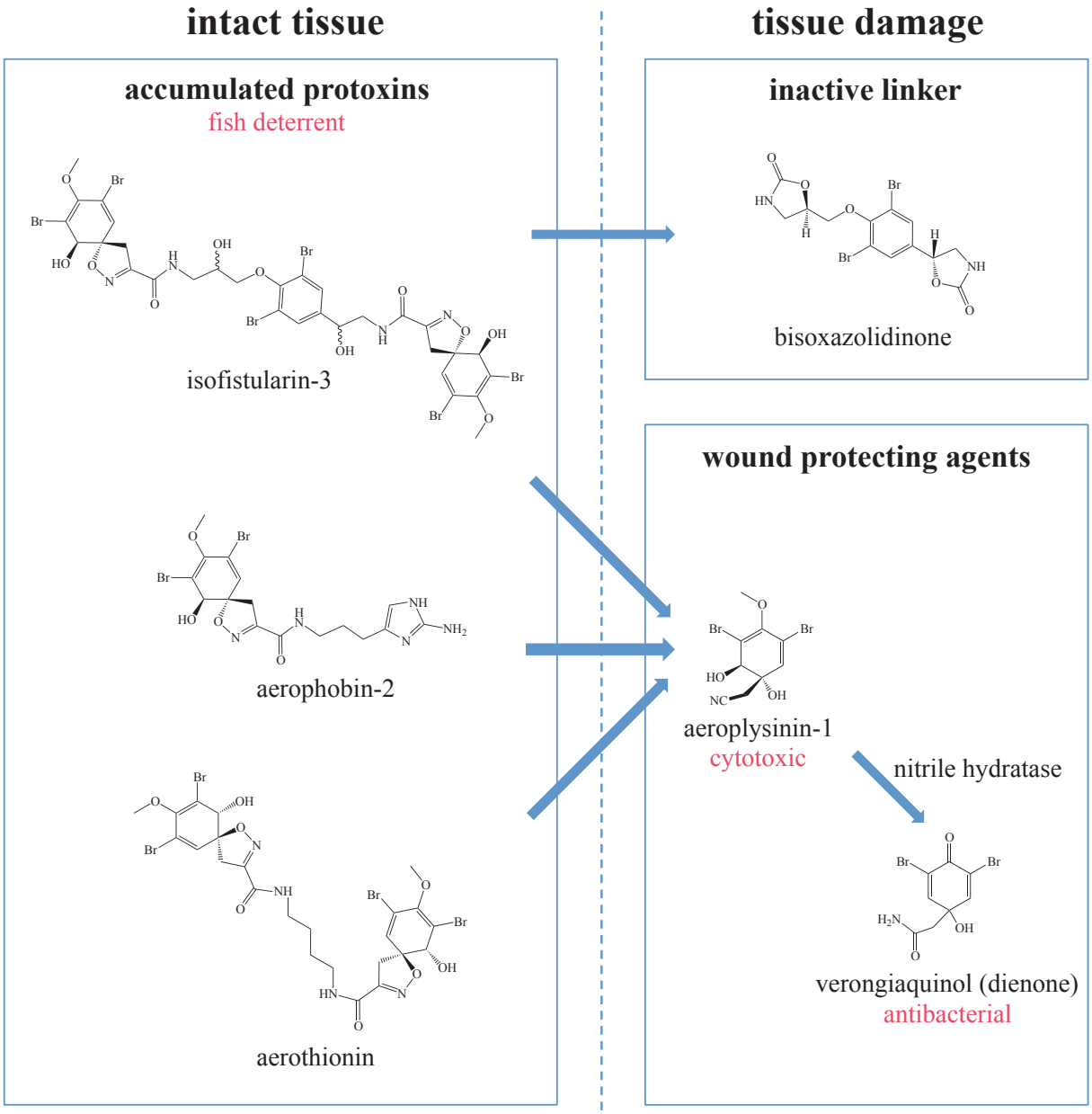

Figure 10. Activated chemical defense in *Aplysina cavernicola* and *A. aerophoba*. Wound-induced bioconversion of fish deterrent *Aplysina* isoxazol-alkoloids to wound protecting agents aeroplysinin-1 and a corresponding dienone.

As mentioned above not only brominated, but also chlorinated congeners of tyrosines were reported among the *Aplysina* alkaloids (figure 11). Dichloroverongiaquinol, the dichloro-analogue of the above mentioned dienone for example (figure 10), also shows prominent antibacterial properties against Gram positive and Gram negative bacteria (D'Ambrosio *et al.*, 1983). 7-Bromo-5-chlorocavernicolin is one structural example of a mixed-halogenated tyorsine congener from *A. cavernicola* (D'Ambrosio *et al.*, 1984).

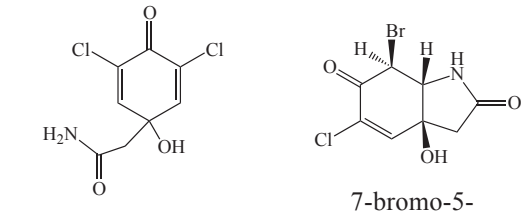

Figure 11. Examples of chlorinated tyrosines among the *Aplysina* alkaloids.

3.3.2.3 Bastadins

True bastadins are oxime-bearing, brominated bis-diaryl ether tetrapeptides, which most commonly occur as macrocycles. In addition to actually 28 macrocyclic congeners three linear bastadins (1-3) are known (Inman and Crews, 2011). The building blocks of bastadins, so called hemibastadins (figure 9), are condensation products of oxime-bearing tyrosine with its amine tyramine. These biosynthetic precursors usually feature mono- or dibromo substituents *ortho* to the phenolic hydroxyls (Butler *et al.*, 1991). The formation of two biaryl ethers, which can be considered as a nucleophilic coupling of a phenolic hydroxyl with a brominated carbon of a second hemibastadin unit, yields a bastaran ring. For the macrocyclic bastadins two possibilities in the hydroxy-ether linkage of the northern bromocatechol bromophenyl ether unit allows a differentiation between the 13,32-dioxa-4,22-diazabastarane- and the 13,32-dioxa-4,22-diazaisobastarane-type of bastadins (figure 12).

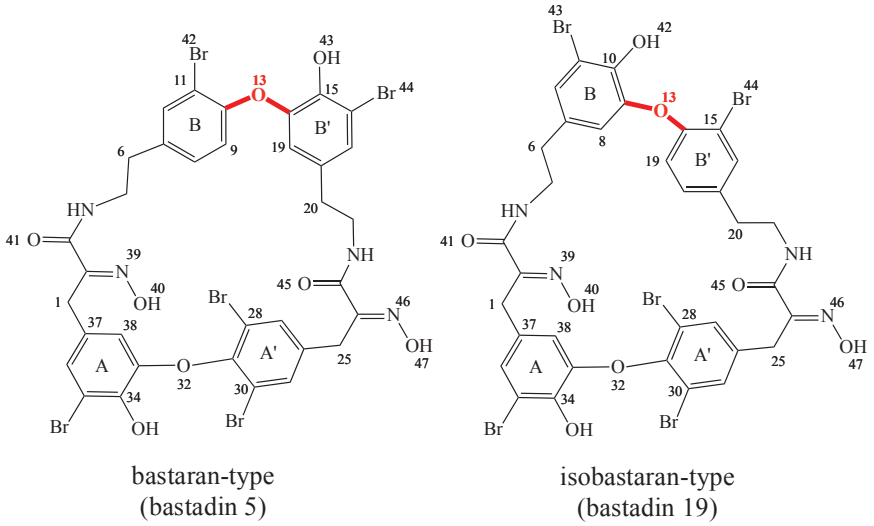

Figure 12. Structures of the macrocyclic constitutional isomers bastadin 5 and 19 indicating the difference in the ether linkage of ring B and B' between bastaran- and isobastarane-type bastadins adapted from Inman and Crews, 2011.

Two exceptions with regard to the biaryl linkage are the linear structures of bastadin 3 and the first trimeric hemibastadin, namely sesquibastadin 1, which was discovered during this study.

Putatively sesquibastadin 1 originates from the two building blocks bastadin 3 and hemibastadin 2 (publication 2). Both compounds share a direct biaryl C-C-linkage instead of the above described ether bridge (figure 13).

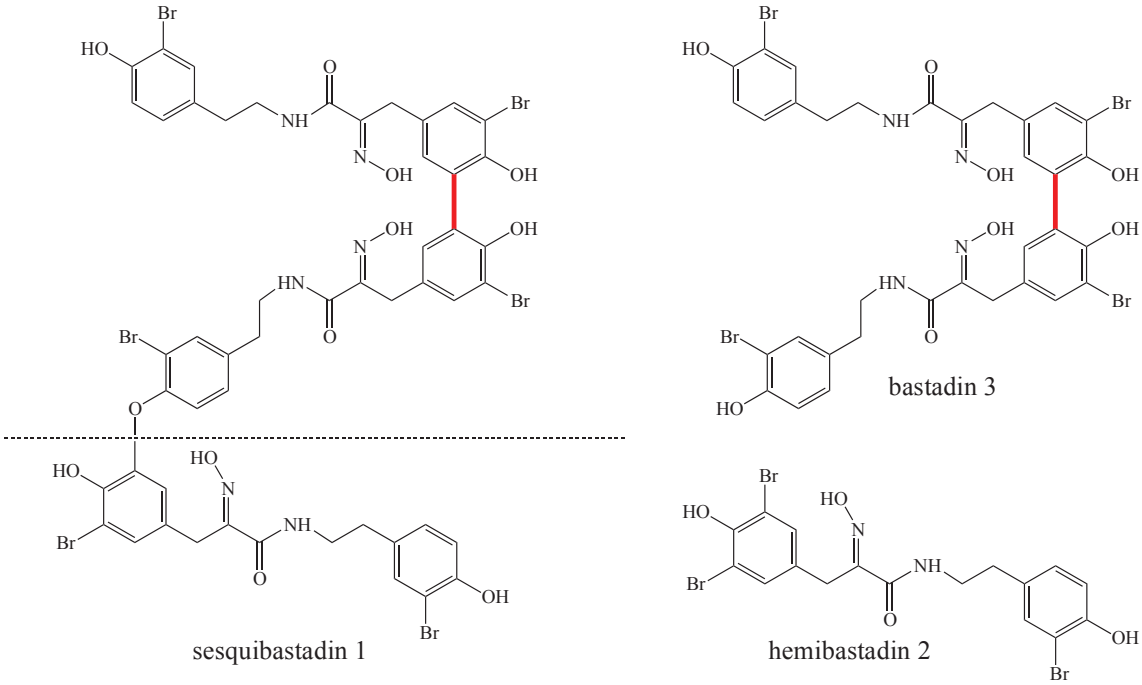

Figure 13. Structures of the trimeric hemibastadin congener sesquibastadin 1 and its building blocks bastadin 3 and hemibastadin 2. The unsual direct biaryl C-C-linkage is shown in red.

The oxime moiety of bastadins is typically reported showing (*E*)-configuration. Nevertheless Inman and Crews propose that bastadins and also closely related psammaplins are biosynthetical similarly produced with the (*Z*)-oximo amide, which subsequently isomerizes to the more thermodynamically stable (*E*)-isomer in solution which is favoured by intramolecular hydrogen bonds (Inman and Crews, 2011). All isolated bastadin congeners investigated during this study were identified as (*E*)-isomers, which was deduced based on the chemical shift of the adjacent methylen groups (figure 12, Pos. 1 and 25) in a ^{13}C-NMR experiment (publication 2). Generally speaking, the differences between individual bastadin derivatives occur with regard to the degree of aromatic bromination, the occurence of double bonds (positions 6/7 and 20/21) and hydroxyl groups (position 7) within the tyramine units and for some derivatives phenolic sulfate esters.

Apart from *Ianthella basta* (Kazlauskas *et al.*, 1980; Pordesimo and Schmitz, 1990) bastadins have been reported from other closely related Verongid sponges such as *Ianthella quadrangulata* (Coll *et al.*, 2002; Greve *et al.*, 2008), *Ianthella reticulata* (Calcul *et al.*, 2010) and *Psammaplysilla purpurea* (Carney *et al.*, 1993). Also among other demosponges such as

the Indian sponge *Dendrilla cactos*, a member of the order Dendroceratida, the occurence of bastadins has been observed (Reddy *et al.*, 2006). Lithothamnin A (figure 14), a metabolite differing from bastadins only in the aromatic substitution pattern by showing meta-meta linkages, that have so far not been reported from sponges, was recently discovered in the red alga *Lithothamnion fragilissimum* (Van Wyk *et al.*, 2011) indicating that the distribution of these brominated tyrosines is not restricted to the phylum of Porifera. This co-occurence in evolutionary distant species gives rise to the hypothesis that the true producers of bastadins and bastadin-like metabolites might be microbial symbionts instead of the hosting macroorganisms. This hypothesis is substantiated by a finding of this study showing that the genes of the above mentioned flavin dependent halogenase (figure 9) are affiliated with sponge symbionts (publication 5).

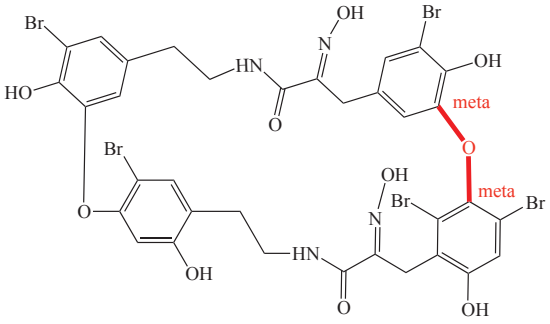

Figure 14. Structure of Lithothamnin A, a bastadin like metabolite with unusual meta-meta linkage (in red) occuring in the red alga *Lithothamnion fragilissimum*.

Several pronounced biological activities of (hemi-)bastadins have been elucidated since their first discovery in 1980 (Kazlauskas *et al.*, 1980). The distinct antifouling properties, in particular the inhibition of barnacle settlement and blue mussel phenoloxidase will be pointed out in section 3.4.3. Most relevant reported activities of bastadins addressing clinical targets can roughly be classified as follows:

- modulation of intracellular Ca^{2+} homeostasis,
- antibacterial activity towards Gram positive and Gram negative bacteria,
- anticancer activities such as cytotoxicity against several cell lines, anti-angiogenic properties and inhibition of molecular targets, e.g. enzymes associated with cancer pathogenesis such as inosine 5'-phosphate dehydrogenase (IMPDH), topoisomerase-II and dehydrofolate reductase.

For bastadin 5 (figure 12) and further bastadin derivatives a selective modulation of the $Ca2^{+}$-release channel of the skeletal sarcoplasmic reticulum (SR) ryanodine receptor-1 (RyR-1) was shown (Mack *et al.*, 1994). Furthermore, bastadins 15 and 20 and 34-O-disulfatobastadin 7 and

10-O-sulfatobastadin 3 showed moderate differential activity as SR Ca^{2+} channel agonists of the RyR-1 FKBP12 complex (Franklin *et al.*, 1996). A further study focussing on the effect of bastadins on Ca^{2+} homeostasis demonstrated that naturally occurring bastadin 10 stabilizes primarily the open conformation of the RyR-1 channel and sensitizes the channel for activation by Ca^{2+} to an extent that it essentially eliminates regulation in the physiological range of this ion (Chen *et al.*, 1999). Later structure-activity studies indicated that bastadin 10 and several synthetic analogues produce an effect identical to that observed for RyR-1 in primary cultures of rat cerebellar granule neurons expressing the cardiac RyR-2 subtype (Zieminska *et al.*, 2007). Synthetic bastadin 5 releases Ca^{2+} from the endoplasmatic reticulum (ER) of neurons in a ryanodine-sensitive way. Further studies indicated that structurally simplified open-chain half bastadins, in particular compounds that carry a dibromocatechol ether moiety as found in bastadin 5, are imitating the activity of naturally occurring bastadins on Ca^{2+} homeostasis in cultured rat cerebellar granule neurons (Zieminska *et al.*, 2008).

Among several investigated bastadin congeners bastadin 3 and hemibastadin 2 (figure 13) proved to be the most potent antibacterial compounds when tested against *Neisseria gonorrhoeae*, *Enterococcus faecalis* and *Staphylococcus aureus* (Pettit *et al.*, 1996). Cytotoxic and antineoplastic attributes of bastadins have additonally been reported in various studies. The first reported cytotoxic activity was stated for bastadins 8 and 9 against the L-1210 leukemia cell line with ED_{50} values of 4.9 μM (Miao *et al.*, 1990). Cytotoxic properties against A-549 lung carcinoma, HT-29 colon adenocarcinoma human tumor, P-388 murine lymphotic leukemia cell lines, and against the non-tumor CV-1 monkey kidney cell line, as well as inhibition of topoisomerase-II and dehydrofolate reductase were discovered for bastadin 14 (Carney *et al.*, 1993). Bastadins 4-7, 12, 3, 21 and 24 were found to possess mean IC_{50} values between 0.6 - 10.1 μM against 36 different human tumor cell lines (Greve *et al.*, 2008). Bastadin 4 isolated showed activity against the colon carcinoma cell line HCT-116 (Calcul *et al.*, 2010). Anti-angiogenic properties of bastadin 6 (figure 15) based on a specific induction of apoptosis in human umbilical vein endothelial cells (HUVEC) were also reported (Aoki *et al.*, 2006). Mechanistically, the authors hypothesized an interaction of bastadin 6 with RyR-3, which may result in a mobilization of intracellular Ca^{2+} and might therefore trigger apoptosis. In a continuative study with synthetic analogues of bastadin 6 Kotoku *et al.* pointed to the oxime function and to the bromination of the aromatic rings as key structural elements with regard to the anti-proliferative effects of bastadin derivatives against HUVECs and KB3-1 cells (Kotoku *et al.*, 2008). The aforementioned bastadin like lithothamnins, also showed moderate

cytotoxic properties, as demonstrated for lithothamnin A (figure 14), exhibiting antiproliferative activities against five human tumor cell lines (Van Wyk *et al.*, 2011).

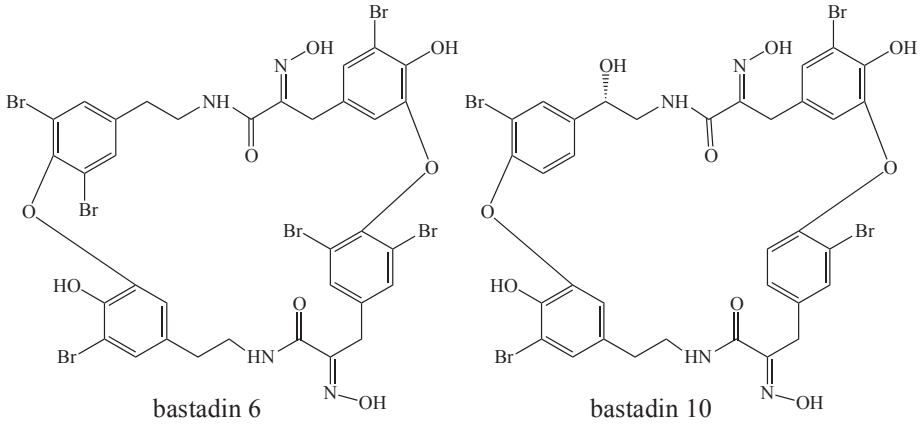

Figure 15. Structures of proapoptotic bastadin 6 and RyR-1 channel modulating bastadin 10.

Due to this diverse profile of various clinically relevant bioactivities bastadins can be stated as highly interesting chemical leads with an enormous potential for modern health sciences.

3.4 Marine Biofouling

3.4.1 Overview and Adhesion Process of Blue Mussel (*Mytilus edulis*)

The undesirable colonization of various submerged substrata in the marine environment like ship hulls or cages in aquaculture by often complex communities of microorganisms, plants and animals is termed biofouling (Callow and Callow, 2002; Yebra *et al.*, 2004). Biofouling processes result from a competition between these pro- and eukaryotic species for space and nutrition (Müller *et al.*, 2013). As a serious global problem biofouling causes extensive material and economic costs as well as a tremendous environmental impact by the worldwide spread of invasive species (Davidson *et al.*, 2009; Schultz *et al.*, 2011; Yebra *et al.*, 2004). According to the US Navy i.e. the increase in friction resistance due to the settlement of fouling organisms such as barnacles (Balanidae) is estimated to cause a 10 % reduction in boat speeds with a 40 % increase in fuel consumption. The overall resulting costs for the US Navy amount to approximately 700 Mio. € p. a. In addition, higher friction rates also lead to an increase in emission of greenhouse gases such as carbon dioxide (CO_2) and sulfur dioxide (SO_2), which are believed to rise up to 72 % untill 2020 as a direct consequence of biofouling (Salta *et al.*, 2010).

The process leading to often highly complex fouling communities is characterized by four main phases (figure 16). Initially, organic particles especially proteins and carbohydrates, adhere to the submerged substrate and serve as nutrients for the subesequently settling microorganisms such as bacteria or diatoms. Among many fouling colonies bacteria of the genus *Vibrio*, such as *V. alginolyticus*, are considered as major microbial constituents generating a so called biofilm. This biofilm conditions the surface further and allows larger organisms such as macroalgae or protozoa to settle. After approximately 21 days the final stage of the fouling process is reached by the settlement of crustaceans such as barnacles (*Balanus amphitrite*) or molluscs like the blue mussel (*Mytilus edulis*) (Yebra *et al.*, 2004).

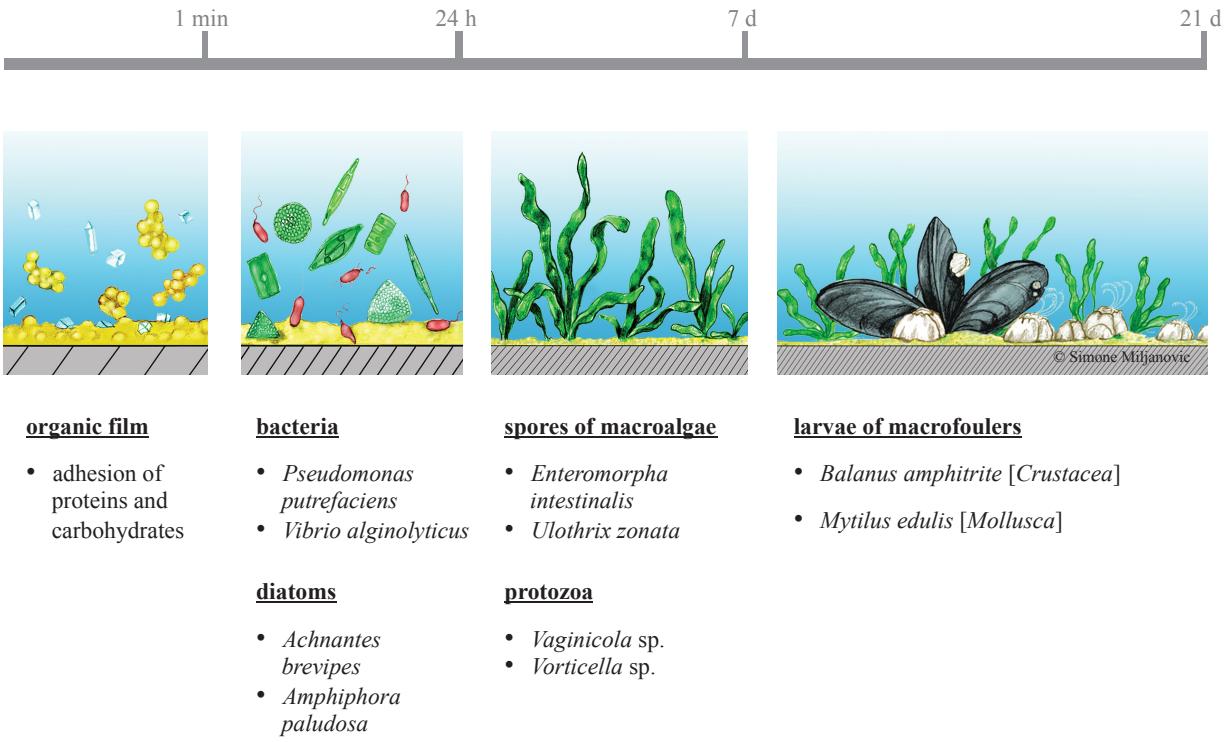

Figure 16. Phases of marine biofouling adapted from Yebra *et al*. (Yebra *et al.*, 2004).

The mechanism of adhesion for the latter of these two macrofoulers is already well understood. The mollusc establishes its firm attachment to any given submerged substrate by the formation of so called byssal threads leading to byssal plaques both contributing to an underwater superglue (Danner *et al.*, 2012). These proteinous structures, also called *Mytilus edulis* foot proteins (Mefp), are mainly characterized by a high content (~30 mol %) of the amino acid 3,4-dihydroxyphenylalanine (DOPA) (Danner *et al.*, 2012). DOPA-residues of Mefp serve as substrates to a phenoloxidase (E.C. 1.14.18.1) (Hellio *et al.*, 2000), that catalyzes the oxidation to highly reactive species such as *ortho*-quinones, that in consequence easily form inter- and intramolecular crosslinks via various mechanisms such as biaryl coupling or michael addtion

(Silverman and Roberto, 2007). The *M. edulis* phenoloxidase can be considered as one key enzyme in the adhesion process and therefore represents an interesting molecular target for future antifouling approaches.

3.4.2 Current Antifouling Approaches: A Depleted Perspective

A huge variety of physical and chemical antifouling (AF) technologies have been developed over several decades, including UV irradiation, ultrasound, electric fields, low friction foul-release polymeric coatings and AF paints such as self-polishing systems (Finnie and Williams, 2010; Guo *et al.*, 2012; Guo *et al.*, 2011; Löschau and Krätke, 2005; Martinelli *et al.*, 2011). Most commonly marine surfaces are coated with AF paints contaning biocides. Among these the best-performing AF approaches are typically based on heavy metals such as copper, lead, mercury, arsenic, and cadmium (Omae, 2003). Already back in ancient times of Carthaginians and Phoenicians (1500–300 BC) heavy metal based AF techniques have been developed to cover ship hulls with pitch and copper platings (WHOI, 1952). In the mid-1960s formulations based on organotin, such as tributyltin (TBT, figure 17), were introduced to the AF market. This approach was marketed to be highly effective at deterring settlement in combination with a low general toxicity level. After more than 20 years being the state of the art among the chemical AF approaches the high efficacy of organotins was found to be primarily based on their acute general toxicity. These most toxic substances ever deliberately introduced into the aquatic environment (Goldberg, 1986) were discovered to be harmful to a range of aquatic biota, including microalgae (Beaumont and Newman, 1986), molluscs, crustaceans (Langston *et al.*, 1990), fish (Wester *et al.*, 1990) and invertebrate communities of seagrass beds (Kelly *et al.*, 1990a; Kelly *et al.*, 1990b). The best documented case reports of the toxic impact of TBT on marine organisms were however those on the Pacific oyster *Crassostrea gigas* and the dogwhelk *Nucella lapillus*. High mortality rates of oyster larvae and a severe malformation of addult oyster shells (Alzieu *et al.*, 1986) as well as imposex in female dogwhelks (Bryan *et al.*, 1987) were discovered as direct effects on high TBT levels in highly frequented boating regions. Since 2008 TBT-based AF paints are banned according to the “International Convention on the Control of Harmful Anti-Fouling Systems on Ships” by the International Maritime Organization (IMO) (IMO, 2002). Therefore, today the most commonly used AF paints are based on copper (Cu) supplemented by so called booster biocides (figure 17) to control Cu-resistant fouling organisms (Voulvoulis, 2006). These include Irgarol 1051 (2-methylthio-4-tertiary-butylamino-6-cyclopropylamino-s-triazine), diuron (1-(3,4-dichlorophenyl)-3,3-dimethyl-urea), zinc pyrithione (2-mercaptopyridine N-oxide zinc salt; ZnPT), copper pyrithione (2-mercaptopyridine N-oxide copper salt; CuPT), chlorothalonil

(2,4,5,6-tetra-chloroisophthalonitrile) and SeaNine 211 (4,5-dichloro-2-n-octyl-4-isothiazolin-3-one; DCOIT) (Konstantinou and Albanis, 2004; Zhou *et al.*, 2006). However, many of the currently used biocides are also a threat for the marine environment (van Wezel and Van Vlaardingen, 2004); some can accumulate at high levels, despite claims for rapid degradation, and have a biocidal effect on non-fouling marine organisms (Bellas, 2006, 2007, 2008; Konstantinou and Albanis, 2004; Thomas and Brooks, 2010). Some are reported to be even more toxic than TBT. For instance, Sea-Nine 211 was found to have a deleterious effect on the embryo-larval stage of the sea urchin, *Paracentrotus lividus*, despite its classification as a safe biocide (Bellas, 2007). Diuron and Irgarol 1051 have been banned by many EU governments in recent years (Cresswell *et al.*, 2006) due to increasing evidence for being environmentally toxic (Munoz *et al.*, 2010). Not only for supplementary booster biocides but also for the major AF paint constituent copper similar restrictions of usage are expected for the future. Washington became recently the first US state to ban copper-based paints (containing more than 0.5 % copper) starting from 2020 for boats less than 20 meters (Trepos *et al.*, 2015). In summary one may state that new eco-friendly solutions for the biofouling issue are highly desirable as the use-risk-profile of current approaches remains unsatisfactory.

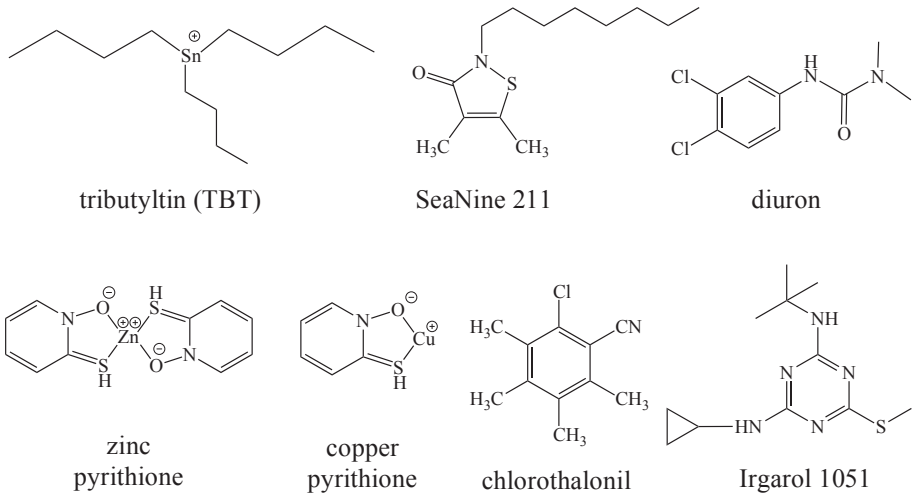

Figure 17. Structures of banned tributyltin and common but debatable booster biocides used in combination with copper in current AF composites.

3.4.3 Sponge-Derived Antifouling Leads

Biomimetic solutions inspired by marine metabolites exhibiting high specificity towards molecular targets of the complex fouling cascade rather than a general toxicity are highly favorable for future AF developments. The world of sessile marine organisms appears as an evolutionary treasure chest for this challenging issue of modern bioprospecting. Due to a high

population density and the reduced mobility among members of sessile marine communities like diverse coral reefs organisms had to develop strategies to protect themselves against physical contact and more specifically against overgrowth and fouling. Mechanical as well as chemical interactions are the two parameters primarily controlling fouling processes in the marine environment (Müller *et al.*, 2013). Investigating the latter recent bioprospecting has identified several promising AF candidates. For naturally occuring as well as synthetic bastadin congeners Ortlepp *et al*. demonstrated an inhibition of the settlement of bay barnacles (*Balanus improvisus*) cyprid larvae (Ortlepp *et al.*, 2007). Among the investigated derivatives macrocyclic bastadin 9 and synthetic 5,5'-dibromohemibastadin-1 (DBHB) showed a strong settlement inhibition (figure 18), but no effect on larval mortality. Targetting the same macrofouler bromotryptophan derived barretins, such as bromobenzisoxazole barettin demonstrated larval settlement inhibition in a low nanomolar range (Hedner *et al.*, 2008). The attachment of another major fouling organism, the zebra mussel (*Dreissena polymorpha*), to a given substrate was inhibited by bromotyrosines including moloka'iamine and hemifistularin-3 at moderate EC_{50} values.

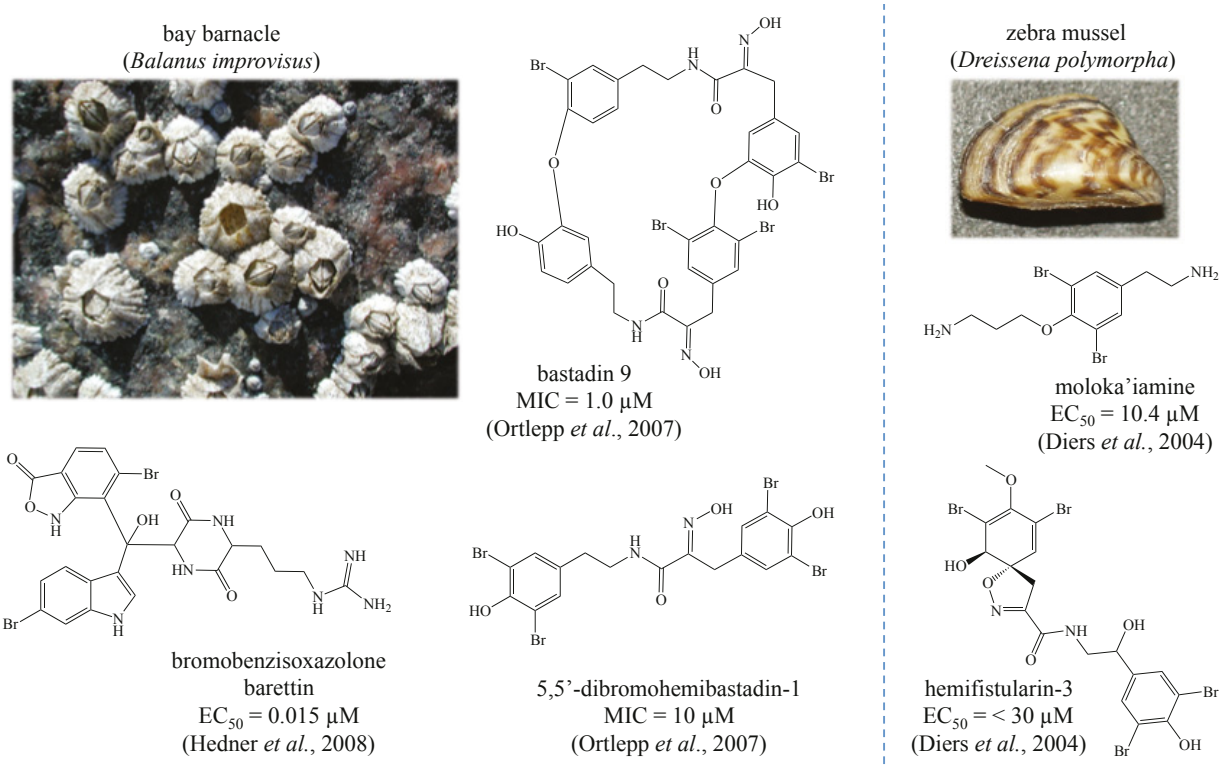

Figure 18. Examples of sponge compounds and their potential to inhibit settlement of respective macrofouling organisms indicated by EC_{50} and MIC values (Diers *et al.*, 2004; Hedner *et al.*, 2008; Ortlepp *et al.*, 2007). Pictures taken from http://wikipedia.org.

For synthetic DBHB and closely related analogues the above mentioned *M. edulis* phenoloxidase (section 3.4.1) was recently discovered as one putative molecular target to inhibit macrofouling (Bayer *et al.*, 2011). Bayer *et al*. assigned the *α*-hydroxyimino-amide moiety as the pharmacophoric core structure being essential for enzyme inhibition due to strong copper coordinating properties (figure 19). Tyrosinyltyramine (TT), a congener bearing a primary amine instead of the oxime, totally failed to inhibit the enzyme. Phenolic residues and bromine substituents as present in DBHB furthermore led to an increase in the inhibitory potential of hemibastadin congeners towards the enzyme. Based on these initial studies further structure-acitivity-relationship studies (SAR) of hemibastadin congeners with regard to blue mussel phenoloxidase inhibition were conducted in this thesis (publication 4).

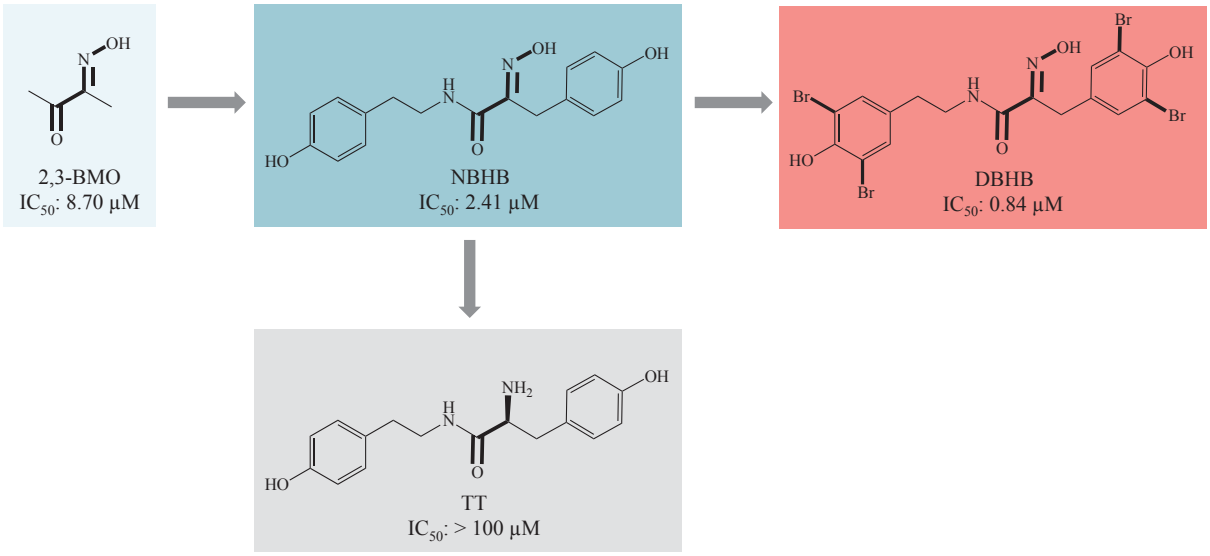

Figure 19. Inhibition of *M. edulis* phenoloxidase by 2,3-BMO (2,3-butandienone monoxime), NBHB (norbromohemibastadin-1), DBHB (5,5'-dibromohemibastadin-1) and TT (tyrosinyltyramine) as indicated by the IC_{50} values of the respective compounds. Pharmacophoric core structures and activity increasing bromine substituents are highlighted in bold. Modified from Bayer *et al*., 2011.

3.5 Aim of the study

In recent bioprospecting investigations metabolites derived from the oceans and especially those from marine sponges have demonstrated an enormous potential as novel clinical leads as well as AF agents. Among this increasing group of marine metabolites the class of halogenated tyrosines has gathered wide interest due to a high structural diversity and pronounced biological activity. One initial aspect of this thesis is to give a review on a small excerpt of compounds from this class, in particular bastadins, *Aplysina* alkaloids and psammaplin A with focus on the respective biological potential (publication 1). Furthermore, this study aims to isolate and identify (novel) bastadin congeners from *I. basta* to contribute to the evaluation of the anticancer potential of this class of marine metabolites (publication 2). Compounds that are isolated from a methanolic sponge extract by several chromatographic procedures and furthermore elucidated with regard to their structure by various spectroscopic methods are then submitted to cell viability assays against a murine lymphoma cell line (L5178Y). Additionally, the bastadin isolates are tested against a panel of protein kinases, that are relevant in neoplastic processes including breast cancer (Aur-A and Aur-B) and non-small-cell lung cancer (EGF-R and VEGF-R2). Further studies on (hemi)bastadins with regard to the anticancer mode of action and here in particular their pro-apoptotic, anti-angiogenic and anti-migratory effects and a putative binding of DBHB to serum albumine is investigated in a further part of the project (publication 3). Apart from the examination of a tentative clinical utilization of halotyrosines the AF potential of synthetic hemibastadin congeners represents another central aspect of this thesis (publication 4). Therefore, a set of closely related compounds is synthesized by preparative organic chemistry and their inhibitory potential against *M. edulis* phenoloxidase is quantified by the determination of the respective IC_{50} values. The aim of this investigation shall lead to a better understanding of the compound enzyme interaction, which may result in a commercial application of AF active hemibastadins in the future. In addition to the biological potential of halotyrosines and a possible biomimetic utilization, chemoecological studies will be subject of this thesis by analyzing the association of bastadins and aerothionin to sponge skeletons (publication 5). In addition, the identification of halotyrosines that are not only associated with but covalently incorporated into the spongineous protein fraction of *A. caverniocal* skeletons represents the final aspect of this study (publication 6).

4 Publication 1

4.1 Sponge Derived Bromotyrosines: Structural Diversity through Natural Combinatorial Chemistry

Published in: „Natural Product Communications“

Impact factor: 0.924

Contribution: 40 %, first author, literature research, manuscript writing

NPC Natural Product Communications

2015
Vol. 10
No. 1
219 - 231

Sponge Derived Bromotyrosines: Structural Diversity through Natural Combinatorial Chemistry

Hendrik Niemann[a,&], Andreas Marmann[a,&], Wenhan Lin[b] and Peter Proksch[a,*]

[a]*Institute of Pharmaceutical Biology and Biotechnology, Heinrich-Heine University, 40225 Düsseldorf, Germany*
[b]*State Key Laboratory of Natural and Biomimetic Drugs, Peking University, Health Science Center, Beijing100191, China*

[&] both authors contributed equally

proksch@hhu.de

Received: August 15th, 2014; Accepted: October 17th, 2014

Sponge derived bromotyrosines are a multifaceted class of marine bioactive compounds that are important for the chemical defense of sponges but also for drug discovery programs as well as for technical applications in the field of antifouling constituents. These compounds, which are mainly accumulated by Verongid sponges, exhibit a diverse range of bioactivities including antibiotic, cytotoxic and antifouling effects. In spite of the simple biogenetic building blocks, which consist only of brominated tyrosine and tyramine units, an impressive diversity of different compounds is obtained through different linkages between these precursors and through structural modifications of the side chains and/or aromatic rings resembling strategies that are known from combinatorial chemistry. As examples for bioactive, structurally divergent bromotyrosines psammaplin A, *Aplysina* alkaloids featuring aerothionin, aeroplysinin-1 and the dienone, and the bastadins, including the synthetically derived hemibastadin congeners, have been selected for this review. Whereas all of these natural products are believed to be involved in the chemical defense of sponges, some of them may also be of particular relevance to drug discovery due to their interaction with specific molecular targets in eukaryotic cells. These targets involve important enzymes and receptors, such as histone deacetylases (HDAC) and DNA methyltransferases (DNMT), which are inhibited by psammaplin A, as well as ryanodine receptors that are targeted by bastadine type compounds. The hemibastadins such as the synthetically derived dibromohemibastadin are of particular interest due to their antifouling activity. For the latter, a phenoloxidase which catalyzes the bioglue formation needed for firm attachment of fouling organisms to a given substrate was identified as a molecular target. The *Aplysina* alkaloids finally provide a vivid example for dynamic wound induced bioconversions of natural products that generate highly efficient chemical weapons precisely when and where needed.

Keywords: Psammaplin A, Bastadin, Aerothionin, Aeroplysinin-1, Dienone, Bromotyrosine, Sponges.

The fact that marine ecosystems cover over 70 % of the surface of the earth and contain about 95 % of the total biosphere, has stimulated natural product chemists for several decades now to embark on bioprospection for new metabolites and drug candidates. The remarkable diversity of natural products reported from marine organisms is due to long evolutionary processes which have favored the accumulation of strongly bioactive compounds. Seemingly primitive and morphologically defenseless organisms like sponges developed ingenious survival strategies which rely heavily on the accumulation of defensive products which protect these organisms from a multitude of stress factors that involve overgrowth by fouling organisms, and predation or invasion by pathogenic microorganisms, to name just a few. Sponges are multicellular sessile invertebrates that have successfully existed on earth for 700-800 million years and can be found in all oceans, even under the Antarctic ice cover. All sponges belong to the phylum Porifera, which is divided into three classes, the Calcarea, Hexactinellida and Demospongiae. Recently a fourth class, the Homoscleromorpha, has been established and separated from the Demospongiae by phylogenetic markers [1]. Sponges are filter-feeders which phagocytose detritus, bacteria and microalgae from the surrounding seawater. Sponges can filter up to 24,000 liters of water per 1 kg weight tissue per day [2]. Structural integrity of the sponges is maintained by siliceous or calcareous spicules and by a spongin skeleton. Interestingly, some of these simple sessile filter feeding organisms are reported to be the oldest living organisms on earth. The artic sponge *Scolymastra joubini* is known to live for 1,500 to 12,000 years [3].

There is an open debate whether all natural products isolated from sponges are produced by sponges or are in fact derived from microorganisms that are inhaled though filter-feeding or that live within the sponges. In fact, a large part of the sponge biomass may consist of associated microorganisms (mainly bacteria). For the sponge *Aplysina aerophoba* associated microbes may account for over 40 % of the sponge biomass [4]. So far the evolutionary processes underlying sponge-microorganism associations are not well understood. Three different scenarios are hypothesized: ancient

Peter Proksch, born 1953. Ph D in Biology in 1980 at the University of Cologne, Germany. From 1980 – 82 Post Doctoral Fellow at the University of California, Irvine. Worked as a scientist at the Universities of Cologne and of Braunschweig from 1982 – 90. Since 1990 as Associate Professor at the University of Wuerzburg and since 1999 as a Full Professor at the University of Duesseldorf. Main areas of scientific research: bioactive natural products from marine sponges and from endophytic fungi. Prof. Proksch is a visting Professor at Peking University, the Ocean University of China at Qingdao and the Chinese Academy of Tropical Agriculture Science, Haikou.

symbiosis maintained by vertical transmission of symbionts, parenteral and environmental symbiont transmission and environmental acquisition of symbionts [5-7].

Apart from their origin and chemoecological functions sponge-derived metabolites are also of considerable interest for bioprospecting. Since resistance of cancer cells and of infectious microorganisms to chemotherapy is a well-known phenomenon that often causes great difficulties during chemotherapy, new drugs that may break resistance and offer alternatives to the currently available anti-cancer drugs or antibiotics are urgently needed. Marine derived compounds including those from sponges that are the most prolific source of bioactive compounds among marine invertebrates [8] have already been shown to offer new drugs for chemotherapy of cancer. Three out of seven currently FDA approved marine drugs either originate from sponges or were modeled based on sponge metabolites, underlining the potential of these compounds as drugs or drug leads. Among them Halaven® (approved for use in the US, Canada and in the EU for the treatment of advanced mamma carcinoma) is the most notable example of a sponge inspired anti-tumor drug. Halaven® is a synthetic macrolide inspired by the naturally occurring halichondrin B that was originally isolated from marine sponges of the genus *Halichondria*, but which is also known to occur in other sponges. In addition, the nucleoside analogues Cytosar-U® and Vira-A® may also be mentioned that were likewise modeled based on compounds isolated from marine sponges [9-11].

This review will focus on selected bromotyrosine derivatives from sponges, their role in chemical ecology and their pharmacological activities which make these compounds interesting for drug discovery. In spite of the rather simple structures of the bromotyrosine and bromotyramine precursors a wealth of structurally divergent metabolites is generated through different linkages between the building blocks and/or structural modifications involving the side chain and the aromatic ring thus bearing resemblances to strategies used in combinatorial chemistry. Within the group of sponges, Demospongiae of the class Verongida have been shown to be the most prolific producers of these metabolites [12, 13]. Examples of bromotyrosines used in this review have all been taken from Verongid sponges. Early reports on naturally occurring mono- and dibromotyrosine in marine invertebrates date back to 1951 [14], when these halogenated amino acids were found as integral constituents of the coral skleroprotein gorgonin. These biogenetic precursors to all naturally occurring bromotyrosine derivatives like psammaplin A, the bastadines and the isoxazoline alkaloids from *Aplysina* sp. that will be covered in this review, are biosynthetically derived from phenylalanine by aromatic hydroxylation catalyzed by phenylalaninhydroxylase (PAH), and bromination presumably catalyzed by halogenases **(**Figure 1) [15]. Bromotyrosine derivatives, however, do not only accumulate within either the cytosol or within cytosolic compartments of sponge cells, from which they can easily be extracted using organic solvents, but may also be covalently bound to sponging, as shown recently for the sponge *Aplysina cavernicola* [15].

Psammaplin A

Psammaplin A consists of two identical subunits, each of them composed of a bromotyrosine and a cysteine derived moiety which are linked by a disulfide bridge (Figure 1) [16]. This compound is primarily, but not exclusively, found in sponges from the order Verongida [17, 18]. Psammaplin A has been described from sponges of the genera *Psammaplysilla* [19] and *Pseudoceratina* [20], both being Verongid sponges, but was also discovered as a product of two associated sponges including *Poecillastra* sp. and *Jaspis* sp., neither of which belong to the order Verongida [21]. Unique structural aspects of psammaplin A are the dense N functionalization in conjunction with S and Br atoms [20]. First described in 1987 from a *Psammaplysilla* sp., initial evaluation of the cytotoxic potential revealed an IC_{50} value of 0.45 µM against P388 cells [22], already indicating the pronounced biological activity of this compound. Over the last decades efforts were made to discover the various biological activities of psammaplin A, such as the antibiotic, antiviral, cytotoxic, fish deterrent and antifouling effects, whereas in the last decade detailed analyses of its pharmacologically relevant molecular targets were conducted.

Analysis of the minimal inhibitory concentrations (MIC) of psammaplin A against twenty-two different methicillin-resistant *Staphylococcus aureus* strains (MRSA) showed MICs ranging from 0.781 - 6.25 µg/mL. The compound was demonstrated to inhibit bacterial DNA synthesis, as well as gyrase activity with IC_{50} values of 2.83 and 100 µg/mL, respectively [23]. The inactivity of psammaplin A against different strains of Gram negative bacteria such as *Escherischia coli*, *Pseudomonas aeruginosa*, *Salmonella typhimurium*, *Klebsiella oxaytoca*, *Enterobacter cloacae* and *Citrobacter freundii*, as well as against a penicillin binding protein isolated from *S. aureus* SG511, demonstrated a narrow range of susceptible bacterial species, but a selective mode of action for the compound [23]. Oh *et al.*, in contrast, observed no antibiotic effect of psammaplin A against *S. aureus*, but instead an inhibition of sortase A and B activity. Sortases are key enzymes involved in the bacterial virulence which are required for the attachment of bacteria to eukaryotic cell surface components like fibrinogen and fibrionectin. In a fibrionectin binding assay, inhibition of sortase A and B by 40 µg/mL of psammaplin A resulted in a decreased adhesion of bacterial cells to fibrionectin coated microtiter plates. Similar results were obtained using bacterial knockout mutants of sortase B and sortase A and B, implying that psammaplin A interfered with bacterial virulence. [24]. By generating a library of psammaplin A derivatives, Nicolaou *et al*. investigated structure activity relationships (SAR) [25]. Over 80 analogues were generated and evaluated against nine different *S. aureus* strains, including methicillin sensitive and resistant strains, and IC_{50} values from 0.09 to >50 µg/mL were measured for the various derivatives. Parallel investigation of the general cytotoxicity against human fibroblasts and lymphocytes, however, indicated a high toxicity of the respective compounds to eukaryotic cells with IC_{50} values from 1.17 - 28.16 µM, respectively (0.78 and 18.7 µg/mL). Due to the toxicity of these compounds their possible use as an antibacterial agent can be ruled out.

Salam *et al*. observed an inhibition of hepatitis C virus NS3 nucleoside triphosphatase (NTPase)/helicase by psammaplin A in a non-competitive manner with IC_{50} values 17 and 32 µM, respectively. Additionally, psammaplin A inhibited viral replication with EC_{50} values of 6.1 and 6.3 µM against two subgenomic replicon cell populations derived from two different genotypes [28]. Again, when viewed against the high toxicity of the compound a possible use of psammaplin A for controlling viral diseases seems unlikely.

Beside possible anti-infective properties, initial toxicity screenings of psammaplin A against A-549, SK-OV-3, SK-MEL-2, XF-498, HCT [18], K-562 [16] and A2780 [29] cancer cells demonstrated a pronounced cytotoxic potential of the compound as expressed by the IC_{50} values that ranged from 0.20 to 1.20 µM. Studies on molecular targets of psammaplin A indicated an inhibition of histone deacetylase (HDAC) and DNA methyltransferase (DNMT). Inhibition of these enzymes leads to cell cycle arrest, apoptosis and

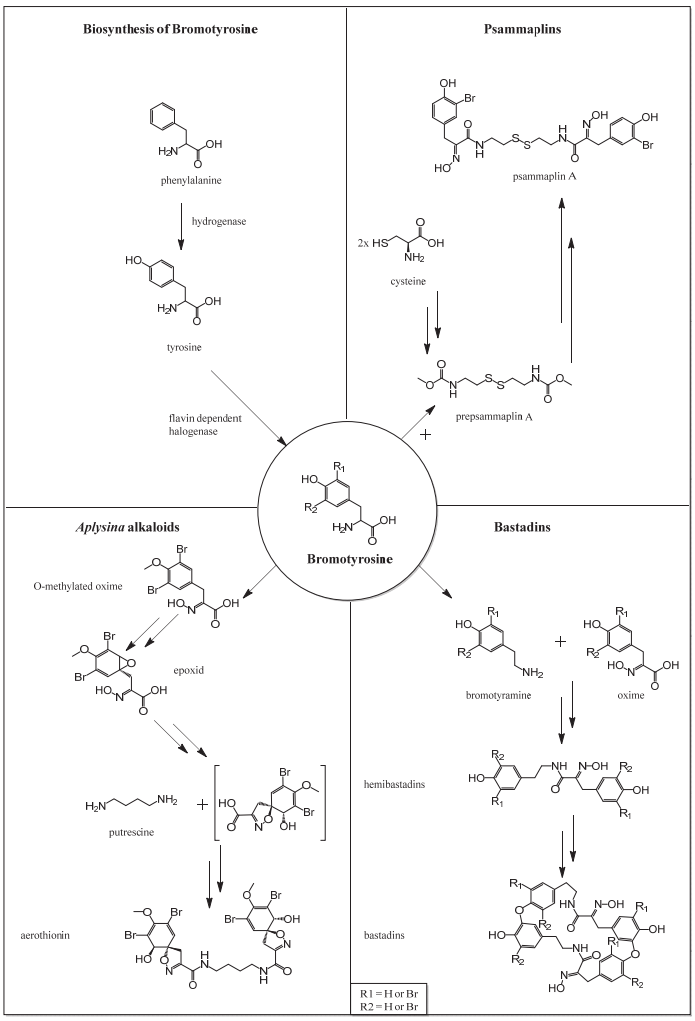

Figure 1: Putative biosynthesis of bromotyrosine derived sponge alkaloids [15, 19, 26, 27].

p53 independent p21 induction [20]. IC_{50} values of psammaplin A amounted to 4.2 nM (+/- 2.4) (HDAC inhibition) and 18.6 nM (DNMT inhibition). In the same study the authors evaluated the activity of psammaplin A in monolayers and in soft agar cell cultures against A549 cells and against MDA-MB-435 cells and reported IC_{50} values of 1.15 and 2.0 µM, respectively [20]. Structure activity studies of a series of psammaplin A analogues revealed the disulfide bridge linked to two bromotyrosine end capped hydroxyimino amides as essential for inhibition of the above mentioned enzymes [20]. Similar observations were made by Ahn *et al*. when investigating cell proliferation of endometrial Ishikawa cancer cells. Psammaplin A was identified as an inducer of the expression of H3 and H4 histone proteins and of the cycline-dependent kinase inhibitor p21 and as a simultaneous down-regulator of pRb, cyclins and CDKs expression, leading to induced cell cycle arrest. Cell cycle analysis of endometrial Ishikawa cancer cells treated with psammaplin A revealed an increased proportion of cells in the G0/G1 and G2/M phase and a decrease of cells in the S phase. Hence, the authors concluded that psammaplin A is a selective inductor of genes related to cell cycle arrest and apoptosis, associated with p53 independent p21 expression [30]. The same cell cycle interferences were observed by Pereira *et al*. in U937 cells, causing an acetylation of the HDAC6 marker α-tubulin [31]. Based on these investigations psammaplin A is characterized as an epigenetic modifier. When studying the inhibition of other potential epigenetic targets, including DNMT1, DNMT3A, SIRT1 and the

p300/CBP HAT domain, no activity of psammaplin A was observed. Additional structure activity relationships that were elucidated using synthetic psammaplin A derivatives in an HDAC1 enzyme assay indicated that the natural product already exhibited optimized structural features. Though the disulfide bridge was identified as a key structural element essential for activity, the free thiol groups are also important for chelating the HDAC co-factor Zn^+ which was pointed out in this study by modeling psammaplin A into the active site of HDAC8 [32]. Out of psammaplins A, B, E and F psammaplin A was shown by Kim *et al*. to be one of the most potent inhibitors of HDAC1 exhibiting an IC_{50} value of 0.003µM. Interestingly, in the same study a positive correlation of intracellular glutathione level and HDAC inhibition was found. When cells were glutathione-depleted with butionine sulfoxime, HDAC inhibition caused by psammaplin A was generally less pronounced giving rise to the hypothesis that intracellular conversion of psammaplin A to its corresponding monomer is responsible for the observed efficacy of the compound as an HDAC inhibitor. The cellular reduction of psammaplin A to its monomers by glutathione is therefore assumed to be a key event in the mechanism of action of this compound [33]. When tested against different HDAC isoforms, psammaplin A showed a 360 fold higher selectivity for HDAC1 over HDAC 6 and was 1000 fold less potent against HDAC7 and 8 [34]. In addition, McCulloch *et al*. were able to identify psammaplin A as an activator of Wnt signaling in STF3 cells, a cell line in which luciferase is constitutively expressed in response to autocrine Wnt signaling. In this study psammaplin A was comparable in regard to its activity with suberoylanilide hydroxamic acid (SAHA), trichostatin A and MS-275 [35]. In addition to HDAC inhibition, psammaplin A was also characterized as a potent inhibitor of DNA methyltransferases DNMT1 and DNMT3A in A549 and U373MG cell lines with IC_{50} values of 7.53 µM in both cases. In this study Kim *et al*. demonstrated that cell treatment with radiation leads to a significantly reduced cell survival of psammaplin A pretreated cells when compared with untreated controls. γH2AX levels, a marker of DNA double strand break, were observed to be constant over a 12 and 24-hour time course in A549 and U373MG cells, respectively, implying an inhibition of DNA repair mechanisms, due to epigenetic modification caused by psammaplin A [36].

Interestingly, Mora *et al*. identified psammaplin A, as an activator of PPARγ in human MCF-7 cells using a luciferase reporter gene assay. Molecular modeling studies additionally suggested an interaction of the compound with the binding site of the PPARγ ligand binding pocket. The EC_{50} value was determined to be 5.7 µM, while the IC_{50} for inhibition of cell proliferation/viability was accessed as 5 µM. Thereby psammaplin A may play a role in cell differentiation and in induction of apoptosis through the activation of PPARγ in addition to the described inhibitory effects on HDAC and DNMT [37].

In addition to the described epigenetic and pro-apoptotic effects of psammaplin A in mammalian cells, the compound was also found to inhibit aminopeptidase N (APN), leading to a suppression of angiogenesis and invasion of cancer cells. APN was inhibited by psammaplin A in a non-competitive manner with an IC_{50} value of 18 µM, resulting in a suppression of cancer invasion and tube formation of endothelial cells treated with basic fibroblast growth factor, while psammaplins B, C, D, A-1 and C1 caused no inhibition. Treatment of different mammalian cell lines with psammaplin A over 72 h, including HepG2, C8161, BAEC, B16/BL6, HT29 and HT1080 cells resulted in IC_{50} values between 3 and >30 µM [38]. Studies on DNA replication, using the SV40 DNA replication assay with radiolabeled dTTP, and pol α-primase assay [39], revealed psammaplin A to inhibit DNA relaxation by inhibition of DNA topoisomerase II with an IC_{50} value of 18.8 µM. Parallel evaluation of cytotoxicity of this compound in K549, SK-OV-3, HCT15 and HCT15/CL02 cell lines yielded EC_{50} values from 0.39 to 3.76 µM thereby connecting topoisomerase II inhibition with cell death. Interestingly, cells incubated with the MDR modulator verapamil showed a 2.1 fold reduction of the EC_{50} value of psammaplin A in HCT15/CL02 cells [40].

Besides the described effects of psammaplin A towards epigenetic targets such as HDAC, the compound also showed moderate IC_{50} (7.0 mM and 70.9 mM, respectively) values with regard to inhibition of farnesyl protein transferase and leucine aminopeptidase (AP-N) [16], further underlining the diversity of psammaplin A targets. Urbaniak *et al*. also identified psammaplin A as an inhibitor of the UDP-4Glc4'-epimerase of *Trypanosoma brucei* TbGaIE as well as mammalian hGaIE with IC_{50} values of 15 ± 5.1 and 3.6 ± 0.5 µM, respectively. When evaluating the cytotoxicity against *T. brucei* and Chinese Hamster CHO-K1 cells EC_{50} values of 2.6 ± 2.4 and 0.9 ± 0.6 µM were determined [41], indicating a non-selective mode of action.

In ecological terms psammaplin A is suspected to act as a fish deterrent [42] and as an antifouling agent [43]. The water soluble psammaplin A sulfate [43] has been shown to be converted to the more lipophilic psammaplin A [42] upon wounding of the sponge. This bioconversion was suggested to be enzymatically catalyzed. Psammaplin A in contrast to its more hydrophilic precursor exhibits significantly stronger antifouling activity [43], while the fish deterrent effects of both compounds are similar [42]. The authors hypothesized that the stronger antifouling activity of the more lipophilic psammaplin A as compared with its sulfate indicates inhibition of an intracellular target in fouling organisms. In addition to antifouling properties, Ortlepp *et al*. observed toxicity of psammaplin A to the larvae of *B. improvisus* with IC_{50} values comparable with concentrations needed for inhibition of larval settlement [43], indicating a non-selective mode of action of the compound with regard to its antifouling properties.

Aerothionin – Aeroplysinin - Dienone – A unique bioconversion cascade involved in sponge chemical defense

Aplysina sponges feature a unique and unusual wound-induced bioconversion of bromoisoxazoline alkaloids which gives rise to the nitrile aeroplysinin-1, which is further converted to a dienone (Figure 2) [12, 44]. The latter two compounds which accumulate following wounding of the sponge tissue have previously been shown to be strongly active against several marine bacteria, whereas aerothionin was found to be inactive [12]. Hence, the formation of aeroplysinin-1 and of the dienone has been proposed to be involved in the antibiotic defense of sponges against invading pathogenic bacteria following disruption of the sponge tissue. First indications in favor of an enzymatically catalyzed conversion of aerothionin to the corresponding low molecular weight products aeroplysinin-1 and dienone were given by Teeyapant *et al.* when observing high amounts of aerothionin when freeze dried sponge samples were extracted in non-aqueous solvents, whereas sponges that were extracted in aqueous solvents yielded large quantities of aeroplysinin-1 and of the dienone instead [12]. Teeyapant and Proksch demonstrated further that treatment of sponge tissue at 90 °C for 5 min prior to extraction inhibited the observed bioconversion of aerothionin to aeroplysinin-1 and the dienone, respectively. Further *in situ* studies on the conversion of aerophobin-2 and aplysinamisin-1 into the dienone by cell free extracts of *A. aerophoba* showed a rapid and almost quantitative transformation to aeroplysinin-1 and to the dienone within 40 seconds after mechanical damage of sponge tissue.

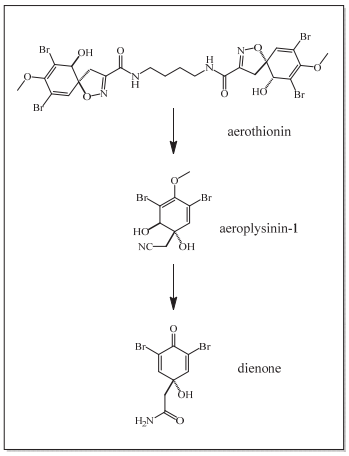

Figure 2: Wound induced bioconversion of aerothionin to aeroplysinin-1 and to the dienone.

When using cell free extracts of other non bromoisoxazoline accumulating sponges, boiled extracts of *A. aerophoba* or assays including known enzyme inhibitors like trichloroacetic acid, no conversion of bromoisoxazoline alkaloids into either aeroplysinin-1 or the dienone was observed [44]. Further evidence for a conversion of bromoisoxazolines by *Aplysina* sponges was provided by a study of Thoms *et al.* who reinvestigated the proposed wound induced bioconversion of sponge alkaloids. *A. aerophoba* was treated in a series of experiments with different disruptive methods thereby injuring the sponge tissue. HPLC analysis of the wounded sponges showed a significant decrease of bromoisoxazolines in damaged sponge tissue, while the amount of aeroplysinin-1 and dienone consistently rose over time. The authors were additionally able to link their observations to the degree of wound induction. Larger disruptions of tissue led to a significantly higher accumulation of aeroplysinin-1 and of the dienone, whereas small damages of sponge tissue caused only minor changes of the alkaloid profiles. It was hypothesized that bromoisoxazoline alkaloids and degrading enzymes are stored in different cellular compartments and are only liberated upon tissue disruption causing the observed bioconversion of sponge alkaloids [45]. Recently Lipowicz *et al.* characterized a manganese dependent nitrile hydratase isolated from *A. cavernicola*, which shows a high substrate-specificity for aeroplysinin-1 and converts it into the dienone. *De-novo* sequencing of the partially purified enzyme by mass spectrometry and comparison with other known nitrile hydratases revealed no homology to known nitrile hydratases, suggesting a unique enzyme to be involved in the alkaloid bioconversion and hence in the chemical defense mechanism of *Aplysina* sponges [46]. In other *Aplysina* species, like *A. cauliformis* and *A. archeri*, no wound activated conversion of bromoisoxazolines into low molecular weight metabolites was observed [47]. However, since the methods used in the latter study differed from those used for investigating the alkaloid bioconversion in *A. aerophoba* or *A. cavernicola* a direct comparison of the results achieved is nevertheless difficult if not impossible.

Aerothionin

Aerothionin, which is one of the bromoisoxazoline alkaloids of the *Aplysina* defense cascade, was first isolated from *A. aerophoba* and *Verongia thiona* in 1970 by Fattorusso *et al*. [48] and identified as spirocyclichexadienylisooxaolone, suspected to be derived from 3,5-dibromotyrosine and ornithine as a product of an intramolecular phenol-oxime coupling giving rise to a symmetrical dimer [48, 49]. It was speculated that 4-hydroxyphenylpyruvic acid oxime is the biogenetic precursor of aerothionin, since both compounds were isolated from *Hymeniacidion sanguinea* [50]. Later on, aerothionin was also found in several other *Aplysina* spp., including *A. geradogreeni* [51], *A. insularis* [47, 52] and *A. cauliformis* [53], but also in the Verongid sponges *Suberea mollis* [54] and *Hymeniacidion sanguinea* [50]. Therefore aerothionin can be considered as being a chemotaxonomic marker of Verongid sponges [55]. Carney and Rinehart were able to demonstrate through feeding experiments using ^{14}C-labeled amino acids that the bromotyrosine unit of bromoisoxazoline alkaloids in *A. fistularis* was derived from phenylalanine, which is subsequently converted to tyrosine [56]. However, the true biosynthetic origin of aerothionin is still questionable, as it is presently unknown whether the compound is derived from the sponge itself or from bacterial symbionts. It was already demonstrated that *A. fistularis* and *A. aerophoba* accumulate aerothionin in sphaerulous cells. Although it seems unlikely that microbial metabolites are translocated to the host cell, the hypothesis of a microbial origin could not be rejected [55]. Remarkable in this context is also the observation that aerothionin was found as a secondary metabolite of the crinoid *Himerometra magnipinna*. Crinoids are not systematically related to sponges which again provokes the question of the actual producer of the compound.

Putz *et al.* were able to demonstrate that the total amounts of bromoisoxazoline alkaloids in *Aplysina* sponges show great variability between different sponge individuals collected in the Adriatic Sea. This study revealed also striking differences of alkaloid patterns in different *Aplysina* specimens, identifying aerothionin as a chemotaxonomic marker of *Aplysina* sponges allocated at depths > 12 m whereas sponges from more shallow depths were characterized by aerophobin-2 and isofistularin-3 as major constituents instead. Transplantation experiments, through which sponges were moved from deeper sites to more shallow waters and vice versa indicated the bromoisoxazoline alkaloid patterns to be stable over a period of 12 months [57]. As shown in a study by Thoms *et al.* aerothionin acts as a fish deterrent to *Blennius sphinx* at ecologically relevant concentrations, whereas the bioconversion products aeroplysinin-1 and dienone showed no fish deterrency. When compared with several other sponge species *Aplysina* spp. were found to be strongly fish deterrent [58]. Feeding experiments involving the pufferfish *Canthigaster rostrata* indicated aerothionin likewise to act as a feeding deterrent [53]. This deterrent effect, however, was not observed for the marine mollusk *Tylodina perversa*, which is a specialized predator on *Aplysina* sponges. Feeding of *T. perversa* on *Aplysina* sponges resulted in a sequestration of aerothionin in mantle tissue, egg masses and mucus. It was speculated that sequestration of aerothionin in these vulnerable tissues or in the defensive mucus serves as an acquired chemical defense for *T. perverse*, whereas the likewise sequestered sponge pigment uranidine provides a perfect camouflage for the mollusks when present on their sponge prey [12, 59, 60].

Previously, aerothionin was isolated from the Verongid sponge *S. mollis*, besides several other bromotyrosine derivatives, and evaluated for its antioxidant, antimicrobial and cytotoxic properties. In this study only a weak antibiotic activity of the compound was detected against *S. aureus*, indicated by a growth inhibition zone of 5 mm in a paper disc diffusion assay [54]. In a further study by

Abou-Shoer *et al.*, aerothinonin caused growth inhibition of *Klebsiella pneumoniae*, expressed by an inhibition zone of 3 mm in the paper disc diffusion assay [61]. Hyphae formation of Streptomyces 85E was inhibited by aerothionin at a concentration of 20 µg/disc [62]. Aerothionin was also evaluated against different *Mycobacterium* strains, including mono- and multi-drug resistant strains of *M. tuberculosis*. Strains of *M. tuberculosis* that were mono-resistant towards isoniazid, rifampicin, streptomycin or ethambutol, respectively, proved susceptible towards aerothionin. The respective MIC values amounted to 12.5 µg/mL. In addition, eight clinical isolates of *M. tuberculosis* with different resistant patterns were also sensitive towards aerothionin, as indicated by MIC values between 6.25 and 25 µg/mL. However, out of eight nontuberculous mycobacterial strains, only three were susceptible to aerothionin, indicating a selective mode of action of the compound against *M. tuberculosis* [51].

Aeroplysinin-1

As mentioned above, aeroplysinin-1 is the first detectable bioconversion product of either aerothionin or of other brominated isoxazoline alkaloids such as isofistularin-3 or aerophobin-2. Aeroplysinin-1 has been shown to exhibit diverse biological activities, including antibiotic, cytotoxic, deterrent and antifouling activity, which may be interpreted in terms of the chemical defense reaction of *Aplysina* sponges explained in more detail above. First isolated in 1972 by Fattorusso *et al.* from *A. aerophoba* [63], aeroplysinin-1 is, like its bromoisoxazoline precursors, taxonomically restricted to the order of Verongid sponges, including *Psammaplysilla purpurea* [64], *A. fistularis* forma *fulva* [65], *Pseudoceratina crassa* [66], *A. aerophoba* [67], *A. cavernicola* [68], *A. cauliformis* [69], *Verongula gigantea* [70] and *A. caissara* [71]. Interestingly the quantity of aeroplysinin-1 was found to be highly variable in a population of *Pseudoceratina crassa* sponges collected from the same depth and in the same region [66]. As shown in a study by Makarieva *et al.* involving 25 Cuban sponges, only those belonging to the order Aplysinidae were able to produce brominated tyrosine derivatives. Out of this group, only four, namely *Aplysina archeri*, *Verongula rigida*, *V. gigantea* and *Aiolochroia crassa* were able to synthesize aeroplysinin-1, but in strikingly different amounts in relation to sponge dry weight [72]. Both reports give further evidence for a bioconversion of sponge alkaloids, as shown for *A. aerophoba* and *A. cavernicola* [66] [72]. In a study on environmental conditions that influence the accumulation of aeroplysinin-1 in sponges Kreuter *et al.* were able to demonstrate that the compound is only produced in the surface tissue of the sponge. Cultivation experiments revealed a positive correlation of aeroplysinin-1 accumulation with regard to UV light and aeration. Sponges cultivated without aeration and UV light were not able to synthesize aeroplysinin-1. Under ideal conditions *V. aerophoba* (syn. *A. aerophoba*) was found to be able to produce up to 13.02 mg aeroplysinin-1 per 100 g sponge [73]. Early studies on antibiotic effects of aeroplysinin-1 already reported activity against *Staphylococcus albus*, *Bacillus cereus* and *B. subtilis*, albeit without mentioning conditions of these experiments and MIC values [63]. Weiss *et al.* were able to demonstrate a strong antibiotic activity of aeroplysinin-1 against *Photobacterium phosphoreum* with an EC_{50} value of 3.45 µM [74]. Furthermore, when evaluating the antibiotic properties of aeroplysinin-1 against several Gram positive and Gram negative bacteria by a paper disc diffusion assay against *Alteromonas* sp., *Cytophaga* sp., *Moraxella* sp., *Pseudomonas fluorescens*, *Serratia plymuthica*, *Vibrio* sp., *Vibrio anaguillarum*, and *Planococcus citreus*, growth inhibition zones of 8 and 30 mm at fixed concentrations of 5, 50 and 100 µg/disc were detected. Both *Vibrio* spp. proved to be most sensitive towards the compound [74]. Aeroplysinin-1 isolated from *Suberea mollis* additionally displayed antimicrobial activities in a paper disc diffusion assay against *S. aureus*, *P. aeruginosa* and *K. pneumoniae*, with inhibition zones of 9 mm, 11 mm and 7 mm, respectively. Antioxidant activity of aeroplysinin-1 at 1 mg/mL was comparable with vitamin E when tested at equimolar concentrations, evaluated by 1,1-diphenyl-2-picylhydrazyl radical assay (DPPH) [61]. Furthermore, aeroplysinin-1 isolated from *A. chiriquensis* and *A. gerardogreeni* collected along the Pacific Coast of Panama, exhibited antiprotozoal activities against chloroquine-resistant *Plasmodium falciparum* and *Trypanosoma cruzi* with IC_{50} values of 17.7 and 37.7 µM, respectively [75]. These results are supported by Galeano *et al.* who observed a growth inhibition of intracellular *T. cruzi* amastigotes at a fixed concentration of 10 µM of aeroplysinin-1 and a severely retarded growth of *Plasmodium falciparum* at 5 µM [76].

Aeroplysinin-1 was reported to have cytostatic effects against the cell line L5178Y with an ED_{50} value of 0.47 ± 0.04 µM [73]. Furthermore, an almost complete growth inhibition of U-937 cells was observed at a fixed concentration of 20 µM aeroplysinin-1 [76]. Early studies on the mode of action of aeroplysinin-1, using Ehrlichs ascites tumor cells (EAT) and HeLa cells in MTT and clonogenic assays, exhibited IC_{50} values of 6.2 ± 0.7 µM and 5.6 ± 0.7 µM, respectively, in continuous incubation over 3 or 4 days, respectively. Incubation for only 2 h led to a drop in IC_{50} values to 8.2 ± 1.0 µM (EAT) and 18.8 ± 2.1 µM (HeLa) in the MTT assay and to 37.0 ± 7.0 µM (EAT) and 27.5 ± 3.0 µM (HeLa) in the clonogenic assay. When aeroplysinin-1 was investigated using cells treated with the glutathione depleting agent buthionine prior to aeroplysinin-1 treatment, even lower IC_{50} values of 0.7 ± 0.2 to 5.4 ± 1.5 µM were detected. Detailed studies on the metabolism of aeroplysinin-1 in EAT cells treated with 2 mM of aeroplysinin-1 using electron paramagnetic resonance spectroscopy, revealed the formation of its corresponding semiquinone radical, which was assumed to be at least partly responsible for the cytotoxicity of the compound [77]. More detailed analyses of the anti-tumor mode of action of aeroplysinin-1 revealed an interaction of the compound with several enzymes, particularly those involved in angiogenesis. In a variety of experimental systems that simulate the sequential events of the angiogenetic process, treatment with aeroplysinin-1 resulted in strong inhibitory effects on angiogenesis in BAE cells, indicated by an effective concentration of the compound of 0.7 µM. Anti-proliferative effects were observed at higher concentrations with an IC_{50} value of 2.1 µM. Capillary tube formation was completely abrogated and an inhibitory effect on the migration capabilities of endothelial cells was observed. Furthermore, aeroplysinin-1 led to a decreased production of matrix metalloproteinase-2 and urokinase in endothelial cells [78]. Using the *in vivo* chorioallantontoic membrane assay, apoptosis-inducing effects of aeroplysinin-1 were observed. These data indicate that aeroplysinin-1 interferes with key events in angiogenesis [79]. Similar results in BAE cells were published by Córdoba *et al.*, who observed an IC_{50} value for aeroplysinin-1 of 29 µM and an MIC of 2 µM for tube formation, giving further evidence for a specific antiangiogenic effect of this natural product [80]. Additional studies on this compound corroborated a directed effect against endothelial cells, using a modified chorioallantontoic membrane assay with monoclonal endothelial markers [81]. A further study, using BAE, HCT-116 and HT-1080 cells, showed again a specific effect of aeroplysinin-1 on endothelial cells, with activation of caspases 2, -3, -8 and -9, as well as a cleavage of apoptotic substrates like poly (ADP-ribose) polymerase and lamin-A. These observations, in combination with dephosphorylation of Bad and mitochondrial cytochrome *c* release, implicate a relevant role of mitochondria in the apoptotic activity of aeroplysinin-1 [79]. Previously, Martínez-Poveda *et al.* were able to demonstrate that this effect is not

restricted to BAE cells, but is also present in human endothelial EVLC-2, RF-24, HUVEC and HMEC cells with IC_{50} values of aeroplysinin-1 between 2.6 - 4.7 μM. More detailed investigations using a gene array assay revealed significant changes in the expression of thrombospondin b1 and monocyte chemoattractant protein-1, which were both down regulated. Western blotting experiments confirmed a down regulation of laterophilin and of the transmembrane domain-containing protein 1, interleukin 1α and matrix metalloproteinase 1. Treatment of THP-1 monocytes as well as HUVEC cells with aeroplysinin-1 resulted in a significantly reduced expression of cyclooxygenase-2 [82]. Kreuter *et al.* were able to prove inhibition of phosphorylation of lipocortin-like proteins by purification of EGF receptor-tyrosine kinase complex from MCF-7 breast carcinoma cells in the presence of aeroplysinin-1 at a concentration of 0.5 μM. MCF-7 cells lost their ability to EGF-mediated cell response in the presence of aeroplysinin-1. These effects were found to be reversible after removal of the compound, and selective to carcinoma cells [83].

In contrast to its biogenetic precursor aerothionin, no fish deterrent effects were observed for aeroplysinin-1 against *B. sphinx* [58], whereas aeroplysinin-1 showed a deterrent effect towards the polyphagous marine gastropod *Littorina littorea*, with an EC_{50} value of 0.1 mM [74]. Deterrency of the compound was also detected against the common Caribbean wrasse *Thalassoma bifaciatum* [44]. Feeding experiments involving the mollusk predator *T. perversa* that feeds on *Aplysina* sponges showed sequestration of aeroplysinin-1, similar to the likewise sponge-derived aerothionin. In this study an enrichment of several bromotyrosine alkaloids, including aeroplysinin-1, was observed, particularly in egg masses of the mollusk [60], underlining the presumed ecological defensive role of the compound. Furthermore, aeroplysinin-1 exhibited a strong growth inhibition against the marine microalgae *Coscinodiscus wailesii* and *Prorocentrum minimum* with IC_{50} values of 5.6 μM [74].

Dienone

This bioconversion product (syn. verongiaquinol [84]) of aeroplysinin-1 was first isolated in 1967 [85], but was later also found in other Verongid sponges including *Verongia cauliformis* and *V. fistularis* [86]. Along with the discovery of the compound its antibiotic potential was recognized [85]. Later on, more detailed studies revealed the antibiotic properties of the dienone to be comparable with those of aeroplysinin-1 showing effects against several Gram positive and Gram negative bacteria in a paper disc diffusion assay against *Alteromonas* sp., *Cytophaga* sp., *Moraxella* sp., *Pseudomonas flourescens*, *Serratia plymuthica*, *Vibrio* sp., *V. anaguillarum*, and *Planococcus citreus*, with growth inhibition zones of 7 and 28 mm at fixed concentrations of 5, 50 and 100 μg/disc. The tested *Vibrio* spp. turned out to be the most sensitive to both compounds [74].

In addition to its antibiotic effects the dienone also showed promising cytotoxic activity. Early studies on the mode of action using Ehrlich's ascites tumor cells and HeLa cells in MTT and clonogenic assays revealed IC_{50} values of the dienone of 26.2 ± 4.1 μM and 15.6 ± 0.6 μM, respectively, during continuous incubation. An incubation for only 2 h led to a decrease of IC_{50} values to 46.1 ± 1.8 μM and 15.6 ± 0.6 μM in the MTT assay and 74.3 ± 3.7 μM and 58.0 ± 10.9 μM in the clonogenic assay. When cells were pretreated with the glutathione depleting agent buthionine, the effect of the dienone was more pronounced, as indicated by lower IC_{50} values of 3.9 ± 1.10 to 15.7 ± 0.5 μM, which were comparable with those of aeroplysinin-1 in the same assay. Electron paramagnetic resonance spectroscopy revealed the formation of its corresponding semiquinone radical, similar to aeroplysinin-1. The semiquinone radical was assumed to be at least partly responsible for the observed cytotoxicity of the dienone [77]. Using a clonogenic GM-CFC/HALO® assay and comparing the cytotoxicity of the dienone with synthetic structural analogues a significant cytotoxicity of this compound was monitored at a dose of 10 μM. Synthetic derivatives, based on non-radical producing phenolic structures did not show this effect [87], confirming the previous results. In addition to cytotoxic effects, Gorshkov *et al.* observed a moderate inhibition of rat brain Na^+/K^+ ATPase with an IC_{50} value of 38 μM [88].

In an ecological perspective, the dienone, like aeroplysinin-1, can be viewed as a broad spectrum wound protecting agent. Beside its cytotoxic and antibiotic properties it inhibits the growth of the marine microalgae *Coscinodiscus wailesii* and *Prorocentrum minimum* with an IC_{50} value of 27.9 μM [74] and of *Phytobacterium phosphoreum* with an EC_{50} value of 1.37 μM [74]. However, a fish deterrent effect was not reported for this compound [58].

Bastadins – Antifouling agents, regulators of cellular Ca^{2+}-homeostasis and potential anticancer drug candidates

Until now, twenty-six different bastadin derivatives have been reported from marine sponges belonging to the genera *Ianthella*, *Psammaplysilla* and *Dendrilla* (all of them from the Demospongiae) [89]. Chemically these metabolites consist of two brominated tyrosine and two brominated tyramine units. Peptidic condensation of the amino acids with their corresponding amines and further oxidation of the α-amino units yielding oxime functionalities, leads to pivotal intermediates of the bastadin biosynthesis, called hemibastadins. Dimerization of hemibastadins via direct carbon-carbon-aryl linkages or arylether bonds results in either open chain or macrocyclic bastadins, the latter being more common. Recently, we have shown that even trimeric hemibastadin congeners, the so called sesquibastadins, occur in the Pacific sponge *Ianthella basta* [90]. We were also able to prove that the distribution of bastadins within the sponge *I. basta* is not restricted to sponge cells, but rather extends to the sponge skeleton as well [15]. Bastadins that are associated with sponge skeletons, which mainly consist of chitin composed collagenous spongin [91] as recently shown for *I. basta* [15], presumably interact with chitinases, as found for other bromotyrosines like psammaplin A [29]. Thus, it may be speculated that bastadins are involved in inhibition of sponge skeletal degradation by e.g. fungal chitinases [15].

The facts that genes of flavin-dependent halogenases, enzymes which are presumably responsible for the incorporation of bromine into the aromatic moieties of bastadins, are known from sponge symbionts [15], and the occurrence of bastadin-like metabolites, called lithothamnins, in the red alga *Lithothamnion fragilissimum* [92], suggest that bastadin type compounds may perhaps either be of symbiotic origin or that symbionts are involved in the biosynthesis of bastadin type compounds.

Several pronounced biological activities of bastadins have been elucidated in the last decade. Ortlepp *et al.* [43] were able to show that bastadins-3, -4, -9 and -16, as well as their putative biogenetic precursor hemibastadin-1, inhibited the settlement of *Balanus improvisus* cyprid larvae, which are among the major macrofouling organisms. The active concentrations of the tested bastadin derivatives were in the range of 1 to 10 μM. Several synthetic analogues of hemibastadin-1, such as 5,5'-dibromohemibastadin-1 (DBHB), exhibited likewise strong inhibitory effects on the settlement of the cyprids at concentrations that were in the same order of magnitude as observed for the naturally occurring compound. The likewise synthetic debromo-hemibastadin-1, which

lacked the bromine substitution of the naturally occurring hemibastadin-1, showed in comparison a less pronounced inhibitory effect, with a minimum dose needed for inhibition of larval settlement of 100 μM, indicating that bromine substitution of the aromatic rings enhances the antifouling activity, but is not an essential structural requirement. Further structure-activity studies pointed to the α-hydroxyimido moiety of hemibastadin type compounds as the prime pharmacophoric substructure. Synthetic hemibastadin derivatives, such as tyrosinyltyramide that lack the α-hydroxyimido moiety, showed no effect on cyprid settlement thus revealing this functionality to be essential for antifouling activity.

Similar structure-activity-relationships for hemibastadins were concluded in a study by Bayer *et al.* [93] who determined the inhibitory activity of various synthetic hemibastadin analogues towards the phenoloxidase of the blue mussel *Mytilus edulis*. This Cu^{2+}-depending enzyme is considered to play a crucial role in oxidative processes that crosslink phenolic residues in the mollusc foot proteins (Mefp), a key mechanism in the formation of bioglue in byssal threads [94]. The oxime in the α-position to the amide substituent in hemibastadin derivatives was shown to be the decisive structural element needed for the formation of a stable Cu^{2+}-complex, indicating that enzyme inhibition, which in turn prevents attachment of blue mussels to a given substrate, is probably caused by chelation of the bivalent metal ions in the active binding side of the phenoloxidase. The significance of an oxime-moiety with regard to antifouling properties of marine-derived natural products has also been demonstrated for other sponge-derived metabolites like diterpenoid alkaloids from *Agelas* species [95]. In summary, (hemi-)bastadins constitute interesting antifouling compounds of sponge origin that suppress settlement of cyprids, probably by targeting phenoloxidases that are involved in the formation of the adhesive proteins that guarantee a firm attachment of macrofouling organisms to a given substrate.

Mack *et al.* [96] showed that bastadin-5 and several other derivatives are selective modulators of the Ca^{2+}-release channel of the skeletal sarcoplasmic reticulum (SR) ryanodine receptor 1 (RyR-1). A full agonism and specificity for the skeletal isoform of RyR-1 was shown, while affinity for the cardiac receptor isoform was significantly lower. Furthermore bastadins-20, -15, 34-*O*-disulfatobastadin-7 and 10-*O*-sulfatobastadin-3 isolated from *Ianthella basta* showed moderate differential activity as SR Ca^{2+} channel agonists of the RyR-1 FKBP12 complex, with EC_{50} values of 20.6, 100 and 13.6 μM [97]. In a further study focusing on the effect of bastadins on Ca^{2+} homeostasis, Chen *et al.* [98] showed that naturally occurring bastadin-10 stabilizes primarily the open conformation of the RyR-1 channel and sensitizes the channel for activation by Ca^{2+} to an extent that it essentially eliminates regulation in the physiological range of this ion. In later structure-activity studies Zieminska *et al.* [99] demonstrated that bastadin-10 and several synthetic bastadins produce an effect identical to that observed for RyR-1 in primary cultures of rat cerebellar granule neurons expressing the RyR-2 (cardiac) subtype. Synthetic bastadin-5 released Ca^{2+} from the endoplasmatic reticulum (ER) of neurons in a ryanodine-sensitive way. It was further found that these effects are closely related to the excess of aromatic bromination of the bastadins, since a bisdebromo analogue of bastadin-10 (BAST218F6) completely lacked the ability to modulate intracellular Ca^{2+} levels. Further studies by Zieminska *et al.* [100] indicated that structurally simplified open-chain half bastadins, in particular compounds that carry a dibromocatechol ether moiety,, as found in bastadin-5 ("western part") (Figure3), are imitating the activity of naturally occurring bastadins on Ca^{2+} homeostasis in cultured rat cerebellar granule neurons.

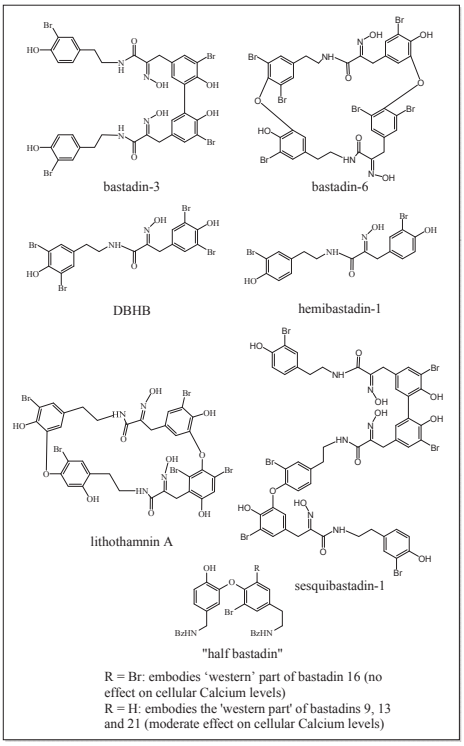

Figure 3: Examples of naturally occurring and synthetic bastadin derivatives.

Cytotoxic and antineoplastic properties of bastadins have been rather intensively investigated so far. The first report on the cytotoxic activity of bastadins was by Miao *et al.* [101], which described the cytotoxic potential of bastadins-8 and -9 against the L-1210 leukemia cell line with ED_{50} values of 4.9 μM. Carney *et al.* [102] discovered cytotoxicity for bastadin 14 against A-549 lung carcinoma, HT-29 colon adenocarcinoma human tumor, P-388 murine lymphotic leukemia cell lines, and against the non-tumor CV-1 monkey kidney cell line with IC_{50} values of 2 - 2.5 μM, as well as inhibition of topoisomerase-II and dehydrofolate reductase with IC_{50} values of 2 and 2.5 μM, respectively. Bastadins-4, -5,- 6, -7, -12, -13, -21 and -24 were found to possess mean IC_{50} values between 0.6 - 10.1 μM against 36 different human tumor cell lines [103]. For bastadin-24 the authors observed *in vitro* tumor cell selectivity towards CNXF SF268 (glioblastoma), LXFA 629L (lung adenocarcinoma), MAXF 401NL (mammary cancer), MEXF 276L (melanoma) and PRXF 22RV1 (prostate cancer) cells with IC_{50} values between 0.33 - 0.53 μM. Bastadin-4 isolated from *Ianthella reticulata* showed activity against the colon carcinoma cell line HCT-116 with an IC_{50} value of 1.28 μM [104]. The linear congener bastadin-3 showed inhibition of 24 different protein kinases, known to be involved in various mechanisms of tumor pathogenesis, with IC_{50} values ranging from 0.1 to 4.1 μM [90]. The trimeric sesquibastadin-1, when screened against the same panel of protein kinases, exhibited some specificity against EGF-R and VEGF-R2 kinases (inter alia) with submicromolar IC_{50} values ranging from 0.6 to 0.8 μM [90], indicating a potential to effect mechanisms related

to angionesis. Anti-angiogenic properties of bastadin-6 based on a specific induction of apoptosis in human umbilical vein endothelial cells (HUVEC) were reported by Aoki *et al.* [105]. Mechanistically, the authors hypothesized an interaction of bastadin-6 with RyR-3, which may result in a mobilization of intracellular Ca^{2+} and therefore trigger apoptosis. In a continuative study with synthetic analogues of bastadin-6 Kotoku *et al.* [106] pointed to the oxime function and to the bromination of the aromatic rings as key structural elements with regard to the anti-proliferative effects of bastadin derivatives against HUVECs and KB3-1 cells. Derivatives where the oxime was masked lacked activity suggesting this moiety to be essential for the formation of hydrogen bond(s) with its target protein and therefore for its anti-angiogenic activity. Changes in the bromination pattern resulted likewise in decreasing activity and/or specificity towards the investigated endothelial cell line. Recently, we have shown that the synthetic hemibastadin derivative DBHB exhibits both *in vitro* anti-angiogenic effects against HUVECs and anti-migratory effects in mouse B16F10 melanoma cells [107]. In *in vivo* experiments DBHB, however, failed to increase the survival of B16F10 melanoma-bearing mice, which we suspected to be due to strong binding of the compound to serum albumin. The aforementioned bastadin like lithothamnins, which show *meta-meta* linkages between the aromatic rings, that have so far not been reported from sponges, also showed moderate cytotoxic properties, as demonstrated for lithothamnin A [92]. This compound exhibited antiproliferative activities against five human tumor cell lines, LOX (IC_{50} = 9.5 µM), SNB-19 (IC_{50} = 7.6 µM), OVCAR-3 (IC_{50} = 7.6 µM), COLO-205 (IC_{50} = 19.0 µM), and MOLT-4 (IC_{50} = 19.0).

Discussion and outlook

This review highlights the ecological importance and pharmacological potential of selected bromotyrosine derivatives from marine sponges. All natural products presented here are assembled from bromotyrosine building blocks involving few enzymatically catalyzed reactions that give rise to a range of structural modifications. The resulting compounds, such as the psammaplins, the bastadins and the *Aplysina* alkaloids, have been shown to be involved in the chemical defense of sponges against predatory fish, fouling organisms or against pathogenic bacteria. Thus, these compounds are part of the remarkable ecological success of these sessile and potentially vulnerable marine invertebrates that has enabled marine sponges to thrive, even in the most stress prone marine habitats that are characterized by intense predation, such as coral reefs [108, 109]. As shown for psammaplin A and its sulfated precursor [43], as well as for the bromoisoxazoline alkaloids of *Aplysina* sponges that are converted to aeroplysinin-1 and a dienone [45, 58], the chemical defense of sponges may be highly dynamic involving a rapid and efficient enzymatically catalyzed conversion of either inactive or less active storage compounds into highly active defense metabolites. Whereas the former are constitutively present in sponge cells the latter are only formed when and where needed, usually at the site of wounding. As shown for the bioconversion cascade in *A. aerophoba* and *A. cavernicola*, this transformation of sponge alkaloids leads to the formation of toxic products that show a multitude of biological activities. Aeroplysinin-1 and the corresponding dienone are not only strong antibiotics that rival even the well-known standard antibiotic chloramphenicol (in fact the dienone had been proposed to be used in aquaculture due to its strong antibiotic activity towards economically important bacterial pathogens [44]), but both compounds also show pronounced cytotoxic effects in eukaryotic cells making them broad spectrum toxins. Whereas this non-selective activity towards prokaryotes and eukaryotes alike is a problem for drug development it represents a very effective defense strategy in an ecological perspective. Broad-spectrum defense metabolites like aeroplysinin-1 and the dienone that act against prokaryotes and eukaryotes alike can be expected to cope successfully with a diversity of aggressors/invaders whereas highly selective defense compounds would not. The same strategy can also be found in other organisms like in terrestrial plants where wounding of plant tissue leads to hydrolysis of cyanogenic glycosides and the formation of toxic HCN. HCN will not only poison invading herbivores or microbes, but will also kill plant tissue at the site of wounding [110]. This can also be expected for the *Aplysina* defense metabolites aeroplysinin-1 and dienone, even though direct toxic effects of these compounds on sponge cells have yet to be demonstrated. Since sponges like plants are able to regenerate tissue losses to a large extent this *kamikaze* attack on invaders can be compensated, whereas it would be detrimental to more highly evolved animals that lack this regenerative capacity.

Even though the bromotyrosine metabolites discussed in this review have all been described from sponges it is by no means clear whether sponges are in all cases also the true producers of these compounds. Sponges are filter feeders and are known to sequester natural products through the food chain, as shown for okadaic acid [111, 112]. On the other hand sponges are also hosts to a multitude of microorganisms that live within the tissues of their host organisms [4]. As recently summarized by our group, highly diverse microbial communities can produce cryptic metabolites that are not present in axenic cultures of microbes. These metabolites can arise during competition and under symbiotic conditions when invading or protecting a certain ecological habitat. It is feasible to assume, that these mechanisms which may lead to activation of usually silent gene clusters are not restricted to inter-microbial competition, but may extend also to interactions between higher organisms and microbes. A prominent example of the latter is the production and accumulation of tetrodotoxin in the pufferfish (*Fugu vermicularis radiatus*) [113] and a xanthid crab (*Atergatis floridus*) [114], as a biosynthetic product of the microbial symbiont *Vibrio* sp. This highly potent neurotoxin is not harmful to the host, but leads to certain death in potential predators, including man.

Regardless of the true biogenetic origin of the discussed bromotyrosines in sponges, the importance of several of these compounds not only for the chemical ecology of sponges but also for the applied side of natural product chemistry is obvious. As demonstrated for the bastadins the antifouling properties of these metabolites are assumed to protect the sponges from epibiontic overgrowth which would be detrimental for a filter feeding organism by obstructing the pores through which a constant flow of water into the sponge body is maintained. For the synthetically derived and structurally more simple hemibastadins like for DBHB the presumed antifouling target is a phenoloxidase. DBHB is believed to act through complexation of copper ions that are present in the catalytic center of the phenoloxidase. The pharmacophoric moiety of DBHB that is responsible for this enzyme inhibition is the alpha-oxime amido functionality that is present in all bastadin-like molecules, including DBHB. As soon as the oxime function is replaced by an amino group the anti-fouling activity and the phenoloxidase inhibition are completely lost, as shown for synthetic DBHB analogues. The bromine substituents of the aromatic rings enhance the antifouling activity (as well as the inhibition of the phenoloxidase), but are, in contrast to the alpha-oxime amido functionality, not essential structural requirements. However, bastadins do not only show antifouling activity but have also been demonstrated to possess antiangiogenic properties making them interesting for cancer chemotherapy. The antiangiogenic mode of action for bastadin-6 relies on modulation of cytoplasmatic Ca^{2+}-levels through interaction with the ryanodine receptor RyR-3,

resulting in a release of Ca^{2+} from the sarcoplasmatic reticulum, followed by induction of apoptotic processes in cancer cells. The alpha-oxime amido function and a specific aromatic bromination pattern were also, in this case, identified as essential structural features with regard to the antiangiogenic potential of the compounds. These structure activity requirements are very similar to those elucidated for the antifouling activity of DBHB. Since copper ions have been shown to be important for angiogenesis [115] an interaction of bastadins with copper, as shown for DBHB before, [93] is a hypothesis for the mode of the antiangiogenic activity of bastadin-6.

A further example of sponge-derived bromotyrosine derivatives is psammaplin A and its sulfated precursor. Psammaplin A not only shows antifouling activity but was also identified as an important regulator of cellular processes which act through inhibition of gene-regulating enzymes like HDAC and DNMT. The interaction with these transcription factors leads to epigenetic modifications as known for other epigenetic modifiers such as suberanilohydroxamic acid (SAHA), which, for example, is used in microbial cultures to activate silent biosynthetic gene clusters [116]. It is possible that psammaplin A is involved in regulating biosynthetic pathways of sponge symbionts, even though no studies have been conducted in this direction so far. However, epigenetic regulations can also cause cell death and may therefore contribute to an unspecific antimicrobial activity of a *bouquet* of sponge-derived compounds to which an invading microorganism is exposed. Histone deacetylases and DNA methyl transferases also represent relevant molecular targets for anticancer research. Due to its pronounced activity against the latter enzymes psammaplin A may also be a future drug lead for anti-cancer chemotherapy, especially since structural modification has been shown to increase considerably the activity of the derivatives compared with the parent compound. Baud *et al*. demonstrated that the affinity of synthetic psammaplin A derivatives towards HDAC 1 and HDAC 6 could be improved by a factor of 45 and 3.4, respectively [117]. Replacing the o-bromophenol moiety of psammaplysin A by a 5-bromoindol function improved not only the inhibitory activity of the derivative towards HDAC and DNMT but rendered the derivative also active with regard to inhibition of NAD^+-dependent SIRT deacetylase enzymes [31]. Further synthetic modification of psammaplin A via substitution with a 3-bromo-phenyl alanine and with a 4`-flourophenyl moiety even shifted the therapeutic application from cytotoxic to antibiotic activity. The therapeutic index, which describes the selectivity of the compound against prokaryotes, was found to shift, when tested against MRSA, from 0.56 for psammaplin A to 37.5 for the synthetic derivative [25].

The significant changes in activity profiles for various synthetic derivatives of psammaplin A, as discussed above, is a text book example that highlights the power of medicinal chemistry when acting on natural product scaffolds. The latter represent *privileged structures* [118] that have been shaped through evolution and hence already possess inherent biological activities. Bromotyrosine derived compounds as featured in this review are especially amenable to structural modifications either by nature or by synthetic chemistry due to their relatively simple structures that can be easily mimicked and further structurally expanded through synthetic approaches, as demonstrated for the various compounds discussed in this review.

References

[1] Gazave E, Lapébie P, Renard E, Vacelet J, Rocher C, Ereskovsky AV, Lavrov DV, Borchiellini C (**2010**) Molecular phylogeny restores the supra-generic subdivision of homoscleromorph sponges (Porifera, Homoscleromorpha). *PloS ONE, **5,*** e14290

[2] Taylor MW, Radax R, Steger D, Wagner M. (**2007**) Sponge-associated microorganisms: evolution, ecology, and biotechnological potential. *Microbiology and Molecular Biology Reviews*, ***71***, 295-347.

[3] Gutt J. (**2006**) Coexistence of macro-zoobenthic species on the Antarctic shelf: an attempt to link ecological theory and results. *Deep Sea Research Part II: Topical Studies in Oceanography*, ***53***, 1009-1028.

[4] Hausmann R, Vitello MP, Leitermann F, Syldatk C. (**2006**) Advances in the production of sponge biomass *Aplysina aerophoba*— A model sponge for ex situ sponge biomass production. *Journal of Biotechnology*, ***124***, 117-127.

[5] Webster NS, Taylor MW, Behnam F, Lücker S, Rattei T, Whalan S, Horn M, Wagner M. (**2010**) Deep sequencing reveals exceptional diversity and modes of transmission for bacterial sponge symbionts. *Environmental Microbiology*, ***12***, 2070-2082.

[6] Schmitt S, Angermeier H, Schiller R, Lindquist N, Hentschel U. (**2008**) Molecular microbial diversity survey of sponge reproductive stages and mechanistic insights into vertical transmission of microbial symbionts. *Applied and Environmental Microbiology*, ***74***, 7694-7708.

[7] Thomas TRA, Kavlekar DP, LokaBharathi PA. (**2010**) Marine drugs from sponge-microbe association—A review. *Marine Drugs*, ***8***, 1417-1468.

[8| Mayer AMS, Rodríguez AD, Taglialatela-Scafati O, Fusetani N. (**2013**) Marine pharmacology in 2009–2011: Marine compounds with antibacterial, antidiabetic, antifungal, anti-inflammatory, antiprotozoal, antituberculosis, and antiviral activities; Affecting the immune and nervous systems, and other miscellaneous mechanisms of action. *Marine Drugs*, ***11***, 2510-2573.

[9] Mayer AMS, Glaser KB, Cuevas C, Jacobs RS, Kem W, Little RD, McIntosh JM, Newman DJ, Potts BC, Shuster DE. (**2010**) The odyssey of marine pharmaceuticals: a current pipeline perspective. *Trends in Pharmacological Sciences*, ***31***, 255-265.

[10] Sagar S, Kaur M, Minneman KP. (**2010**) Antiviral lead compounds from marine sponges. *Marine Drugs*, ***8***, 2619-2638.

[11] Yasuhara-Bell J, Lu Y. (**2010**) Marine compounds and their antiviral activities. *Antiviral Research*, ***86***, 231-240.

[12] Teeyapant R, Kreis P, Wray V, Witte L, Proksch P. (**1993**) Brominated secondary compounds from the marine sponge *Verongia aerophoba* and the sponge feeding gastropod *Tylodina perversa*. *Zeitschrift für Naturforschung C. A journal of biosciences*, ***48***, 640-644.

[13] Faulkner DJ. (**2000**) Marine pharmacology. *Antonie van Leeuwenhoek*, *77*, 135-145.

[14] Roche J, Rand M, Yagi Y(**1951**) The presence of monobromotyrosine in gorgonins. *Comptes Rendus Chimie*, ***232***, 570-571.

[15] Kunze K, Niemann H, Ueberlein S, Schulze R, Ehrlich H, Brunner E, Proksch P, Pée K-Hv. (**2013**) Brominated skeletal components of the marine demosponges, *Aplysina cavernicola* and *Ianthella basta*: Analytical and biochemical investigations. *Marine Drugs*, ***11***, 1271-1287.

[16] Shin J, Lee HS, Seo Y, Rho JR, Cho KW, Paul VJ. (**2000**) New bromotyrosine metabolites from the sponge *Aplysinella rhax*. *Tetrahedron*, ***56***, 9071-9077.

[17] Bergquist PR, Wells RJ. (**1983**) Chemotaxonomy of the Porifera: the development and current status of the field. *Marine Natural Products: Chemical and Biological Perspectives*, ***5***, 1-50.

[18] Shinde PB, Lee YM, Dang HT, Hong J, Lee CO, Jung JH. (**2008**) Cytotoxic bromotyrosine derivatives from a two-sponge association of *Jaspis* sp. and *Poecillastra* sp. *Bioorganic & Medicinal Chemistry Letters*, ***18***, 6414-6418.

[19] Jiménez C, Crews P. (**1991**) Novel marine sponge derived amino acids 13. Additional psammaplin derivatives from *Psammaplysilla purpurea*. *Tetrahedron*, ***47***, 2097-2102.

[20] Piña IC, Gautschi JT, Wang GYS, Sanders ML, Schmitz FJ, France D, Cornell-Kennon S, Sambucetti LC, Remiszewski SW, Perez LB, Bair KW, Crews P. (**2003**) Psammaplins from the sponge *Pseudoceratina purpurea*: Inhibition of both histone deacetylase and DNA methyltransferase. *Journal of Organic Chemistry*, ***68***, 3866-3873.

Publication 1

[21] Jung JH, Sim CJ, Lee CO. (**1995**) Cytotoxic compounds from a two-sponge association. *Journal of Natural Products*, ***58***, 1722-1726.
[22] Quiñoà E, Crews P. (**1987**) Phenolic constituents of *Psammaplysilla*. *Tetrahedron Letters*, ***28***, 3229-3232.
[23] Kim D, Lee IS, Jung JH, Yang SI. (**1999**) Psammaplin A, a natural bromotyrosine derivative from a sponge, possesses the antibacterial activity against methicillin-resistant *Staphylococcus aureus* and the DNA gyrase-inhibitory activity. *Archives of Pharmacal Research*, ***22***, 25-29.
[24] Oh KB, Oh MN, Kim JG, Shin DS, Shin J. (**2006**) Inhibition of sortase-mediated *Staphylococcus aureus* adhesion to fibronectin via fibronectin-binding protein by sortase inhibitors. *Applied Microbiology and Biotechnology*, ***70***, 102-106.
[25] Nicolaou KC, Hughes R, Pfefferkorn JA, Barluenga S. (**2001**) Optimization and mechanistic studies of psammaplin A type antibacterial agents active against methicillin-resistant *Staphylococcus aureus* (MRSA). *Chemistry - A European Journal*, ***7***, 4296-4310.
[26] Leone-Stumpf D. (**2001**) Synthesis and chromatography of [RuCp]+-labelled diaryl ether peptoids as precursors of the bastadins from the marine sponge *Ianthella basta*. Combined Faculties for the Natural Sciences and for Mathematics, Ruperto-Carola University of Heidelberg, Germany, PhD thesis
[27] Tymiak AA, Rinehart Jr KL. (**1981**) Biosynthesis of dibromotyrosine-derived antimicrobial compounds by the marine sponge *Aplysina fistularis* (*Verongia aurea*). *Journal of the American Chemical Society*, ***103***, 6763-6765.
[28] Salam KA, Furuta A, Noda N, Tsuneda S, Sekiguchi Y, Yamashita A, Moriishi K, Nakakoshi M, Tsubuki M, Tani H, Tanaka J, Akimitsu N. (**2013**) Psammaplin A inhibits hepatitis C virus NS3 helicase. *Journal of Natural Medicines*, ***67***, 765-772.
[29] Tabudravu JN, Eijsink VGH, Gooday GW, Jaspars M, Komander D, Legg M, Synstad B, van Aalten DMF. (**2002**) Psammaplin A, a chitinase inhibitor isolated from the fijian marine sponge *Aplysinella rhax*. *Bioorganic & Medicinal Chemistry*, ***10***, 1123-1128.
[30] Ahn MY, Jung JH, Na YJ, Kim HS. (**2008**) A natural histone deacetylase inhibitor, psammaplin A, induces cell cycle arrest and apoptosis in human endometrial cancer cells. *Gynecologic Oncology*, ***108***, 27-33.
[31] Pereira R, Benedetti R, Pérez-Rodríguez S, Nebbioso A, García-Rodríguez J, Carafa V, Stuhldreier M, Conte M, Rodríguez-Barrios F, Stunnenberg HG, Gronemeyer H, Altucci L, de Lera ÁR. (**2012**) Indole-derived psammaplin A analogues as epigenetic modulators with multiple inhibitory activities. *Journal of Medicinal Chemistry*, ***55***, 9467-9491.
[32] García J, Franci G, Pereira R, Benedetti R, Nebbioso A, Rodríguez-Barrios F, Gronemeyer H, Altucci L, de Lera AR. (**2011**) Epigenetic profiling of the antitumor natural product psammaplin A and its analogues. *Bioorganic & Medicinal Chemistry*, ***19***, 3637-3649.
[33] Kim DH, Shin J, Kwon HJ. (**2007**) Psammaplin A is a natural prodrug that inhibits class I histone deacetylase. *Experimental and Molecular Medicine*, ***39***, 47-55.
[34] Baud MGJ, Leiser T, Haus P, Samlal S, Wong AC, Wood RJ, Petrucci V, Gunaratnam M, Hughes SM, Buluwela L, Turlais F, Neidle S, Meyer-Almes FJ, White AJP, Fuchter MJ. (**2012**) Defining the mechanism of action and enzymatic selectivity of psammaplin A against its epigenetic targets. *Journal of Medicinal Chemistry*, ***55***, 1731-1750.
[36] Kim HJ, Kim JH, Chie EK, Young PD, Kim IA. (**2012**) DNMT (DNA methyltransferase) inhibitors radiosensitize human cancer cells by suppressing DNA repair activity. *Radiation Oncology*, ***7***, 39.
[37] Mora FD, Jones DK, Desai PV, Patny A, Avery MA, Feller DR, Smillie T, Zhou YD, Nagle DG. (**2006**) Bioassay for the identification of natural product-based activators of peroxisome proliferator-activated receptor-γ (PPARγ): The marine sponge metabolite psammaplin A activates PPARγ and induces apoptosis in human breast tumor cells. *Journal of Natural Products*, ***69***, 547-552.
[38] Shim JS, Lee HS, Shin J, Kwon HJ. (**2004**) Psammaplin A, a marine natural product, inhibits aminopeptidase N and suppresses angiogenesis in vitro. *Cancer Letters*, ***203***, 163-169.
[39] Jiang Y, Ahn EY, Ryu SH, Kim DK, Park JS, Yoon HJ, You S, Lee BJ, Lee DS, Jung JH. (**2004**) Cytotoxicity of psammaplin A from a two-sponge association may correlate with the inhibition of DNA replication. *BMC Cancer*, ***4***, 70-77.
[40] Kim D, Lee IS, Jung JH, Lee CO, Choi SU. (**1999**) Psammaplin A, a natural phenolic compound, has inhibitory effect on human topoisomerase II and is cytotoxic to cancer cells. *Anticancer Research*, ***19***, 4085-4090.
[41] Urbaniak MD, Tabudravu JD, Msaki A, Matera KM, Brenk R, Jaspars M, Ferguson MAJ. (**2006**) Identification of novel inhibitors of UDP-Glc 4′-epimerase, a validated drug target for african sleeping sickness. *Bioorganic and Medicinal Chemistry Letters*, ***16***, 5744-5747.
[42] Thoms C, Schupp PJ. (**2008**) Activated chemical defense in marine sponges-a case study on *Aplysinella rhax*. *Journal of Chemical Ecology*, ***34***, 1242-1252.
[43] Ortlepp S, Sjögren M, Dahlström M, Weber H, Ebel R, Edrada R, Thoms C, Schupp P, Bohlin L, Proksch P. (**2007**) Antifouling activity of bromotyrosine-derived sponge metabolites and synthetic analogues. *Marine Biotechnology*, ***9***, 776-785.
[44] Ebel R, Brenzinger M, Kunze A, Gross HJ, Proksch P. (**1997**) Wound activation of protoxins in marine sponge *Aplysina aerophoba*. *Journal of Chemical Ecology*, ***23***, 1451-1462.
[45] Thoms C, Ebel R, Proksch P. (**2006**) Activated chemical defense in *Aplysina* sponges revisited. *Journal of Chemical Ecology*, ***32***, 97-123.
[46] Lipowicz B, Hanekop N, Schmitt L, Proksch P. (**2013**) An aeroplysinin-1 specific nitrile hydratase isolated from the marine sponge *Aplysina cavernicola*. *Marine Drugs*, ***11***, 3046-3067.
[47] Puyana M, Fenical W, Pawlik JR. (**2003**) Are there activated chemical defenses in sponges of the genus *Aplysina* from the Caribbean? *Marine Ecology Progress Series*, ***246***, 127-135.
[48] Fattorusso E, Minale L, Sodano G, Moody K, Thomson RH. (**1970**) Aerothionin, a tetrabromo-compound from *Aplysina aerophoba* and *Verongia thiona*. *Journal of the Chemical Society D: Chemical Communications*, ***12***, 752-753.
[49] Moody K, Thomson RH, Fattorusso E, Minale LT, Sodano G. (**1972**) Aerothionin and homoaerothionin: two tetrabromospirocyclohexadienyl-isoxazoles from *Verongia* sponges. *Journal of the Chemical Society, Perkin Transactions, **1***, 18-24.
[50] Cimino G, De Stefano S, Minale L. (**1975**) Occurrence of 4-hydroxyphenylpyruvic acid oxime in the marine sponge *Hymeniacidon sanguinea*. *Experientia*, ***31***, 756-757.
[51] Encarnacion-Dimayuga R, Ramirez MR, Luna-Herrera J. (**2003**) Aerothionin, a bromotyrosine derivative with antimycobacterial activity from the marine sponge *Aplysina gerardogreeni* (Demospongia). *Pharmaceutical Biology*, ***41***, 384-387.
[52] Fendert T, Wray V, Van Soest RW, Proksch P. (**1999**) Bromoisoxazoline alkaloids from the Caribbean sponge *Aplysina insularis*. *Zeitschrift für Naturforschung C*, ***54***, 246-252.
[53] Gochfeld DJ, Kamel HN, Olson JB, Thacker RW. (**2012**) Trade-offs in defensive metabolite production but not ecological function in healthy and diseased sponges. *Journal of Chemical Ecology*, ***38***, 451-462.
[54] Shaala LA, Bamane FH, Badr JM, Youssef DTA. (**2011**) Brominated arginine-derived alkaloids from the Red Sea sponge *Suberea mollis*. *Journal of Natural Products*, ***74***, 1517-1520.
[55] Nuñez CV, de Almeida EVR, Granato AC, Marques SO, Santos KO, Pereira FR, Macedo ML, Ferreira AG, Hajdu E, Pinheiro US, Muricy G, Peixinho S, Freeman CJ, Gleason DF, Berlinck RGS. (**2008**) Chemical variability within the marine sponge *Aplysina fulva*. *Biochemical Systematics and Ecology*, ***36***, 283-296.
[56] Carney JR, Rinehart KL. (**1995**) Biosynthesis of brominated tyrosine metabolites by *Aplysina fistularis*. *Journal of Natural Products*, ***58***, 971-985.

[57] Putz A, Kloeppel A, Pfannkuchen M, Brummer F, Proksch P. (**2009**) Depth-related alkaloid variation in Mediterranean *Aplysina* sponges. *Zeitschrift für Naturforschung C*, ***64***, 279-287.

[58] Thoms C, Wolff M, Padmakumar K, Ebel R, Proksch P. (**2004**) Chemical defense of Mediterranean sponges *Aplysina cavernicola* and *Aplysina aerophoba*. *Zeitschrift für Naturforschung C*, ***59***, 113-122.

[59] Thoms C, Ebel R, Hentschel U, Proksch P. (**2003**) Sequestration of dietary alkaloids by the spongivorous marine mollusc *Tylodina perversa*. *Zeitschrift für Naturforschung C*, ***58***, 426-432.

[60] Ebel R, Marin A, Proksch P. (**1999**) Organ-specific distribution of dietary alkaloids in the marine opisthobranch *Tylodina perversa*. *Biochemical Systematics and Ecology*, ***27***, 769-777.

[61] Abou-Shoer MI, Shaala LA, Youssef DTA, Badr JM, Habib AAM. (**2008**) Bioactive brominated metabolites from the Red Sea sponge *Suberea mollis*. *Journal of Natural Products*, ***71***, 1464-1467.

[62] Ankudey FJ, Kiprof P, Stromquist ER, Chang LC. (**2008**) New bioactive bromotyrosine-derived alkaloid from a marine sponge *Aplysinella* sp. *Planta Medica*, ***74***, 555-559.

[63] Fattorusso E, Minale L, Sodano G. (**1972**) Aeroplysinin-1, an antibacterial bromo-compound from the sponge *Verongia aerophoba*. *Journal of the Chemical Society, Perkin Transactions, **1***, 16-18.

[64] Chang CW, Weinheimer AJ. (**1977**) 2-Hydroxy, 3, 5-dibromo, 4-methoxyphenylacetamide. A dibromotyrosine metabolite from *Psammoposilla purpurea*. *Tetrahedron Letters*, ***18***, 4005-4007.

[65] Ciminiello P, Costantino V, Fattorusso E, Magno S, Mangoni A, Pansini M. (**1994**) Chemistry of Verongida sponges, II. Constituents of the Caribbean sponge *Aplysina fistularis* forma *fulva*. *Journal of Natural Products*, ***57***, 705-712.

[66] Ciminiello P, Fattorusso E, Magno S, Pansini M. (**1995**) Chemistry of Verongida sponges, IV. Comparison of the secondary metabolite composition of several specimens of *Pseudoceratina crassa*. *Journal of Natural Products*, ***58***, 689-696.

[67] Teeyapant R, Proksch P. (**1993**) Biotransformation of brominated compounds in the marine sponge *Verongia aerophoba*—Evidence for an induced chemical defense? *Naturwissenschaften*, ***80***, 369-370.

[68] Ciminiello P, Fattorusso E, Forino M, Magno S, Pansini M. (**1997**) Chemistry of verongida sponges VIII[1]-bromocompounds from the mediterranean sponges *Aplysina aerophoba* and *Aplysina cavernicola*. *Tetrahedron*, ***53***, 6565-6572.

[69] Ciminiello P, Dell'Aversano C, Fattorusso E, Magno S, Pansini M. (**1999**) Chemistry of Verongida sponges. 9.1 Secondary metabolite composition of the Caribbean sponge *Aplysina cauliformis*. *Journal of Natural Products*, ***62***, 590-593.

[70] Ciminiello P, Dell'Aversano C, Fattorusso E, Magno S, Pansini M. (**2000**) Chemistry of Verongida sponges. 10.1 Secondary metabolite composition of the Caribbean sponge *Verongula gigantea*. *Journal of Natural Products*, ***63***, 263-266.

[71] Saeki BM, Granato AC, Berlinck RGS, Magalhães A, Schefer AB, Ferreira AG, Pinheiro US, Hajdu E. (**2003**) Two unprecedented dibromotyrosine- derived alkaloids from the Brazilian endemic marine sponge *Aplysina caissara*. *Journal of Natural Products*, ***65***, 796-799.

[72] Makarieva TN, Stonik VA, Alcolado P, Elyakov YB. (**1981**) Comparative study of the halogenated tyrosine derivatives from Demospongiae (Porifera). *Comparative Biochemistry and Physiology Part B: Comparative Biochemistry*, ***68***, 481-484.

[73] Kreuter MH, Robitzki A, Chang S, Steffen R, Michaelis M, Kljajić Z, Bachmann M, Schröder HC, Müller WE. (**1992**) Production of the cytostatic agent aeroplysinin by the sponge *Verongia aerophoba* in *in vitro* culture. *Comparative Biochemistry and Physiology Part C: Comparative Pharmacology*, ***101***, 183-187.

[74] Weiss B, Ebel R, Elbrächter M, Kirchner M, Proksch P. (**1996**) Defense metabolites from the marine sponge *Verongia aerophoba*. *Biochemical Systematics and Ecology*, ***24***, 1-12.

[75] Gutiérrez M, Capson TL, Guzmán HM, González J, Ortega-Barría E, Quiñoá E, Riguera R. (**2005**) Antiprotozoal activity against *Plasmodium falciparum* and *Trypanosoma cruzi* of aeroplysinin-1 isolated from the new sponge *Aplysina chiriquensis*. *Pharmaceutical Biology*, ***43***, 762-765.

[76] Galeano E, Thomas OP, Robledo S, Munoz D, Martinez A. (**2011**) Antiparasitic bromotyrosine derivatives from the marine sponge *Verongula rigida*. *Marine Drugs*, ***9***, 1902-1913.

[77] Koulman A, Proksch P, Ebel R, Beekman AC, van Uden W, Konings AW, Pedersen JA, Pras N, Woerdenbag HJ. (**1996**) Cytoxicity and mode of action of aeroplysinin-1 and a related dienone from the sponge *Aplysina aerophoba*. *Journal of Natural Products*, ***59***, 591-594.

[78] Rodríguez-Nieto S, González-Iriarte M, Carmona R, Muñoz-Chápuli R, Medina MA, Quesada AR. (**2002**) Antiangiogenic activity of aeroplysinin-1, a brominated compound isolated from a marine sponge. *The FASEB Journal*, ***16***, 261-263.

[79] Martínez-Poveda B, Rodríguez-Nieto S, García-Caballero M, Medina MÁ, Quesada AR. (**2012**) The antiangiogenic compound aeroplysinin-1 induces apoptosis in endothelial cells by activating the mitochondrial pathway. *Marine Drugs*, ***10***, 2033-2046.

[80] Córdoba R, Tormo NS, Medarde AF, Plumet J. (**2007**) Antiangiogenic versus cytotoxic activity in analogues of aeroplysinin-1. *Bioorganic & Medicinal Chemistry*, ***15***, 5300-5315.

[81] González-Iriarte M, Carmona R, Pérez-Pomares JM, Macías D, Medina MÁ, Quesada AR, Muñoz-Chápuli R. (**2003**) A modified chorioallantoic membrane assay allows for specific detection of endothelial apoptosis induced by antiangiogenic substances. *Angiogenesis*, ***6***, 251-254.

[82] Martínez-Poveda B, García-Vilas JA, Cardenas C, Melgarejo E, Quesada AR, Medina MA. (**2013**) The brominated compound aeroplysinin-1 inhibits proliferation and the expression of key pro-inflammatory molecules in human endothelial and monocyte cells. *PloS one*, ***8***, e55203.

[83] Kreuter MH, Leake RE, Rinaldi F, Müller-Klieser W, Maidhof A, Müller WE, Schröder HC. (**1990**) Inhibition of intrinsic protein tyrosine kinase activity of EGF-receptor kinase complex from human breast cancer cells by the marine sponge metabolite (+)-aeroplysinin-1. *Comparative Biochemistry and Physiology Part B: Comparative Biochemistry*, ***97***, 151-158.

[84] D'Ambrosio M, Guerriero A, Pietra F. (**1984**) Novel, racemic or nearly-racemic antibacterial bromo-and chloroquinols and γ-lactams of the verongiaquinol and the cavernicolin type from the marine sponge *Aplysina* (= Verongia) *cavernicola*. *Helvetica chimica acta*, ***67***, 1484-1492.

[85] Sharma GM, Burkholder PR. (**1967**) Studies on antimicrobial substances of sponges. I. Isolation, purification, and properties of a new bromine-containing antibacterial substance. *The Journal of Antibiotics*, ***20***, 200-203.

[86] Andersen RJ, Faulkner DJ. (**1973**) A novel antibiotic from a sponge of the genus *Verongia*. *Tetrahedron Letters*, ***14***, 1175-1178.

[87] Sallam AA, Ramasahayam S, Meyer SA, Sayed KAE. (**2010**) Design, synthesis, and biological evaluation of dibromotyrosine analogues inspired by marine natural products as inhibitors of human prostate cancer proliferation, invasion, and migration. *Bioorganic & Medicinal Chemistry*, ***18***, 7446-7457.

[88] Gorshkov BA, Shestak OP, Gorshkova IA, Makar'eva TN, Novikov VL, Stonik VA. (**1992**) Synthesis of verongiaquinol and related compounds and study of their inhibiting action on rat brain Na^+, K^+-ATPase. *Chemistry of Natural Compounds*, ***28***, 128-129.

[89] Carroll AR, Kaiser SM, Davis RA, Moni RW, Hooper JN, Quinn RJ. (**2010**) A bastadin with potent and selective δ-opioid receptor binding affinity from the Australian sponge *Ianthella flabelliformis*. *Journal of Natural Products*, ***73***, 1173-1176.

[90] Niemann H, Lin W, Müller WE, Kubbutat M, Lai D, Proksch P. (**2012**) Trimeric hemibastadin congener from the marine sponge *Ianthella basta*. *Journal of Natural Products*, ***76***, 121-125.

[91] Brunner E, Ehrlich H, Schupp P, Hedrich R, Hunoldt S, Kammer M, Machill S, Paasch S, Bazhenov VV, Kurek DV, Arnold T, Brockmann S, Ruhnow M, Born R (**2009**) Chitin-based scaffolds are an integral part of the skeleton of the marine demosponge *Ianthella basta*. *Journal of Structural Biology*, ***168***, 539-547.

[92] Van Wyk AW, Zuck KM, McKee TC. (**2011**) Lithothamnin A, the first bastadin-like metabolite from the red alga *Lithothamnion fragilissimum*. *Journal of Natural Products*, ***74***, 1275-1280.

[93] Bayer M, Hellio C, Maréchal JP, Frank W, Lin W, Weber H, Proksch P. (**2011**) Antifouling bastadin congeners target mussel phenoloxidase and complex copper (II) ions. *Marine Biotechnology*, ***13***, 1148-1158.

[94] Hellio C, Bourgougnon N, Gal YL. (**2000**) Phenoloxidase (EC 1.14. 18.1) from the byssus gland of *Mytilus edulis*: purification, partial characterization and application for screening products with potential antifouling activities. *Biofouling*, ***16***, 235-244.

[95] Hertiani T, Edrada-Ebel R, Ortlepp S, van Soest RW, de Voogd NJ, Wray V, Hentschel U, Kozytska S, Müller WE, Proksch P. (**2010**) From anti-fouling to biofilm inhibition: New cytotoxic secondary metabolites from two Indonesian *Agelas* sponges. *Bioorganic & Medicinal Chemistry*, ***18***, 1297-1311.

[96] Mack MM, Molinski TF, Buck ED, Pessah IN. (**1994**) Novel modulators of skeletal muscle FKBP12/calcium channel complex from *Ianthella basta*. Role of FKBP12 in channel gating. *Journal of Biological Chemistry*, ***269***, 23236-23249.

[97] Franklin MA, Penn SG, Lebrilla CB, Lam TH, Pessah IN, Molinski TF. (**1996**) Bastadin 20 and bastadin *O*-sulfate esters from *Ianthella basta*: novel modulators of the Ry1R FKBP12 receptor complex. *Journal of Natural Products*, ***59***, 1121-1127.

[98] Chen L, Molinski TF, Pessah IN. (**1999**) Bastadin 10 stabilizes the open conformation of the ryanodine-sensitive Ca^{2+} channel in an FKBP12-dependent manner. *Journal of Biological Chemistry*, ***274***, 32603-32612.

[99] Zieminska E, Stafiej A, Pitsinos EN, Couladouros EA, Moutsos V, Kozlowska H, Toczylowska B, Lazarewicz JW. (**2007**) Synthetic bastadins modify the activity of ryanodine receptors in cultured cerebellar granule cells. *Neurosignals*, ***15***, 283-292.

[100] Zieminska E, Lazarewicz JW, Couladouros EA, Moutsos VI, Pitsinos EN. (**2008**) Open-chain half-bastadins mimic the effects of cyclic bastadins on calcium homeostasis in cultured neurons. *Bioorganic & Medicinal Chemistry Letters*, ***18***, 5734-5737.

[101] Miao S, Andersen RJ, Allen TM. (**1990**) Cytotoxic metabolites from the sponge *Lanthella basta* collected in Papua New Guinea. *Journal of Natural Products*, ***53***, 1441-1446.

[102] Carney JR, Scheuer PJ, Kelly-Borges M. (**1993**) A new bastadin from the sponge *Psammaplysilla purpurea*. *Journal of Natural Products*, ***56***, 153-157.

[103] Greve H, Kehraus S, Krick A, Kelter G, Maier A, Fiebig HH, Wright AD, Kõnig GM. (**2008**) Cytotoxic bastadin 24 from the Australian sponge *Ianthella quadrangulata*□. *Journal of Natural Products*, ***71***, 309-312.

[104] Calcul L, Inman WD, Morris AA, Tenney K, Ratnam J, McKerrow JH, Valeriote FA, Crews P. (**2010**) Additional insights on the bastadins: Isolation of analogues from the sponge *Ianthella* cf. *reticulata* and exploration of the oxime configurations. *Journal of Natural Products*, ***73***, 365-372.

[105] [105] Aoki S, Cho SH, Ono M, Kuwano T, Nakao S, Kuwano M, Nakagawa S, Gao JQ, Mayumi T, Shibuya M., Kobayashi M. (**2006**) Bastadin 6, a spongean brominated tyrosine derivative, inhibits tumor angiogenesis by inducing selective apoptosis to endothelial cells. *Anti-Cancer Drugs*, ***17***, 269-278.

[106] Kotoku N, Hiramatsu A, Tsujita H, Hirakawa Y, Sanagawa M, Aoki S, Kobayashi M. (**2008**) Structure-activity relationships study of bastadin 6, an anti-angiogenic brominated-tyrosine derived metabolite from marine sponge. *Archiv der Pharmazie*, ***341***, 568-577.

[107] Mathieu V, Wauthoz N, Lefranc F, Niemann H, Amighi K, Kiss R, Proksch P. (**2013**) Cyclic versus hemi-bastadins. Pleiotropic anti-cancer effects: from apoptosis to anti-angiogenic and anti-migratory effects. *Molecules*, ***18***, 3543-3561.

[108] Proksch P. (**1999**) Chemical defence in marine ecosystems. *Annual Plant Reviews*, ***3***, 134-154.

[109] Aerts LAM, Van Soest RWM. (**1997**) Quantification of sponge/coral interactions in a physically stressed reef community, NE Colombia. *Marine ecology progress series. Oldendorf*, ***148***, 125-134.

[110] Osbourn AE. (**1996**) Preformed antimicrobial compounds and plant defense against fungal attack. *The Plant Cell*, ***8***, 1821.

[111] Dickey RW, Bobzin SC, Faulkner DJ, Bencsath FA, Andrzejewski D. (**1990**) Identification of okadaic acid from a Caribbean dinoflagellate, *Prorocentrum concavum*. *Toxicon*, ***28***, 371-377.

[112] Bialojan C, Takai A. (**1988**) Inhibitory effect of a marine-sponge toxin, okadaic acid, on protein phosphatases. Specificity and kinetics. *Biochemical Journal*, ***256***, 283-290.

[113] Lee MJ, Jeong DY, Kim WS, Kim HD, Kim CH, Park WW, Park YH, Kim KS, Kim HM, Kim DS. (**2000**) A tetrodotoxin-producing *Vibrio* strain, LM-1, from the puffer fish *Fugu vermicularis radiatus*. *Applied and Environmental Microbiology*, ***66***, 1698-1701.

[114] Noguchi T, Jeon JK, Arakawa O, Sugita H, Deguchi Y, Shida Y, Hashimoto K. (**1986**) Occurrence of tetrodotoxin and anhydrotetrodotoxin in *Vibrio* sp. isolated from the intestines of a xanthid crab, *Atergatis floridus*. *Journal of Biochemistry*, ***99***, 311-314.

[115] Finney L, Vogt S, Fukai T, Glesne D. (**2009**) Copper and angiogenesis: unravelling a relationship key to cancer progression. *Clinical and Experimental Pharmacology and Physiology*, ***36***, 88-94.

[116] Nützmann HW, Reyes-Dominguez Y, Scherlach K, Schroeckh V, Horn F, Gacek A, Schümann J, Hertweck C, Strauss J, Brakhage AA. (**2011**) Bacteria-induced natural product formation in the fungus Aspergillus nidulans requires Saga/Ada-mediated histone acetylation. *Proceedings of the National Academy of Sciences*, ***108***, 14282-14287.

[117] Baud MGJ, Leiser T, Meyer-Almes FJ, Fuchter M. (**2011**) New synthetic strategies towards psammaplin A, access to natural product analogues for biological evaluation. *Organic & Biomolecular Chemistry*, ***9***, 659-662.

[118] Evans BE, Rittle KE, Bock MG, DiPardo RM, Freidinger RM, Whitter WL, Lundell GF, Veber DF, Anderson PS. (**1988**) Methods for drug discovery: development of potent, selective, orally effective cholecystokinin antagonists. *Journal of Medicinal Chemistry*, ***31***, 2235-2246.

5 Publication 2

5.1 Timeric Hemibastadin Congener from the Marine Sponge *Ianthella basta*

Published in: „Journal of Natural Products“

Impact factor: 3.947

Contribution: 80 %, first author, conducting most of the experiments, manuscript writing

JOURNAL OF NATURAL PRODUCTS

Note

pubs.acs.org/jnp

Trimeric Hemibastadin Congener from the Marine Sponge *Ianthella basta*

Hendrik Niemann,[†] Wenhan Lin,[‡] Werner E. G. Müller,[§] Michael Kubbutat,[⊥] Daowan Lai,*[,†] and Peter Proksch*[,†]

[†]Institute of Pharmaceutical Biology and Biotechnology, Heinrich-Heine University, Universitätsstrasse 1, 40225 Düsseldorf, Germany

[‡]State Key Laboratory of Natural and Biomimetic Drugs, Peking University, Beijing 100191, People's Republic of China

[§]Institute of Physiological Chemistry and Pathobiochemistry, Johannes-Gutenberg-University, Duesbergweg 6, 55128 Mainz, Germany

[⊥]ProQinase GmbH, Breisacher Strasse 117, 79106 Freiburg, Germany

Supporting Information

ABSTRACT: The first naturally occurring trimeric hemibastadin congener, sesquibastadin 1 (**1**), and the previously reported bastadins 3, 6, 7, 11, and 16 (**2**–**6**) were isolated from the marine sponge *Ianthella basta*, collected in Indonesia. The structure of **1** was elucidated on the basis of 1D and 2D NMR measurements and by HRMS. Among all the isolated compounds, the linear sesquibastadin 1 (**1**) and bastadin 3 (**2**) showed the strongest inhibition rates for at least 22 protein kinases (IC_{50} = 0.1–6.5 μM), while the macrocyclic bastadins (**3**–**6**) demonstrated a strong cytotoxic potential against the murine lymphoma cell line L5178Y (IC_{50} = 1.5–5.3 μM).

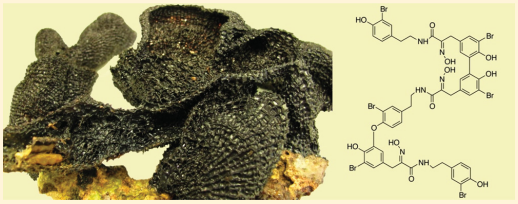

Since their first discovery more than 30 years ago from marine sponges of the order Verongida, bastadin derivatives have attracted wide attention due to their pronounced biological activities. Bastadins are known for their antifouling,[1] antimicrobial,[2,3] and anti-inflammatory[4] activities. They furthermore modulate Ca^{2+}-release from the sarcoplasmic reticulum[5−7] and may show δ-opioid receptor binding affinity.[8] In addition, antineoplastic activities have been reported for bastadins that may be modulated by inhibition of topoisomerase-II,[9] DHFR,[9] or IMP dehydrogenase[10] or by antiangiogenic effects.[11,12] Thus, this group of marine natural products is of considerable interest, both as molecular tools and for bioprospecting. Structurally, bastadins consist of brominated tyrosine and tyramine derivatives that are linked by a peptide bond, forming a hemibastadin unit, which is the putative biogenetic precursor to the bastadins. Formation of the bastadins requires two hemibastadin moieties that are linked via an ether bridge or by carbon−carbon bonds. The amino group of the bromotyrosine units is typically oxidized to yield an oxime function. So far there are 26 naturally occurring bastadin derivatives from sponges.[8] The recently discovered lithothamnin A indicates that similar metabolites differing from the bastadins only in the aromatic substitution pattern can also be found in red algae.[13]

We now have isolated the first trimeric hemibastadin derivative, which was named sesquibastadin 1 (**1**) (Figure 1), from a specimen of the marine sponge *Ianthella basta* and report on the structure elucidation of the new compound. In addition, five known derivatives, bastadins 3 (**2**),[2] 6 (**3**),[2] 7 (**4**),[2] 11 (**5**),[4] and 16 (**6**),[14] were likewise obtained. All compounds were investigated for their cytotoxicity in a cellular assay using the murine lymphoma cell line L5178Y and in a biochemical assay involving 24 different protein kinases that represent potential targets for anticancer chemotherapy.

Positive HRESIMS of **1** indicated pseudomolecular ion clusters centered at m/z 1412.81374 $[M + H]^+$. Isotope-induced signal splitting revealed six bromines within the molecule. When measured at low-resolution ESIMS conditions, two prominent fragments of **1** could be detected at m/z 421 (dibromo cluster) and m/z 682 (tribromo cluster) (Figure S9). The same fragment ions could also be observed for bastadin 3 (**2**), indicating that **1** is partially composed of **2**. Moreover, the molecular weight and isotopic pattern suggested hemibastadin 2 as the other building unit of **1**.

This assumption was confirmed by inspection of the 1D and 2D NMR spectra of **1** (Table 1). Downfield resonances at δ_H 11.84, 11.82, and 11.79, as well as three triplets of amide protons at δ_H 8.03, 7.94, and 7.93, as observed in the ^{1}H NMR spectrum, indicated the presence of three 2-oxime amide moieties within the molecule. In addition, the total number of 15 aromatic and 18 aliphatic protons indicated the presence of a trimeric hemibastadin. Inspection of ^{1}H NMR and COSY spectra suggested three 1,2,4-trisubstituted and three unsymmetrical

Received: October 31, 2012
Published: December 18, 2012

dx.doi.org/10.1021/np300764u | *J. Nat. Prod.* 2013, 76, 121−125

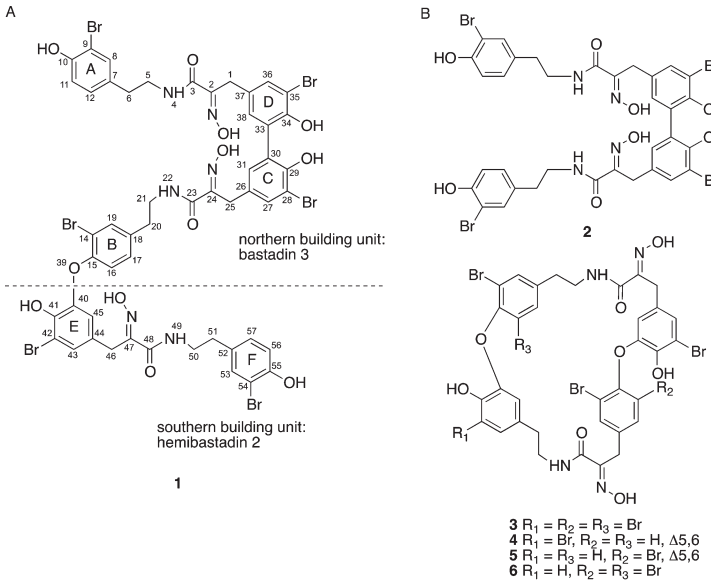

Figure 1. (A) Sesquibastadin 1 (**1**) and its putative biogenetic building units; (B) known bastadins 3, 6, 7, 11, and 16 (**2**–**6**).

1,2,3,5-tetrasubstituted phenyl rings and three ethylamido and three isolated benzylic methylene functionalities. Two of the 1,2,4-trisubstituted phenyl ring systems (rings A and F) showed overlapping signals, especially the entirely overlapped doublet at δ_H 6.84 (H-11, H-56), indicating a high rate of similarity for these two ring systems within the molecule. The positions of rings A and F were assigned at the northern and southern ends of the linear molecule, respectively, to form a "quasi symmetry". All three ABX systems were found to be attached to ethylamido moieties on the basis of long-range couplings observed in the COSY spectrum between H_2-6 (δ_H 2.63), H-12 (δ_H 6.97), and H-8 (δ_H 7.29) (ring A), H_2-51 (δ_H 2.60), H-53 (δ_H 7.27), and H-57 (δ_H 6.95) (ring F), and H_2-20 (δ_H 2.73), H-19 (δ_H 7.53), and H-17 (δ_H 7.14) (ring B). Similarly, the attachment of the three isolated methylene chains to three meta-coupling aromatic spin systems was established on the basis of long-range couplings observed in the COSY spectrum, including correlations between H_2-1 (δ_H 3.73), H-36 (δ_H 7.33), and H-38 (δ_H 6.94) (ring D), H_2-25 (δ_H 3.72), H-27 (δ_H 7.32), and H-31 (δ_H 6.93) (ring C), and H_2-46 (δ_H 3.63), H-45 (δ_H 6.61), and H-43 (δ_H 7.11) (ring E). HMBC correlations confirmed the composition of the six aliphatic chains, the aromatic systems, and their mutual connections (Figure 2). Strong three-bond correlations could be observed between the methylene protons and the ortho carbons in each neighboring benzene ring, as shown in Table 1. Key correlations were found between δ_H 6.93 (H-31) and 6.94 (H-38) and δ_C 127.6 (C-30, and C-33), which confirmed the C-30–C-33 direct linkage between the two meta-coupling aromatic spin systems (rings C and D). As mentioned above, the two northern hemibastadin subunits of **1** form the known symmetric structure of **2**, which was confirmed by comparison of ^{1}H and ^{13}C NMR data. The addition of a further hemibastadin subunit during the biosynthesis of **1** caused a loss in symmetry and therefore induced extra ^{1}H and ^{13}C resonances appearing only with a small difference in chemical shifts compared to the corresponding resonances found for **2** (Table 1). In particular, the NMR data for rings A, C, and D of **1** are almost identical to those of bastadin 3 (**2**),[2] which corroborated that **1** is partially composed of **2**. Further confirmation for the constitution of the aliphatic side chains and their attachment to the neighboring benzene rings was found in a ROESY spectrum. Especially the correlations found for the amide protons (H-4, H-22, H-49) to their neighboring ethyl (H_2-5, H_2-6; H_2-20, H_2-21; H_2-50, H_2-51) but also to the isolated methylene functionalities (H_2-1, H_2-25, H_2-46) confirmed all previously made conclusions about the arrangement of the aliphatic chains. The chemical shifts of C-40 (δ_C 144.5) and C-41 (δ_C 144.0) were indicative of two vicinal oxygen substituents, while the chemical shift of C-42 (δ_C 110.9) and the chemical shifts of CH-43 (δ_C 127.9, δ_H 7.11) were consistent with a bromine substituted at C-42 in ring E.[16] Moreover, the molecular weight suggested that the southern hemibastin unit was connected to the northern "bastadin 3" unit through an ether bond. The possibility of an ether linkage between C-15 (ring B) and C-41 (ring E) was ruled out from a biogenetic point of view, since such aryl–ether linkage has never been found in bastadins[8,16] and their similar derivatives[13] so far. Key ROESY correlations observed between δ_H 6.74 (H-16) and δ_H 6.61 (H-45) provided evidence for an ether linkage between C-15 (ring B) and C-40 (ring E). The geometries of all three oxime functionalities were deduced on the basis of the ^{13}C NMR chemical shifts. Because the α benzylic carbons resonated at δ_C 27.7 (C-1, C-25) and δ_C 27.8 (C-46), the adjacent oxime groups must have the *E* geometry.[15] The possibility of a genuine *Z* geometry and subsequent isomeration to *E* geometry during extraction and storage, as shown recently for bastadin 19,[16] was not investigated in this study. However, the fact that sesquibastadin 1 (**1**) was already observed during HPLC analysis of the initial extract from *I. basta* argues against this possibility, as isomerization of the oxime group can be expected to affect the retention time, which was unchanged for **1**.

dx.doi.org/10.1021/np300764u | *J. Nat. Prod.* 2013, 76, 121–125

Table 1. NMR Spectroscopic Data and HMBC and ROESY Correlations for Sesquibastadin 1 (1) in DMSO-d_6[a]

position	δ_C	δ_H (J in Hz)	ROESY	HMBC[b]
1	27.7, CH_2	3.73, s[c]	H4, H36, H38	2, 3, 36, 37, 38
2	151.51, C[d]			
2═N-OH		11.82, s[e]		2
3	163.0, C[f]			
4		7.94, t (6.0)[g]	H1, H5, H6	3, 5
5	40.4, CH_2	3.30, q-like[h]		3, 6, 7
6	33.6, CH_2[i]	2.63, t (7.6)[j]	H4, H5, H8, H12	5, 8, 12
7	131.4, C			
8	132.6, CH	7.29, d (2.0)[k]	H6	6, 9, 10, 12
9	109.0, C			
10	152.3, C			
10-OH		9.99, s[l]		9, 10, 11
11	116.2, CH	6.84, d (8.2)	H12	7, 9, 10, 12
12	128.8, CH	6.97, dd (2.0, 8.2)[m]	H6, H11	6, 8, 10
14	112.8, C			
15	151.2, C			
16	118.94, CH	6.74, d (8.3)	H17, H45	14, 15, 18
17	129.3, CH	7.14, dd (2.0, 8.3)	H16, H20	15, 19, 20
18	136.5, C			
19	133.3, CH	7.53, d, (2.0)	H20	14, 15, 17, 20
20	33.8, CH_2	2.73, t (7.4)	H17, H19, H21, H22	17, 18, 19, 21
21	40.1, CH_2	3.36[n]		18, 20, 23
22		8.03, t (5.9)	H20, H21, H25	21, 23
23	162.9, C[f]			
24	151.48, C[d]			
24═N-OH		11.79, s[e]		24
25	27.7, CH_2	3.72, s[c]	H22, H27, H31	23, 24, 26, 27, 31
26	129.2, C			
27	132.1, CH	7.32, d, (2.0)[o]	H25	25, 28, 29, 31
28	111.2, C			
29	149.6, C			
30	127.6, C			
31	131.1, CH	6.93, d, (2.0)[p]	H25	25, 27, 29, 30, 33
33	127.6, C			
34	149.6, C			
35	111.2, C			
36	132.1, CH	7.33, d, (2.1)[o]	H1	1, 34, 35, 38
37	129.2, C			
38	131.1, CH	6.94, d (2.1)[p]	H1	1, 30, 33, 34, 36
40	144.5, C			
41	144.0, C			
42	110.9, C			
43	127.9, CH	7.11, d (2.0)	H46	41, 42, 44, 45, 46
44	128.9, C			
45	118.87, CH	6.61, d (2.0)	H16, H46	40, 41, 43, 46
46	27.8, CH_2	3.63, s	H43, H45, H49	43, 44, 45, 47, 48
47	151.7, C[d]			
47═N-OH		11.84, s[e]		47
48	163.1, C[f]			
49		7.93, t (6.0)[g]	H46, H50, H51	48, 50
50	40.4, CH_2	3.26, q-like[h]	H49, H51	48, 51, 52
51	33.5, CH_2[i]	2.60, t (7.6)[j]	H49, H50, H53, H57	49, 53, 57
52	131.4, C			
53	132.6, CH	7.27, d (2.0)[k]	H51	51, 54, 55, 57
54	109.0, C			
55	152.3, C			
55-OH		9.99, s		54, 55, 56
56	116.2, CH_2	6.84, d (8.2)	H57	52, 54, 55, 57
57	128.8, CH_2	6.95, dd, (2.0, 8.2)[m]	H51, H56	51, 53, 55

[a]Measured in 600 MHz (^{1}H), and 150 MHz (^{13}C); chemical shifts were referenced to the solvent peak (δ_H 2.50 for ^{1}H, δ_C 39.5 for ^{13}C). [b]HMBC correlations are from proton(s) stated to the indicated carbon. [c−k,m,o,p]Assignments may be interchanged within the same column. [l]Chemical shifts for the other phenolic OH: δ_H 8.87 (2H, br s, 29-OH, and 34-OH), 9.81 (1H, br s, 41-OH) [n]Signal overlapped with the water peak.

Inhibition of protein kinases by **1**−**6** was determined using a panel of 24 different enzymes (Table 2). Sesquibastadin 1 (**1**) and bastadin 3 (**2**), both linear bastadin congeners, were most active and showed comparable activity profiles against at least 22 protein kinases, with IC_{50} values ranging from 0.1 to 6.5 μM. Sesquibastadin 1 (**1**) caused potent inhibition of the receptor tyrosine kinases EGF-R (IC_{50} = 0.6 μM) and VEGF-R2 (IC_{50} = 0.6 μM), both being overexpressed in non-small-cell lung cancer cells, and of TIE2 (IC_{50} = 0.6 μM). Inhibition of Aurora A and B, both being serine/threonine kinases that are important for the cell cycle and overregulated in breast cancer cells, was most pronounced for **2**, with IC_{50} values of 0.1 μM against Aurora A and 0.5 μM against Aurora B. Similar inhibition was shown for **2** against TIE2 (IC_{50} = 0.8 μM). Overall, **2** indicated the widest activity spectrum by inhibiting all studied protein kinases at (sub)micromolar concentrations. On the other hand, the macrocyclic bastadins 6 (**3**), 7 (**4**), 11 (**5**), and 16 (**6**) were considerably less active or even inactive when studied in the biochemical assay. This was especially pronounced for **5** and **6**. Additionally, **1**−**6** were evaluated for their cytotoxic potential against mouse lymphoma cells (L5178Y). Here, bastadins 6, 7, 11, and 16 (**3**−**6**) inhibited cell proliferation, with IC_{50} values (μM) of 1.5, 5.3, 3.7, and 1.9, respectively, while compounds **1** and **2** exhibited no activity. Thus, the pronounced inhibition of the studied protein kinases in the biochemical assay by compounds **1** and **2** did not correlate with a significant reduction in lymphoma cell growth and *vice versa*, which is particularly significant for bastadin 11 (**5**), which showed no activity against any of the kinases of the panel but a strong inhibition of lymphoma cell growth. Therefore a different mode of action rather than inhibition of protein kinases can be assumed for compounds **3**−**6**. Similar activity results for **1** and **2** in the bioassays indicated that the addition of a third hemibastadin subunit as in the case of **1** did not lead to a distinct change in the activity profiles. The lack of activity of compounds **1** and **2** in the cellular assay cannot presently be explained, but may be due to hindered uptake of the compounds by the lymphoma cells.

dx.doi.org/10.1021/np300764u | *J. Nat. Prod.* 2013, 76, 121−125

Table 2. Protein Kinase Inhibition Activities (IC_{50}, μM) for compounds 1−6

	kinase											
compound	AKT1	ARK5	Aur-A	Aur-B	B-RAF VE	CDK2/CycA	CDK4/CycD1	CK2-alpha1	COT	EGF-R	EPHB4	ERBB2
1		1.7	2.6	2.3	1.7	6.5	1.4		1.3	0.6	3.4	2.1
2	1.9	1.8	0.1	0.5	2.7	1.6	1.5	4.1	1.6	1.3	3.4	2.1
3			1.7	2.9			3.6		4.8	2.0		7.0
4		3.2	3.9	2.6	4.4		2.6		3.3	1.5	7.7	2.8
5												
6			1.3	1.6			4.0			2.9		4.5

	kinase										
compound	FLT3	IGF1-R	FAK	INS-R	MET	PDGFR-beta	PLK1	SAK	SRC	TIE2	VEGF-R2	VEGF-R3
1	1.4	1.0	3.5	1.4	0.8	4.0	6.4	0.7	0.7	0.6	0.6	1.6
2	2.4	2.3	2.1	2.9	1.1	3.3	3.9	4.1	1.9	0.8	1.2	2.8
3	5.3											
4	2.9	1.7	7.3	4.4	2.8	10.2		1.9	2.0	1.8	1.3	3.2
5												
6												

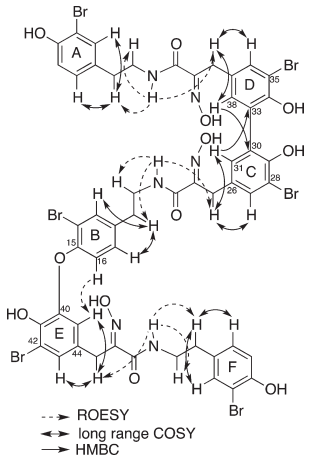

Figure 2. Key correlations for **1** obtained from 2D NMR spectra.

EXPERIMENTAL SECTION

General Experimental Procedures. UV spectra were measured in a Perkin-Elmer Lambda 25 UV/vis spectrometer. IR spectra were measured in a Shimadzu IRAffinity-1 FT-IR spectrometer. NMR spectra were recorded in DMSO-d_6 on Bruker Avance III-600 and/or Bruker DRX 500 spectrometers. High-resolution mass measurements were performed on a Bruker UHR-QTOF maXis 4G. Low-resolution ESI mass spectra were recorded on a Thermoquest Finnigan LCQDeca connected to an Agilent 1100 Series LC. Analytical HPLC investigations for all compounds were performed on a Dionex Ultimate 3000 System employing a DAD and a Knauer VertexPlus column (125 × 4 mm, Eurospher 100-10, C18). Semipreparative purification was accomplished on a Merck Hitachi system consisting of an L-7400 UV detector and an L-7100 pump connected with a Kipp&Zonen flatbed recorder. The attached column was a Knauer VertexPlus C18 column (300 × 8 mm, Eurospher 100-10).

Animal Material. A specimen of *Ianthella basta* was collected at Ambon (Indonesia) in August 1996, subsequently identified by Dr. Rob W. M. van Soest, and stored in EtOH at −20 °C in a sealed plastic container until extraction. A voucher specimen (reference number ZMAPOR17857) is deposited at the Zoological Museum, Amsterdam, The Netherlands.

Extraction and Isolation. The thawed sponge material (80.0 g wet weight) was homogenized with a blender and extracted three times with 3 L of MeOH, stirring at room temperature for 24 h each cycle. Extracts were combined and concentrated by rotary evaporation to yield 4.51 g of a brown crude extract. HPLC-DAD analysis was performed for the crude extract and for every subsequently obtained subfraction. Liquid−liquid extraction yielded hexane (0.52 g), EtOAc (1.23 g), BuOH (1.18 g), and H_2O fractions (1.57 g). The EtOAc fraction was further subjected to vacuum liquid chromatography over ODS using gradient elution from H_2O containing increasing proportions of MeOH, followed by a final elution with 0.1% TFA in MeOH, to yield 10 fractions. HPLC-DAD analysis indicated fraction 5 (20% H_2O/MeOH, 555.2 mg) to be of further interest, based on the presence of typical bastadin UV spectra. Size exclusion chromatography over Sephadex LH-20 with MeOH/CH_2Cl_2 (50:50 v/v) as mobile phase was performed to further divide fraction 5 into seven subfractions. All subfractions were subsequently purified by semi-preparative HPLC in a gradient system of H_2O/MeOH or H_2O/CH_3CN, to afford sesquibastadin 1 (**1**, 7.5 mg), bastadin 3 (**2**, 31.8 mg), bastadin 6 (**3**, 11.1 mg), bastadin 7 (**4**, 8.0 mg), bastadin 11 (**5**, 10.3 mg), and bastadin 16 (**6**, 13.2 mg) as amorphous, white solids.

Sesquibastadin 1 (1): white, amorphous solid (7.5 mg, 0.009%); UV (λ_{max}, MeOH) (log ε) 207.7 (5.06), 282.2 (4.10) nm; FT-IR ν_{max} 3734, 3649, 3628, 3273 (br), 2955, 2918, 2918, 2849, 1699, 1645, 1636, 1609, 1558, 1539, 1506, 1489, 1472, 1456, 1418, 1281, 1234, 1204, 1180, 1043, 1022, 988 cm^{-1}; ^1H NMR (600 MHz, DMSO-d_6) and ^{13}C NMR (150 MHz, DMSO-d_6) data see Table 1; HRESIMS (TOF) m/z 1412.81374 $[M + H]^+$ (calcd for $C_{51}H_{45}{}^{79}Br_3{}^{81}Br_3N_6O_{12}$ 1412.81343).

Bastadins 3, 6, 7, 11, and 16 (2−6). NMR and MS data matched the previously published data.[2,4,14]

Protein Kinase Inhibition Assays. The tested protein kinases were AKT1, ARK5, Aurora A, Aurora B, B-RAF VE, CDK2/CycA, CDK4/CycD1, CK2-alpha1, COT, EGF-R, EPHB4, ERBB2, FAK, FLT3, IGF1-R, INS-R, MET, PDGFR-beta, PLK1, SAK, SRC, TIE2, VEGF-R2, and VEGF-R3. Experiments were conducted as described before.[17]

Cytotoxicity Assays. Cytotoxicity was tested against mouse lymphoma cells (L5178Y) using a tetrazolium-based colorimetric (MTT) assay as described before.[18]

ASSOCIATED CONTENT

Supporting Information

1D and 2D NMR and high-resolution mass spectra for sesquibastadin 1 (**1**) are available free of charge via the Internet at http://pubs.acs.org.

dx.doi.org/10.1021/np300764u | *J. Nat. Prod.* 2013, 76, 121−125

AUTHOR INFORMATION

Corresponding Author
*Tel: +49 211 81 14187 (D.L.), +49 211 81 14163 (P.P.). Fax: +49 211 81 11923. E-mail: laidaowan123@gmail.com (D.L.), proksch@uni-duesseldorf.de (P.P.).

Notes
The authors declare no competing financial interest.

ACKNOWLEDGMENTS

P.P. thanks BMBF for support. We thank E. Ferdinandus and L. A. Pattisina (Marine Science Center, Fisheries Faculty, Pattimura University, Ambon, Indonesia) and Sudarsono (Faculty of Pharmacy, Gadjah Mada University, Yogyakarta, Indonesia) for collecting the sponges.

REFERENCES

(1) Bayer, M.; Hellio, C.; Maréchal, J.-P.; Frank, W.; Lin, W.; Weber, H.; Proksch, P. *Mar. Biotechnol.* **2011**, *13*, 1148−1158.
(2) Kazlauskas, R.; Raymond, O. L.; Murphy, P. T.; Wells, R. J.; Blount, J. F. *Aust. J. Chem.* **1981**, *34*, 765−786.
(3) Gulavita, N. K.; Wright, A. E.; McCarthy, P. J.; Pomponi, S. A.; Kelly-Borges, M. *J. Nat. Prod.* **1993**, *56*, 1613−1617.
(4) Pordesimo, E. O.; Schmitz, F. J. *J. Org. Chem.* **1990**, *55*, 4704−4709.
(5) Franklin, M. A.; Penn, S. G.; Lebrilla, C. B.; Lam, T. H.; Pessah, I. N.; Molinski, T. F. *J. Nat. Prod.* **1996**, *59*, 1121−1127.
(6) Masuno, M. N.; Hoepker, A. C.; Pessah, I. N.; Molinski, T. F. *Mar. Drugs* **2004**, *2*, 176−184.
(7) Mack, M. M.; Molinski, T. F.; Buck, E. D.; Pessah, I. N. *J. Biol. Chem.* **1994**, *269*, 23236−23249.
(8) Carroll, A. R.; Kaiser, S. M.; Davis, R. A.; Moni, R. W.; Hooper, J. N. A.; Quinn, R. J. *J. Nat. Prod.* **2010**, *73*, 1173−1176.
(9) Carney, J. R.; Scheuer, P. J. *J. Nat. Prod.* **1993**, *56*, 153−157.
(10) Jaspars, M.; Rali, T.; Laney, M.; Schatzman, R. C.; Diaz, M. C.; Schmitz, F. J.; Pordesimo, E. O.; Crews, P. *Tetrahedron* **1994**, *50*, 7367−7374.
(11) Aoki, S.; Cho, S.-h.; Ono, M.; Kuwano, T.; Nakao, S.; Kuwano, M.; Nakagawa, S.; Gao, J.-Q.; Mayumia, T.; Shibuya, M.; Kobayashi, M. *Anti-Cancer Drugs* **2006**, *17*, 269−278.
(12) Aoki, S.; Cho, S.-h.; Hiramatsu, A.; Kotoku, N.; Kobayashi, M. *J. Nat. Med.* **2006**, *60*, 231−235.
(13) Van Wyk, A. W. W.; Zuck, K. M.; McKee, T. C. *J. Nat. Prod.* **2011**, *74*, 1275−1280.
(14) Park, S. K.; Jurek, J.; Carney, J. R.; Scheuer, P. J. *J. Nat. Prod.* **1994**, *57*, 407−410.
(15) Arabshahi, L.; Schmitz, F. J. *J. Org. Chem.* **1987**, *52*, 3584−3586.
(16) Calcul, L.; Inman, W. D.; Morris, A. A.; Tenney, K.; Ratnam, J.; McKerrow, J. H.; Valeriote, F. A.; Crews, P. *J. Nat. Prod.* **2010**, *73*, 365−372.
(17) Aly, A. H.; Edrada-Ebel, R.; Indriani, I. D.; Wray, V.; Müller, W. E. G.; Totzke, F.; Zirrgiebel, U.; Schächtele, C.; Kubbutat, M. H. G.; Lin, W. H.; Proksch, P.; Ebel, R. *J. Nat. Prod.* **2008**, *71*, 972−980.
(18) Ebrahim, W.; Kjer, J.; El Amrani, M.; Wray, V.; Lin, W.; Ebel, R.; Lai, D.; Proksch, P. *Mar. Drugs* **2012**, *10*, 1081−1091.

Supporting Information

A Trimeric Hemibastadin Congener from the Marine Sponge *Ianthella basta*

Hendrik Niemann,[†] *Wenhan Lin,*[‡] *Werner E. G. Müller,*[§] *Michael Kobbutat,*[⊥] *Daowan Lai,*[†,*]

Peter Proksch[†,*]

[†] Institute of Pharmaceutical Biology and Biotechnology, Heinrich-Heine University, Universitätsstrasse 1, 40225 Düsseldorf, Germany,

[‡] State Key Laboratory of Natural and Biomimetic Drugs, Peking University, Beijing 100191, People's Republic of China,

[§] Institute of Physiological Chemistry und Pathobiochemistry, Johannes-Gutenberg-University, Duesbergweg 6, 55128 Mainz, Germany,

[⊥] ProQinase GmbH, Breisacher Strasse 117, 79106 Freiburg, Germany

* Corresponding authors.

Tel.: +49 211 81 14187 (D.L.), +49 211 81 14163 (P.P.). Fax: +49 211 81 11923.

E-mail: laidaowan123@gmail.com (D.L.), proksch@uni-duesseldorf.de (P.P.).

Table of Contents

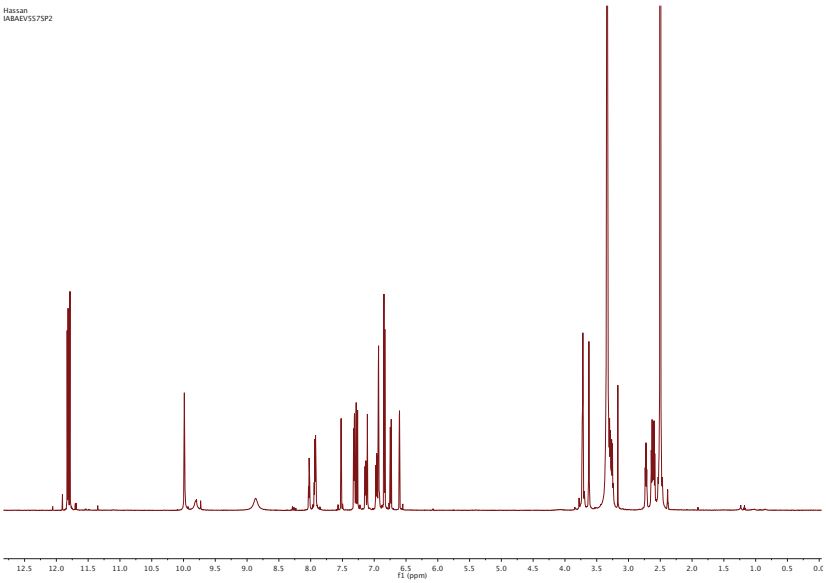

Figure S1-1. [1]H NMR Spectrum of Sesquibastadin 1 (**1**) (600 MHz, DMSO-d_6)

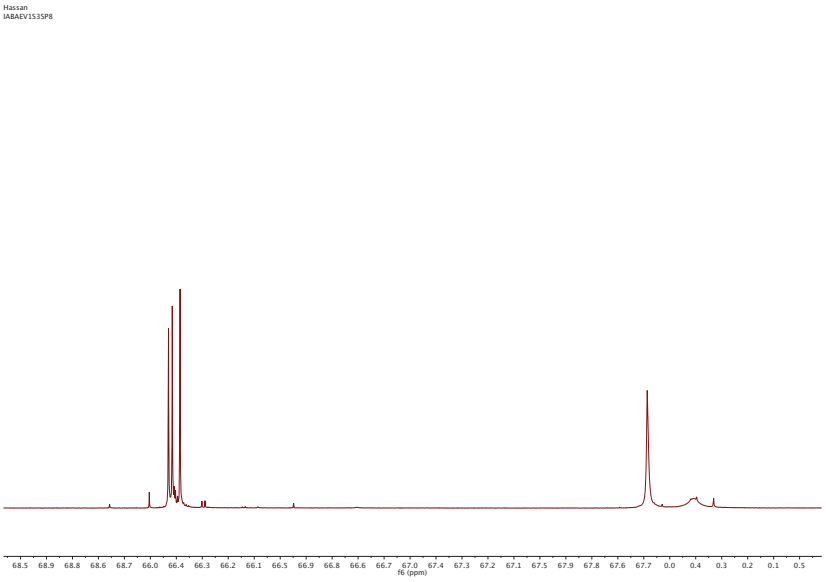

Figure S1-2. [1]H NMR Spectrum of **1** (expansion oxime region, 600 MHz, DMSO-d_6)

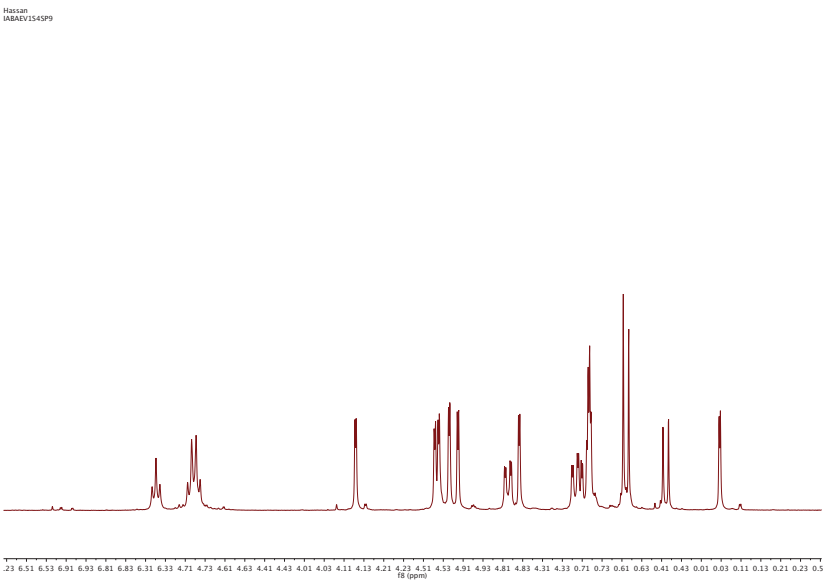

Figure S1-3. [1]H NMR Spectrum **1** (expansion aromatic region, 600 MHz, DMSO-d_6)

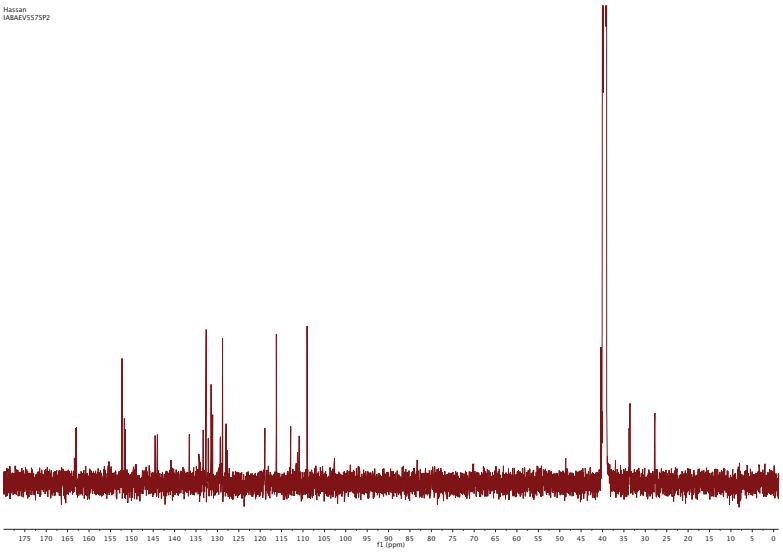

Figure S2. [13]C NMR Spectrum **1** (150 MHz**,** DMSO-d_6*)*

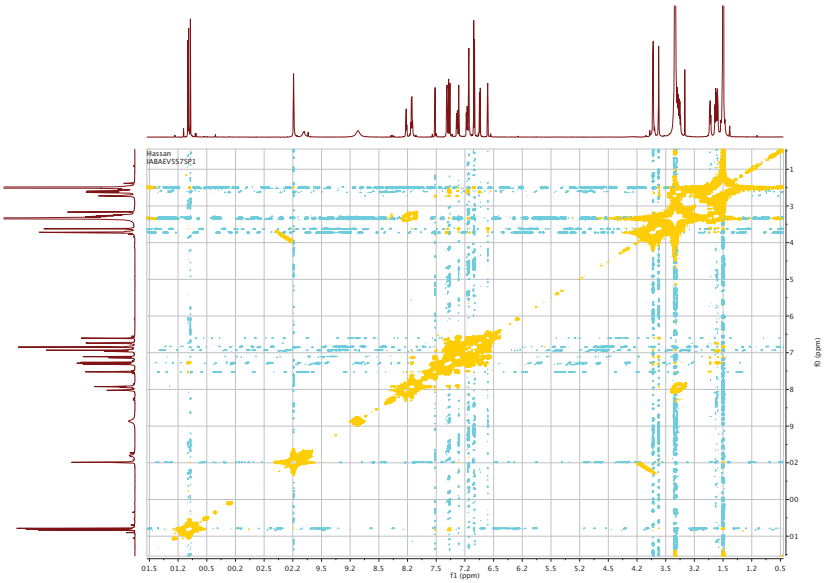

Figure S3. ^{1}H-^{1}H COSY Spectrum of **1** (DMSO-d_6)

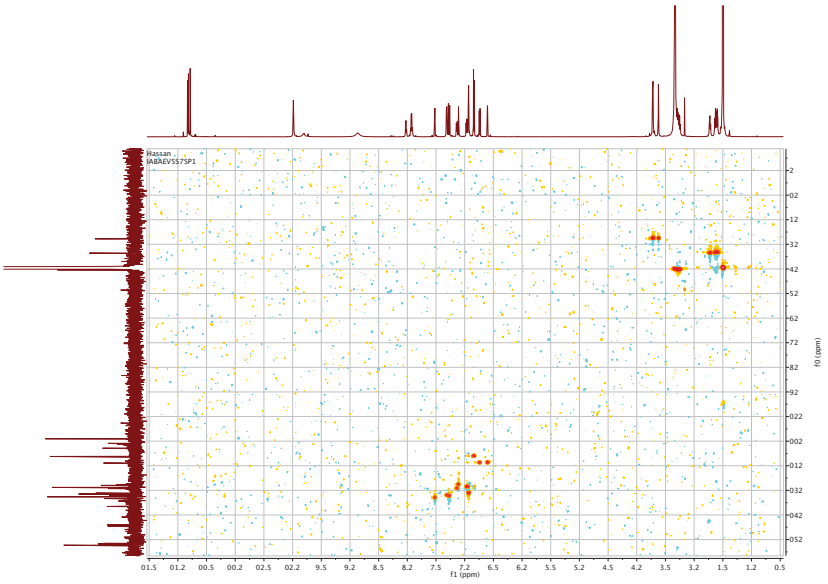

Figure S4. HMQC Spectrum of **1** (DMSO-d_6)

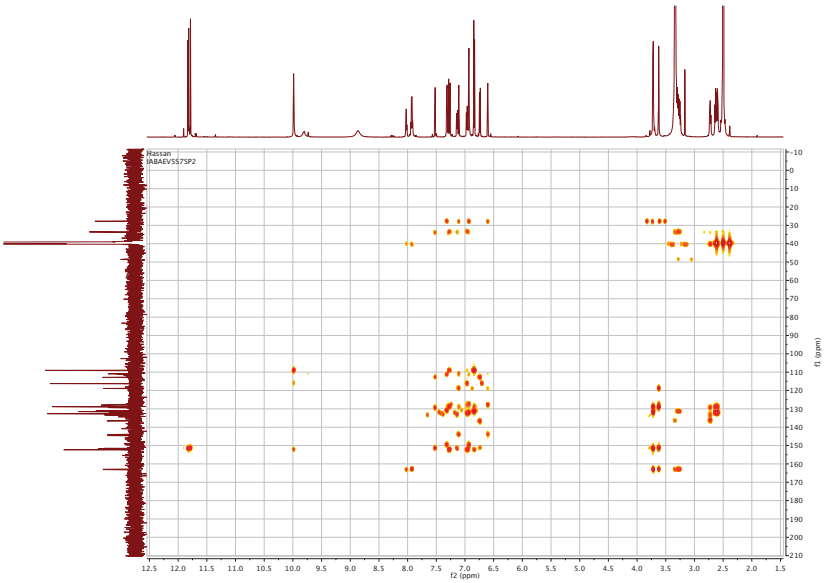

Figure S5. HMBC Spectrum of **1** (DMSO-d_6)

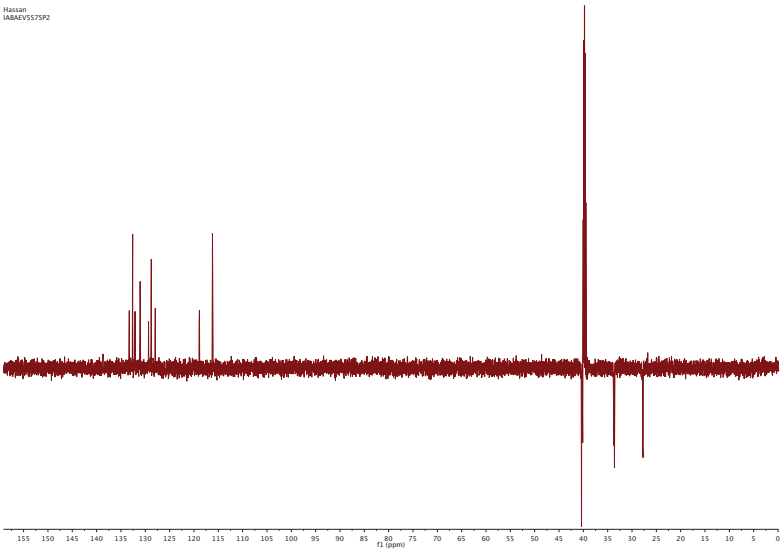

Figure S6. DEPT Spectrum of **1** (DMSO-d_6)

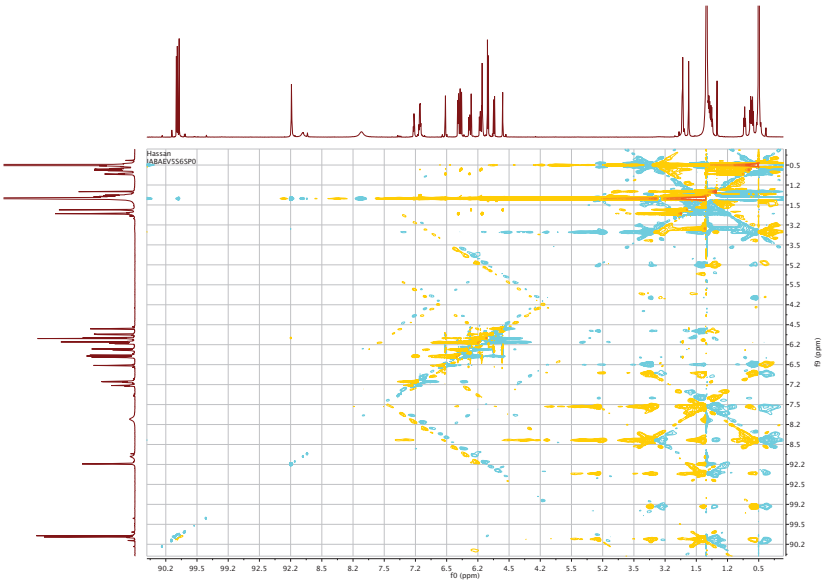

Figure S7. ROESY Spectrum of **1** (DMSO-d_6)

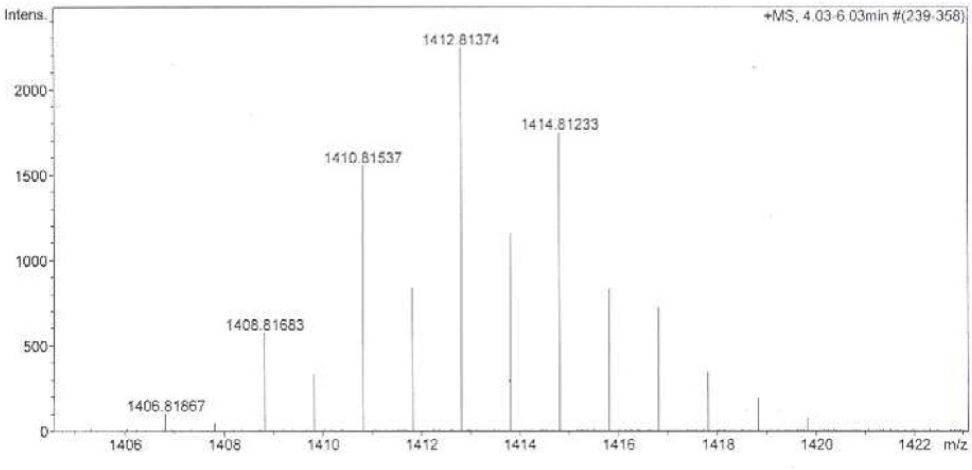

Figure S8. High Resolution Mass Spectrum of **1** (MeOH)

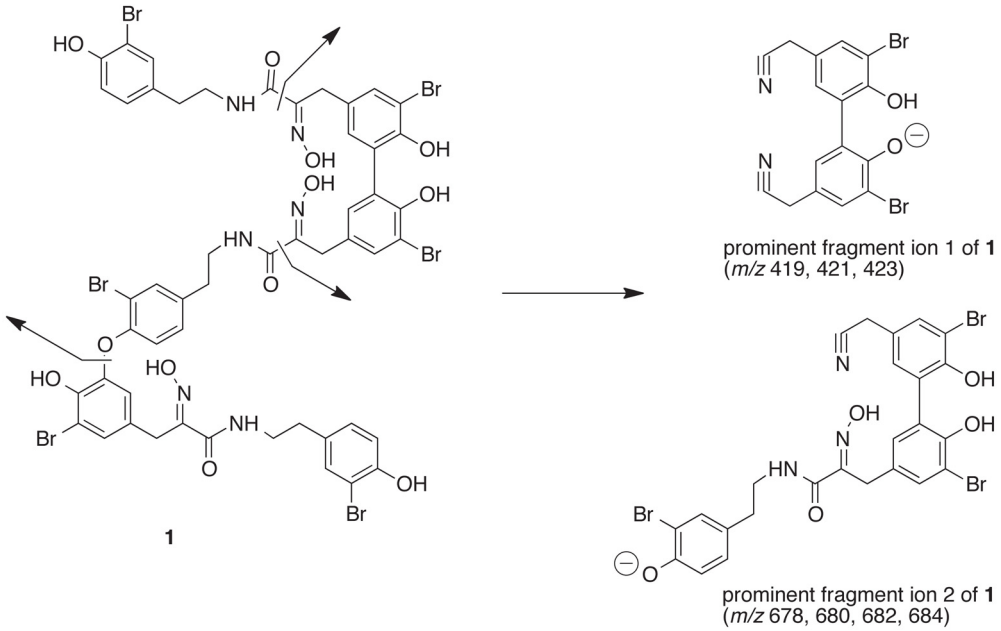

Figure S9 Plausible Fragmentation Pathway for **1**

6 Publication 3

6.1 Cyclic *versus* Hemi-Bastadins. Pleiotropic Anti-Cancer Effects: from Apoptosis to Anti-Angiogenic and Anti-Migratory Effects

Published in: „Molecules“

Impact factor: 2.095

Contribution: 20 %, conducting one set of experiments (determination of DBHB affinity to albumin), manuscript writing

Publication 3

Molecules **2013**, *18*, 3543-3561; doi:10.3390/molecules18033543

OPEN ACCESS

molecules

ISSN 1420-3049

www.mdpi.com/journal/molecules

Article

Cyclic *versus* Hemi-Bastadins. Pleiotropic Anti-Cancer Effects: from Apoptosis to Anti-Angiogenic and Anti-Migratory Effects

Véronique Mathieu [1,*], Nathalie Wauthoz [2], Florence Lefranc [3], Hendrik Niemann [4], Karim Amighi [2], Robert Kiss [1] and Peter Proksch [4]

[1] Laboratoire de Toxicologie, Faculté de Pharmacie, Université Libre de Bruxelles (ULB), Campus de la Plaine, Boulevard du Triomphe, 1050 Brussels, Belgium; E-Mail: rkiss@ulb.ac.be

[2] Laboratoire de Pharmacie Galénique et de Biopharmacie, Faculté de Pharmacie, Université Libre de Bruxelles (ULB), Campus de la Plaine, Boulevard du Triomphe, 1050 Brussels, Belgium; E-Mails: nawautho@ulb.ac.be (N.W.); kamighi@ulb.ac.be (K.A.)

[3] Service de Neurochirurgie, Hôpital Erasme, ULB, Route de Lennik, 1070 Brussels, Belgium; E-Mail: fllefran@ulb.ac.be

[4] Institute of Pharmaceutical Biology and Biotechnology, Heinrich-Heine University Düsseldorf, Universitätsstrasse 1, 40225 Düsseldorf, Germany; E-Mails: hendrik.niemann@uni-duesseldorf.de (H.N.); proksch@uni-duesseldorf.de (P.P.)

* Author to whom correspondence should be addressed; E-Mail: vemathie@ulb.ac.be; Tel.: +32-478-317-388.

Received: 16 January 2013; in revised form: 4 February 2013 / Accepted: 8 March 2013 / Published: 19 March 2013

Abstract: Bastadins-6, -9 and -16 isolated from the marine sponge *Ianthella basta* displayed *in vitro* cytostatic and/or cytotoxic effects in six human and mouse cancer cell lines. The *in vitro* growth inhibitory effects of these bastadins were similar in cancer cell lines sensitive to pro-apoptotic stimuli *versus* cancer cell lines displaying various levels of resistance to pro-apoptotic stimuli. While about ten times less toxic than the natural cyclic bastadins, the synthetically derived 5,5'-dibromohemibastadin-1 (DBHB) displayed not only *in vitro* growth inhibitory activity in cancer cells but also anti-angiogenic properties. At a concentration of one tenth of its *in vitro* growth inhibitory concentration, DBHB displayed actual antimigratory effects in mouse B16F10 melanoma cells without any sign of cytotoxicity and/or growth inhibition. The serum concentration used in the cell culture media markedly influenced the DBHB-induced antimigratory effects in the B16F10 melanoma cell population. We are currently developing a specific inhalation formulation

Publication 3

for DBHB enabling this compound to avoid plasmatic albumin binding through its direct delivery to the lungs to combat primary as well as secondary (metastases) tumors.

Keywords: bastadins; hemibastadins; angiogenesis; apoptosis; cancer

1. Introduction

First isolated in the 1980s [1,2] and in the 1990s [3] from the sponge *Ianthella basta*, bastadins have attracted wide attention due to their pronounced biological activities. Chemically, bastadins are formed by brominated tyrosine and tyramine derivatives (Figure 1) that are linked by a peptide bond to build a hemibastadin unit. Two moieties of these putative precursors form the bastadins either by carbon bonds or by the more common ether bridges. Both, linear and macrocyclic derivatives occur in nature. The amino group of the bromotyrosine unit is typically oxidized to yield an oxime function. Approximately thirty natural bastadins have been reported so far [4–7], with full chemical syntheses successfully developed for some of them. Several novel derivatives, including hemibastadin congeners [8–10] that exhibit remarkable anti-fouling activity [11,12], have also been generated. For example, 5,5'-dibromohemibastadin-1 (DBHB; **8**; Figure 1) suppresses the settling of barnacle larvae through the inhibition of the blue mussel phenoloxidase that is involved in the firm attachment of fouling organisms to a given substrate [12]. Bastadins and congeners also display activity with respect to ryanodine-sensitive Ca^{2+} channels (ryanodine receptors) [13–15].

Several reports have described the cytotoxic activity of various bastadins towards cancer cells [16,17], as well as their anti-angiogenic activity [18–20]. While their pro-apoptotic effects have been demonstrated in endothelial cells with respect to their cytotoxic activity [21], the mechanisms of action through which bastadins delay cancer cell growth have not yet been elucidated, to the best of our knowledge. In addition, preliminary investigations carried out in our group showed that bastadins display similar *in vitro* growth inhibitory effects in cancer cells that display actual sensitivity to pro-apoptotic stimuli *versus* cancer cells that display various levels of resistance to pro-apoptotic stimuli (unpublished data), as it is detailed in the current study for bastadins-6 (**1**; Figure 1), -9 (**2**; Figure 1) and -16 (**3**; Figure 1), and also for DBHB (**8**; Figure 1) and other related compounds (Figure 1).

The fact that various bastadins and DBHB are able to overcome the intrinsic resistance of cancer cells to pro-apoptotic stimuli is of potential clinical importance. In addition to the well-known multidrug resistance (MDR) phenotype of various cancer cell types that resist conventional chemotherapy [22], the intrinsic resistance of cancer cells to pro-apoptotic stimuli can also lead to dismal prognoses, as reported for gliomas [23], melanomas [24], non-small-cell lung cancers (NSCLCs) [25] and esophageal cancers [26]. Metastatic cancer cells are also resistant to pro-apoptotic stimuli because they must resist anoikis during their metastatic journey [27,28]. Because a cell cannot migrate and divide simultaneously, there should be an inverse relationship between the levels of cancer cell migration and their sensitivity to pro-apoptotic stimuli [29,30]. In other words, antimigratory compounds that are not inherently cytotoxic can be as effective as cytotoxic compounds in combatting aggressive cancer cells. In addition, antimigratory compounds can increase the efficiency of cytotoxic drugs against apoptosis-resistant cancer cells, by decreasing the migration of these cancer cells [29,30].

For example, cilengitide is a cyclo[Arg-Gly-Asp-D-Phe-(NMeVal)] (cRGD) compound that acts as an antimigratory agent that targets the α(v)β(3) and α(v)β(5) integrins, which govern not only endothelial but also cancer cell adhesion; affecting thus both endothelial (angiogenesis) and cancer cell migratory (metastasis) processes, this compound has been assayed in multiple clinical trials, including studies on aggressive types of cancers [31,32].

Figure 1. Compounds under study.

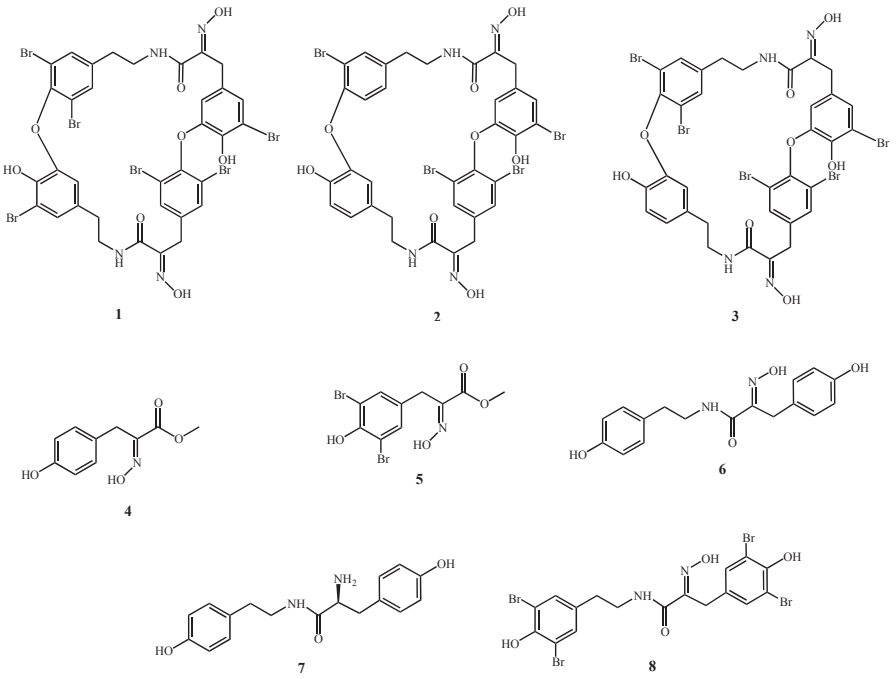

The present study examined: (i) the characterization of the *in vitro* cytostatic *versus* cytotoxic effects of bastadins-6, -9 and -16 in multiple cancer cell lines (including several cancer cell lines displaying various levels of resistance to pro-apoptotic stimuli); (ii) the bastadin-9-induced effects on cell cycle kinetics and apoptotic features in human SKMEL-28 melanoma and U373 glioblastoma cells; (iii) the anti-angiogenic effects of DBHB; (iv) the antimigratory effects of DBHB; (v) the influence of the serum concentration in cell culture media on DBHB-induced antimigratory effects in B16F10 melanoma cells and the binding affinity of DBHB to albumin; and (vi) a first evaluation of the *in vivo* analysis of DBHB-related activity as measured by the survival of B16F10 melanoma-bearing mice.

2. Results and Discussion

2.1. In Vitro *Growth Inhibitory Concentrations*

The eight compounds whose chemical structures are illustrated in Figure 1 were assayed using the MTT colorimetric test to determine the concentration that reduced global cancer cell growth by 50% for six cancer cell lines cultured for three days in the presence of the drug of interest (Table 1).

Publication 3

Table 1. *In vitro* growth inhibitory concentrations that reduce cell growth by 50% (IC_{50}; μM) for compounds **1**–**8** (Figure 1) following culturing of the cancer cell lines with the compound of interest for 72 h (MTT colorimetric assay).

Compounds	Carcinoma		Glioma		Melanoma		Mean ± SEM
	MCF-7 (breast)	A549 (NSCLC)	Hs683 (oligodendroglioma)	U373 (astroglioma)	B16F10 *	SKMEL28	
1	4	3	3	3	4	4	4.0 ± 0.2
2	8	7	4	7	5	7	6.0 ± 0.6
3	7	8	4	11	6	7	7.0 ± 0.9
4	>100	>100	>100	>100	75	>100	>96
5	94	>100	>100	>100	86	>100	>97
6	>100	>100	>100	>100	45	>100	>91
7	>100	>100	>100	>100	63	>100	>94
8	68	68	70	73	58	76	69 ± 3

* All the cell lines are of human origin except the B16F10 melanoma, which is of murine origin. NSCLC means non-small-cell lung cancer.

The data shown in Table 1 clearly indicate that cyclic bastadins [bastadin-6, -9 and -16 (**1**–**3**)] display higher *in vitro* growth inhibitory effects than hemibastadins such as DBHB. However, this latter revealed a weak activity with a mean IC_{50} growth inhibitory activity of 69 μM over all cancer cell lines, including the A549 NSCLC [33], SKMEL-28 melanoma [34] and U373 [35] cell lines that exhibit various levels of resistance to pro-apoptotic stimuli. The cancer cell lines sensitive to pro-apoptotic stimuli, including the MCF-7 breast cancer [36], the Hs683 oligodendroglioma [35] and the B16F10 melanoma [34] cell lines, did not display higher sensitivity to bastadins and DBHB than the A549, SKMEL-28 and U373 cancer cells. These data suggest that bastadins and DBHB display their anti-cancer activities regardless to their sensitivity to apoptosis. Therefore, we hypothesized that induction of apoptosis should not be the primary mechanism of action of these compounds that could thus be used to combat models associated with, at least partial, intrinsic resistance to pro-apoptotic stimuli. If at first glance, DBHB appeared to have rather weak activity (at least in terms of IC_{50} *in vitro* growth inhibitory concentrations), it must kept in mind that temozolomide, the most efficacious drug used clinically to treat glioblastoma [23], has IC_{50} *in vitro* growth inhibitory concentrations ranging between 220 (U373) and 956 (Hs683) μM, depending on the glioma cell line [37]. The same features were observed for another widely used compound to combat various cancer types, *i.e.*, carboplatin, whose IC_{50} growth inhibitory concentrations ranged between 11 (A549) and 149 (SKMEL-28) μM [38].

A comparison of the analyzed compounds clearly reveals that the studied bastadin derivatives **1**–**3**, which can be envisioned as dimeric hemibastadin congeners, show the strongest activity in all cell lines investigated in this study. Differences in activity between the individual bastadins are only minor, as reflected by their similar IC_{50} values. Among the synthetically derived hemibastadin derivatives **6**–**8**, compound **8** (DBHB) shows the best activity, which can be traced back to its brominated aromatic rings, as is evident from comparison of **8** with the debromo analogue **6**. Hydrolysis of **8** and subsequent methylation yields **5** as one biogenetic building block. The fact that **5** is devoid of activity in almost all studied cell lines suggests that at least two bromotyrosine derived units must be fused as present in **8** for obtaining appreciable activity in the studied cellular systems. Dimerization of a

hemibastadin unit such as present in **8** which gives rise to bastadin derivatives (e.g., **1**–**3**) leads to a further enhancement of activity suggesting that the size of the molecule in addition to bromination of the aromatic rings is a further factor which influences the cellular activity of the studied compounds.

2.2. Quantitative Videomicroscopy Analyses

While effective at determining the metabolic activity of cells, the colorimetric MTT assay cannot provide information as whether a compound decreases the global growth of normal or cancerous cells through cytotoxic, cytostatic, or anti-adhesive features or a mix of several of these features. To elucidate the specific features of bastadin derived anti-cancer effects, we used quantitative videomicroscopy to characterize these growth inhibitory effects [30,39]. The effects induced by bastadins-6, -9 and -16 (compounds **1**–**3**) on human SKMEL-28 melanoma and U373 glioblastoma cells are shown in Figure 2. We have chosen the concentration of 10 μM in order to compare the three cyclic bastadin effects on both cell lines at a similar dosis which corresponds to the IC_{50} of bastadin-16 on U373 cancer cells (11 μM) and which is closed to the IC_{50} values of bastadin-16 on SKMEL-28 (7 μM) and of bastadin-9 on both U373 and SKMEL-28 cells (7 μM).

The white and bright objects in Figure 2A correspond either to dying cells (e.g., cytotoxic effects) or to cells blocked in mitosis (cytostatic effects). A global growth ratio (the GGR index) was thus calculated for each compound (Figure 2). For both the controls and the treated cells, the global growth (GG) was first calculated by dividing the number of cells on the image at 24, 48 and 72 h by the number of cells on the first image. The GGR index was calculated by dividing the GG values calculated for the treated SKMEL-28 or U373 cancer cells by the GG values calculated for the control. As shown in Figure 2, at the same dosage of 10 μM, bastadin-6 (**1**) is the most potent compound, followed by bastadin-9 (**2**) and then bastadin-16 (**3**) for both cell lines, consistent with the potency data obtained with the colorimetric MTT assay (Table 1). In contrast, bastadin-9 (**2**) and -16 (**3**) appeared less active in the SKMEL-28 melanoma cells as assayed with quantitative videomicroscopy than by the MTT colorimetric assay (Table 1; Figure 2). The marked decrease in the total number of mitoses over the 72 h period observed with these compounds (marked effects except with bastadin-16 on U373 glioblastoma cells; Figure 2C) suggested that they exert their anti-cancer activities through primary cytostatic effects. These later were distinguished from cytotoxic effects on the basis of the dynamic movies and particularly the timelines associated with the compound-induced effects: blocking of proliferation was first observed and led, when sustained, at some cell death at the end of the experiment depending on the compound and the cell line under consideration with bastadin-6 (**1**) being the most cytotoxic one. These data suggest that the bastadin-mediated effects could at least partly depend on the cell cycle kinetic characteristics of the cancer cells analyzed. To further examine these effects, flow cytometry analyses were performed, as detailed in the next section.

Figure 2. (**A**) Images of SKMLEL-28 and U373 cells left untreated or treated with 10 µM of bastadins at 10 µM during 72 h. Scale bar: 100 µm. (**B**) Global Growth Ratio for each experiment at 24 (open bars), 48 (gray bars) and 72 h (black bars) of treatment. (**C**) Number of mitoses that occurred over the 72 h period of observation for each experimental condition (control *versus* bastadin treated cells at 10 µM). Data are expressed as the means ± SEM.

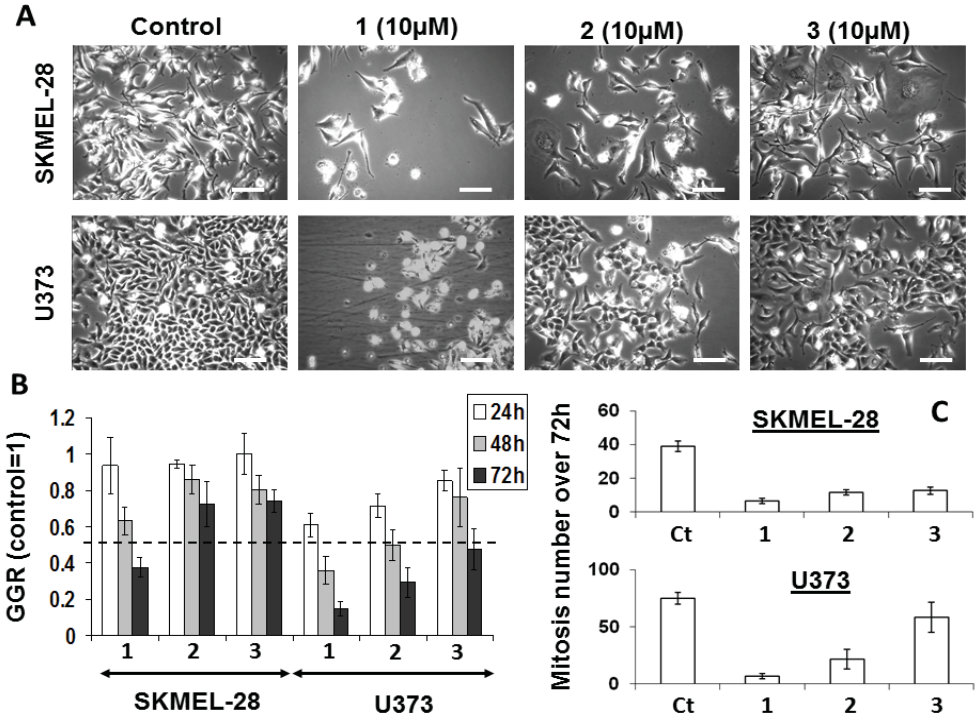

2.3. Cell Cycle Kinetics versus Pro-Apoptotic Features

Using flow cytometry, we examined the influence of bastadin-9 (**2**, for which we had sufficient amount of material) on both the cell cycle kinetics and the apoptotic features in SKMEL-28 melanoma and U373 glioblastoma cells (Figure 3). Bastadin-9 (10 µM) decreased the proportion of proliferating SKMEL-28 melanoma cells characterized by a decrease in the S phase with an increase in G1 phase. This decrease is consistent with the cytostatic effects determined using quantitative videomicroscopy (Figure 2C). This compound increased in a time-dependent manner the proportion of dying cells in the preG1 fraction in SKMEL-28 melanoma cells only (Figure 3A as compared to Figure 3B for U373 cell line). TUNEL analyses determination of the levels of apoptotic cells confirmed the bastadin-9 (**2**) apoptosis induction in about one-third of the SKMEL-28 melanoma cells (Figure 3C), as also observed in the quantitative videomicroscopy experiments while no effects could be observed with respect to U373 glioblastoma cells (Figure 3B,D). In addition to the negative and positive controls furnished by the manufacturer, we also used a positive control, narciclasine (1 µM), which is an isocarbostyril compound isolated from *Narcissus* bulbs, on the PC-3 prostate cancer cells [36]. The pro-apoptotic effects induced by bastadin-9 (**2**) in SKMEL-28 melanoma cells (and subsequent cell death measured

by increasing preG1 cells; Figure 3A) were of lower magnitude than those induced by narciclasine in PC-3 prostate cancer cells (Figure 3C). Nevertheless, **2** induced both cytostatic and then cytotoxic effects in SKMEL-28 melanoma cells, a feature that should correspond with several distinct mechanisms of action for exerting its growth inhibitory effects in these melanoma cells.

Figure 3. (**A** and **B**) Propidium iodide cell cycle analyses of SKMEL-28 and U373 cancer cells respectively, either left untreated or treated with 10 µM of (**2**). The results are presented as the means of the 3 replicates of the experiment. (**C** and **D**) Proportion of apoptotic cells (percentages) by TUNEL staining in SKMEL-28 and U373 cells, respectively. In addition to the negative and positive controls provided with the kit, we included two additional controls using PC-3 prostate cancer cells untreated or treated for 72 h with narciclasine (narci) at 1 µM. Each replicate result is presented as a black dot.

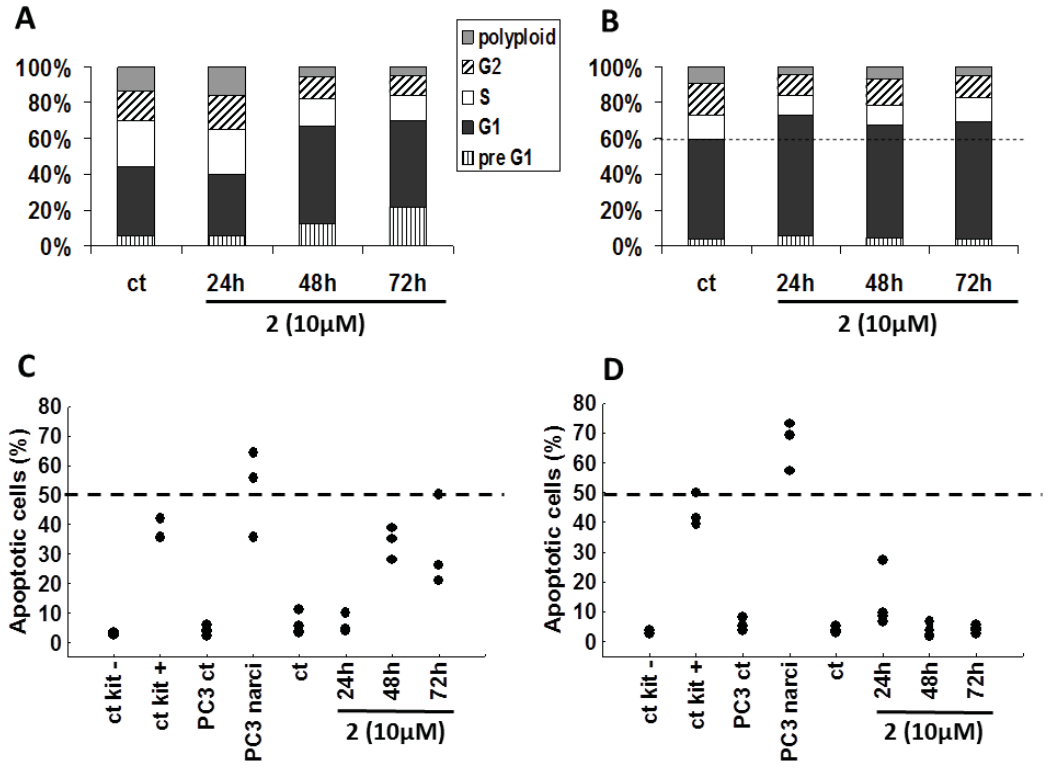

By contrast, it seems that bastadin-9 could overcome the intrinsic resistance of the U373 glioblastoma cells through pure cytostatic but not cytotoxic effects. The underlying molecular pathways have yet to be identified. As mentioned earlier, bastadins and congeners display activity with respect to the ryanodine-sensitive Ca^{2+} channels (ryanodine receptors; RyRs) [13–15]. Bastadin-induced cytotoxic and/or cytostatic effects could possibly be due, at least partly, to bastadin-induced modifications in the actin cytoskeleton organization through modulation of the RyRs [40,41], with modifications in the actin cytoskeleton organization leading to cytotoxic, not cytostatic, effects in endothelial cells [42] as well as in cancer [29,30,34] cells. As emphasized by Mackrill [43], RyRs are

high conductance intracellular cation channels that release calcium ions from stores, such as the endoplasmic and sarcoplasmic reticulum, with altered RyR gating being implicated in a wide range of diseases, including cancer. However, Mackrill [43] also emphasizes that the available pharmacological tools for manipulating RyR gating are generally unsuitable for clinical, veterinary or agricultural use, owing to their lack of selectivity, their inappropriate solubility in the aqueous or lipid environment, or the generation of side-effects. It is possible that the bastadin-mediated cytostatic and/or cytotoxic effects in cancer cells occur by targeting the RyRs. Whether bastadins affect cells in a cytostatic and/or cytotoxic manner may depend on the type of cell studied and the concentrations used.

While naturally occurring bastadins are difficult to isolate or to synthesize in large quantities, DBHB (**8**) can be easily synthesized in multigram amounts, supporting our decision to pursue our investigations with DBHB (**8**). Indeed, DBHB (**8**) turned out to exert cytostatic effects at its IC_{50} growth inhibitory concentration on B16F10 apoptosis-sensitive melanoma cells with marked cell shape modification (data not shown) while it behaves as an anti-migratory compound at lower concentrations devoid of any cytotoxic and/or cytostatic effects as illustrated in the next sections. Whether DBHB does or not target RyRs at these low nontoxic concentrations for which it displays anti-migratory effects remains to be determined.

*2.4. DBHB (**8**) Exhibits Anti-Angiogenic Activity*

Guided by the fact that several naturally occurring bastadins are reported to exhibit anti-angiogenic effects [18–21], we evaluated if DBHB (**8**) also exhibits anti-angiogenic effects. Treatment of two human umbilical vein endothelial cell (HUVEC) lines, *i.e.*, HTG06 and HTG08, with 70 μM DBHB (**8**; the mean IC_{50} concentration on cancer cells; Table 1) induced marked anti-angiogenic effects in both HUVEC lines, as illustrated in Figure 4. The DBHB-induced inhibition of the HUVEC tubulogenesis correlated with anti-migratory but not cytotoxic effects, as shown in Figure 4. As shown below, DBHB (**8**) also exhibits anti-migratory effects without cytotoxic and/or cytostatic effects in melanoma cells at even lower concentrations than those used here for analyzing DBHB-induced anti-angiogenic effects.

Aoki *et al.* [21] observed that bastadin-6 inhibits vascular endothelial growth factor (VEGF)- or basic fibroblast growth factor (bFGF)-dependent proliferation of HUVECs with a 20- to 100-fold selectivity in comparison with normal fibroblasts (3Y1) or several tumor cell lines (KB3-1, K562 and Neuro2A). These authors also reported that bastadin-6 inhibited the VEGF- or bFGF-induced tubular formation, the VEGF-induced migration of HUVECs and the VEGF- or bFGF-induced *in vivo* neovascularization in the mice corneal assay. Bastadin-6 also suppressed the growth of s.c. inoculated A431 solid tumor in immunodeficient mice at 100 mg/kg (intraperitoneal) [21]. While bastadin-6 has been reported to induce apoptotic cell death in HUVECs [21], our data on DBHB (**8**) reported here, suggest a mechanism of action that is anti-migratory but non-cytostatic and non-cytotoxic in HUVECs: when considering evolution of HUVEC cell populations over the first hours, we observed marked anti-angiogenic effects while cellular spreading and cell population evolution are still present (Figure 4). Our observations with DBHB (**8**) in endothelial cells could therefore differ from those reported by Aoki *et al.* [21] for bastadin-6.

Figure 4. Representative images of the tubular network formation of HUVEC endothelial cells when cultured on Matrigel over a 24 h period. Two distinct HUVECs primary cultures, HTG06 and HTG08, were used. Treatment with DBHB (**8**) at 70 µM completely impaired the ability of endothelial cells to form these networks.

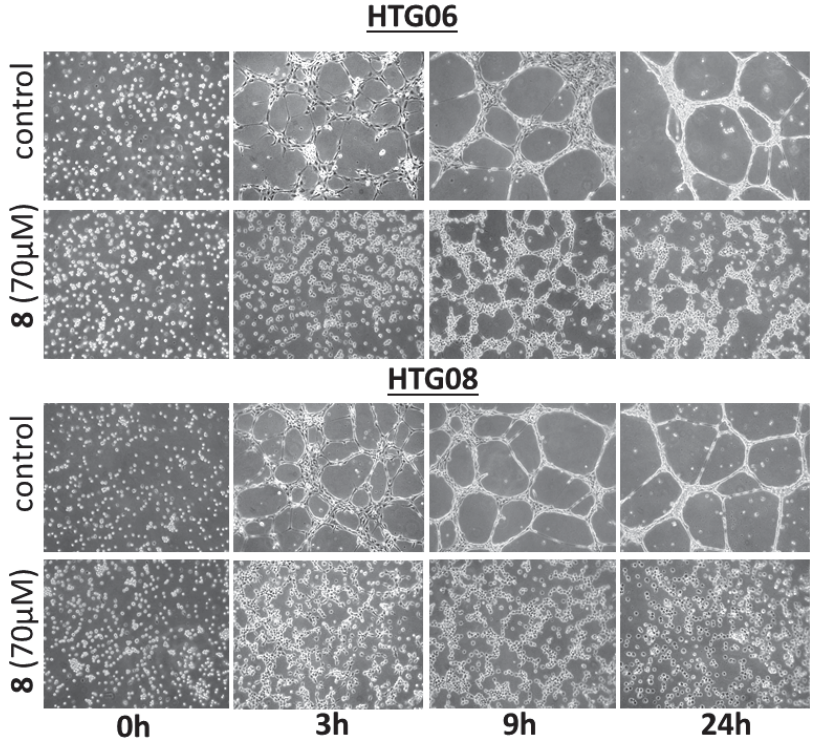

2.5. Direct Impact of Serum on the Anti-Migratory Properties of DBHB (**8**) *in B16F10 Melanoma Cells, with a Potential Involvement of Albumin*

The anti-migratory effects observed above with endothelial cells led us to investigate whether DBHB could display anti-migratory effects on cancer cells. We made use of quantitative scratch wound assays [29,30] for this purpose with the mouse B16F10 melanoma cells.

An image of a B16F10 melanoma scratch wound at "0 h" and the same scratch wound after 6 h of culture are shown in Figure 5A. The area percentages covered by B16F10 melanoma cells colonizing the white rectangle in the scratch wound over time have been quantitatively determined by means of computer-assisted phase-contrast microscopy [29,30]. The left panel of Figure 5B clearly shows that DBHB (**8**) only delayed the wound healing process of B16F10 mouse melanoma cells. To identify whether this effect related to anti-migratory and/ or to anti-proliferative effects, we decreased serum concentration to 1% to minimize the proliferative contribution to the wound healing. While not expected, we discovered that the 50 µM DBHB concentration when used in 1% FBS culture medium led to very high cytotoxic effects with cell death occurring within the first two hours of treatment (data not shown). We had to decrease DBHB till 10 µM to avoid any effect on cell proliferation as assessed

by quantitative videomicroscopy in Figure 5C,D. Similar data were obtained with respect to SKMEL-28 cells (Figure 5D). Interestingly, the B16F10 cell shape morphology seemed more affected by the DBHB in a 1% FBS culture than at the same concentration of DBHB in 10% FBS, a feature that could, at least partly, explain the anti-migratory effects observed (Figure 5B).

Figure 5. Anti-migratory effects of DBHB (**8**) on cancer cells. (**A**) Image of a wound made in confluent B16F10 cells at t = 0 h and 6 h after. Quantification of the area of the white rectangle healed over time is shown in (**B**) for cells cultured in 10 *vs.* 1% FBS. Black dots: control; open dots: DBHB treated condition at 50 µM or 5 µM as indicated. (**C**) Images of B16F10 cells left untreated or treated for 48 h with DBHB at 10 µM. (**D**) Quantitative data of B16F10 and SKMEl-28 cell growth ratio (control condition GGR = 1) when treated with 10 µM of DBHB for 24 h (gray bars) and 48 h (black bars). All data are expressed as the mean ± SEM.

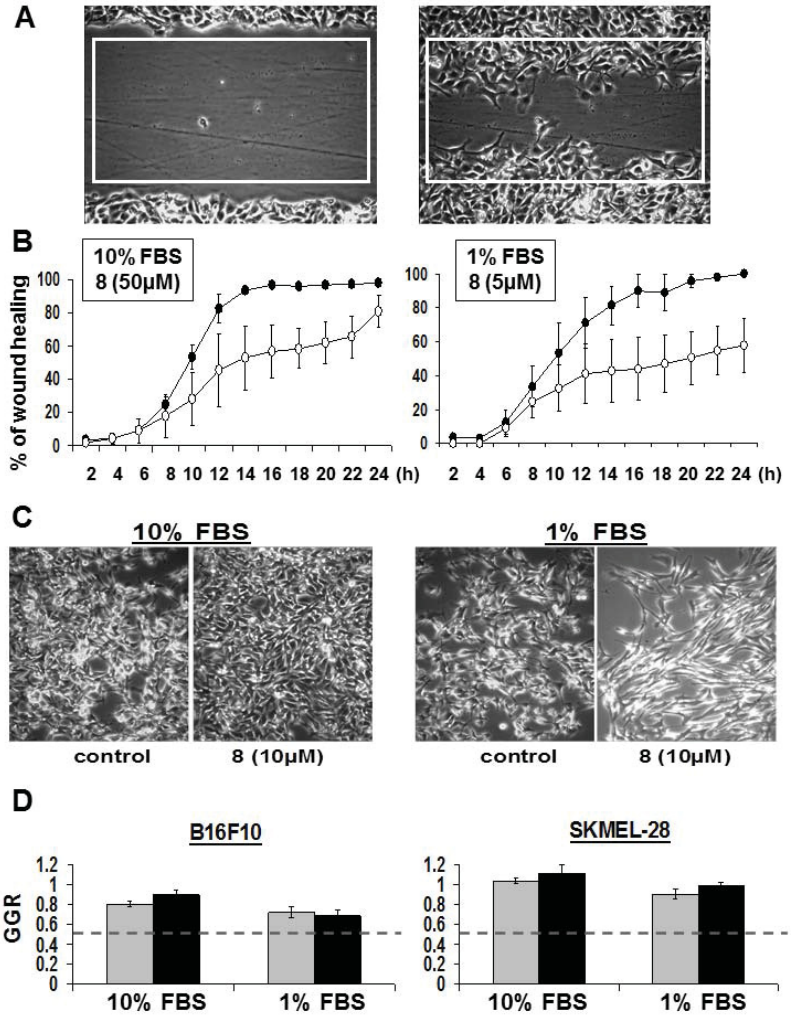

We thus compared the recolonization of the wound induced by 50 μM DBHB (*i.e.*, the IC_{50} growth inhibitory concentration of DBHB as measured using the MTT colorimetric assay (Table 1)) when B16F10 melanoma cells were cultured in medium supplemented with 10% of FBS to the ones induced by 5 μM in 1% FBS supplemented medium. The data in Figure 5B show that the 50 μM DBHB delayed the B16F10 melanoma cell migration during the first 24 h of observation and then this anti-migratory effect was lost. Lowering the DBHB concentration from 50 to 5 μM and the serum concentration from 10 to 1% induced higher DBHB anti-migratory effects than in the previous experimental conditions. At these lower DBHB and serum concentrations, a 50% inhibition of the B16F10 migration was still observed at 24 h when full colonization (100%) of the rectangle had been completed by the B16F10 melanoma cells in the control condition (Figure 5B). Thus, while lowering the FCS concentration from 10 to 1% only slightly delayed but did not impair the B16F10 cell migratory properties (see the control curves in Figure 5B), this ten-fold decrease in serum concentration allowed the even reduced DBHB concentration to inhibit cell migration more markedly.

The anti-migratory (non-cytostatic and non-cytotoxic) effects of DBHB in endothelial (Figure 4) and cancer cells (Figure 5A,B), are consistent with previously published data on bastadin- and DBHB-related antifouling properties [11,12]. Indeed, DBHB induced an inhibition of the larval settlement of *Balanus improvisus* without being toxic to either these larvae or the brine shrimp larvae [12]. By contrast, cyclic bastadins are toxic with poor, if any, antifouling activity at nontoxic concentrations [12].

Considering that the serum concentration affected the DBHB-induced effects on cell growth, death and migration (Figure 5), we hypothesized that DBHB could interact with albumin, one of the major components of plasma. As shown in Figure 6, DBHB binds strongly to albumin, whose concentration could thus impair DBHB-induced anti-migratory effects on both cancer and endothelial cells *in vivo*.

Figure 6. Binding curve of DBHB to albumin. Indirect quantification of bound DBHB (**8**) was performed after TCA precipitation. Data are presented for ratio of DBHB/ albumin of 1/4 to 5/1.

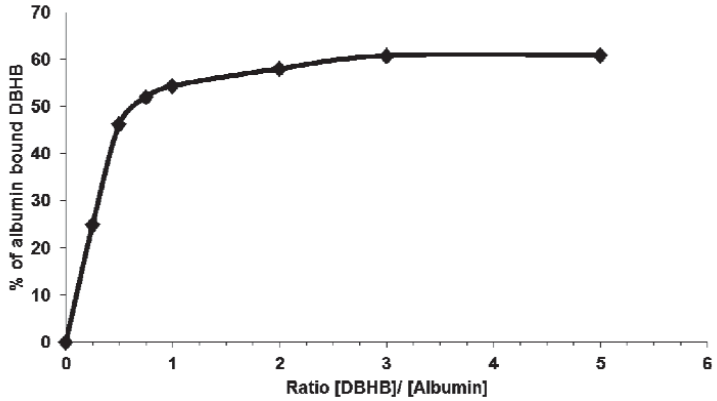

2.6. In Vivo *Analyses of DBHB* (**8**) *Activity in B16F10 Melanoma-Bearing Mice*

The *in vitro* anticancer activity in 6/6 cancer cell lines (Table 1) and the anti-angiogenic effects in 2/2 HUVEC lines of DBHB led us to assay this compound's *in vivo* anticancer activity. The

formulation we developed for DBHB to deliver 40 mg/kg with chronic i.v. administrations of the compound (*i.e.*, 200 µL of i.v. administration volume at a concentration of 5 mg/mL) to 25 g mice was made in NaCl 0.9% (see Experimental for details). The formulation was a relatively homogeneous suspension of DBHB compatible with chronic i.v. administrations (data not shown).

Preliminary toxicological experiments revealed that chronic i.v. administrations of 40 mg/kg DBHB to healthy mice (not grafted with tumors) induced no toxic side effects in terms of mouse behavior, weight and survival (data not shown). This dosage could lead in theory to a 10 fold IC_{50} plasmatic concentration at the injection time.

We then analyzed the DBHB *in vivo* antitumor activity using the mouse B16F10 melanoma model that, once injected i.v. in the tail vein of mice, rapidly develop aggressive lung pseudometastases [44]. The non-toxic dose of 40 mg/kg dose of DBHB (**8**) was chronically injected i.v. nine times, *i.e.*, three times a week (Monday, Wednesday, Friday) for three consecutive weeks, with the first injection occurring on the 5th day post-tumor cell grafting to mice bearing B16F10 melanoma-related lung pseudometastases. On the 5th day post B16F10 melanoma cell injection in the tail, lung pseudometastases can already be found at the histological level. Temozolomide was used as a reference compound and administered at the same dose (40 mg/kg) as DBHB and schedule, as we previously reported for this compound with the B16F10 melanoma model [44].

At these conditions, DBHB had no significant *in vivo* therapeutic benefits in the B16F10 model, neither as a single agent nor in combination with temozolomide (data not shown). To fully evaluate DBHB for *in vivo* anticancer activity, the development of specific formulations to prevent the albumin binding in the plasma is needed for the future.

3. Experimental

3.1. Sample Collection, Extraction and Purification of bastadin 6 (**1**), *bastadin 9* (**2**) *and bastadin 16* (**3**)

A specimen of the marine sponge *Ianthella basta* was collected at Ambon Tanjung Island, Indonesia in August 1996 and stored in ethanol at −20 °C until extraction. Taxonomic identification was performed by the Zoological Museum, Amsterdam, The Netherlands (reference number ZMAPOR17857). After freeze drying, the material (121 g) was ground and then macerated with acetone, followed by methanol. Each extraction cycle was performed four times for five hours with 800 mL of solvent. Acetone and MeOH extracts were combined and evaporated under vacuum to yield a dried crude extract of approximately 30 g in weight. A liquid-liquid partition led to four fractions (hexane 2 g; EtOAc 5 g; *n*-BuOH 3.5 g; H_2O 17.1 g). HPLC-DAD analysis indicated the EtOAc- and BuOH fraction to be of further interest. The EtOAc fraction was further subjected to vacuum liquid chomatography (VLC) using a gradient system from hexane over EtOAc over CH_2Cl_2 to MeOH to obtain 21 fractions. Compound **1** was eluted with 45% hexane/55% EtOAc, **2** with 40% hexane/60% EtOAc and both were further purified by size exclusion chromatography in 100% MeOH and semi-preparative HPLC utilizing an appropriate gradient system to yield 21.6 mg (**1**) and 1.9 mg (**2**), respectively. Bastadin 16 (**3**, 34.2 mg) were obtained from the BuOH fraction after further purification via size exclusion chromatography in 100% MeOH and semi-preparative HPLC.

3.2. Chemical Syntheses

Methyl-[2-hydroxyimino-3-(4-hydroxyphenyl)]-propionate (**4**). 4-Hydroxyphenylpyruvic acid (3 mmol) was suspended in H_2O (50 mL) and NaOH (5%) was added to dissolve the acid completely. Hydroxylamine·HCl (20 mmol), dissolved in H_2O (20 mL) was added to the solution and the pH was adjusted to approx. 8–9 with 5% NaOH. This solution was stirred for one hour at 60 °C and thereafter the pH was readjusted to 8–9 with 5% NaOH. The solution was heated once more for two hours at 60 °C and was left to cool down to room temperature. The cold solution was adjusted with HCl to pH 1 and extracted with ether. The obtained residue was recrystallized from ether/petroleum ether (60–80 °C) to yield [2-hydroxyimino-3-(4-hydroxyphenyl)] propionic acid as white crystals. The oxime (4 mmol) was dissolved in dimethylformamide (30 mL) and diazabicycloundecane (DBU, 4 mmol) was added. After cooling on ice methyl iodide (20 mmol) was added and the reaction was left stirring at 4 °C for 3 h. Thereafter water (100 mL) was added and the solution was extracted with ether. The traces of dimethylformamide were removed from the ether residue under vacuum. The product was recrystallized from ether/petroleum ether (60–80 °C) to yield white crystals of **4**, which served also as a precursor for the following syntheses of **5**, **6** and **8**.

Methyl-[2-hydroxyimino-3-(3,5-dibromo-4-hydroxyphenyl)]-propionate (**5**). The dibromo methylester **5** was prepared by a bromination of **4**. A bromine solution (0.1 M) was freshly prepared in dichloromethane and 50 mL of this solution were added to an ether solution of **4** (1 mmol). The reaction was left for 24 hours at room temperature. The organic solution was washed with diluted sodium hydrogen sulphite and sodium hydrogen carbonate solution and dried under reduced pressure. The residue was purified by chromatography on silica gel to give the main product of **5**.

Norbromohemibastadin-1 (**6**). Norbromohemibastadin-1 (**6**) was synthesized as reported earlier [12].

L-Tyrosine-tyramide A (**7**). L-Tyrosine-tyramide A (**7**) was synthesized as reported earlier [12].

5,5'-Dibromohemibastadin-1 (**8**). DBHB (**8**) was synthesized as reported earlier [12].

3.3. Determination of the In Vitro *Growth Inhibitory Concentrations*

Six cancer cell lines were obtained from the European Collection of Cell Cultures (ECACC; Salisbury, UK), the American Type Culture Collection (ATCC; Manassas, VA, USA) or the Deutsche Sammlung von Mikroorganismen and Zellkulturen (DSMZ, Braunschweig, Germany). These six cell lines included the MCF-7 breast cancer (DSMZ code ACC115), the A549 NSCLC (DSMZ code ACC107), the Hs683 oligodendroglioma (ATCC code HTB-138), the U373 glioblastoma (ECACC code 89081403), and the SKMEL-28 (ATCC code HTB-72) and B16F10 (ATCC code CRL-6475) melanoma cell lines. The cells were cultured in RPMI (Lonza, Verviers, Belgium) medium supplemented with 10% heat inactivated fetal bovine serum (Lonza). All culture media were supplemented with 4 mM glutamine, 100 µg/mL gentamicin, and 200 U/mL penicillin and 200 µg/mL streptomycin (Lonza). The overall growth level of the human cancer cell lines was determined using a colorimetric MTT (3-[4,5-dimethylthiazol-2-yl-diphenyltetrazolium bromide, Sigma, Diegemy, Belgium) assay as detailed previously [34–36]. Each experimental condition was performed in six replicates.

3.4. Computer-Assisted Phase Contrast Microscopy (Quantitative Videomicroscopy)

The direct visualization of the compound-induced cytostatic and/ or cytotoxic effects for the human U373 glioblastoma, human SKMEL-28 melanoma and mouse B16F10 melanoma cells was recorded as described previously [30,39]. Briefly, the quantitative videomicroscopy experiment was designed to capture digital images of the cell culture every four minutes for a 72 h period, providing 1,080 digitized images that can be visualized as dynamic movies that were approximately 1 min in length [30,39].

3.5. Flow Cytometry

Cell cycle analysis (propidium iodide staining) and apoptosis detection were performed simultaneously in U373 and SKMEL-28 cells with the APO TUNEL detection kit (BD Pharmingen, Erembodegem, Belgium) following the manufacturer's recommendations. A similar procedure was described in [44]. Narciclasine, an isocarbostyril isolated from *Narcissus* bulbs was assayed on PC-3 prostate cancer cells (DSMZ code ACC465) as a positive control for the apoptosis measurements [36]. The experiment was performed once in triplicate.

3.6. In Vitro *Anti-Angiogenesis Analyses*

Human HUVECs were established as primo cultures according to a method we described previously [42]. Their ability to form tubular networks was evaluated by seeding 100,000 cells/well in a six well plate containing pure Matrigel (BD Pharmingen) [42]. Experiments were conducted once, in triplicate, with 5 images per well taken at time = 0 h, 3 h, 6 h, 9 h and 24 h.

*3.7. Formulating DBHB (**8**) for* in Vivo *Analyses*

DBHB was formulated as a suspension at a concentration of 5 mg/mL in a solution of NaCl 0.9% for i.v. infusion (B. Braun, Diegem, Belgium). To ensure homogeneity, the pre-mix was vortexed and then homogenized using a high speed homogenizer composed of an IKA® T10 Basic rotor connected to an SN10 G5 dispersing element (Boutersem, Belgium) at a speed of 24,000 rpm for 5 min in an ice bath to avoid temperature increases during the process, which could possibly damage the compound. A solution of NaCl 0.9% for infusion was chosen as the dispersant medium to ensure that the injection suspension has the same osmolality as the blood fluid.

3.8. The in Vivo *Model of Lung Pseudometastases from Mouse B16F10 Melanoma*

We injected 250,000 B16F10 melanoma cells per mouse into the tail vein of C57Bl/6 6 week old female mice (Charles River, France). Lung pseudometastases developed, leading to animal death within 3 to 4 weeks without treatment [44]. Eleven mice per experimental condition were used. Treatments used in the present study are detailed in section 3.6 of Results and Discussion. The experiment was conducted with the authorization no. LA1230568 of the Animal Ethics Committee of the Federal Department of Health, Nutritional Safety, and the Environment (Belgium).

3.9. Scratch Wound Assay

The procedure used in the scratch wound assays was described previously [29,30]. Briefly, cells were seeded and cultured in 25 cm² flasks with 10% FBS until confluence. The wound was manually performed with a 200 µL pipette tip. Cells were washed before exposure to compound **8** at the appropriate FBS concentration (1 or 10%) or left untreated in the same medium and placed in the videomicroscopy incubator device. The experiments were conducted once, in quadruplicate. We were unable to use the software for one sample because of contrast difficulty (n = 3 for the control condition at 1% FBS).

*3.10. Determination of DBHB (**8**) Affinity to Albumin*

The albumin binding affinity of **8** was investigated with an HPLC based assay. A DBHB (**8**) stock solution (0.1 mM in 50% MeOH) was prepared and differing amounts of the stock were added to seven different 2 mL glass vials containing an albumin (Sigma-Aldrich) solution (0.1 mM in 50% MeOH). MeOH (50%) was added to end up with molar ratios (DBHB: albumin) of 1:4, 1:2, 3:4, 1:1, 2:1, 3:1 and 5:1 in a final volume of 2 mL. The samples were mixed thoroughly by utilizing a vortex for approximately 10 s each and subsequently incubated under shaking (200 rpm) at 37 °C for 1 h. Then, all samples where centrifuged at 13.300 rpm for 10 min. 50 µL of the supernatant of all samples were injected into a Dionex Ultimate 3000 HPLC System and the concentration was calculated on the basis of quantification via AUC integration. A three point calibration was performed with DBHB (**8**) samples, treated identically to the samples above. The amount of DBHB (**8**) was determined indirectly as follows:

$$n\,(\text{bound}) = n\,(100\%) - n\,(\text{free})$$

4. Conclusions

Bastadins, at least bastadin-6, -9 and -16 (compounds **1**–**3**), exhibit cytotoxic *versus* cytostatic effects at single digit µM concentrations for several mouse and cancer cell lines. While the anti-cancer effects are of similar levels in cancer cells sensitive to pro-apoptotic stimuli *versus* cancer cells displaying various levels of resistance to pro-apoptotic stimuli, the type of effects, *i.e.*, cytotoxic *versus* cytostatic, depend on the cell type analyzed. With an approximately ten times weaker *in vitro* growth inhibitory effect on the investigated cancer cell lines compared with bastadin-6, -9 and -16 (**1**–**3**), DBHB (5,5'-dibromohemibastadin; (8) exhibited both anti-angiogenic (HUVECs) and anti-migratory effects in mouse B16F10 melanoma cells. The anti-migratory effects that appeared at one-tenth of the IC_{50} *in vitro* growth inhibitory concentration were antagonized by increasing percentages of serum in the culture media of the B16F10 melanoma cells. Further experiments demonstrated that DBHB bound strongly to albumin, possibly explaining the treatment failure of DBHB delivered through the i.v. route in an *in vivo* tumor model. Anti-migratory compounds that decrease the migration levels of cancerous cells may increase sensitivity of those cancer cells to the cytotoxic damages experienced with conventional chemotherapy and radiotherapy. This suggests that an anti-migratory compound such as DBHB, which is also anti-angiogenic, could be delivered prior to conventional radiotherapy and/or chemotherapy to sensitize migrating cancer cells to these conventional therapies.

While our *in vivo* experiments with DBHB failed to increase the survival of B16F10 melanoma-bearing mice, it may be possible in the future to develop inhalation formulations to deliver DBHB directly to the lung (thus avoiding albumin binding) as we recently demonstrated for temozolomide [45,46]. Lung cancer may be an ideal first clinical target for these compounds because it is a deadly disease with dismal prognoses and a high resistance to conventional as well as targeted therapies [47–49]. The local delivery of an anti-migratory, but non-cytostatic and non-cytotoxic, agent such as DBHB, with limited systemic side effects, could contribute added therapeutic benefits to conventional cytotoxic radiotherapy and chemotherapy and even targeted therapies (kinase inhibitors; anti-receptor antibodies) in the specific combat against lung cancers.

Acknowledgments

Authors warmly thank Thierry Gras for his excellent technical assistance in cell cultures. Robert Kiss is a Director of Research with the *Fonds National de la Recherche Scientifique* (FNRS, Belgium). Peter Proksch wants to thank the Federal Ministry of Education and Research (BMBF) for support.

References

1. Kazlauskas, R.; Lidgard, R.O.; Murphy, P.T.; Well, R.J. Brominated tyrosine-derived metabolites from the sponge *Ianthella basta*. *Tetrahedron Lett.* **1980**, *21*, 2277–2280.
2. Kazlauskas, R.; Lidgard, R.O.; Murphy, P.T.; Well, R.J.; Blount, J.F. Brominated tyrosine-derived metabolites from the sponge *Ianthella basta*. *Aust. J. Chem*. **1981**, *34*, 765–786.
3. Park, S.K.; Park, H.; Scheuer, P.J. Isolation and structure determination of a new bastadins from the marine sponge *Ianthella basta*. *Bull. Korean Chem. Soc.* **1994**, *15*, 534–537.
4. Pettit, G.R.; Butler, M.S.; Bass, C.G.; Doubek, D.L.; Williams, M.D.; Schmidt, J.M.; Pettit, R.K.; Hooper, J.N.; Tackett, L.P.; Filiatrault, M.J. Antineoplastic agents, 326. The stereochemistry of bastadins 8, 10, and 12 from the Bismarck archipelago marine sponge *Ianthella basta*. *J. Nat. Prod*. **1995**, *58*, 680–688.
5. Coll, J.C.; Kearns, P.S.; Rideout, J.A.; Sankar, V. Bastadin 21, a novel isobastarane metabolite from the Great Barrier Reef marine sponge *Ianthella quadrangulata*. *J. Nat. Prod*. **2002**, *65*, 753–756.
6. Calcul, L.; Inman, W.D.; Morris, A.A.; Tenney, K.; Ratman, J.; McKerrow, J.H.; Valeriote, F.A.; Crews, P. Additional insights on the bastadins: Isolation of analogues from the sponge *Ianthella cf. reticulata* and exploration of the oxime configurations. *J. Nat. Prod.* **2010**, *73*, 365–372.
7. Carroll, A.R.; Kaiser, S.M.; Davis, R.A.; Moni, R.W.; Hooper, J.N.; Quinn, R.J. A bastadins with potent and selective delta-opioid receptor binding affinity from the Australian sponge *Ianthella flabelliformis*. *J. Nat. Prod.* **2010**, *73*, 1173–1176.
8. Couladouros, E.A.; Pitsinos, E.N.; Moutsos, V.I.; Sarakinos, G. A general method for the synthesis of bastaranes and isobastaranes: First total synthesis of bastadins 5, 10, 12, 16, 20, and 21. *Chemistry* **2004**, *11*, 406–421.
9. Masuno, M.N.; Pessah, I.N.; Olmstead, M.M.; Molinski, T.F. Simplified cyclic analogues of bastadins-5. Structure-activity relationships for modulation of the Ryr1/FKBP12 Ca^{2+} channel complex. *J. Med. Chem.* **2006**, *49*, 4497–4511.

Publication 3

10. Zieminska, E.; Lazarewicz, JW.; Couladouros, E.A.; Moutsos, V.I.; Pitsinos, E.N. Open-chain half-bastadins mimic the effects of cyclic bastadins and calcium homeostasis in cultured neurons. *Bioorg. Med. Chem. Lett.* **2008**, *18*, 5734–5737.
11. Ortlepp, S.; Sjögren, M.; Dahlström, M.; Weber, H.; Ebel, R.; Edrada, R.; Thoms, C.; Schupp, P.; Bohlin, L.; Proksch, P. Antifouling activity of bromotyrosine-derived sponge metabolites and synthetic analogues. *Mar. Biotechnol.* **2007**, *9*, 776–785.
12. Bayer, M.; Hellio, C.; Maréchal, J.P.; Frank, W.; Lin, W.; Weber, H.; Proksch, P. Antifouling bastadins congeners target mussel phenoloxidase and complex copper(II) ions. *Mar. Biotechnol.* **2011**, *13*, 1148–1158.
13. Chen, L.; Molinski, T.F.; Pessah, I.N. Bastadin 10 stabilizes the open conformation of the ryanodine-sensitive Ca^{2+} channel in an FKBP12-dependent manner. *J. Biol. Chem*. **1999**, *274*, 32603–32612.
14. Masuno, M.N.; Hoepker, A.C.; Pessah, I.N.; Molinski, T.F. 1-*O*-Sulfatobastadins-1 and -2 from *Lanthella basta* (Pallas). Antagonists of the RyR1-FKBP12 Ca^{2+} channel. *Mar. Drugs* **2004**, *2*, 176–184.
15. Zieminska, E.; Stafiej, A.; Pitsinos, E.N.; Couladouros, E.A.; Moutsos, V.; Kozlowska, H.; Toczylowska, B.; Lazarewicz, J.W. Synthetic bastadins modify the activity of ryanodine receptors in cultured cerebellar granule cells. *Neurosignals* **2006**, *15*, 283–292.
16. Reddy, A.V.; Ravinder, K.; Narasimhulu, M.; Sridevi, A.; Satyanarayana, N.; Kondapi, A.K.; Venkateswarlu, Y. New anticancer bastadins alkaloids from the sponge *Dendrilla cactos*. *Bioorg. Med. Chem.* **2006**, *14*, 4452–4457.
17. Greve, H.; Kehraus, S.; Krick, A.; Kelter, G.; Maier, A.; Fiebig, H.H.; Wright, A.D.; König, G.M. Cytotoxic bastadin 24 from the Australian sponge *Ianthella quadrangulata*. *J. Nat. Prod.* **2008**, *71*, 309–312.
18. Kotoku, N.; Tsujita, H.; Hiramatsu, A.; Mori, C.; Koizumi, N.; Kobayashi, M. Efficient total synthesis of bastadins 6, an anti-angiogenic brominated tyrosine-derived metabolite from marine sponge. *Tetrahedron* **2005**, *61*, 7211–7218.
19. Kotoku, N.; Hiramatsu, A.; Tsujita, H.; Hirakawa, Y.; Sanagawa, M.; Aoki, S.; Kobayashi, M. Structure-activity relationship study of bastadins 6, an anti-angiogenic brominated-tyrosine derived metabolite from marine sponge. *Arch. Pharm*. **2008**, *341*, 568–577.
20. Aoki, S.; Cho, S.H.; Hiramatsu, A.; Kotoku, N.; Kobayashi, M. Bastadins, Cyclic tetramers of brominated-tyrosine derivatives, Selectively inhibit the proliferation of endothelial cells. *J. Nat. Med.* **2006**, *60*, 231–235.
21. Aoki, S.; Cho, S.H.; Ono, M.; Kuwano, T.; Nakao, S.; Kuwano, M.; Nakagawa, S.; Gao, J.Q.; Mayumi, T.; Shibuya, M.; Kobayashi, M. Bastadin 6, a spongean brominated tyrosine derivative, inhibits tumor angiogenesis by inducing selective apoptosis to endothelial cells. *Anticancer Drugs* **2006**, *17*, 269–278.
22. Chen, K.G.; Sikic, B.I. Molecular pathways: Regulation and therapeutic implications of multidrug resistance. *Clin. Cancer Res*. **2012**, *18*, 1863–1869.
23. Lefranc, F.; Sadeghi, N.; Camby, I.; Metens, T.; De Witte, O.; Kiss, R. Present and potential future issues in glioblastoma treatment. *Expert Rev. Anticancer Ther*. **2006**, *6*, 719–732.
24. Maira, F.; Catania, A.; Candido, S.; Russo, A.E.; McCubrey, J.A.; Libra, M.; Malaponte, G.; Fenga, C. Molecular targeted therapy in melanoma: A way to reverse resistance to conventional drugs. *Curr. Drug Deliv*. **2012**, *9*, 17–29.

Publication 3

25. Fennell, D.A.; Swanton, C. Unlocking Pandora's box: personalizing cancer cell death in non-small cell lung cancer. *EPMA J.* **2012**, *3*, 6.
26. Bruyère, C.; Lonez, C.; Duray, A.; Cludts, S.; Ruysschaert, J.M.; Saussez, S.; Yeaton, P.; Kiss, R.; Mijatovic, T. Considering temozolomide as a novel potential treatment for esophageal cancer. *Cancer* **2011**, *117*, 2004–2016.
27. Nagaprashantha, L.; Vartak, N.; Awasthi, S.; Awasthi, S.; Singhal, S.S. Novel anti-cancer compounds for developing combinatorial therapies to target anoïkis-resistant tumors. *Pharm. Res.* **2012**, *29*, 621–636.
28. Okayama, H. Cell cycle control by anchorage signaling. *Cell Signal*. **2012**, *24*, 1599–1609.
29. Mathieu, V.; Mijatovic, T.; Van Damme, M.; Kiss, R. Gastrin exerts pleitropic effects on human melanoma cell biology. *Neoplasia* **2005**, *7*, 930–943.
30. Mégalizzi, V.; Mathieu, V.; Mijatovic, T.; Gailly, P.; Debeir, O.; De Neve, N.; Van Damme, M.; Bontempi, G.; Haibe-Kains, B.; Decaestecker, C.; *et al*. 4-IBP, A sigma1 receptor agonist, Decreases the migration of human cancer cells, Including glioblastoma cells, *in vitro* and sensitizes them *in vitro* and *in vivo* to cytotoxic insults of proapoptotic and proautophagic drugs. *Neoplasia* **2007**, *9*, 358–369.
31. Tabatabai, G.; Tonn, J.C.; Stupp, R.; Weller, M. The role of integrins in glioma biology and anti-glioma therapies. *Curr. Pharm. Des*. **2011**, *17*, 2402–2410.
32. Svensen, N.; Walton, J.G.; Bradley, M. Peptides for cell-selective drug delivery. *Trends Pharmacol. Sci*. **2012**, *33*, 186–192.
33. Mathieu, A.; Remmelink, M.; D'Haene, N.; Penant, S.; Gaussin, J.F.; Van Ginckel, R.; Darro, F.; Kiss, R.; Salmon, I. Development of a chemoresistant orthotopic human non-small cell lung carcinoma models in nude mice: Analyses of tumor heterogeneity in relation to the immunohistochemical levels of expression of ciclooxygenase-2, ornitine decarboxylase, lung-related resistance protein, prostaglandine-E synthetase, and glutathione-S-transferase-alpha (GST)-alpha, GST-mu, and GST-pi. *Cancer* **2004**, *101*, 1908–1918.
34. Van Goietsenoven, G.; Hutton, J.; Becker, J.P.; Lallemand, B.; Robert, F.; Lefranc, F.; Pirker, C.; Vandenbussche, G.; Van Antwerpen, P.; Evidente, A.; *et al*. Targeting of eEF1A with Amaryllidaceae isocarbostyrils as a strategy to combat melanomas. *FASEB J.* **2010**, *24*, 4575–4584.
35. Ingrassia, L.; Lefranc, F.; Dewelle, J.; Pottier, L.; Mathieu, V.; Spiegl-Kreinecker, S.; Sauvage, S.; El Yazidi, M.; Dehoux, M.; Berger, W.; *et al*. Structure-activity relationship analysis of novel derivatives of narciclasine (an Amaryllidaceae isocarbostyril derivative) as potential anticancer agents. *J. Med. Chem*. **2009**, *52*, 1100–1104.
36. Dumont, P.; Ingrassia, L.; Rouzeau, S.; Ribaucour, F.; Thomas, S.; Roland, I.; Darro, F.; Lefranc, F.; Kiss, R. The amaryllidaceae isocarbostyril narciclasine induces apoptosis by activation of the death receptor and/or mitochondrial pathways in cancer cells but not in normal fibroblasts. *Neoplasia* **2007**, *9*, 766–776.
37. Goffin, E.; Lamoral-Theys, D.; Tajedinne, N.; de Tullio, P.; Mondin, L.; Lefranc, F.; Gailly, P.; Rogister, B.; Kiss, R.; Pirotte, B. *N*-Aryl-*N*'-(chroman-4-yl)ureas and thioureas display *in vitro* anticancer activity and selectivity on apoptosis-resistant glioblastoma cells: Screening, synthesis of simplified derivatives, and structure-activity relationship analysis. *Eur. J. Med. Chem.* **2012**, *54*, 834–844.

38. Lallemand, B.; Masi, M.; Maddau, L.; De Lorenzi, M.; Dam, R.; Cimmino, A.; Moreno Y Banuls, L.; Andolfi, A.; Kiss, R.; Mathieu, V.; *et al*. Evaluation of *in vitro* anticancer activity of sphaeropsidins A-C, fungal rearranged pimarane diterpenes, and semisynthetic derivatives. *Phytochem. Lett.* **2012**, *5*, 770–775.
39. Delbrouck, C.; Doyen, I.; Belot, N.; Decaestecker, C.; Ghanooni, R.; de Lavareille, A.; Kaltner, H.; Choufani, G.; Danguy, A.; Vandenhoven, G.; *et al*. Galectin-1 is overexpressed in nasal polyps under budesonide and inhibits eosinophil migration. *Lab. Invest.* **2002**, *82*, 147–158.
40. Guzman, R.E.; Bolanos, P.; Delgado, A.; Rojas, H.; DiPolo, R.; Caputo, C.; Jaffe, E.H. Depolymerization and rearrangement of actin filaments during exocytosis in rat peritoneal mast cells: involvement of ryanodine-sensitive calcium stores. *Pflugers Arch.* **2007**, *454*, 131–141.
41. Bose, D.D.; Thomas, D.W. The actin cytoskeleton differentially regulates NG115–401L cell ryanodine receptor and inositol 1,4,5-triphosphate receptor induced calcium signaling pathways. *Biochem. Biophys. Res. Commun*. **2009**, *379*, 594–599.
42. Lefranc, F.; Mijatovic, T.; Mathieu, V.; Rorive, S.; Decaestecker, C.; Debeir, O.; Brotchi, J.; Van Ham, P.; Salmon, I.; Kiss, R. Characterization of gastrin-induced proangiogenic effects *in vivo* in orthotopic U373 experimental human glioblastomas and *in vitro* in human umbilical vein endothelial cells. *Clin. Cancer Res.* **2004**, *10*, 8250–8265.
43. Mackrill, J.J. Ryanodine receptor calcium channels and their partners as drug targets. *Biochem. Pharmacol.* **2010**, *79*, 1535–1543.
44. Mathieu, V.; Le Mercier, M.; De Neve, N.; Sauvage, S.; Gras, T.; Roland, I.; Lefranc, F.; Kiss, R. Galectin-1 knockdown increases sensitivity to temozlomide in a B16F10 mouse metastatic melanoma model. *J. Invest. Dermatol*. **2007**, *127*, 2399–2410.
45. Wauthoz, N.; Deleuze, P.; Hecq, J.; Roland, I.; Saussez, S.; Adanja, I.; Debeir, O.; Decaestecker, C.; Mathieu, V.; Kiss, R.; *et al*. *In vivo* assessment of temozolomide local delivery for lung cancer inhalation therapy. *Eur. J. Pharm. Sci*. **2010**, *39*, 402–411.
46. Wauthoz, N.; Deleuze, P.; Saumet, A.; Duret, C.; Kiss, R.; Amighi, K. Temozolomide-based dry powder formulations for lung tumor-related inhalation treatment. *Pharm. Res*. **2011**, *28*, 762–775.
47. Black, A.; Morris, D. Personalized medicine in metastatic non-small-cell lung cancer: Promising targets and current clinical trials. *Curr. Oncol.* **2012**, *19*, S73–S85.
48. Ganguli, A.; Wiegand, P.; Gao, X.; Carter, J.A.; Botterman, M.F.; Ray, S. The impact of second-line agents on patients' health-related quality of life in the treatment for non-small cell lung cancer: A systematic review. *Qual. Life Res*. **2012**, in press.
49. Nakata, A.; Gotoh, N. Recent understanding of the molecular mechanisms for the efficacy and resistance of EGF receptor-specific tyrosine kinase inhibitors in non-small cell lung cancer. *Expert Opin. Ther. Targets* **2012**, *16*, 771–781.

Sample Availability: Samples of the compounds **1**–**8** are available from the authors.

7 Publication 4

7.1 SAR of Sponge Inspired Hemibastadin Congeners Inhibiting Blue Mussel Phenoloxidase

Accepted for publication in: „Marine Drugs“ (05/05/2015)

Impact factor: 3.512

Contribution: 70 %, first author, conducting most of the syntheses, compound characterization, manuscript writing

Publication 4

Mar. Drugs **2015**, *13*, 1-x manuscripts; doi:10.3390/md130x000x

OPEN ACCESS

marine drugs

ISSN 1660-3397

www.mdpi.com/journal/marinedrugs

Communication

SAR of Sponge-Inspired Hemibastadin Congeners Inhibiting Blue Mussel Phenoloxidase

Hendrik Niemann [1], Jens Hagenow [1], Mi-Young Chung [1], Claire Hellio [2,3], Horst Weber [1] and Peter Proksch [1,*]

[1] Institute of Pharmaceutical Biology and Biotechnology, Heinrich-Heine-University Düsseldorf, Universitätsstrasse 1, Geb. 26.23, Düsseldorf 40225, Germany; E-Mails: hendrik.niemann@hhu.de (H.N.); jens.hagenow@hhu.de (J.H.); mi-young.chung@hhu.de (M.-Y.C.); horst.weber@hhu.de (H.W.)

[2] LEMAR UMR 6539 UBO CNRS Ifremer IRD, European Institute of Marine Studies (IUEM), Université de Bretagne Occidentale (UBO), European University of Brittany (UEB), Technopole Brest-Iroise, Plouzané 29280, France; E-Mail: Claire.Hellio@univ-brest.fr

[3] Biodimar, Université de Bretagne Occidentale (UBO), European University of Brittany (UEB), 6 Avenue Victor Le Gorgeu, CS93837, Brest cedex 3 29238, France

* Author to whom correspondence should be addressed; E-Mail: proksch@hhu.de; Tel.: +49-211-811-4163; Fax: +49-211-811-1923.

Academic Editor: Orazio Taglialatela-Scafati

Received: 27 January 2015 / Accepted: 5 May 2015 / Published:

Abstract: Hemibastadin derivatives, including the synthetically-derived 5,5′-dibromohemibastadin-1 (DBHB), are potent inhibitors of blue mussel phenoloxidase (PO), which is a key enzyme involved in the firm attachment of this invertebrate to substrates and, thus, a promising molecular target for anti-fouling research. For a systematic investigation of the enzyme inhibitory activity of hemibastadin derivatives, we have synthesized nine new congeners, which feature structural variations of the DBHB core structure. These structural modifications include, e.g., different halogen substituents present at the aromatic rings, different amine moieties linked to the (*E*)-2-(hydroxyimino)-3-(4-hydroxyphenyl)propionic acid, the presence of free *vs.* substituted aromatic hydroxyl groups and a free *vs.* methylated oxime group. All compounds were tested for their inhibitory activity towards the target enzyme *in vitro*, and IC_{50} values were calculated. Derivatives, which structurally closely resemble sponge-derived hemibastadins, revealed superior enzyme inhibitory properties *vs.* congeners featuring structural moieties that are absent in

the respective natural products. This study suggests that natural selection has yielded structurally-optimized antifouling compounds.

Keywords: antifouling; hemibastadin; phenoloxidase; sponges; copper; *Mytilus edulis*

1. Introduction

The world-wide ban of tributyltin (TBT) as an effective, but highly-toxic constituent of anti-fouling (AF) paints in 2008 has spurred the search for eco-friendly alternatives. Currently used compositions of antifouling paints, which are primarily based on copper in addition to so-called booster biocides, like cybutryne (Irgarol®), 3-(3,4-dichlorophenyl)-1,1-dimethylurea (Diuron®), zinc pyrithione (ZnPT), copper pyrithionine (CuPT) and chlorothalonil, have shown similar or even more severe toxic properties than TBT [1]. Therefore, also for these latter formulations, restrictions of usage, as already decided by the U.S. senate in 2011, will confine their use for maritime industries in the future. Washington became recently the first U.S. state to ban copper-based paints (containing more than 0.5% copper) from 2020 for boats less than 20 m [2]. It is thus urgent to develop new eco-friendly antifouling solutions using innovative concepts, such as biomimetic approaches and the use of compounds with high target specificity, but low general toxicity. Among invertebrate epibionts, blue mussels (*Mytilus edulis*) are considered to be one of the major macrofouling organisms that are known to readily settle on any kind of submerged, hard surface, such as ship hulls, cages used for aquaculture and others. Substrate attachment of *M. edulis* is established through adhesive plaques connected to a byssus stem. The formation of these plaques is catalyzed by a copper-depending phenol oxidase (PO) (E.C. 1.14.18.1), which oxidizes phenolic residues, such as tyrosine, to catechols, like 3,4-dihydroxy-L-phenylalanin (L-DOPA). The catechols are then further converted to *O*-quinones, which are present in so-called *M. edulis* foot proteins (Mefps) [3]. The redox-chemistry of L-DOPA mainly affects the formation of molecular networks within Mefps [4]. Being highly reactive chemical species, these *O*-quinone-bearing scleroproteins easily form intermolecular covalent cross-links with bionucleophils [5]. Until now, ten Mefps have been identified, while for Mefp-1, a firm attachment to substrates, like glass, plastic, wood, concrete and even Teflon®, has been shown [6].

In previous studies, sponge-derived hemibastadin derivatives and, in particular, their synthetic analogues, such as 5,5′-dibromohemibastadin-1 (DBHB) (**1**), demonstrated significant antifouling, but low/no general toxic properties towards marine invertebrates, thus highlighting these compounds as promising candidates for future anti-fouling applications [7,8]. DBHB (**1**) was subsequently shown to inhibit blue mussel PO *in vitro*, and the first structure-activity relationships for this compound and structurally related derivatives were reported [8]. It was shown that the α-hydroxyimino-amide moiety of hemibastadins represents an important pharmacophoric substructure of **1**, which is responsible for the strong copper-chelating properties of this compound, thereby presumably causing enzyme inhibition. Furthermore, the presence of bromine substituents at the phenolic rings of **1** increased the enzyme inhibitory properties. We have now synthesized a set of further hemibastadin analogues featuring structural modifications with regard to the substitution pattern of the aromatic rings, the amine substituents and the oxime group. All compounds were then analyzed for their inhibitory

activity against blue mussel PO, thereby allowing more detailed predictions on important structural features for future hemibastadin-derived antifouling candidates.

2. Results and Discussion

Hemibastadins consist of a brominated tyrosine moiety featuring an oxime function instead of the amino group and a likewise brominated tyramine unit linked to tyrosine through an amide bond. These compounds are the putative biogenetic building blocks of the more complex bastadins, all of them being typical secondary metabolites of the pacific elephant ear sponge (Ianthella basta). The synthetically-derived DBHB (**1**) was reported by our group as one of the strongest inhibitors of blue mussel PO known so far [8]. The synthetic hemibastadin analogues reported in this study (Figure 1) include several structural variations of the parent compound DBHB (**1**). In detail, we replaced the bromine atoms of the former by further halogen atoms, such as chlorine or iodine (**4**,**5**), methylated the phenolic hydroxyl groups, as well as the oxime function (**6**) and substituted the tyramine subunit of DBHB (**1**) by other acyclic or cyclic (including aromatic) amine substituents (**7**–**12**). In addition to these, newly-generated analogues of **1**, norbomohemibastadin-1 (**2**) and tyrosinyltyramine (**3**) that were available from our previous investigation [8] were included in this comparative study on PO inhibition (Figure 2). Analysis of this larger set of compounds suggested the following central structure-activity-relationship (SAR) statements:

Replacement of the bromine atoms of DBHB (**1**) by either chlorine (**4**) or iodine (**5**) resulted only in a negligible reduction of the inhibitory activity of the resulting analogues with very similar IC_{50} values of **4** (1.14 μM) and **5** (1.19 μM) compared to that of **1** (0.81 μM) (Figure 2). Complete loss of halogen substituents as present in norbromohemibastadin-1 (**2**) had a slightly more pronounced effect on the activity (IC_{50} 2.41 μM), indicating that the presence of bulky halogen atoms ortho to the phenolic hydroxyl groups increases the inhibitory activity, albeit only to a small extent. The actual size of the halogen substituents seems to be less important, as indicated by the very similar IC_{50} values of the chlorinated, brominated and iodinated analogues (**1**,**4**,**5**) of **2** (Figure 2).

Substitution of the tyramine unit of DBHB (**1**) by other aliphatic amines (**7**–**9**) had a clearly stronger effect and resulted in a considerable decrease of enzyme inhibitory activity of the different analogues when compared to DBHB (**1**) (Figure 2). The decline in inhibition of congeners bearing other araliphatic amines (**10**–**12**) was even more severe. The presence of the bulky and electron-rich tryptamine moiety *vs.* tyramine as present in Compound **12** resulted in a complete loss of activity. The importance of the p-hydroxyl function of brominated tyramine for the enzyme inhibitory activity of hemibastadin derivatives is apparent upon comparison of **1** with Compound **10**, which exhibits a phenylethylamine moiety instead of tyramine, which causes a strong reduction of inhibitory activity (Figure 2).

It was shown previously that the amine moiety is not an essential structural element that is required for the inhibition of blue mussel PO, as the small synthetic compound 2,3-butanedione monoxime (**13**) that features the alpha-oxo oxime group of the hemibastadins is likewise an enzyme inhibitor [8]. Nevertheless, one may hypothesize that the presence of two phenolic rings in the more active norbromohemibastadin-1 (**2**) with an IC_{50} of 2.41 μM compared to 8.70 μM for **13** [8] provides a better fit of the inhibitor to the enzyme and/or is involved in the stabilization of the enzyme-inhibitor complex.

Methylation of both the oxime moiety and the phenolic hydroxyl groups of DBHB (**1**) caused a more than twenty-fold reduction of the enzyme inhibitory activity of **6** compared to the parent compound **1** (Figure 2).

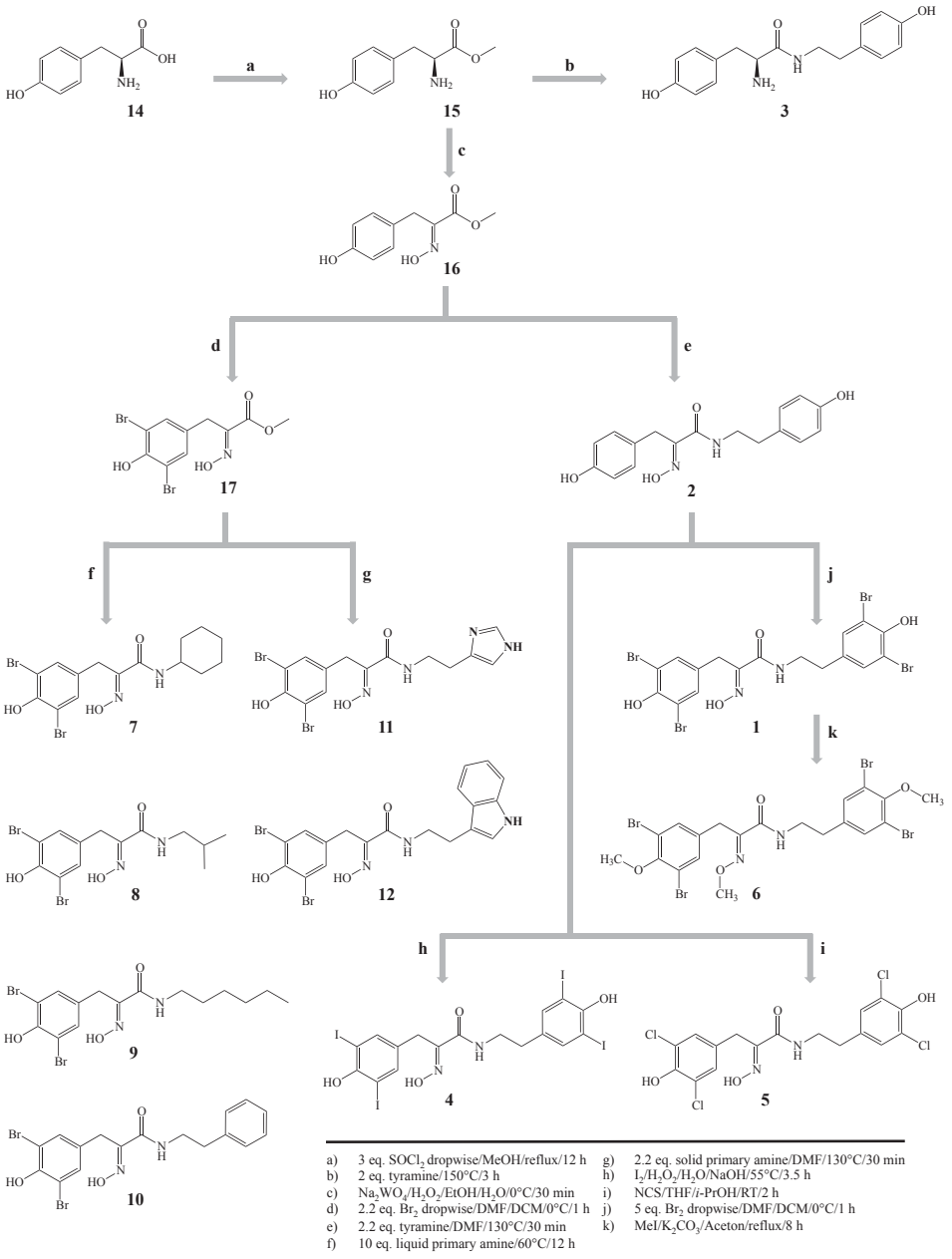

Figure 1. Synthetic approaches to the hemibastadin derivatives reported in this study.

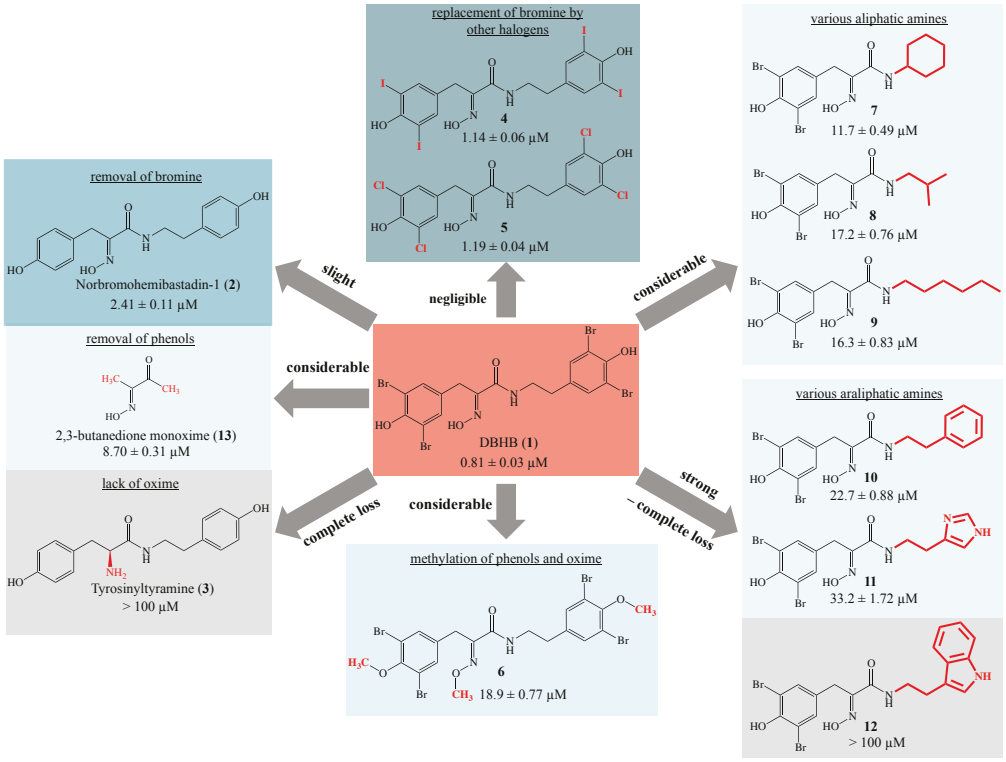

Figure 2. Inhibition of blue mussel phenoloxidase (PO) by 5,5′-dibromohemibastadin-1 (DBHB) (**1**) and its analogues as indicated by their IC_{50} values. Data for Compounds **2**, **3** and **13** were derived from a previous investigation [8].

However, methylation of the oxime hydroxyl group does not have a detrimental effect on the inhibitory activity, as is the case of tyrosinyltyramine (**3**), the latter being completely inactive with regard to the inhibition of blue mussel PO [8]. The alpha-oxo oxime substructure that is shared by the hemibastadins, as well as by 2,3-butanedione monoxime (**13**) has been shown to be responsible for the complexation of copper atoms that are present in the catalytic center of blue mussel PO [8]. Whether inhibition of blue mussel PO by DBHB (**1**) and by some of its derivatives is caused by direct complexation of copper ions in the active site of the enzyme or whether hemibastadins form a pre-Michaelis complex, which leads to a hindered substrate supply, as shown recently for the mushroom tyrosinase inhibitor tropolone [9], remain to be elucidated in future investigations.

3. Experimental Section

3.1. General Experimental Procedures

All reagents used in this study were purchased from commercial suppliers. Solvents for reactions and column chromatography were used at per analysis quality. MiliQ water and HiPerSolv CHROMANORM® Methanol (VWR) were used for HPLC analysis and purification steps. Thin-layer chromatography

(TLC) was performed using aluminum-backed plates coated with silica gel 60, F254 (Merck, Darmstadt, Germany), and compound spots were visualized by a UV lamp (LAMAG) at λ_{max} = 254 nm. Column chromatography was executed using silica gel (Macherey-Nagel, Silica 60 M, 0.04–0.063 mm). HPLC analysis was performed on a Dionex Ultimate 3000 System employing a Knauer VertexPlus Column (125 × 4 mm, Eurospher 100–10, C18). ESI mass spectra were recorded on a Thermoquest Finnigan LCQDeca connected to an Agilent 1100 Series LC. Preparative purification was performed on a Varian Prepstar connected to a Varian Prostar UV-detector. Semipreparative purification was accomplished on a Merck Hitachi system consisting of an L-7400 UV detector and an L-7100 pump connected with a Kipp&Zonen flatbed recorder with a Knauer VertexPlus C18 column (300 × 8 mm, Eurospher 100–10). All NMR spectra were recorded on a Bruker DRX 500 spectrometer (500 MHz ^{1}H, Bruker, Billerica, MA, USA) and are presented in the Supporting Information.

3.2. Blue Mussel PO Inhibition Assay

PO activity was measured spectrophotometrically as described earlier [3]. The purified enzyme was incubated at 25 °C with 10 mM L-DOPA in 50 mM phosphate buffer of pH 6.8. PO activity was determined by monitoring the increase of absorbance at 475 nm. One unit of enzyme activity was defined as the amount of enzyme that catalyzes the formation of 1 μmol dopachrome per minute under the described experimental conditions. Hemibastadin congeners were added to the assay at concentrations of up to 50 μg/mL. In addition, the biocide TBT (10 μg/mL) was used as a positive standard. Aliquots of pure enzyme were incubated for 2 h with hemibastadin analogues, then the enzyme activity was recorded with L-DOPA or catechol (10 mM) as substrates. All assays were run in triplicate. The results are presented as the concentration of compounds that reduces enzyme velocity by 50% (IC_{50} values). IC_{50} values were calculated using MINITAB (Version 14).

3.3. Synthetic Procedures

Hemibastadin analogues were synthesized by an optimized and extended method, as described earlier [7,8] (Figure 1). Structures were confirmed via LC-ESI-MS and ^{1}H-NMR (for spectra of new hemibastadin congeners see supporting information).

3.3.1. L-Tyrosine-methyl Ester (**15**)

L-Tyrosine (**14**, 10.06 g, 55.53 mmol) was converted into the methyl ester (**15**) by dropwise addition of three equivalents thionyl chloride ($SOCl_2$, 12.08 mL, 166.59 mmol) in methanol (100 mL) on ice. After complete addition of $SOCl_2$, the suspension was heated under reflux for 12 h. The resulting solution was concentrated *in vacuo* and the pH was adjusted to 8 with $NaHCO_3$, followed by exhaustive extraction with ethyl acetate. The organic phase was separated and dried over anhydrous magnesium sulfate. After solvent evaporation, 9.86 g of L-tyrosine-methyl ester (**15**) were obtained as a white, amorphous powder (50.53 mmol, 91.0%). Positive mode ESI-MS analysis revealed the pseudomolecular ion $[M + H]^+$ at *m/z* 196.

3.3.2. (*E*)-Methyl 2-(hydroxyimino)-3-(4-hydroxyphenyl)propanoate (**16**)

Oxidation of **15** to **16** was carried out according to a modified procedure of Boehlow *et al.* [10]. The ester **15** (8.59 g, 44 mmol) was dissolved in ethanol (100 mL) and stirred on ice. After the addition of H_2O (76 mL), equimolar amounts of sodium tungstate dihydrate ($Na_2WO_4 \cdot 2H_2O$, 44 mmol) and H_2O_2 (30% aqueous solution, 44 mL), the solution was stirred until the color changed into pale yellow, and TLC analysis (SiO_2, dichloromethane, ethyl acetate 3:1) revealed a complete turnover of the educt. After exhaustive extraction with ethyl acetate, the combined organic phases were washed with aqueous sodium hydrogen sulfite (2 × 100 mL) and H_2O (2 × 100 mL) and dried over anhydrous magnesium sulfate. The solvent was removed *in vacuo* to yield a pale yellow powder. The crude product was further purified by column chromatography (SiO_2, dichloromethane, ethyl acetate 3:1), and 7.09 g of pure **16** (33.90 mmol, 77.0%) were obtained as a nearly white amorphous powder. All spectral data were in accordance with previously reported values [10].

3.3.3. (*E*)-Methyl 3-(3,5-dibromo-4-hydroxyphenyl)-2-(hydroxyimino)propanoate (**17**)

The ester **16** (1 g, 4.78 mmol) was dissolved in dimethylformamide (10 mL) and diluted with dichloromethane (60 mL). After cooling on crushed ice, a solution of bromine (11 mL 1M-Br_2 in dichloromethane) was added dropwise during 20 min of stirring and cooling in the absence of light. TLC analysis was used to control complete bromination. Excessive bromine was reduced by the addition of aqueous 10% sodium hydrogen sulfite solution until the brown color was converted to pale yellow. The water phase was separated and extracted exhaustively with ethyl acetate. Both organic phases were washed with water, then combined and dried over anhydrous magnesium sulfate. After solvent evaporation, the resulting crude product was purified by column chromatography (SiO_2, dichloromethane, ethyl acetate 5:1) to yield 1.53 g of pure **17** (4.17 mmol, 87.3%) as an amorphous white powder. All spectral data were in accordance with previously reported values [10].

3.3.4. 5,5′-Dibromohemibastadin-1 (**1**) and Norbromohemibastadin-1 (**2**)

DBHB (**1**) and nobromohemibastadin-1 (**2**) were synthesized by replication of the protocol published earlier [8]. All spectral data were in accordance with previously reported values [8].

3.3.5. Tyrosinyltyramine (**3**)

Tyrosinyltyramine (**3**) was synthesized by replication of the protocol published earlier, and all spectral data were in accordance with [7].

3.3.6. Tetraiodo-norbromohemibastadin-1 (**4**)

Tetraiodo-norbromohemibastadin-1 (**4**) was synthesized by iodination of **2**, utilizing a modified method of Wada *et al.* [11]. Briefly, **2** (157.0 mg, 0.5 mmol) was dissolved in diluted sodium hydroxide solution (5 mL, pH 10), and H_2O_2 (30% aqueous solution, 0.12 mL) and iodine (I_2, 152.0 mg, 0.6 mmol) were added. The solution was stirred at 55 °C for 3 h. Excessive iodine was reduced by the addition of aqueous 10% sodium hydrogen sulfite solution. After solvent evaporation

in vacuo, the resulting crude product was purified by column chromatography (SiO_2, hexan, ethyl acetate, 4:1), and pure **4** (3.7 mg, 4.5 µmol, 0.9%) was obtained. **4**: ^{1}H (500 MHz, DMSO-d_6) δ 11.90 (s, 1H), 9.40 (s, 1H), 9.35 (s, 1H), 8.02 (t, J = 5.9 Hz, 1H), 7.56 (s, 2H), 7.54 (s, 2H), 3.65 (s, 2H), 3.30–3.26 (m, 2H), 2.61 (t, J = 7.2 Hz, 2H); ESI-MS $[M + H]^+$ *m/z* 818.7.

3.3.7. Tetrachloro-norbromohemibastadin-1 (**5**)

To a solution of **2** (157.0 mg 0.5 mmol) in a mixture of tetrahydrofuran (3 mL) and isopropanol (1 mL), *N*-chlorosuccinimide (333.8 mg, 2.5 mmol) was added in portions, and the suspension was stirred at room temperature for 2 h. After solvent evaporation *in vacuo*, the crude product was purified via column chromatography (SiO_2, dichloromethane, ethyl acetate 1:1), and semipreparative HPLC (gradient system of 0.1% trifluoro acetic acid and methanol) was conducted to obtain pure **5** as a yellow solid (3.7 mg, 8.2 µmol, 1.6%). **5**: ^{1}H (500 MHz, DMSO-d_6) δ 11.90 (s, 1H), 9.93 (s, 1H), 9.85 (s, 1H), 7.99 (t, J = 5.8 Hz, 1H), 7.15 (s, 2H), 7.14 (s, 2H) 3.69 (s, 2H), 3.33 (m, 2H), 2.67 (t, J = 7.0 Hz, 2H); ESI-MS $[M + H]^+$ 453.3, $[M - H]^-$ *m/z* 451.3.

3.3.8. Tri-*O*-methyl-5,5′-dibromohemibastadin-1 (**6**)

Methylation of both phenolic hydroxyls and of the oxime function of **1** (189 mg, 0.3 mmol) was achieved in acetone (6 mL) by the addition of potassium carbonate (207.0 mg, 1.5 mmol) and iodomethane (63.9 mg, 0.45 mmol), heating under reflux for 8 h and additional stirring at RT for 12 h. After solvent evaporation and subsequent purification of the crude product via semipreparative HPLC (gradient system of 0.1% trifluoro acetic acid and methanol), pure **6** (46.0 mg, 0.07 mmol, 23.0%) was obtained as a white powder. **6**: ^{1}H (500 MHz, DMSO-d_6) δ 8.27 (t, J = 5.8 Hz, 1H), 7.47 (s, 2H), 7.42 (s, 2H), 3.97 (s, 3H), 3.76–3.75 (m, 8H), 3.35 (t, J = 6.9 Hz, 2H), 2.73 (t, J = 6.9 Hz, 1H); ESI-MS $[M + H]^+$ *m/z* 672.9.

3.3.9. Amides Resulting from Liquid Primary Amines (**7**–**10**)

For the preparation of Compounds **7**–**10**, four aliquots of **17** (200 mg, 0.96 mmol) were dissolved in ten equivalents (9.6 mmol) of a liquid primary amine (for **7**: 1.11 mL cyclohexylamine; for **8**: 0.82 mL isobutylamine; for **9**: 1.26 mL *n*-hexylamine; for **10**: 1.21 mL phenethylamine), respectively, and stirred at 60 °C for 12 h in an open flask. For the general work-up, the crude products (**7**–**10**) were diluted with ethyl acetate (50 mL) and aqueous 10% HCl (10 mL). After separation, the aqueous phase was extracted exhaustively with ethyl acetate. The organic phases were combined and dried over anhydrous magnesium sulfate. After solvent evaporation, the resulting solids were further purified by column chromatography (SiO_2, dichloromethane, ethyl acetate 3:1) to obtain the pure compounds:

N-cyclohexyl-3-(3,5-dibromo-4-hydroxyphenyl)-2-(2-hydroxyimino)-propanamide (**7**): 371.8 mg (89.2%), ^{1}H-NMR (500 MHz, DMSO-d_6) δ 11.83 (s, 1H), 9.77 (s, 1H), 7.71 (d, J = 8.0 Hz, 1H), 7.35 (s, 2H), 3.69 (s, 2H), 3.66–3.53 (m, 1H), 1.72–1.62 (m, 3H), 1.55 (d, J = 11.0 Hz, 1H), 1.32–1.18 (m, 5H), 1.13–1.02 (m, 2H); ESI-MS $[M + H]^+$ *m/z* 435.1.

N-(2-methyl-propyl)-3-(3,5-dibromo-4-hydroxyphenyl)-2-(2-hydroxyimino)-propanamide (**8**): 385.5 mg (98.4%), ^{1}H (500 MHz, DMSO-d_6) δ 11.87 (s, 1H), 9.77 (s, 1H), 8.00 (t, J = 6.6 Hz, 1H),

7.34 (s, 2H), 3.71 (s, 2H), 2.95 (t, *J* = 6.6 Hz, 2H), 1.82–1.69 (1H, m), 0.80 (d, *J* = 6.6 Hz, 6H); ESI-MS $[M + H]^+$ *m/z* 409.0.

N-hexyl-3-(3,5-dibromo-4-hydroxyphenyl)-2-(2-hydroxyimino)-propanamide (**9**): 383.9 mg (91.7%), ^{1}H (500 MHz, DMSO-d_6) δ 11.86 (s, 1H), 9.76 (s, 1H), 7.98 (t, *J* = 6.6 Hz, 1H), 7.34 (s, 2H), 3.70 (s, 2H), 3.11 (dd, 2H, *J* = 6.6, 6.9 Hz), 1.40 (t, 2H, *J* = 6.9 Hz), 0.83 (t, *J* = 6.5 Hz, 3H); ESI-MS $[M + H]^+$ *m/z* 436.9.

N-2-phenylethyl-3-(3,5-dibromo-4-hydroxyphenyl)-2-(2-hydroxyimino)-propanamide (**10**): 409.0 mg (93.4%), ^{1}H (500 MHz, DMSO-d_6) δ 11.89 (s, 1H), 9.74 (s, 1H), 7.98 (t, *J* = 5.9 Hz, 1H), 7.34 (s, 2H), 7.25 (t, *J* = 7.4 Hz, 2H), 7.20–7.14 (m, 3H), 3.70 (s, 2H), 3.37 (dt, *J* = 5.9, 7.4 Hz, 2H), 2.75 (t, *J* = 7.4 Hz, 2H); ESI-MS $[M + H]^+$ *m/z* 457.2.

3.3.10. Amides Resulting from Solid Primary Amines (**11**, **12**)

Compounds **11** and **12** were obtained by triturating two aliquots of **17** (200 mg, 0.96 mmol) with the corresponding solid primary amine (each 2.11 mmol; for **11**: 234.5 mg histamine; for **12**: 338.1 mg tryptamine), adding dimethylformamide (3 mL) and melting at 130 °C for 30 min in an open flask. The resulting crude products were purified utilizing preparative HPLC (gradient system of 0.1% trifluoro acetic acid and methanol) to obtain the pure compounds:

N-[2-(4-imidazolyl)-ethyl]-3-(3,5-dibromo-4-hydroxyphenyl)-2-(2-hydroxyimino)-propanamide (**11**): 274.5 mg (64.1%), ^{1}H (500 MHz, DMSO-d_6) δ 14.27 (s, 1H), 11.98 (s, 1H), 9.81 (s, 1H), 8.96 (s, 1H), 8.21 (t, *J* = 6.0 Hz, 1H), 7.41 (s, 1H), 7.32 (s, 1H), 3.68 (s, 2H), 3.44 (dt, *J* = 6.0, 6.9 Hz, 2H), 2.83 (t, *J* = 6.9 Hz, 2H); ESI-MS $[M + H]^+$ *m/z* 447.2.

N-[2-(3-indolyl)-ethyl]-3-(3,5-dibromo-4-hydroxyphenyl)-2-(2-hydroxyimino)-propanamide (**12**): 274.8 mg (57.8%), ^{1}H (500 MHz, DMSO-d_6) δ 11.92 (s, 1H), 10.79 (s, 1H), 9.78 (s, 1H), 8.06 (t, *J* = 5.9 Hz, 1H), 7.54 (d, *J* = 7.8 Hz, 1H), 7.37 (s, 2H), 7.33 (d, *J* = 8.0 Hz, 1H), 7.14 (s, 1H), 7.06 (dd, *J* = 7.5, 7.8 Hz, 1H), 6.96 (dd, *J* = 7.5, 8.0 Hz, 1H), 3.72 (s, 2H), 3.43 (m, 2H, overlapped with solvent signal), 2.85 (t, *J* = 7.6 Hz, 2H); ESI-MS $[M + H]^+$ *m/z* 496.2.

4. Conclusions

In conclusion, among all synthetic analogues analyzed in this study, the natural product-like DBHB (**1**), which features all of the structural elements that are present in the sponge-derived hemibastadin and bastadin derivatives, showed the strongest inhibition of blue mussel PO. It is known that the enzyme inhibitory activity of DBHB (**1**) is paralleled by its strong antifouling activity, as demonstrated in experiments using barnacle larvae [7]. Naturally-occurring hemibastadins and bastadins show likewise strong anti-fouling activity against barnacle larvae [7]. Even though the latter had so far not been evaluated with regard to the inhibition of blue mussel PO, their close structural similarity to DBHB (**1**) strongly suggests that they will share the inhibitory activity of **1**. Based on the comparative investigations carried out in this study, it appears that natural selection has resulted in the accumulation of bastadin-like anti-fouling metabolites in the sponge. Since the preparation of DBHB (**1**) is comparatively simple, this synthetic compound is at the moment the most promising representative of bastadin-like compounds with regard to the inhibition of blue mussel PO.

Acknowledgments

The authors gratefully acknowledge financial support from the Arbeitsgemeinschaft industrieller Forschungsvereinigungen Projekt GmbH (AiF, Grant No. KF2388402AJ3).

Author Contributions

HN, JH and HW conducted syntheses of all investigated hemibastadin congeners in assistance of MYC. HN, JH, HW and PP analyzed spectroscopic data of LC-MS and NMR experiments. CH performed phenoloxidase inhibition assays and analyzed resulting data. PP and HW supervised all synthetic procedures. This manuscript was mainly written by HN, PP, HW and CH.

Conflicts of Interest

The authors declare no conflict of interest.

References

1. Bao, V.W.W.; Leung, K.M.Y.; Qiu, J.-W.; Lam, M.H.W. Acute toxicities of five commonly used antifouling booster biocides to selected subtropical and cosmopolitan marine species. *Mar. Pollut. Bull.* **2011**, *62*, 1147–1151.
2. Trepos, R.; Pinori, E.; Jonsson, P.R.; Berglin, M.; Svenson, J.; Coutinho, R.; Lausmaa, J.; Hellio, C. Innovative approaches for the development of new copper-free marine antifouling paints. *J. Ocean Technol.* **2015**, in press.
3. Hellio, C.; Bourgougnon, N.; Gal, Y.L. Phenoloxidase (E.C. 1.14.18.1) from the byssus gland of Mytilus edulis: Purification, partial characterization and application for screening products with potential antifouling activities. *Biofouling* **2000**, *16*, 235–244.
4. Numata, K.; Baker, P.J. Synthesis of adhesive peptides similar to those found in blue mussel (*Mytilus edulis*) using papain and tyrosinase. *Biomacromolecules* **2014**, *15*, 3206–3212.
5. Aladaileh, S.; Rodney, P.; Nair, S.V.; Raftos, D.A. Characterization of phenoloxidase activity in sydney rock oysters (*Saccostrea glomerata*). *Comp. Biochem. Physiol. B Biochem. Mol. Biol.* **2007**, *148*, 470–480.
6. Silverman, H.G.; Roberto, F.F. Understanding marine mussel adhesion. *Mar. Biotechnol.* **2007**, *9*, 661–681.
7. Ortlepp, S.; Sjögren, M.; Dahlström, M.; Weber, H.; Ebel, R.; Edrada, R.; Thoms, C.; Schupp, P.; Bohlin, L.; Proksch, P. Antifouling activity of bromotyrosine-derived sponge metabolites and synthetic analogues. *Mar. Biotechnol.* **2007**, *9*, 776–785.
8. Bayer, M.; Hellio, C.; Maréchal, J.-P.; Frank, W.; Lin, W.; Weber, H.; Proksch, P. Antifouling bastadin congeners target mussel phenoloxidase and complex copper(II) ions. *Mar. Biotechnol.* **2011**, *13*, 1148–1158.
9. Ismaya, W.T.; Rozeboom, H.J.; Weijn, A.; Mes, J.J.; Fusetti, F.; Wichers, H.J.; Dijkstra, B.W. Crystal structure of Agaricus bisporus mushroom tyrosinase: Identity of the tetramer subunits and interaction with tropolone. *Biochemistry* **2011**, *50*, 5477–5486.

10. Boehlow, T.R.; Harburn, J.J.; Spilling, C.D. Approaches to the synthesis of some tyrosine-derived marine sponge metabolites: Synthesis of verongamine and purealidin N. *J. Org. Chem.* **2001**, *66*, 3111–3118.
11. Wada, Y.; Harayama, Y.; Kamimura, D.; Yoshida, M.; Shibata, T.; Fujiwara, K.; Morimoto, K.; Fujioka, H.; Kita, Y. The synthetic and biological studies of discorhabdins and related compounds. *Org. Biomol. Chem.* **2011**, *9*, 4959–4976.

Supplementary Information

SAR of Sponge Inspired Hemibastadin Congeners Inhibiting Blue Mussel Phenoloxidase

Hendrik Niemann [1], Jens Hagenow [1], Mi-Young Chung [1], Claire Hellio [2,3], Horst Weber [1] and Peter Proksch [1,*]

[1] Institute of Pharmaceutical Biology and Biotechnology, Heinrich-Heine-Universitaty Düsseldorf, Universitätsstrasse 1, Geb. 26.23, Düsseldorf 40225, Germany; E-Mails: hendrik.niemann@hhu.de (H.N.), jens.hagenow@hhu.de (J.H.), mi-young.chung@hhu.de (M.C.), horst.weber@hhu.de (H.W.), proksch@hhu.de (P.P.)

[2] LEMAR UMR 6539 UBO CNRS Ifremer IRD, European Institute of Marine Studies (IUEM), Université de Bretagne Occidentale (UBO), European University of Brittany (UEB), Technopole Brest-Iroise, 29280 Plouzané, France.

[3] Biodimar, Université de Bretagne Occidentale (UBO), European University of Brittany (UEB), 6 Avenue Victor Le Gorgeu, CS93837, 29238 Brest cedex 3, France.

* Author to whom correspondence should be addressed; E-Mail: proksch@hhu.de (P.P.);
Tel.: +49-211-81-14163; Fax: +49-211-81-11923.

Figure S1. [1]H-NMR spectrum of tetraiodo-norbromohemibastadin-1 (**4**)

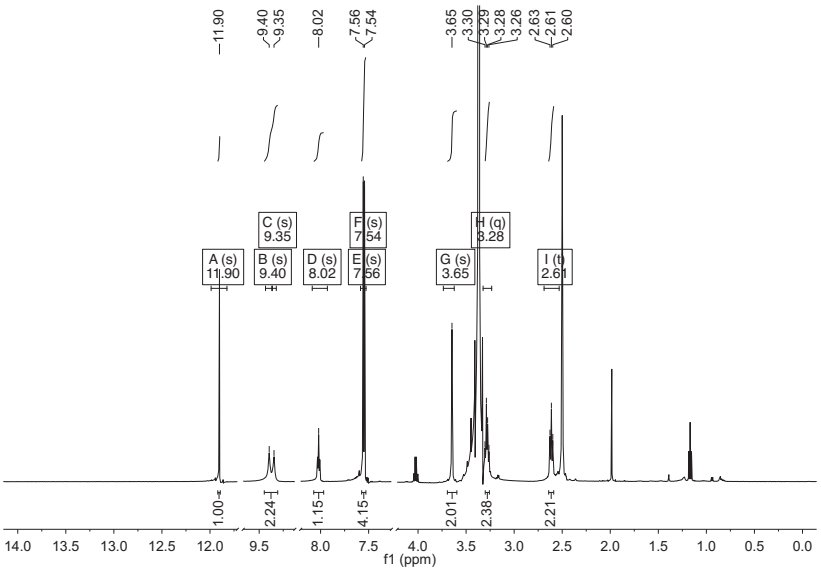

Figure S2. [1]H-NMR spectrum of tetrachloro-norbromohemibastadin-1 (**5**)

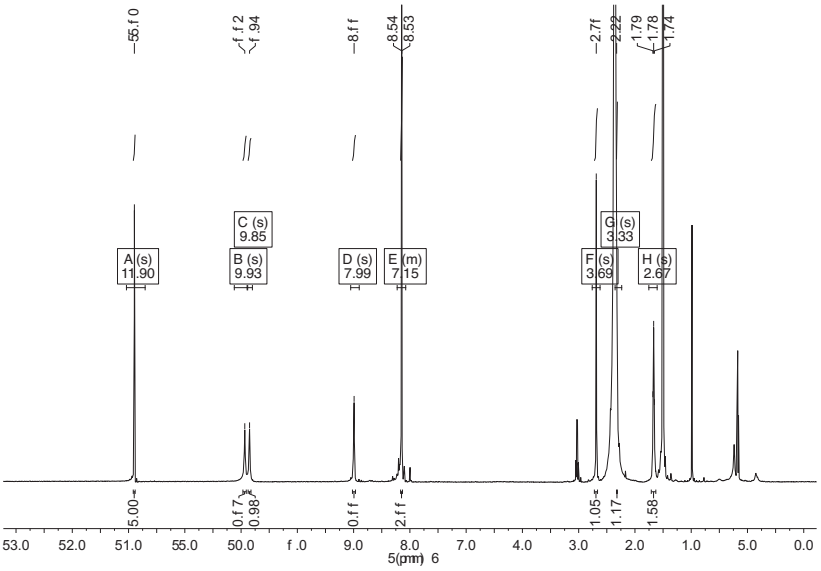

Figure S3. [1]H-NMR spectrum of trimethoxy-5,5'-dibromohemibastadin-1 (**6**)

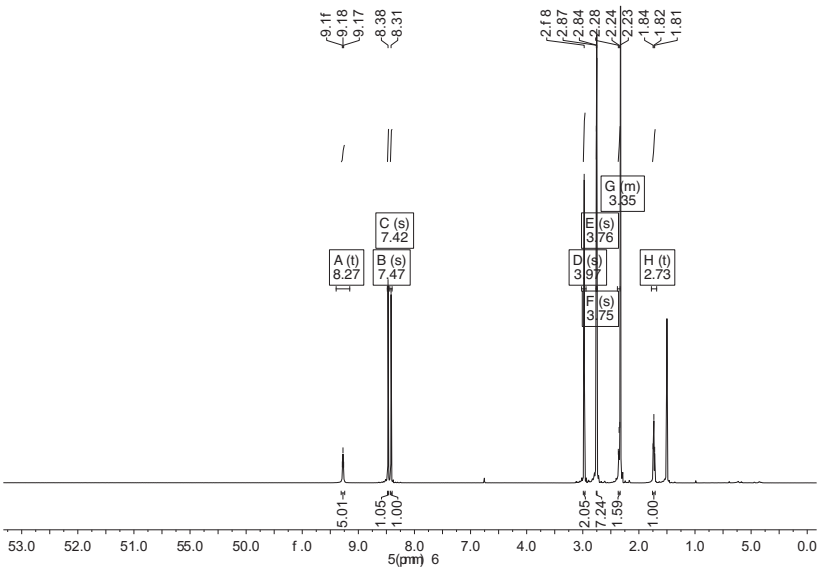

Figure S4. [1]H-NMR spectrum of N-cyclohexyl-3-(3,5-dibromo-4-hydroxyphenyl)-2-(2-hydroxyimino)-propanamide (**7**)

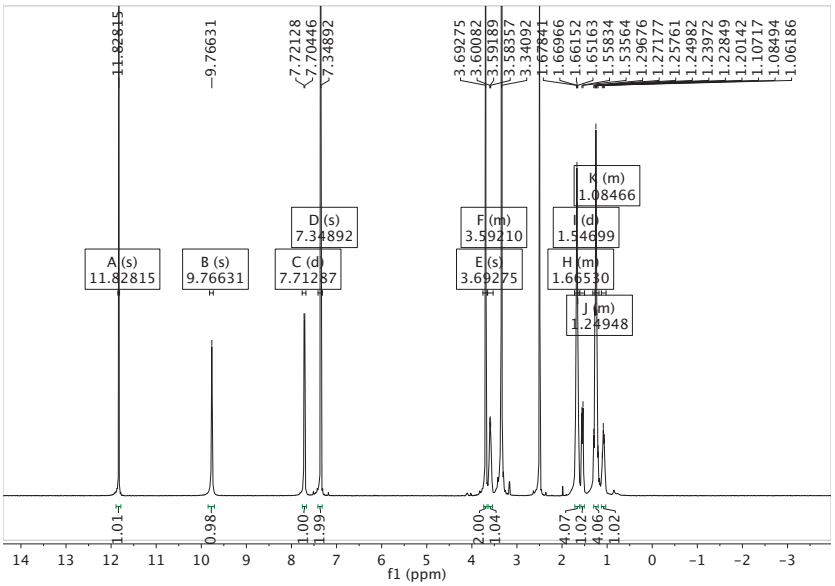

Figure S5. [1]H-NMR spectrum of N-(2-methyl-propyl)-3-(3,5-dibromo-4-hydroxyphenyl)-2-(2-hydroxyimino)-propanamide (**8**)

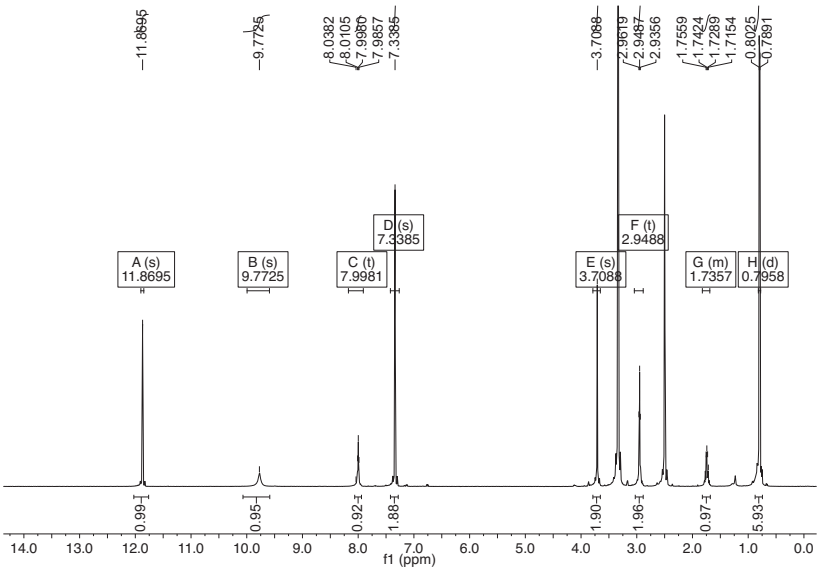

Figure S6. [1]H-NMR spectrum of N-hexyl-3-(3,5-dibromo-4-hydroxyphenyl)-2-(2-hydroxyimino)-propanamide (**9**)

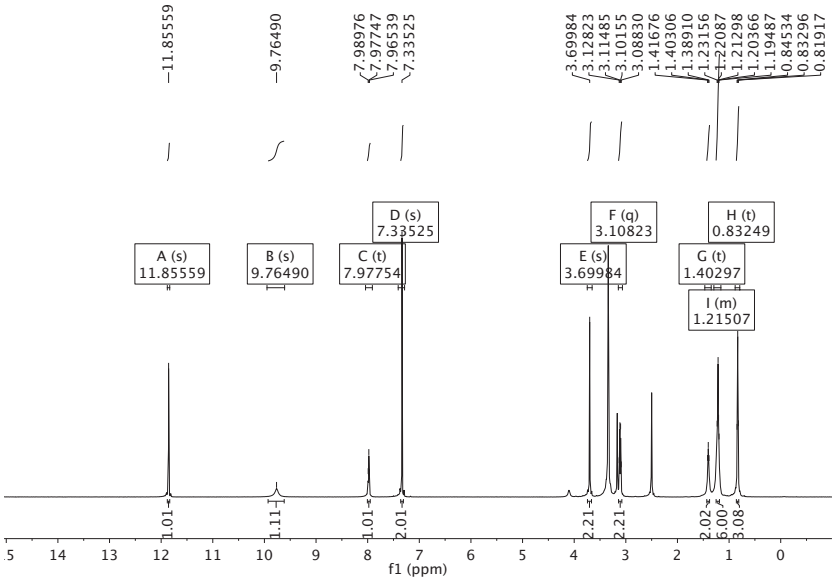

Figure S7. [1]H-NMR spectrum of N-2-phenylethyl-3-(3,5-dibromo-4-hydroxyphenyl)-2-(2-hydroxyimino)-propanamide (**10**)

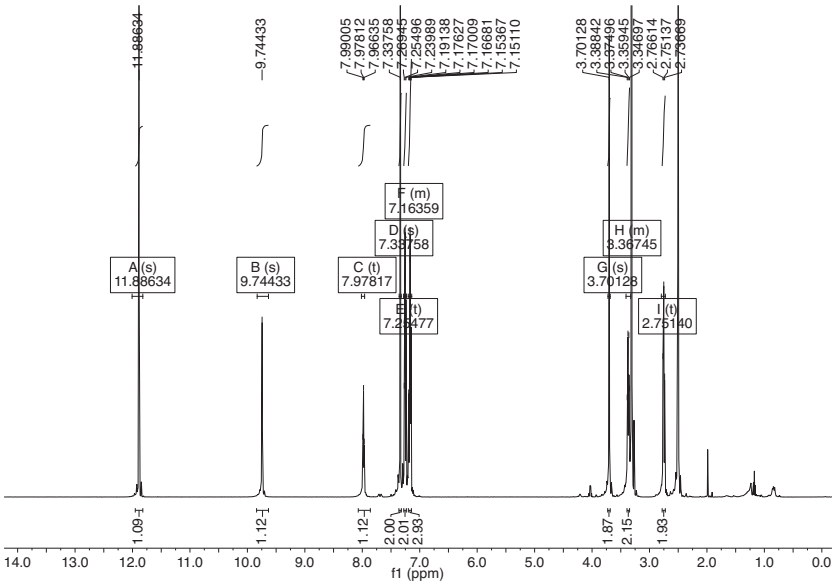

Figure S8. [1]H-NMR spectrum of N-[2-(4-imidazolyl)-ethyl]-3-(3,5-dibromo-4-hydroxyphenyl)-2-(2-hydroxyimino)-propanamide (**11**)

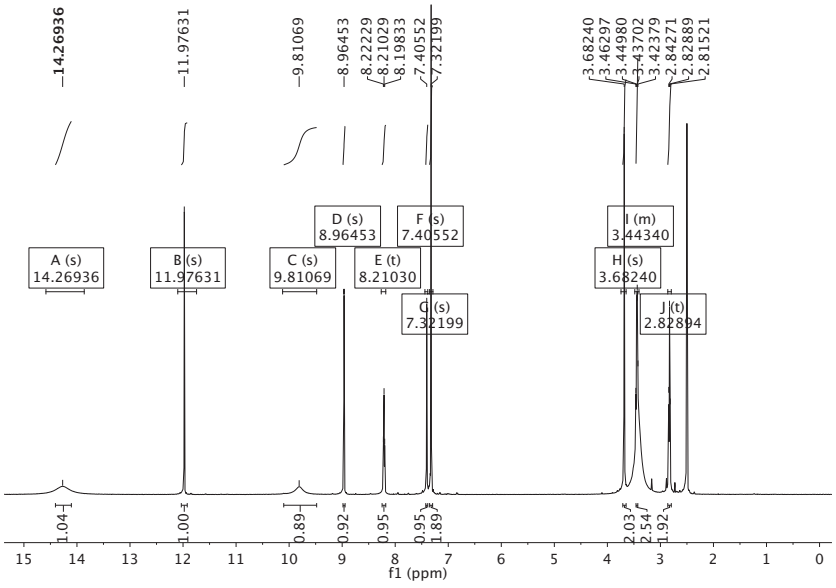

Figure S9. [1]H-NMR spectrum of N-[2-(3-indolyl)-ethyl]-3-(3,5-dibromo-4-hydroxyphenyl)-2-(2-hydroxyimino)-propanamide (**12**)

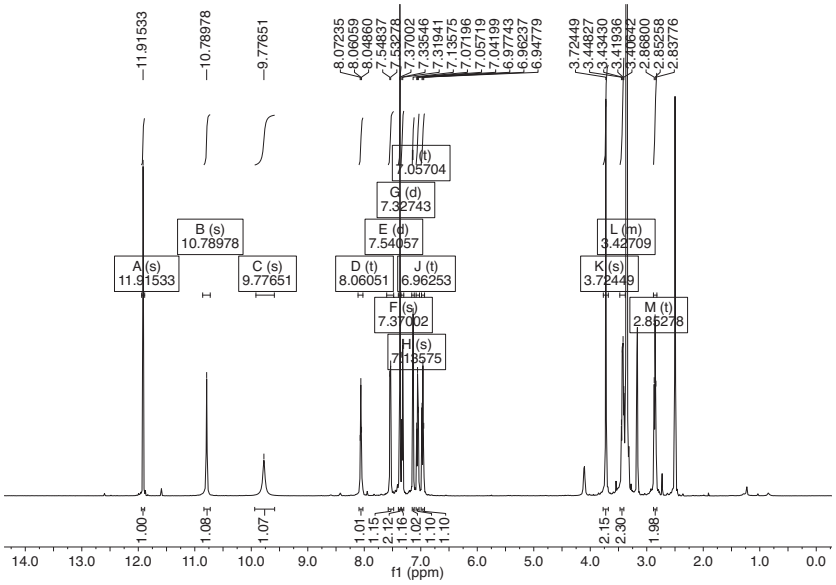

8 Publication 5

8.1 Brominated Skeletal Components of the Marine Demosponges, *Aplysina cavernicola* and *Ianthella basta*: Analytical and Biochemical Investigations

Published in: „Marine Drugs“

Impact factor: 3.512

Contribution: 30 %, conducting two sets of experiments (HPLC and LCMS analyses of skeleton MeOH extracts from *Ianthella basta* and *Aplysina cavernicola*), manuscript writing

Publication 5

Mar. Drugs **2013**, *11*, 1271-1287; doi:10.3390/md11041271

OPEN ACCESS

Marine Drugs

ISSN 1660-3397

www.mdpi.com/journal/marinedrugs

Article

Brominated Skeletal Components of the Marine Demosponges, *Aplysina cavernicola* and *Ianthella basta*: Analytical and Biochemical Investigations

Kurt Kunze [1], Hendrik Niemann [2], Susanne Ueberlein [3], Renate Schulze [3], Hermann Ehrlich [4], Eike Brunner [3,*], Peter Proksch [2] and Karl-Heinz van Pée [1]

[1] General Biochemistry, TU Dresden, Dresden 01062, Germany;
E-Mails: kurt.kunze@chemie.tu-dresden.de (K.K.);
Karl-Heinz.vanPee@chemie.tu-dresden.de (K.-H.P.)

[2] Institute of Pharmaceutical Biology and Biotechnology, Heinrich Heine University Duesseldorf, Universitaetsstrasse 1, Geb. 26.23, Duesseldorf 40225, Germany;
E-Mails: hendrik.niemann@uni-duesseldorf.de (H.N.); proksch@uni-duesseldorf.de (P.P.)

[3] Bioanalytical Chemistry, TU Dresden, Dresden 01062, Germany;
E-Mails: susanne.ueberlein@chemie.tu-dresden.de (S.U.);
renate.schulze@chemie.tu-dresden.de (R.S.)

[4] Institute of Experimental Physics, TU Bergakademie Freiberg, Freiberg 09596, Germany;
E-Mail: hermann.ehrlich@physik.tu-freiberg.de

* Author to whom correspondence should be addressed; E-Mail: eike.brunner@tu-dresden.de;
Tel.: +49-351-4633-7152; Fax: +49-351-4633-7188.

Received: 16 February 2013; in revised form: 18 March 2013 / Accepted: 26 March 2013 / Published: 17 April 2013

Abstract: Demosponges possess a skeleton made of a composite material with various organic constituents and/or siliceous spicules. Chitin is an integral part of the skeleton of different sponges of the order Verongida. Moreover, sponges of the order Verongida, such as *Aplysina cavernicola* or *Ianthella basta*, are well-known for the biosynthesis of brominated tyrosine derivates, characteristic bioactive natural products. It has been unknown so far whether these compounds are exclusively present in the cellular matrix or whether they may also be incorporated into the chitin-based skeletons. In the present study, we therefore examined the skeletons of *A. cavernicola* and *I. basta* with respect to the presence of bromotyrosine metabolites. The chitin-based-skeletons isolated from these sponges indeed contain significant amounts of brominated compounds, which are not easily extractable from the skeletons by common solvents, such as MeOH, as shown by HPLC analyses in combination with NMR and IR spectroscopic measurements. Quantitative

potentiometric analyses confirm that the skeleton-associated bromine mainly withstands the MeOH-based extraction. This observation suggests that the respective, but yet unidentified, brominated compounds are strongly bound to the sponge skeletons, possibly by covalent bonding. Moreover, gene fragments of halogenases suggested to be responsible for the incorporation of bromine into organic molecules could be amplified from DNA isolated from sponge samples enriched for sponge-associated bacteria.

Keywords: demosponges; brominated tyrosine-derivatives; halogenase; HPLC; NMR; IR

1. Introduction

Approximately 70% of the surface of our planet is covered by water, making the oceans the biggest habitat on earth that exhibits a high and still largely unexplored biodiversity. Numerous marine organisms are known to produce bioactive compounds [1,2], including, foremost, sponges [3]. Sponges are multicellular organisms [4,5] and represent the oldest and most primitive metazoans. These sessile animals have successfully adapted to various environments and show a global distribution. Sponges are not restricted to the seas, but occur also in fresh water, even though the majority of known sponge taxa live in the sea. In spite of their sessile nature and lack of morphological defense mechanisms (excluding spiculae), sponges, in most cases, successfully withstand predators, as well as overgrowth by fouling organisms. The evolutionary success of sponges is mainly due to an effective chemical defense that is based on deterrent, cytotoxic and/or antibiotically active compounds [3,6–8] that protect sponges from predators, such as fishes or mollusks, from overgrowth by fouling organisms and from infections caused by microbial pathogens.

Demosponges form the largest class of sponges [9]. They possess a skeleton made of a composite material with various organic constituents, such as proteins (spongin) [10], polysaccharides (chitin) [11,12] and/or siliceous spicules [9,13]. Chitin is an integral component of various invertebrates. Ehrlich *et al.* reported for the first time the presence of chitin as an integral part of the skeleton of different sponges of the order Verongida [11]. Meanwhile, chitin could also be found in the skeletons of further demosponges, like in species of the genus *Aplysina* [11,14], in *Verongula gigantea* [14] and in *Ianthella basta* [12]. All demosponge species, which were so far shown to exhibit a chitin-based skeleton, belong to the order Verongida.

Moreover, the order Verongida is well-known for the biosynthesis of brominated tyrosine-derivates, such as bastadin derivates or isoxazoline alkaloids [15,16]. These secondary metabolites have been shown to act against predators [6], competing marine invertebrates [17] or against bacteria [15]. For example, brominated tyrosine-derived compounds from the Verongida sponge, *Aplysinella rhax*, moderately inhibit bacterial chitinase [18]. Earlier investigations [11,14] demonstrated that the chitin-based skeletons of Verongida sponges contain tightly attached/incorporated organic compounds of yet unknown structure. This leads to the question: which organic compounds in addition to chitin adhere to the skeletons? Since brominated compounds, such as bromotyrosine derivatives, are characteristic natural products of Verongida sponges, such as *Aplysina* sp. or *I. basta*, it is possible that these compounds are not only present in the cellular matrix, but may also be incorporated into the

chitin-based skeletons. Early investigations showed the presence of aerothionin in the spherulous cells of the marine sponge *Aplysina fistularis* [19]. There is, however, also an earlier report demonstrating the localization of brominated compounds in the spherulous cells, as well as the skeletal fibers of *Aplysina aerophoba* [20]. That means the localization of bromotyrosine derivatives, as well as their origin within the sponge and the biosynthetic pathway leading to these molecules remain to be elucidated. Based on earlier studies [21,22], biosynthetic pathways leading to bastadins and isoxazoline alkaloids, such as aerothionin, can be proposed as described in Figure 1.

Figure 1. Hypothetical pathway for the biosynthesis of aerothionin in *A. cavernicola* and bastadins in *I. basta* according to Tymiak and Rinehart [21] and Leone-Stumpf [22]. Data available for biological halogenation reactions strongly suggest the involvement of flavin-dependent halogenases in the bromination reactions occurring during aerothionin and bastadin biosynthesis. The compound in brackets has not been isolated yet.

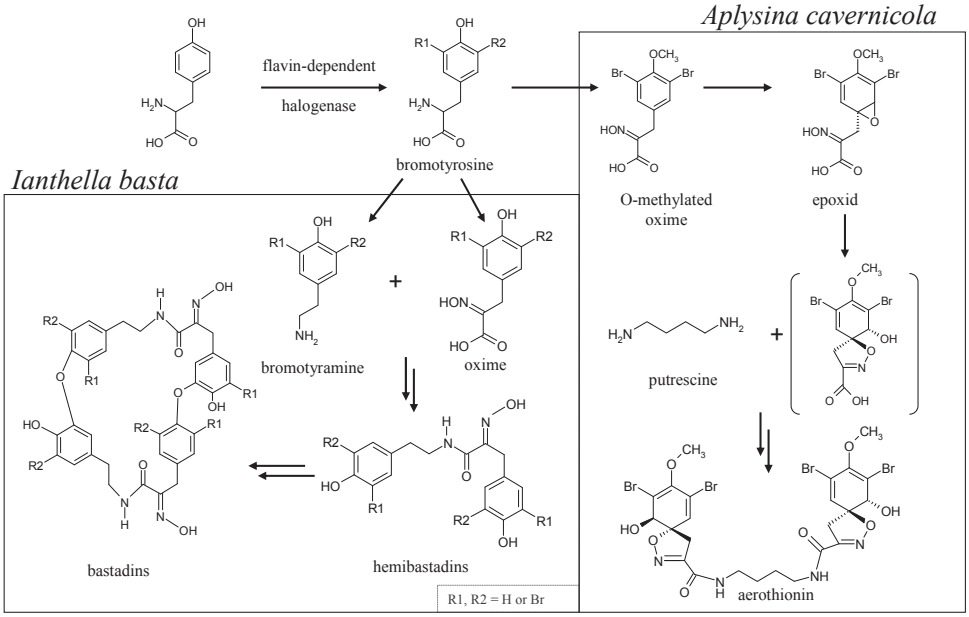

In recent years, it became increasingly evident that numerous compounds isolated from sponges are actually produced by bacterial symbionts [23]. The separation of the sponge from the bacterial symbionts with subsequent cultivation of the "bacterial free" sponge and the bacterial symbionts alone is not possible. Instead, the issue of the producing organism can be dealt with using molecular genetics. Accumulation of bacterial symbionts and isolation of their DNA allows the search for genes required for the biosynthesis of the respective metabolite using PCR primers or suitable probes for specific genes. In the case of bromotyrosines (aerothionin and bastadins; Figure 1) isolated from *A. cavernicola* and *I. basta*, suitable target genes are non-ribosomal peptide synthetase genes or genes coding for enzymes catalyzing the incorporation of bromine. In the last few years, it became evident that flavin-dependent halogenases are the type of halogenating enzymes involved in the regioselective incorporation of halogen atoms into aromatic and other compounds activated for attack by an

electrophilic halogen species [24]. The data gathered on flavin-dependent halogenases using different substrates should allow the construction of specific probes and PCR primers for the search for halogenase genes involved in the biosynthesis of the bromotyrosine derivatives produced by *A. cavernicola* and *I. basta*. Cloning of the respective genes with larger flanking regions and subsequent sequencing should at least allow for the decision of whether the producing organism is a bacterial symbiont or a eukaryote. If the producing organism turns out to be a bacterial symbiont, cloning of the complete gene cluster will allow the identification of the genes required for the biosynthesis of these bromotyrosine derivatives and the elucidation of the biosynthetic pathway.

The goal of the present study was to examine the skeletons of *A. cavernicola* and *I. basta* with respect to bromotyrosine metabolites. If present, these compounds were to be identified and compared to those occurring in the cellular matrix. Additionally, the DNA of the sponges, *A. cavernicola* and *I. basta*, was to be analyzed for the presence of halogenase genes likely to be involved in the biosynthesis of the brominated sponge-derived alkaloids, thereby addressing the question of whether microbial symbionts are the true producers of these compounds.

2. Results and Discussion

2.1. Isolation and Characterization of the Sponge Skeletons

The formerly described isolation [14] of pure chitin-scaffolds from marine sponges—which are an integral part of the sponge skeletons—is based on treatment with NaOH. This alkaline extraction, however, results in the hydrolytic degradation of any other skeleton-associated or incorporated biomolecules, such as bromotyrosine derivatives. Therefore, an alternative, milder extraction method had to be developed, which allows effective extraction and cleaning of the intact skeletons from other sponge components without chemical deterioration of labile constituents. H_2O and TE100 (10 mM Tris-HCl, 100 mM EDTA, pH 8) are "mild" solvents, which do not substantially modify biomolecules. Thus, TE buffers are commonly used in molecular biology/biochemistry to isolate, purify and store biomolecules (e.g., [25–28]). The optimized extraction procedure based on the treatment of the integer sponge with H_2O and TE100 is described in the Experimental Section. Figure 2 displays the results of these extraction experiments. It could be shown that TE100 extraction is favorable, especially in the case of the skeletons of *A. cavernicola*, since H_2O-based extraction took more than four weeks.

It was also observed that the skeleton of *I. basta* extracted with TE100 is slightly brighter compared to extraction with H_2O. This indicates that pigments are removed from the skeletons of *I. basta* by TE100. H_2O-based skeleton isolation was, therefore, preferred for *I. basta*. Apart from this observation, the microscopic images do not show any morphological damage caused by the extraction process. To analyze the chemical composition of the isolated skeletons, ATR FTIR and NMR studies were carried out. Figure 3 shows the ATR FTIR spectra of *A. cavernicola* after the different extraction steps before methanol extraction (see Figure 2). When comparing the spectra of the skeleton samples with those of the reference α-chitin, it becomes evident that characteristic vibrations of chitin are already visible in the TE100-treated sample. However, comparison of the spectra also reveals several striking differences. The amide II band occurs at 1550 cm^{-1} in pure chitin, whereas it is found at 1515 cm^{-1} in the skeleton samples. The intensity of both amide bands relative to the bands between

1000 and 1200 cm^{-1} (C–O stretching vibrations) is much higher in the skeleton samples compared with chitin. Moreover, the band at 1235 cm^{-1} observed for the skeleton samples does not occur in pure chitin. This wavenumber falls into the characteristic range of C–O and C–N stretching vibrations. These differences between the skeleton samples and pure chitin already indicate the presence of other organic compounds, probably amino acids/peptides/proteins or their derivatives attached to the chitin in the skeleton samples. Practically the same results were obtained for *I. basta* (see Supporting Information, Figure S1).

Figure 2. Scheme demonstrating the preparation of sponge skeletons, including skeleton isolation by H_2O or TE100, MeOH-based extraction of the skeletons and extraction of the chitin-based scaffold by NaOH (top: *A. cavernicola*, scale bar: 100 µm; bottom: *I. basta*, scale bar: 100 µm). The treatment procedures are described in Section 3.

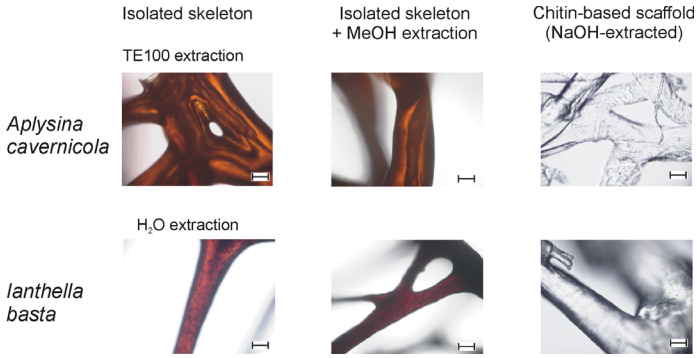

Figure 3. ATR FTIR spectra of the *A. cavernicola* skeleton samples after different isolation/preparation steps, except for MeOH extraction (see Figure 2). For comparison, the spectrum of an α-chitin reference sample is also shown. The assignment of the various bands is given in the Supporting Information, Table S1. The corresponding results obtained for *I. basta* are shown in the Supporting Information, Figure S1.

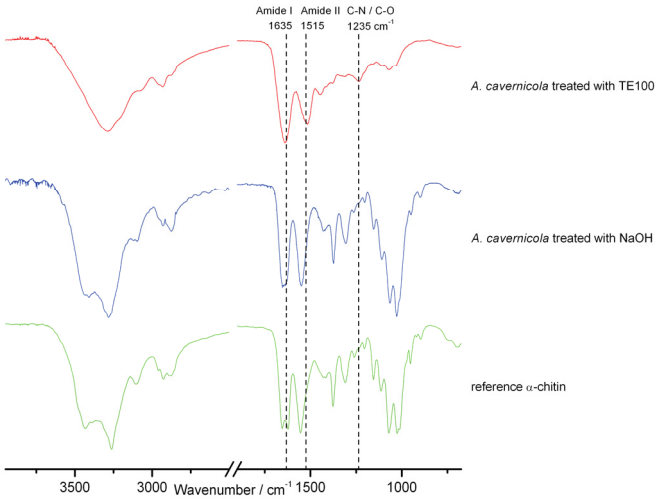

This is consistent with the observations made by ^{13}C solid-state NMR spectroscopy. The $^{13}C\{^1H\}$ CP MAS NMR spectra of *A. cavernicola* (Figure 4) clearly show the presence of further organic components in addition to the chitin scaffold. The spectrum of aerothionin, a major bromotyrosine derivative found in *A. cavernicola*, is also shown in Figure 4. The ^{13}C solid-state NMR spectrum of the *A. cavernicola* skeleton indeed shows several narrow signals characteristic of aerothionin, which are, however, very weak (see, also, Supporting Information, Figure S7). In addition to these narrow signals, the spectrum exhibits broader and more intense signals in the same characteristic regions of aromatic carbons/carbonyls, as well as in the aliphatic region, indicating the presence of organic material other than chitin in analogy to the infrared spectra described above. In order to prove that bromotyrosines or their derivatives may be present in the isolated sponge skeletons, the bromine content of the skeleton samples was measured by potentiometric titration following the protocol described in Section 3. (see also [29]). A bromine content of 40 µg Br per milligram sponge skeleton was measured before MeOH treatment (see below, Table 1).

Figure 4. $^{13}C\{^1H\}$ CP MAS NMR spectra of the skeletons of *A. cavernicola* after TE100 treatment. For comparison, the spectra of the pure chitin scaffold obtained after NaOH treatment and of pure aerothionin are also shown. The signal assignments follow from the inserts (for aerothionin, see, also, Supporting Information, Figure S2). The corresponding results obtained for *I. basta* are shown in the Supporting Information, Figures S3 and S4. * denotes spinning sidebands.

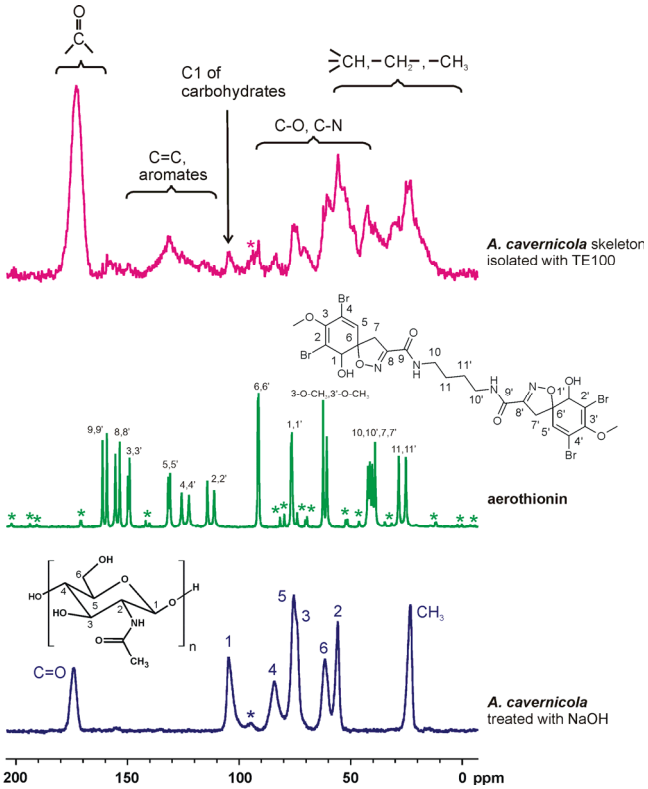

Table 1. Bromine contents of *A. cavernicola* and *I. basta* after different isolation/extraction steps measured by potentiometry. ***** Note that the bromine concentrations are related to the dry weight of the respective samples after the different isolation/extraction steps, thus representing the relative bromine contents in the remaining material.

	A. cavernicola **mg Br/g dry weight ***	***I. basta*** **mg Br/g dry weight ***
Sponge tissue	60 ± 5	72 ± 10
Skeleton (isolated)	40 ± 3	51 ± 4
Skeleton after MeOH extraction	35 ± 2	44 ± 4
Scaffold after NaOH treatment	0	0

In summary, it can, therefore, be stated that bromotyrosines or bromotyrosine derivatives may indeed be tightly bound to the skeletons. Since the extraction of these compounds from integer sponge samples usually relies on a MeOH-based extraction procedure [30], we have chosen this established protocol in order to extract the—spectroscopically detected—skeleton-associated compounds.

2.2. The Effect of MeOH Extraction upon the Isolated Sponge Skeletons

Both the MeOH-treated sponge skeletons and the MeOH extracts obtained from *A. cavernicola* and *I. basta* skeleton samples were analyzed. Surprisingly, the MeOH treatment did not result in any pronounced changes of the ATR FTIR and $^{13}C\{^{1}H\}$ CP MAS NMR spectra compared with the skeletons before MeOH extraction (see Supporting Information, Figures S5 and S6). This indicates that the established MeOH-based method extracts only small amounts of organic material from the skeletons. Most importantly, in order to decide whether or not brominated organic compounds are found among the remaining MeOH-insoluble, *i.e.*, tightly skeleton-associated organic material, the bromine content in the samples after the different isolation/extraction steps was measured by potentiometry. The results of these measurements are summarized in Table 1. Both sponges exhibit a similar behavior. The sponge tissue before any extraction procedure exhibits the highest relative amount of bromine. The isolated skeleton samples possess lower bromine concentrations. That means that the soluble parts of the sponge—which are removed from the skeletons by TE100 or H_2O treatment—contain higher concentrations of brominated compounds than the skeletons. Nevertheless, the isolated skeleton samples do still exhibit a significant amount of bromine-containing compounds, which are obviously not soluble in TE100 or H_2O. Subsequent MeOH treatment only results in the removal of a rather insignificant amount of bromine from the skeletons for both sponges, indicating that the majority of brominated skeletal compounds is strongly—maybe covalently—bound to the skeletons. In contrast, the NaOH treatment results in the complete removal of bromine from the sponge skeletons. These observations are in agreement with the described spectroscopic observations showing that the strongly skeleton-associated organic compounds are completely removed from the chitin-based scaffolds by NaOH. That means that the bromine found in the sponge skeletons is mainly associated with the NaOH-extractable, strongly skeleton-associated organic material.

Moreover, the MeOH extracts were analyzed by the established HPLC-based method (see Experimental Section). HPLC analysis of a skeleton extract from *A. cavernicola* showed trace amounts of aerothionin, which was confirmed by the on-line recorded UV spectrum and comparison of the

retention time with an authentic standard. The concentration was, however, too small to allow quantification. Several compounds with UV spectra typical for bromotyrosine derivatives were detected by HPLC in the MeOH extracts of *I. basta*. Comparison of the HPLC profiles from the skeleton extracts obtained from H_2O-treatment with a crude MeOH extract of fresh sponge tissue from the same specimen of *I. basta* (Figure 5) shows a high degree of analogy.

Figure 5. HPLC-DAD chromatograms of fresh sponge and H_2O-treated skeleton extracts of *I. basta* with the peaks of identified bastadins 3, 4, 6, 7, 9 and 16 detected at λ = 235 nm.

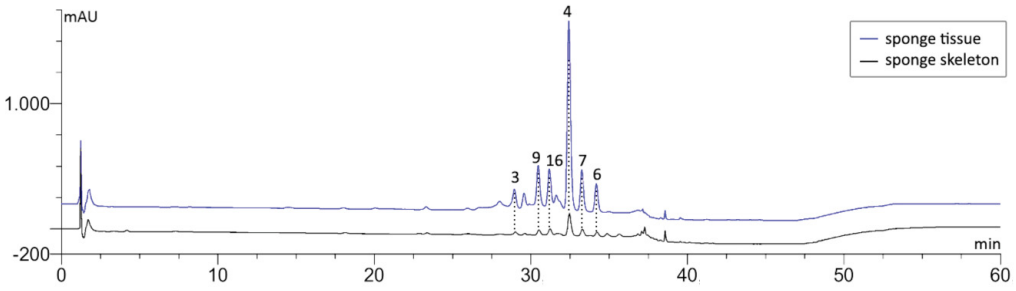

Comparison of the retention times of the six major peaks in the chromatogram of the H_2O-treated skeleton extract with authentic standards isolated from the same sponge specimen indicates the presence of bastadins 3, 4, 6, 7, 9 and 16 (see Supporting Information, Figure S8, for structures). Further confirmation for this tentative identification was achieved by LC-MS and comparison of the resulting pseudomolecular ions. A typical molecular ion cluster of a brominated compound was found in the negative mode at *m/z* 941.1 $[M - H]^-$, which indicates the presence of bastadin 3 (see Supporting Information, Figure S9, for the spectrum). HPLC-based comparison of the bastadin profiles present in extracts of sponge tissue and in extracts of the skeleton revealed the same major constituent (bastadin 4, Table 2) for both extracts, albeit at different percentages. Whereas bastadin 4 accounted for 56% of all detected bastadin derivatives in the tissue extract, this number decreased to 41% in the extract obtained from the skeleton. The percentages of several minor bastadins showed an opposite trend. For example, whereas bastadin 16 amounts to 10% of the bastadin profile from sponge tissue, the same compound reaches 20% in extracts from the skeleton. However, the total bastadin concentration found in the skeleton extracts of *I. basta* amounts to only 0.51 mg per gram dry weight. In contrast, an almost 300-fold higher total bastadin concentration was measured for the tissue extract (Table 2). This shows that most of the previously identified MeOH-extractable bromotyrosine derivatives, such as aerothionin and bastadins, were already removed from the sponge skeletons by TE100 or H_2O, indicating the localization of these compounds in sponge cells and/or symbionts.

In summary, it can therefore be stated that the total concentration of MeOH-soluble bromotyrosine derivatives in the sponge skeletons is very low for both species under study. It is, however, remarkable that the sponge skeletons contain a considerable amount of bromine even after exhaustive MeOH extraction. It should be noted that these compounds, which are tightly bound to the skeleton, could not be extracted by other common solvents, such as acetone, urea and ethylenediaminetetraacetic acid/sodium dodecyl sulfate. Therefore, we conclude that the skeletons contain insoluble, *i.e.*, strongly bound brominated compounds, which have not yet been identified.

Table 2. Contents of known bastadins identified in MeOH extracts of the *I. basta* skeleton and in sponge tissue.

Bastadin No.	Bastadin Content in Isolated Skeleton/ mg g^{-1} dry weight	Bastadin Content in Sponge Tissue/ mg g^{-1} dry weight
3	0.02	7
9	0.05	15
16	0.10	14
4	0.21	77
7	0.07	15
6	0.06	10
total	0.51	138

2.3. Genetic Analyses

DNA isolated from samples of the two sponges enriched for bacterial symbionts was found to be contaminated with pigments and required further purification to allow for its use in PCR and cloning experiments. This purification was achieved by size exclusion chromatography (see Supporting Information, Figure S10). Using the purified DNA, 600 bp gene fragments could be detected by PCR (Figure 6). The fragment obtained from bacteria associated with *I. basta* showed high homology to known genes of flavin-dependent halogenases accepting tyrosine or tyrosine derivatives as substrates. The amplified fragment from symbionts of *I. basta* shows high similarity (98%) to *bhaA*, a flavin-dependent halogenase from balhimycin biosynthesis in the bacterium, *Amycolatopsis balhimycina* (Figure 7, [31]). Like in bastadins and aerothionin, balhimycin contains a halogenated tyrosine derivative, indicating that the amplified halogenase gene fragment might also code for a halogenase accepting tyrosine or a tyrosine derivative as a substrate and might thus be part of the bastadin biosynthetic gene cluster. The high similarity to *bhaA* also suggests that the genes for bastadin biosynthesis originate from symbiotic bacteria. Hence, these genes should be clustered, too. The 600 bp gene fragment obtained from the bacterial symbionts enriched from *A. cavernicola* could not be sequenced. Thus, a second primer pair (HaloDetect_for/rev) was used, which allowed the PCR-amplification of a 300 bp gene fragment (Figure 6). The amino acid sequence derived from this gene fragment is almost identical (99%) to a putative halogenase gene fragment cloned from *A. cavernicola*-associated bacteria [23]. However, the substrate of this halogenase, as well as the putative biosynthetic pathway it might be involved in, are yet unknown. In order to obtain information about the regions flanking the halogenase genes and to allow cloning of the biosynthetic gene clusters, metagenomic cosmid libraries will be constructed and screened for the halogenase genes using the amplified fragments as probes. It can, however, be stated that our genetic analyses point towards the presence of halogenase genes of symbiotic origin. This is in line with the above described observation that the majority of the previously known bromotyrosine derivatives can be removed from the sponge skeletons simply by TE100 or H_2O. The above-described observation of strongly skeleton-associated brominated compounds raises the question of whether or not these substances are also of symbiotic origin.

Figure 6. Detection of genes of flavin-dependent halogenases in metagenomic DNA of *A. cavernicola* (*Ac*) and *I. basta* (*Ib*) via degenerated primer PCR; left: primer pair TyrhalA_for/rev; right: primer pair HaloDetect_for/rev; +: fragment of *clohal* (flavin-dependent halogenase from the clorobiocin biosynthetic gene cluster) as a positive control; −: H_2O as a negative control.

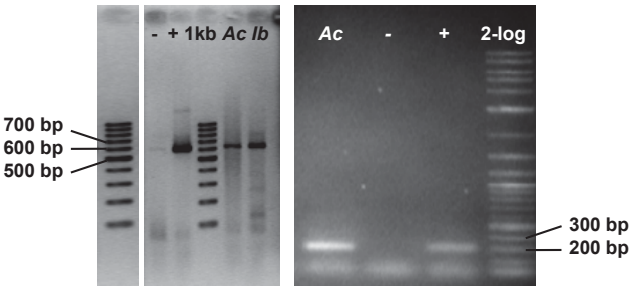

Figure 7. Comparison of the amino acid sequence derived from the 600 bp halogenase gene fragment obtained from bacteria associated with *I. basta* (Ib) to the halogenase BhaA from balhimycin biosynthesis [31] and of the 300 bp halogenase gene fragment from bacteria associated with *A. cavernicola* (Ac) with a halogenase gene fragment (Acclone 1) isolated by Bayer *et al.* from *A. cavernicola* [23]. Non-identical amino acids are shaded in grey.

```
BhaA       1 KGVVVREGCAVTDVVEDGERVTGARYTDPDGTEREVSARFVIDASGNKSR

Ib         1 AGVVVREGCAVTDVVEDGERVTGARYTDPDGTEREVSARFVIDASGNKSR


BhaA      51 LYTKVGGSRNYSEFFRSLALFGYFEGGKRLPEPVSGNILSVAFDSGWFWY

Ib        51 LYTKVGGSRNYSEFFRSLALFGYFEGGKRLPEPVSGNILSVAFDSGWFWY


BhaA     101 IPLSDTLTSVGAVVRREDAEKIQGDREKALNTLIAECPLISEYLADATRV

Ib       101 IPLSDTLTSVGAVVRREDAEKIQGDREKALNTLIAECPLIAEYLADATRV


BhaA     151 TTGRYGELRVRKDYSYQQETYWRPGMILVGDAACFVDPVFSSGVH

Ib       151 TTGRYGELRVRKDYSYQLETYWRPGMILVGDAACFVDPLFSRGVS



Acclone1   1 VVGPMDGLIRDRKGRPHEIFFEEVGNCAEIERRIAPGHQCRPVSVMKDFS

Ac         1 VVGPMDGLIRDRKGRPHEIFFEEVGNCAEIERRIAPAHQCRPVSVMKDFS


Acclone1  51 YRIDKMAGDGWIAIGDAFSFI

Ac        51 YRIDKMAGDGWIAIGDAFSFI
```

3. Experimental Section

3.1. Isolation of the Skeletons

3.1.1. Sponge Samples

The *A. cavernicola* sample was collected in the Mediterranean Sea (Hydra-Institute, Elba, Italy, www.hydra-institute.com [32]) and purchased from the Hydra Institut für Meereswissenschaften AG (Munich, Germany). The entire sponge was shock frozen immediately after underwater collection and was always kept frozen on dry ice during transport and storage. *I. basta* samples were collected by Prof. P. Schupp at Western Shoals in Apra Harbor (Guam); see also [12].

3.1.2. H_2O Extraction

Small pieces of *A. cavernicola* (approximately 10 g wet sponge) or *I. basta* (5–10 cm²) were soaked in 40 mL of distilled water for two weeks. Subsequently, the samples were transferred into freshly distilled water for 24 h. This procedure was repeated two times under continuous shaking.

3.1.3. TE100 Extraction

Small pieces of *A. cavernicola* (approximately 10 g wet sponge) or *I. basta* (5–10 cm^2) were soaked in 40 mL of TE100 (10 mM Tris-HCl, 100 mM EDTA, pH 8) for two weeks. Subsequently, the samples were transferred into freshly distilled water for 24 h. This was repeated six times under continuous shaking.

3.1.4. NaOH Extraction

Alkaline extraction was performed for extraction of the pure chitin-based skeletons, which were used as a reference. According to [14], the samples were treated with 2.5 M NaOH for 24 h. The remaining fibrous skeletal material was neutralized. In a second step, the samples were treated with 20% acetic acid for 24 h. Subsequently, the remaining fibrous skeleton material was neutralized. This procedure was repeated until a colorless fibrous material remained.

3.1.5. Methanol Extraction of the Purified Skeletons

The purified skeletons were put into 200 mL of methanol and sonicated for 1 min. Under stirring, the samples were treated with methanol for 24 h. Subsequently, the solvent was changed, and the skeletons were stirred in fresh methanol for a further 24 h. This procedure was repeated two times. Finally, all methanol extracts were combined, reduced in volume with a rotary evaporator and analyzed by HPLC. For *A. cavernicola*, extraction with methanol was followed by an acetonitrile extraction. For this purpose, the skeletons were put into 200 mL of acetonitrile and stirred for 24 h. Subsequently, the solvent was changed, and the skeletons were stirred in fresh acetonitrile for further 24 h. All acetonitrile extracts were combined, reduced in volume and analyzed by HPLC. Finally, the extracted skeletons were freeze-dried.

3.2. HPLC

3.2.1. General Procedures

All analytical HPLC-DAD measurements were carried out on a Dionex Ultimate 3000 System employing a Knauer VertexPlus Column (125 × 4 mm, Eurospher 100–10, C18). The different gradient settings for analysis of samples from both sponges are shown in the Supporting Information, Table S2. The flow rate was adjusted to 1 mL min^{-1}. The detection wavelength was set to $\lambda = 235$ nm. Crude extracts of *A. cavernicola* and of *I. basta* skeletons were dissolved in MeOH prior to HPLC analysis. Low resolution ESI mass spectra were recorded on-line using a Thermoquest Finnigan LCQDeca connected to an Agilent 1100 Series LC.

3.2.2. Identification of Brominated Metabolites

Brominated metabolites present in the skeleton extracts were detected based on their retention times, a comparison with authentic standards and on their on-line ESI mass spectra.

3.2.3. Quantification of Brominated Metabolites

The identified metabolites were quantified by peak integration using an external standard. Bastadin 3 was utilized as the external standard for bastadin derivatives from *I. basta* to establish the calibration graph shown in the Supporting Information (Figure S11). The contents of bromotyrosine metabolites were calculated as mg g^{-1} of the dried skeleton or of freeze dried sponge tissue.

3.3. Light Microscopy

Small pieces of the skeletons were put on a sample holder. Microscopic studies were carried out on a Keyence BZ-8000K microscope. The images were acquired at 10-fold magnification.

3.4. FTIR Spectroscopy

IR spectra were recorded using a Bruker FTIR spectrometer IFS 88. The samples were deposited on SPECAC Golden-Gate-ATR equipment. The spectra were measured in the range from 4000 cm^{-1} to 650 cm^{-1} with a spectral resolution of 0.5 cm^{-1}. Each spectrum was recorded by the accumulation of 1000 scans. Subsequently, an ATR intensity correction was carried out. The spectra were baseline corrected and normalized to the most intensive band at about 1625 cm^{-1}.

3.5. NMR Spectroscopy

Solid-state ^{13}C NMR spectra of the skeletons of the sponges were recorded on a Bruker Avance 800 spectrometer at a ^{13}C resonance frequency of 201.19 MHz using a commercial 3.2 mm triple-resonance (^{1}H, ^{13}C, ^{15}N) E-free MAS NMR probe. During signal acquisition, SPINAL ^{1}H-decoupling was applied [33]. The MAS frequency was 16 kHz. The spectra were recorded with a recycle delay of 3 s.

3.6. Bromine Determination by Potentiometric Titration

Small pieces (approximately 10 mg dry sample) of the samples were combusted by the method of Schöniger [29]. The samples were wrapped in ashless filter paper and trapped in a platinum grid, which was attached to the stopper of an Erlenmeyer flask. The Erlenmeyer flask contained 10 mL ultrapure water acidified with 2% HNO_3 as the absorbent. The flask was flushed with pure oxygen, while the sample was ignited and put in the Erlenmeyer flask to ensure complete burning without loss. For complete absorption, the flask was allowed to equilibrate overnight. Afterwards, 2 mL of the resulting solution were diluted to 20 mL and measured by potentiometric titration. Accordingly, a silver nitrate solution (2 mM for whole sponge, 0.5 mM for skeletons) was added in 0.1 mL increments (see Supporting Information, Figure S12). To validate the described sample combustion, the amount of bromine in a reference sample (4-bromochlorobenzene) of known bromine concentration was measured. Within a recovery rate of 95% (±10%), the expected bromine concentrations could be detected by the described combustion and potentiometric titration method. In addition, the accuracy of this method was tested by adding 1 mL of a 1 mM KBr-solution to several digested samples. The corresponding amount of added bromine could also be detected within the experimental error of 10%, demonstrating the validity of the applied method.

3.7. DNA Analysis

3.7.1. Enrichment of Symbiotic Bacteria

The symbiont enrichment procedure was adapted from Ouyang *et al*. [28]. Two grams of sponge material were sliced into small pieces and homogenized using a mortar and a pestle. Cells were suspended in 10 mL TE buffer (10 mM Tris-HCl, 1 mM EDTA, pH 8.0, 4 °C) and filtered through a nylon mesh (42 µm pore size). To eliminate sponge debris and dirt, the suspension was centrifuged at 250× *g* for 1 min at 4 °C. Cells were pelleted at 8000× *g* for 20 min at 4 °C. Finally, the cell pellet was washed three times with 10 mL TE100 buffer (10 mM Tris-HCl, 100 mM EDTA, pH 8.0, 4 °C) to remove sponge pigments. Microscopic analysis of the obtained cells revealed that the samples still contained sponge cells and a comparably high amount of bacterial cells.

3.7.2. Extraction of Metagenomic DNA

According to Schirmer *et al.* [34], 0.5 g of symbiont enriched cell pellets were resuspended in 2 mL lysis buffer (0.5 M NaCl, 10 mM Tris-HCl, 100 mM EDTA, pH 8.0) and treated with lysozyme (200 mg mL^{-1} for 1 h at 37 °C), followed by a second lysis step with 1% SDS and 0.5 mg mL^{-1} proteinase K for 2 h at 50 °C. The DNA was purified three times by phenol-extraction, followed by one chloroform extraction step and finally precipitated over night at −20 °C with isopropanol. The DNA pellet was washed with ice cold 70% ethanol and dissolved in 100 µL H_2O.

3.7.3. Purification of DNA by Size Exclusion Chromatography

The solution of the extracted DNA still showed brownish contaminations (probably humic/fulvic acid-like substances), which inhibited further applications, such as digestion with restriction enzymes

and PCR. To eliminate these contaminations, a size exclusion chromatographic step using a Superdex 200 column (Pharmacia Biotech) was employed. The molecular weight of humic/fulvic acid-like contamination is much smaller than 200 kDa. DNA with the size of 10 kb has an approximate molecular mass of 600 MDa. DNA after extraction had an average length between 20 and 40 kb. Thus, pure DNA will be in the last fractions of the void volume, whereas contaminations will elute much later. 1 mL of DNA solution in TEN buffer (10 mM Tris-HCl, 1 mM EDTA, 150 mM NaCl, pH 8.0) was loaded onto the column and eluted with TEN buffer. Elution was monitored at 254 nm, and fractions containing the high molecular weight DNA were collected and pooled. To avoid digestion of the DNA by contaminating nucleases, a final phenol extraction step was used. The purified DNA was diluted in ddH_2O.

3.7.4. Detection of Halogenase Genes

The degenerated primer pair (TyrhalA_for: 5′-TACCAGGTCGAGCGSDBNMVNTCCGAC-3′ and TyrhalA_rev: 5′-CGGGACSACGAARCASGCSGCGTCBCC-3′) and (HaloDetect_for: 5′-GGAC GGCTGGTTCTGGNHNATHCC-3′ and HaloDetect_rev: 5′-CACGCCGCGGGAGWANANNGG RTC-3′) were constructed using sequence data of published and unpublished data for identified and potential tyrosine halogenases. These primers were used for PCR for the detection of halogenase genes. Gene fragments were amplified with *taq*-polymerase (Fermentas) in ThermoPolII-buffer (NEB) containing 2 nmol $MgCl_2$, 4% DMSO, 1 pmol of the degenerated primer pair and 0.1 pmol dNTPs in a total volume of 25 µL. One microliter of metagenomic DNA (approx. 20 ng μL^{-1}) was used as the template. Initial denaturation was performed at 98 °C for 5 min. Elongation was carried out at 68 °C for 1 min (600 bp fragment) and 40 s (250 bp fragment) after a 30 s annealing period at 55 °C. Denaturation between cycles was done at 98 °C for 30 s. The final elongation step was performed at 68 °C for 5 min. PCR fragments obtained after 30 cycles were isolated using the GeneJET™ Purification Kit (Fermentas) and sequenced (MWG-eurofins). A BLAST search using the amino acid sequences derived from the DNA sequences of the fragments was performed to detect similarities with published halogenases.

4. Conclusions

In summary, the following conclusions can be drawn from our study:

(i) Genetic analyses reveal the presence of flavin-dependent halogenase genes in the sponges, *A. cavernicola* and *I. basta*. These genes are likely to originate from symbionts of the sponges. This agrees well with the observations of Bayer *et al.* [23]. Both gene fragments show high similarity to bacterial halogenase genes. It can, therefore, be assumed that the previously identified bromotyrosine derivatives in *A. cavernicola* and *I. basta*—aerothionin and bastadins—respectively, are probably of symbiotic origin.

(ii) Moreover, our analytical studies show that the majority of the previously identified bromotyrosine derivatives are not associated with the sponge skeletons. They can easily be removed from the skeletons by TE100 or even H_2O treatment. This is in line with the aforementioned conclusion that these compounds are produced by symbionts.

(iii) However, a considerable amount of bromine-bearing organic molecules were found to be MeOH-insoluble. These strongly skeleton-associated compounds withstand the established extraction protocol and remain tightly associated with the sponge skeleton. It is tempting to speculate that these compounds are involved in the chemical defense of the skeleton, e.g., by inhibiting chitinases as discussed in the introduction section or by other biological activities. The extraction of these yet unidentified molecules—which may even be covalently bound to the chitin-based scaffolds—without severe chemical damage remains to be the subject of future work, including the elucidation of their ecological function/biological activity and biosynthetic pathway.

Acknowledgments

Thanks are due to P. Schupp (Oldenburg) for providing us with the *I. basta* sample. Financial support from the German Research Foundation (DFG grant no. Br 1278/17-1, PE 348/27-1, PR 229/15-1 and EH 394/1-1) is gratefully acknowledged. Furthermore, we acknowledge support by the Open Access Publication Funds of the TU Dresden. Thanks are further due to S. Machill and S. Paasch for excellent experimental assistance.

Conflict of Interest

The authors declare no conflict of interest.

References

1. Blunt, J.W.; Copp, B.R.; Hu, W.P.; Munro, M.H.G.; Northcote, P.T.; Prinsep, M.R. Marine natural products. *Nat. Prod. Rep.* **2009**, *26*, 170–244.
2. Montaser, R.; Luesch, H. Marine natural products: A new wave of drugs? *Future Med. Chem.* **2011**, *3*, 1475–1489.
3. Proksch, P.; Putz, A.; Ortlepp, S.; Kjer, J.; Bayer, M. Bioactive natural products from marine sponges and fungal endophytes. *Phytochem. Rev.* **2010**, *9*, 475–489.
4. Müller, W.E.G. Origin of metazoa: Sponges as living fossils. *Naturwissenschaften* **1998**, *85*, 11–25.
5. Li, C.-W.; Chen, J.-Y.; Hua, T.-E. Precambrian sponges with cellular structures. *Science* **1998**, *279*, 879–882.
6. Thoms, C.; Wolff, M.; Padmakumar, K.; Ebel, R.; Proksch, P. Chemical defense of Mediterranean sponges *Aplysina cavernicola* and *Aplysina aerophoba*. *Z. Naturforsch. C* **2004**, *59*, 113–122.
7. Thoms, C.; Ebel, R.; Proksch, P. Activated chemical defense in *Aplysina* sponges revisited. *J. Chem. Ecol.* **2006**, *32*, 97–123.
8. Paul, V.J.; Ritson-Williams, R.; Sharp, K. Marine chemical ecology in benthic environments. *Nat. Prod. Rep.* **2011**, *28*, 345–387.
9. Wehner, R.; Gehring, W.J. *Zoologie*; Georg Thieme Verlag: Stuttgart, Germany, 2007; pp. 698–699.

10. Bergquist, P.R.; Cook, S.D.C. Order Verongida Bergquist, 1978. In *Systema Porifera: A Guide to the Classification of Sponges*; Hooper, J.N.A., van Soest, R.W.M., Eds.; Kluwer Academic/ Plenum Publishers: New York, NY, USA, 2002; Volume I, pp. 1081–1096.
11. Ehrlich, H.; Maldonado, M.; Spindler, K.-D.; Eckert, C.; Hanke, T.; Born, R.; Goebel, C.; Simon, P.; Heinemann, S.; Worch, H. First evidence of chitin as a component of the skeletal fibers of marine sponges. Part I. Verongidae (Demospongia: Porifera). *J. Exp. Zool. B Mol. Dev. Evol.* **2007**, *308*, 347–356.
12. Brunner, E.; Ehrlich, H.; Schupp, P.; Hedrich, R.; Hunoldt, S.; Kammer, M.; Machill, S.; Paasch, S.; Bazhenov, V.V.; Kurek, D.V.; *et al*. Chitin-Based scaffolds are an integral part of the skeleton of the marine demosponge *Ianthella basta*. *J. Struct. Biol.* **2009**, *168*, 539–547.
13. Uriz, M.-J.; Turon, X.; Becerro, M.A.; Agell, G. Siliceous spicules and skeleton frameworks in sponges: Origin, diversity, ultrastructural patterns, and biological functions. *Microsc. Res. Tech*. **2003**, *62*, 279–299.
14. Ehrlich, H.; Ilan, M.; Maldonado, M.; Muricy, G.; Bavestrello, G.; Kljajic, Z.; Carballo, J.L.; Shiaparelli, S.; Ereskovsky, A.V.; Schupp, P.; *et al*. Three-Dimensional chitin-based scaffolds from Verongida sponges (Demospongiae: Porifera). Part I. Isolation and identification of chitin. *Int. J. Biol. Macromol.* **2010**, *47*, 132–140.
15. Teeyapant, R.; Woerdenbag, H.; Kreis, P.; Hacker, J.; Wray, V.; Witte, L.; Proksch, P. Antibiotic and cytotoxic activity of brominated compounds from the marine sponge *Verongia aerophoba*. *Z. Naturforsch. C* **1993**, *48*, 939–945.
16. Faulkner, D.J. Marine pharmacology. *Antonie Van Leeuwenhoek* **2000**, *77*, 135–145.
17. Weiss, B.; Ebel, R.; Elbrächter, M.; Kirchner, M.; Proksch, P. Defence metabolites from the marine sponge *Verongia aerophoba*. *Biochem. Syst. Ecol.* **1996**, *24*, 1–12.
18. Tabudravu, J.N.; Eijsink, V.G.H.; Gooday, G.W.; Jaspars, M.; Komander, D.; Legg, M.; Synstad, B.; van Aalten, D.M.F. Psammaplin A, a Chitinase Inhibitor Isolated from the Fijian Marine Sponge *Aplysinella rhax*. *Bioorg. Med. Chem.* **2002**, *10*, 1123–1128.
19. Thomson, J.E.; Barrow, K.D.; Faulkner, D.J. Localization of two brominated metabolites, aerothionin and homoaerothionin, in spherulous cells of the marine sponge *Aplysina fistularis* (=*Verongia thiona*). *Acta Zool.* **1981**, *64*, 199–210.
20. Turon, X.; Becerro, M.A.; Uriz, M.J. Distribution of brominated compounds within the sponge *Aplysina aerophoba*: Coupling X-ray microanalysis with cryofixation techniques. *Cell Tissue Res.* **2000**, *301*, 311–322.
21. Tymiak, A.A.; Rinehart, L.R., Jr. Biosynthesis of dibromotyrosine-derived antimicrobial compounds by the marine sponge *Aplysina fistularis* (*Verongia aurea*). *J. Am. Chem. Soc.* **1981**, *103*, 6763–6765.
22. Leone-Stumpf, D. Synthesis and Chromatography of $[RuCp]^{+}$-labelled Diaryl Ether Peptoids as Precursors of the Bastadins from the Marine Sponge *Ianthella basta*. PhD Thesis, Combined Faculties for the Natural Sciences and for Mathematics, Ruperto-Carola University of Heidelberg, Heidelberg, Germany, November 2001.
23. Bayer, K.; Scheuermayer, M.; Fieseler, L.; Hentschel, U. Genomic mining for novel $FADH_2$-dependent halogenases in marine sponge-associated microbial consortia. *Mar. Biotechnol.* **2013**, *15*, 63–72.

24. Van Pée, K.-H. Enzymatic chlorination and bromination. *Methods Enzymol.* **2012**, *516*, 237–257.
25. Chow, T.Y.K. Purification of yeast—*E. coli* shuttle plasmid suitable for high transformation frequency in *E. coli*. *Nucleic Acids Res*. **1989**, *17*, 8391.
26. Bollet, C.; Gevaudan, M.J.; de Lamballerie, X.; Zandotti, C.; de Micco, P. A simple method for the isolation of chromosomal DNA from Gram positive or acid-fast bacteria. *Nucleic Acids Res.* **1991**, *19*, 1955.
27. Wang, H.; Zhang, L.; Zhang, F.; An, H.; Chen, S.; Li, H.; Wang, P.; Wang, X.; Wang, Y.; Yang, H. Investigation on the morphology of precipitated chemicals from TE buffer on solid substrates. *Surf. Rev. Lett*. **2007**, *14*, 1121–1128.
28. Ouyang, Y.; Dai, S.; Xie, L.; Ravi Kumar, M.S.; Sun, W.; Sun, H.; Tang, D.; Li, X. Isolation of high molecular weight DNA from marine sponge bacteria for BAC library construction. *Mar. Biotechnol*. **2010**, *12*, 318–325.
29. Schöniger, W. Eine mikroanalytische Schnellbestimmung von Halogenen in organischen Substanzen. *Mikrochem. Acta* **1995**, *1*, 123–129.
30. Ebada, S.S.; Edrada, R.A.; Lin, W.; Proksch, P. Methods of isolation, purification and structural elucidation of bioactive secondary metabolites from marine invertebrates. *Nat. Protoc.* **2008**, *3*, 1820–1831.
31. Pelzer, S.; Süßmuth, R.; Heckmann, D.; Recktenwald, J.; Huber, P.; Jung, G.; Wohlleben, W. Identification and analysis of the balhimycin biosynthetic gene cluster and its use for manipulating glycopeptide biosynthesis in *Amycalotopsis mediterranei* DSM5908. *Antimicrob. Agents Chemother.* **1999**, *43*, 1565–1573.
32. Institut für angewandte Hydrobiologie; HYDRA AG; HYDRA Institut für Meereswissenschaften AG; HYDRA Büro für Gewässerökologie Mürle & Ortlepp GbR; HYDRA Wiesloch—Dipl-Biol. Andreas Becker. Available online: http://www.hydra-institute.com (accessed on 10 April 2013).
33. Fung, B.M.; Khitrin, A.K.; Ermolaev, J. An improved broadband decoupling sequence for liquid crystals and solids. *J. Magn. Reson.* **2002**, *142*, 97–101.
34. Schirmer, A.; Gadkari, R.; Reeves, C.D.; Ibrahim, F.; DeLong, E.F.; Hutchinson, C.R. Metagenomic analysis reveals diverse polyketide synthase gene clusters in microorganisms associated with the marine sponge *Discodermia dissoluta*. *Appl. Environ. Microbiol.* **2005**, *71*, 4840–4849.

Supporting Information

Table S1. Assignment of the IR bands in Figure 3 and Figure S1 (below).

A. cavernicola **(H_2O/TE100)**		***A. cavernicola*** **(NaOH)**	***I. basta*** **(H_2O/TE100)**		***I. basta*** **(NaOH)**	**α-chitin**	**Assignment**
Wavenumber/ cm^{-1}		Wavenumber/ cm^{-1}	Wavenumber/ cm^{-1}		Wavenumber/ cm^{-1}	Wavenumber/ cm^{-1}	
		898			897	898	CH_x deformation (o.o.p.)
				921		920	
		949			950	953	
1033		1027	1037		1029	1025	C-O-C/C-O stretching
1072	1069	1065	1068	1063	1068	1071	
1111	1108	1109	1111	1118	1112	1113	
		1154	1155	1156	1155	1155	
		1203			1203	1205	Amide III
1234	1235		1233				
		1263		1255	1262	1260	
1316	1314	1306		1325	1306	1309	
	1380	1374	1376		1375	1376	CH_x deformation
				1398		1415	
1447	1445	1429	1447		1430	1430	
1519	1515	1550	1522	1588	1554	1554	Amide II
1634	1639		1638		1631	1622	Amide I
		1642			1653	1654	
2876 (shoulder)	2876 (shoulder)	2875	2876 (shoulder)	2875 (shoulder)	2874	2876	CH_x stretching
2931	2933	2930	2929		2923	2927	
2958				2957	2955	2959	
		3096					N-H stretching
		3121			3114	3103	
3277	3285	3283	3279	3270	3285	3262	
		3409			3436	3432	O-H stretching

Figure S1. ATR FTIR spectra of the purified skeletons of *I. basta* after different treatment steps.

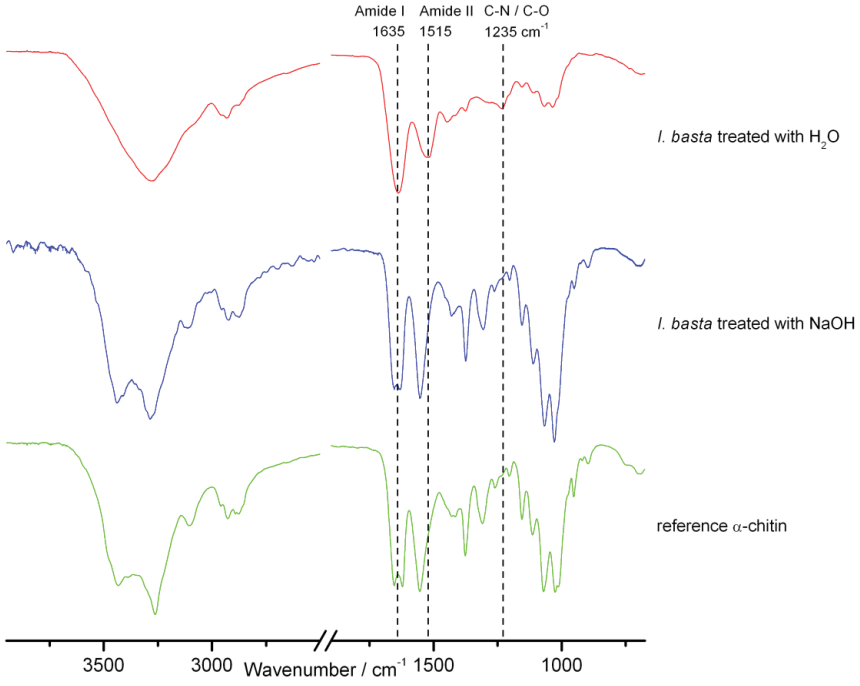

Figure S2. $^{13}C\{^{1}H\}$ CP MAS NMR spectrum and structure of aerothionin as well as assignment table of the observed ^{13}C NMR signals. This symmetric molecule exhibits two pairwise identical carbon positions (e.g., 1 and 1′) which exhibit identical chemical shifts in the liquid-state NMR spectra [1]. The observation of two signals in the solid-state NMR spectrum indicates the presence of two crystallographically different positions for solid aerothionin. * denotes spinning sidebands.

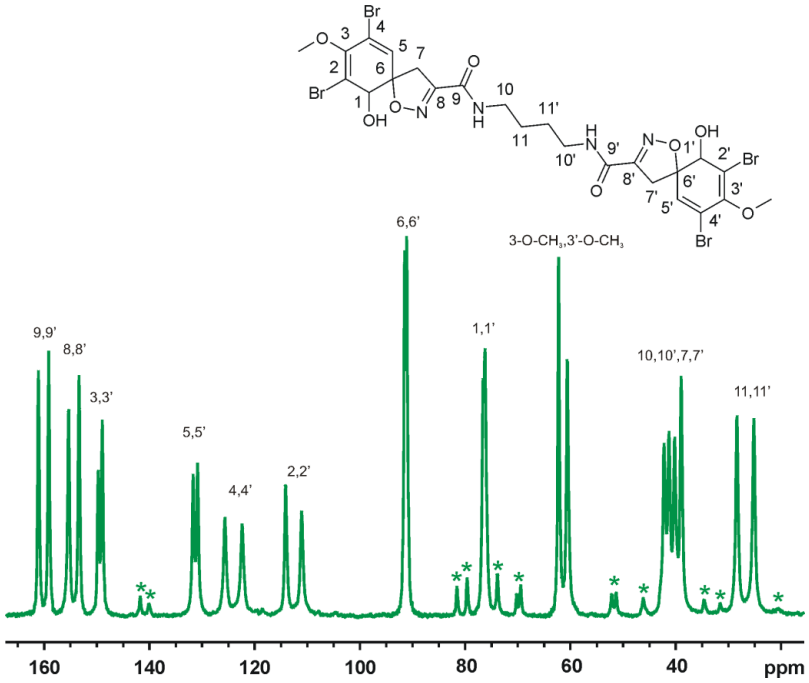

^{13}C NMR signal/ppm	Assignment
25; 28	11/11′
39; 40; 41; 42	7/7′/10/10′
61; 62	3-*O*-CH_3/3′-*O*-CH_3
76; 77	1/1′
91; 92	6/6′
111; 114	2/2′
122; 126	4/4′
131; 132	5/5′
149; 150	3/3′
153; 155	8/8′
159; 161	9/9′

Figure S3. $^{13}C\{^{1}H\}$ CP MAS NMR spectra of the skeletons of *I. basta* after TE100 treatment. For comparison, the spectra of the pure chitin-scaffold obtained after NaOH treatment and of synthetic 5,5′-dibromohemibastadin-1 are also shown. For signal assignments see Figure 4 and Figure S4. * denotes spinning sidebands.

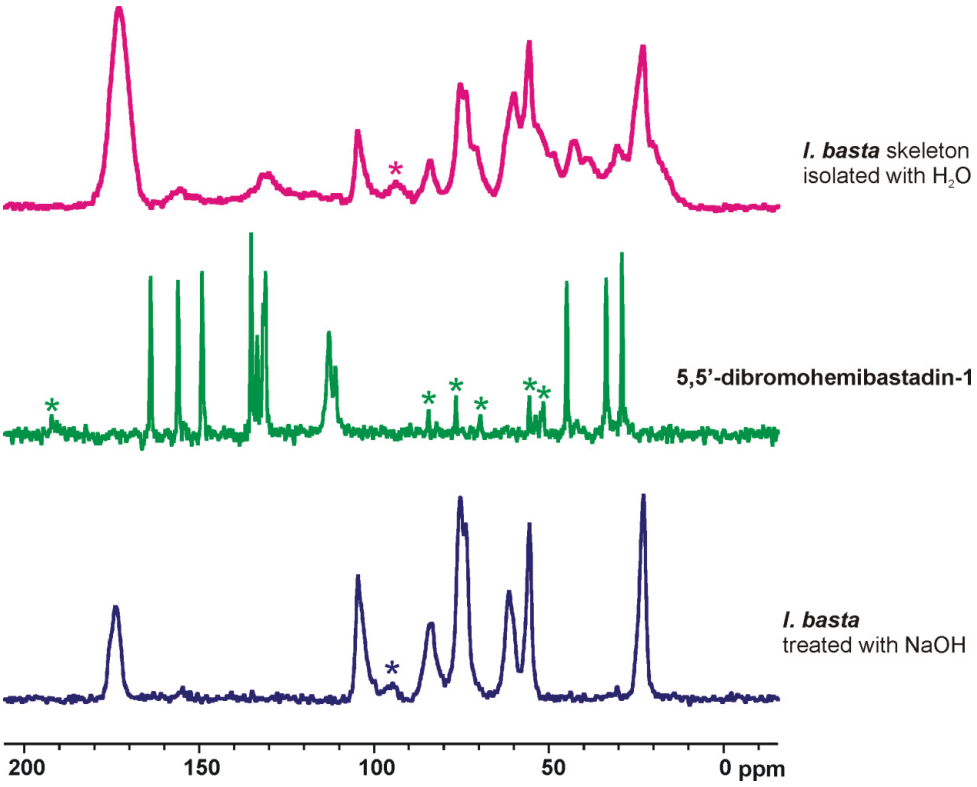

Figure S4. $^{13}C\{^{1}H\}$ CP MAS NMR spectrum, structure of 5,5′-dibromohemibastadin-1 and assignment table of the ^{13}C NMR signals. * denotes spinning sidebands.

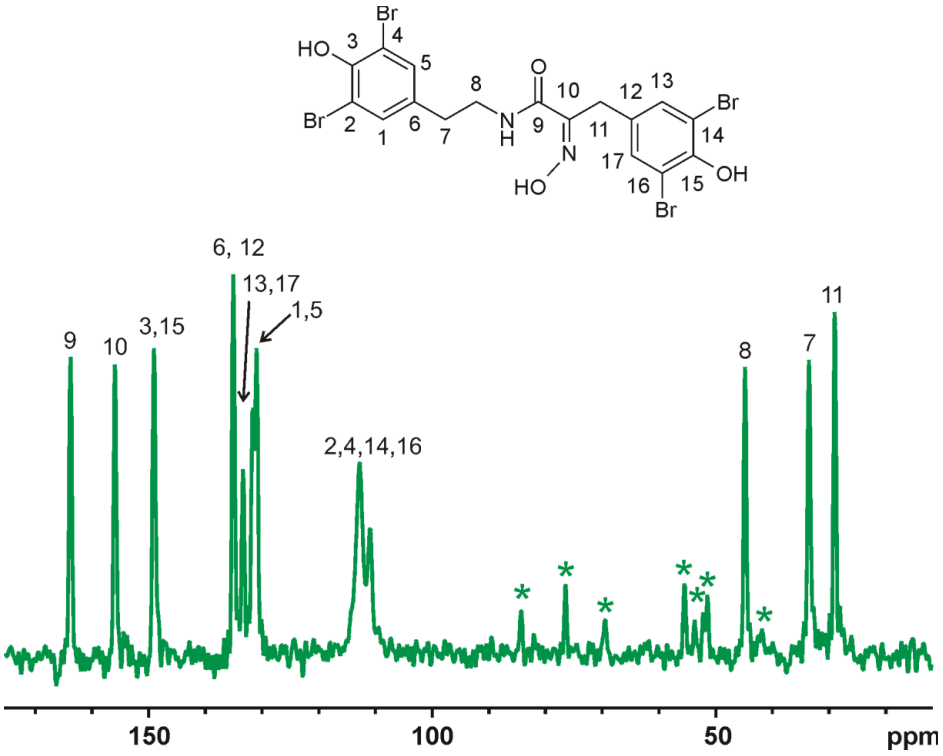

^{13}C NMR signal/ppm	Assignment
29	11
36	7
45	8
111; 113	2/4/14/16
131; 132	1/5
133	13/17
135	6/12
149	3/15
156	10
163	9

Figure S5. ATR FTIR spectra of the purified skeletons of *A. cavernicola* and *I. basta* before and after the MeOH extraction.

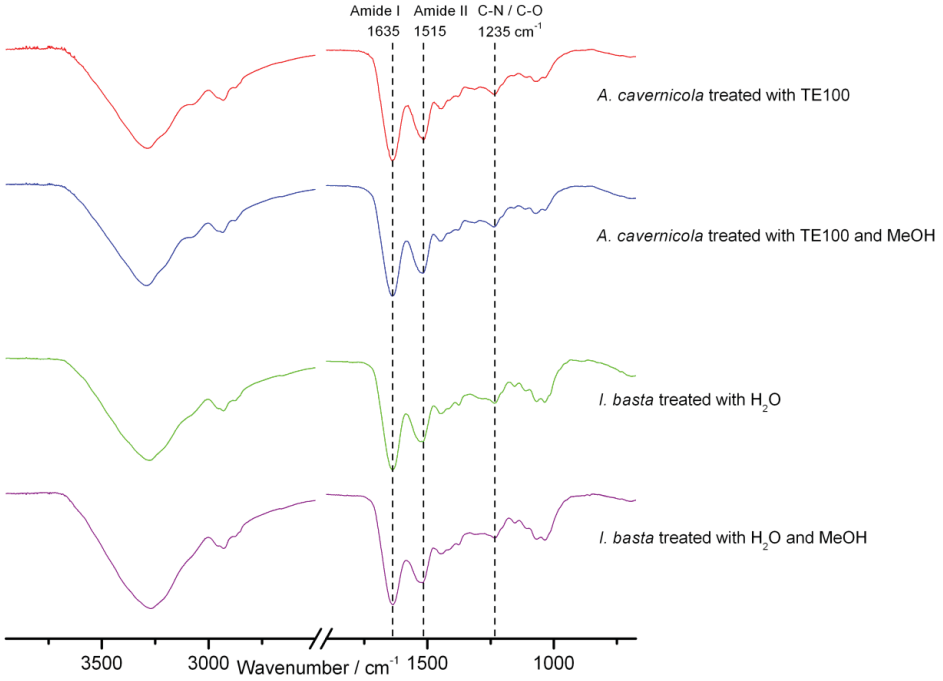

Figure S6. $^{13}C\{^{1}H\}$ CP MAS NMR spectra of the purified skeletons of *A. cavernicola* and *I. basta* before and after the MeOH extraction.

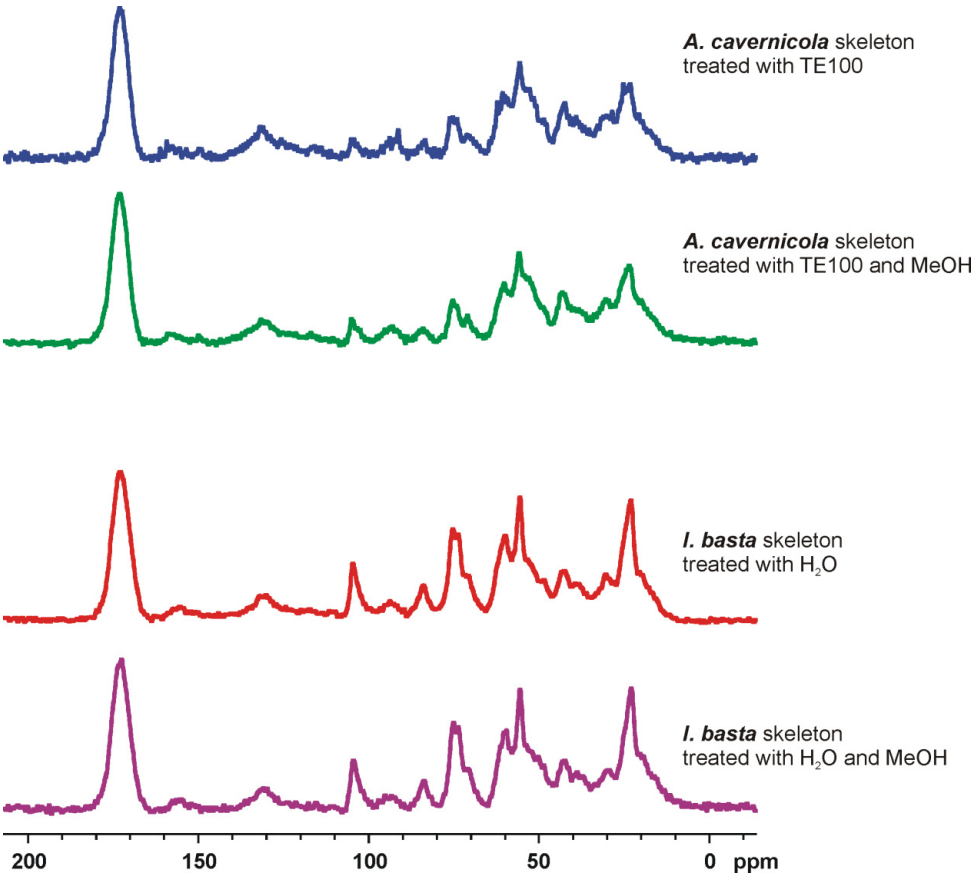

Figure S7. Selected region from the $^{13}C\{^{1}H\}$ CP MAS NMR spectra of the purified skeletons of *A. cavernicola* before and after MeOH extraction and of aerothionin. Note the presence of weak, characteristic signals due to aerothionin before MeOH extraction which disappear after MeOH treatment.

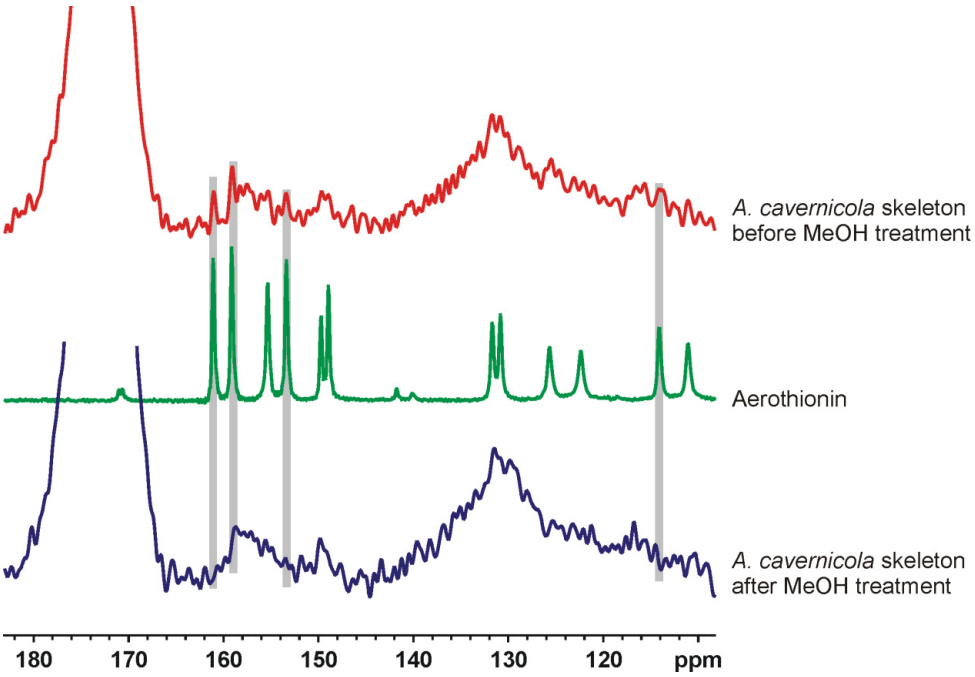

Figure S8. Chemical structures of bromotyrosines identified in the skeleton extracts; (**A**) bastadins 3, 4, 6, 7, 9 and 16 from *I*. *basta*; (**B**) aerothionin from *A*. *cavernicola*.

A

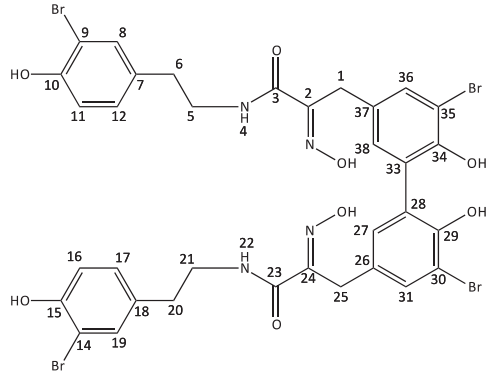

bastadin 3

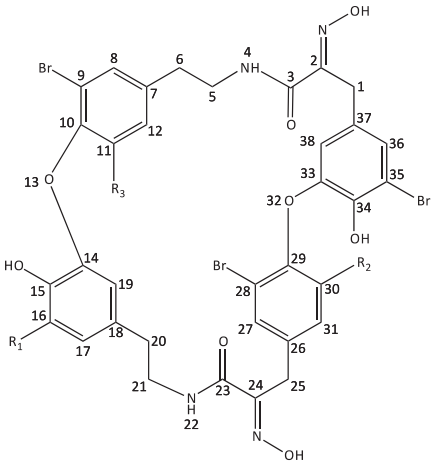

bastadin 4: $R_1 = R_2 = Br$, $R_3 = H$, $\Delta^{5,6}$
bastadin 6: $R_1 = R_2 = R_3 = Br$
bastadin 7: $R_1 = Br$, $R_2 = R_3 = H$, $\Delta^{5,6}$
bastadin 9: $R_1 = R_3 = H$, $R_2 = Br$
bastadin 16: $R_1 = H$, $R_2 = R_3 = Br$

B

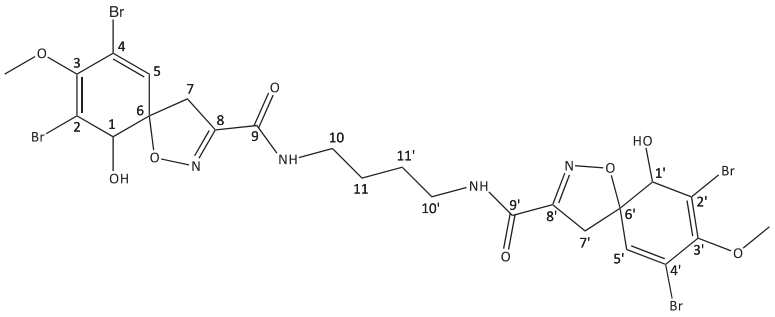

aerothionin

Figure S9. (**A**) Direct injection-ESI-mass spectrum of pure bastadin 3 standard obtained from *I. basta* tissue extract; (**B**) LC-ESI-mass spectrum obtained from a constituent of the *I. basta* skeleton extract. Based on this mass spectrum, this compound was identified as bastadin 3.

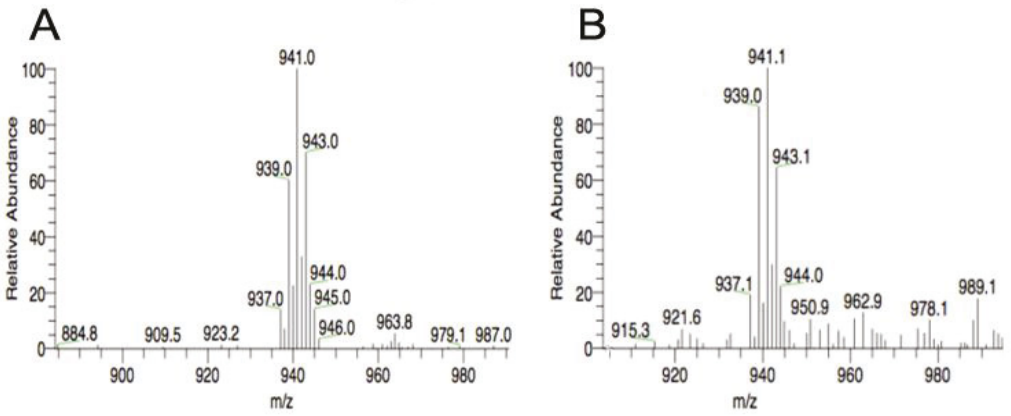

Figure S10. Removal of contaminating pigments (2) from the DNA (1) isolated from bacteria associated with *A. cavernicola*.

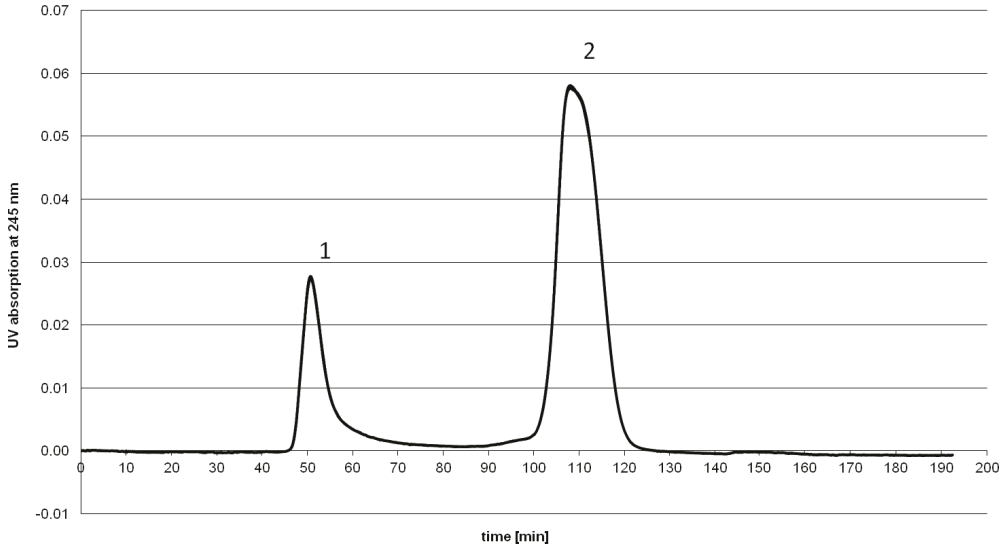

Table S2. Gradient systems for HPLC analysis of *I. basta* and *A. cavernicola*; eluent A: 0.1% formic acid in water, eluent B: MeOH.

I. basta			***A. cavernicola***		
time [min]	**eluent A [%]**	**eluent B [%]**	**time [min]**	**eluent A [%]**	**eluent B [%]**
0	60	40	0	90	10
5	60	40	5	90	10
34	25	75	35	0	100
35	0	100	45	0	100
50	90	10	50	90	10
60	90	10	60	90	10

Figure S11. Calibration graph of bastadin 3 for external standard quantification of bastadin derivatives in MeOH-extracts of sponge tissue and skeleton.

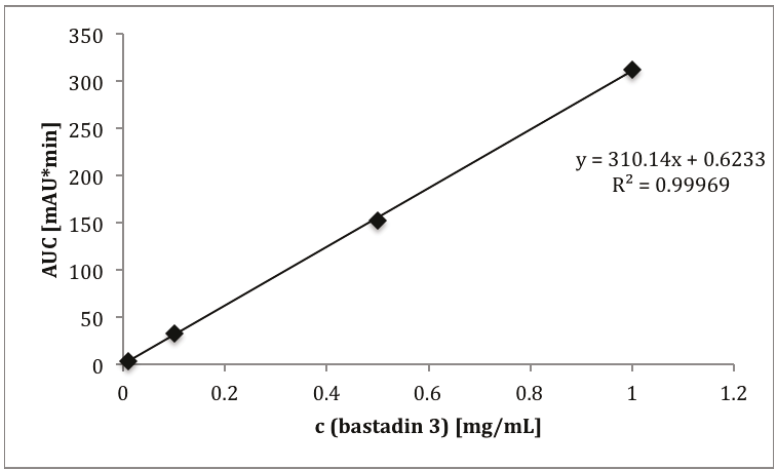

Figure S12. Potentiometric titration curves for quantitative bromine determination in *A. cavernicola* skeleton samples before and after MeOH-extraction. The step in the titration curve represents the bromide ions. The bromine concentration can be determined from the $AgNO_3$ concentration at the inflection point of this potential step.

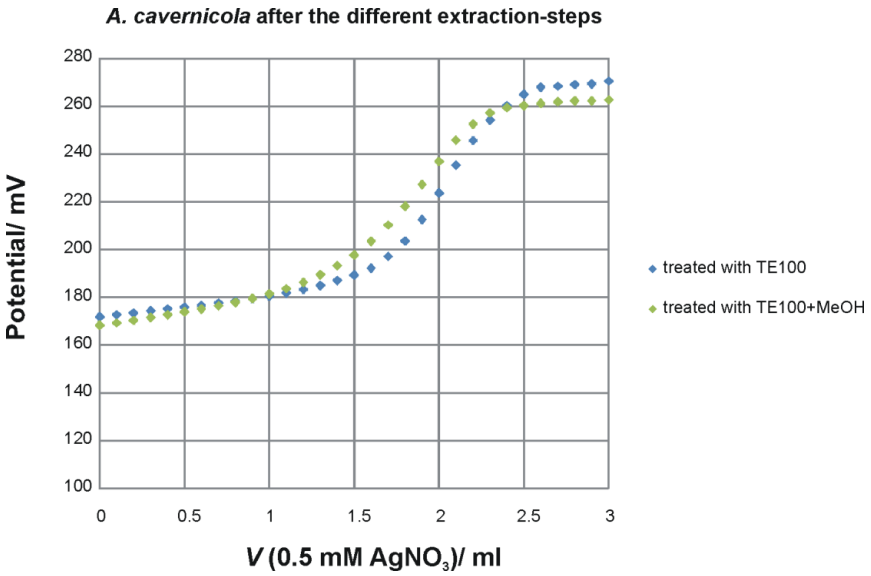

References

1. Kalaitzis, J.A.; Davis, R.A.; Quinn, R.J. Unequivocal ^{13}C NMR assignment of cyclohexadienyl rings in bromotyrosine-derived metabolites from marine sponges. *Magn. Reson. Chem.* **2012**, *50*, 749–754.

9 Publication 6

9.1 The Skeletal Amino Acid Composition of the Marine Demosponge *Aplysina cavernicola*

Published in: „Marine Drugs“

Impact factor: 3.512

Contribution: 30 %, conducting one set of experiments (LCMS analysis of *Aplysia cavernicola* skeleton hydrolysates), manuscript writing

Mar. Drugs **2014**, *12*, 4417-4438; doi:10.3390/md12084417

OPEN ACCESS

marine drugs

ISSN 1660-3397

www.mdpi.com/journal/marinedrugs

Article

The Skeletal Amino Acid Composition of the Marine Demosponge *Aplysina cavernicola*

Susanne Ueberlein [1], Susanne Machill [1], Hendrik Niemann [2], Peter Proksch [2] and Eike Brunner [1,*]

[1] Bioanalytical Chemistry, TU Dresden, Dresden 01062, Germany;
E-Mails: susanne.ueberlein@chemie.tu-dresden.de (S.U.);
susanne.machill@chemie.tu-dresden.de (S.M.)

[2] Institute of Pharmaceutical Biology and Biotechnology, Heinrich Heine University Düsseldorf, Universitaetsstrasse 1, Geb. 26.23, Düsseldorf 40225, Germany;
E-Mails: hendrik.niemann@uni-duesseldorf.de (H.N.); proksch@uni-duesseldorf.de (P.P.)

* Author to whom correspondence should be addressed; E-Mail: eike.brunner@tu-dresden.de;
Tel.: +49-351-4633-7152; Fax: +49-351-4633-7188.

Received: 3 June 2014; in revised form: 23 July 2014 / Accepted: 24 July 2014 / Published: 8 August 2014

Abstract: It has been discovered during the past few years that demosponges of the order Verongida such as *Aplysina cavernicola* exhibit chitin-based skeletons. Verongida sponges are well known to produce bioactive brominated tyrosine derivatives. We could recently demonstrate that brominated compounds do not exclusively occur in the cellular matrix but also in the skeletons of the marine sponges *Aplysina cavernicola* and *Ianthella basta*. Our measurements imply that these yet unknown compounds are strongly, possibly covalently bound to the sponge skeletons. In the present work, we determined the skeletal amino acid composition of the demosponge *A. cavernicola* especially with respect to the presence of halogenated amino acids. The investigations of the skeletons before and after MeOH extraction confirmed that only a small amount of the brominated skeleton-bound compounds dissolves in MeOH. The main part of the brominated compounds is strongly attached to the skeletons but can be extracted for example by using $Ba(OH)_2$. Various halogenated tyrosine derivatives were identified by GC-MS and LC-MS in these $Ba(OH)_2$ extracts of the skeletons.

Publication 6

Keywords: demosponges; skeletons; amino acid composition; halogenated amino acids; GC-MS; LC-MS

1. Introduction

Sponges (*Porifera*) belong to the oldest *Metazoans* and are the simplest animals on earth [1,2]. Although they do not possess morphological defense strategies, these sessile filter feeders successfully withstand the attacks of predators, as well as overgrowth by fouling organisms or bacterial infections. This evolutionary success is mainly due to an effective chemical defense based on deterrent, cytotoxic and/or antibiotically active compounds [3–6].

Sponges possess a skeleton which consists of a composite of natural biomaterials containing organic constituents and/or inorganic compounds. One function of these skeletons is mechanical support, that means the prevention of the collapse of the sponge body [7,8]. Furthermore, the skeletons seem to play a role in the protection against predators. For example, Hill *et al.* showed that the sponge *Anthosigmella varians* increases the spicule concentration during the attack of predators [9,10].

Based on the skeletal composition, the phylum *Porifera* is divided into three classes: Calcareous sponges (*Calcarea*), glass sponges (*Hexactinellida*), and demosponges (*Demospongia*) [11]. Demosponges form the largest class and possess a skeleton made of a composite material with different organic compounds like proteins [12] and polysaccharides [13,14]. They can also contain siliceous spicules [11,15]. The skeletons of three taxonomic orders of demosponges (Dendroceratida, Dictyoceratida, Verongida) are characterized by the lack of siliceous spicules. Instead, their skeletons contain spongin, a collagenous protein [16].

Until now, the chemical composition of spongin has not been exactly defined. Gross *et al.* isolated two morphologically distinct forms of spongin described as “spongin A” and “spongin B” [17]. Spongin fibers are more resistant than collagen fibers against enzymatic digestion [18]. Today, spongin is characterized as a halogenated protein [16]. Ehrlich *et al.* demonstrated recently that the polysaccharide chitin is an integral part of the skeleton of different demosponges of the order Verongida [13,14,19]. So far, chitin could be found in the skeletons of the genus *Aplysina* [13,19], in the skeletons of *Verongula gigantea* [19], *Ianthella basta* [14], and the freshwater demosponge *Spongilla lacustris* [20]. Moreover, chitin could be isolated from a million year old fossil of the basal demosponge *Vauxia gracilenta* [21].

It is unknown yet how the organic components such as proteins (spongin) are connected with the chitin in sponge skeletons [16]. However, there is a variety of examples in nature showing that proteins are strongly bound to chitin. For example, Hackman suggested that proteins are covalently bound to chitin in different insects and crustacea [22]. Blackwell *et al.* developed a model for the three-dimensional structure of an insect chitin-protein complex with chitin fibrils surrounded by layers of proteins [23].

Furthermore, Verongida sponges such as *A. cavernicola* are well-known for the biosynthesis of brominated tyrosine derivatives—characteristic bioactive natural products [24,25]. Up to now it has remained unclear whether these compounds are exclusively present in the cellular matrix or whether

they may also be incorporated into the chitin-based skeletons. Earlier investigations showed that aerothionin, a typical brominated tyrosine-derivative, is present in the spherulous cells of the marine sponge *Aplysina fistularis* [26]. Another earlier report demonstrated that the brominated compounds are localized also in the skeletal fibers of the demosponge *Aplysina aerophoba* [27]. We recently demonstrated that brominated compounds occur not exclusively in the cellular matrix but also in the skeletons of the marine sponges *A. cavernicola* and *I. basta*. The bromine content of the skeletons of these sponges was measured by quantitative potentiometric titration. A MeOH treatment only resulted in the removal of rather insignificant amounts of bromine. It was therefore concluded that these yet unknown brominated compounds are strongly, possibly covalently bound to the chitin-based sponge skeletons [28]. The structure and composition of these compounds is yet unknown. One possibility could be a covalent incorporation of halogenated amino acids into the skeletons.

Until now the pure skeletal amino acid composition of the chitin-containing Verongida sponges has been completely unknown since only the amino acid compositions of the commercial unbleached sponge *Hippospongia equina* and of the bath sponge *Spongia officinalis obliqua* which both belong to the order Dictyoceratida have been investigated [29,30]. The analyses of these sponges indicated that not only proteinogenic amino acids but also halogenated tyrosines occur in these sponges. Iodated tyrosines were found in *Hippospongia equina* [29], while iodated as well as brominated tyrosines could be detected in *Spongia officinalis obliqua* [30].

In contrast to these previous studies, the goal of the present study was to examine the pure skeletal amino acid composition of the Verongida sponge *A. cavernicola*, especially with respect to halogenated compounds. We therefore isolated the sponge skeletons as described previously [28]. Furthermore, we developed a method to analyze the amino acid composition of the skeletons. In order to evaluate the influence of the established MeOH extraction upon the skeletal amino acid composition, the sponge skeletons were studied before and after MeOH extraction. MeOH is widely used for the extraction of bioactive natural products like aerothionin [31]. In addition, the MeOH extract was analyzed in order to identify possible MeOH-extractable soluble components.

2. Results and Discussion

2.1. Examination of the Skeletons by SEM

The morphology of the isolated sponge skeletons before and after MeOH treatment was studied by scanning electron microscopy (SEM) (Figure 1). The SEM image of the isolated skeletons before MeOH treatment shows a skeletal fiber network system with network fibers composed of concentric multilayers. The core channel of these fibers is filled with a porous material, a pith. The SEM images of the skeletons after MeOH extraction show the same network of fibers with concentric multilayered channels. However, the porous core material is removed by the MeOH treatment showing that this material is only loosely attached to the inner layer surface. This MeOH-soluble pith material represents only 1.4% of the total mass of the isolated sponge skeleton.

Moreover, subsequent energy dispersive X-ray spectroscopy (EDX) measurements show that bromine, chlorine, and iodine are present in the skeletons before as well as after MeOH extraction

(see supporting information Figures S1 and S2). This is in line with our aforementioned hypothesis that halogenated compounds are tightly attached/covalently bound to the sponge skeletons.

Figure 1. Scanning electron microscopy (SEM) images of the skeletons of *A. cavernicola* before MeOH extraction (left) and after MeOH extraction (right), scale bars: 40 µm (top), 20 µm (bottom).

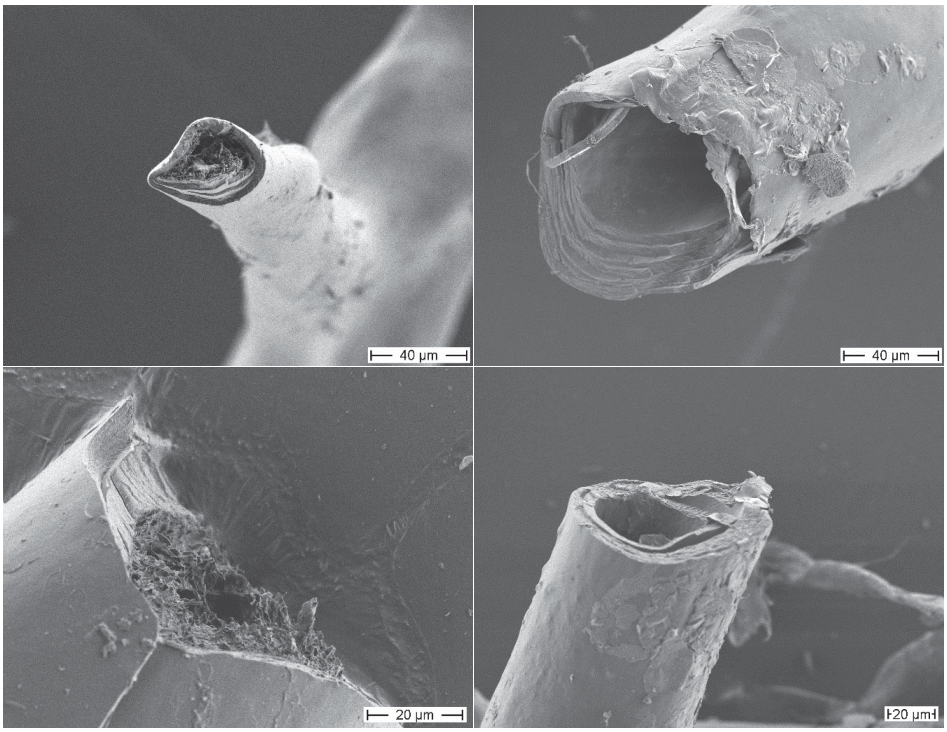

2.2. Amino Acid Extraction, Selection of the Derivatization Agent and the Internal Standard for GC-MS

Alkaline extraction of pure chitin scaffolds from marine sponges using NaOH as previously described by Ehrlich *et al.* [19] leads to a degradation and removal of all other skeleton-associated or incorporated biomolecules such as brominated tyrosine-derivatives or proteins like spongin—but leaves the chitin undissolved. The proteins are hydrolyzed, e.g., disintegrated into their amino acids by this treatment. These extracts, however, contain a huge amount of NaOH which interferes with the further analytical procedure. In order to circumvent this problem, a saturated $Ba(OH)_2$ solution was used as extracting and hydrolyzing agent. Subsequently it was investigated whether the $Ba(OH)_2$ treatment had the same effect as the NaOH treatment. ATR-FTIR measurements (Figure 2) and microscopic studies (Figure 3) show that the $Ba(OH)_2$ as well as the NaOH extraction lead to the removal of all other organic material (cf. [28]) apart from the pure chitin scaffolds. The remaining chitin represents 8.0% ± 1.4% of the mass of the isolated sponge skeleton. In contrast to NaOH, however, the $Ba(OH)_2$ extract can be easily neutralized by adding H_2SO_4. The resulting $BaSO_4$ forms a

precipitate which is separated by centrifugation whereas the extracted amino acids and other soluble compounds remain in the supernatant. After freeze drying, these extracted compounds can be identified by gas chromatography-mass spectrometry (GC-MS). The latter technique requires a preceding derivatization of the compounds.

Figure 2. Attenuated total reflectance infrared (ATR-IR) spectra of the purified chitin-scaffolds of *A. cavernicola* after $Ba(OH)_2$ and NaOH treatment.

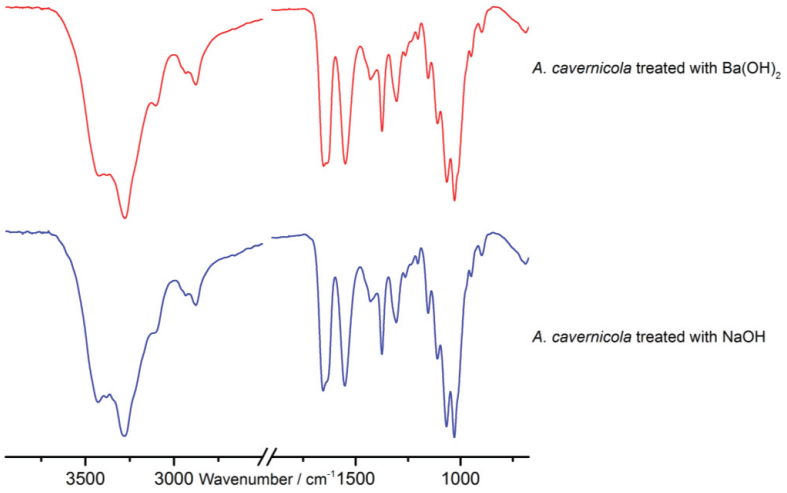

Figure 3. Light microscopic images of the purified chitin-scaffolds of *A. cavernicola* after $Ba(OH)_2$ (left) and NaOH treatment (right); scale bars: 100 µm.

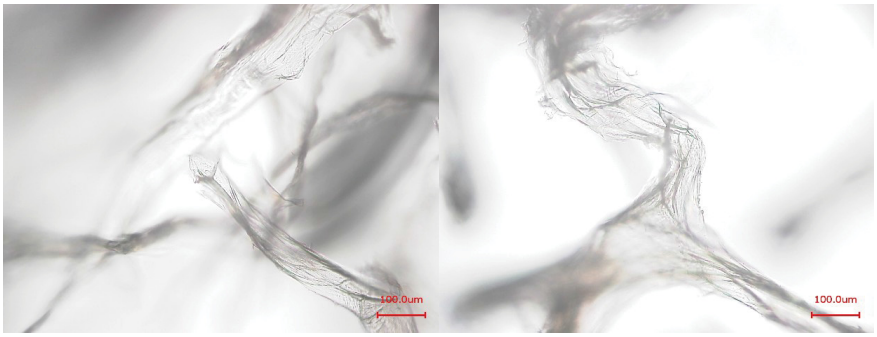

For this purpose, the derivatization agent *N*-*tert*-butyldimethylsilyl-*N*-methyltrifluoroacetamide (MTBSTFA) containing 1% *tert*-butyldimethylchlorosilane (TBDMSCl) was selected since *tert*-butyldimethylsilyl (TBDMS) derivatives of amino acids are more stable than the traditional trimethylsilyl (TMS) derivatives [32]. The amino acids were identified based on their mass spectra and—If available—By comparison with standards. Therefore, the relative retention times of the amino acids found in the extract were compared with the pure reference compounds (standards). The compound 5-Bromotryptophan was selected as an internal standard due to its similarity with the halogenated

compounds found in the skeletons, *i.e.*, the brominated aromatic ring system. This internal standard shows two GC-signals due to different degrees of derivatization (first peak: two TBDMS groups; second peak: three TBDMS groups).

2.3. GC-MS Analysis of the Skeletal Amino Acid Composition

2.3.1. Skeletal Amino Acid Composition before MeOH Extraction

The isolated skeletons [28] of the demosponge *A. cavernicola* were treated with a saturated $Ba(OH)_2$ solution and derivatized using MTBSTFA as described in Section 2.2 and in the Experimental Section. The GC-MS measurements of the isolated *A. cavernicola* sponge skeletons show the presence of various amino acids (see Table 1 and Figure 4).

Table 1. Amino acids detected in the $Ba(OH)_2$ extract of isolated *A. cavernicola* sponge skeletons before MeOH treatment. Components with ***** could not be verified with pure standards due to the lack of availability of these reference compounds.

Peak	*tert*-Butyldimethylsilyl (TBDMS)-Derivative	Proteinogenic	Halogenated
1	Alanine	X	
2	Glycine	X	
3	α-Aminobutyric Acid (AABA)		
4	Valine	X	
A	Urea		
5	Leucine	X	
6a	Serine (2 TBDMS)	X	
7	Proline	X	
8	Oxoproline		
9a	Hydroxyproline (2 TBDMS)		
6b	Serine (3 TBDMS)	X	
10a	Threonine (3 TBDMS)	X	
10b	Threonine (3 TBDMS)	X	
11	Phenylalanine	X	
12	Aspartic Acid	X	
9b	Hydroxyproline (3 TBDMS)		
13	Glutamic Acid	X	
14	Ornithine		
15	Lysine	X	
B	Aerothionin or its derivatives		
16	Arginine	X	
17	Histidine	X	
18	Tyrosine	X	
19	Tryptophan	X	
20	3-Monochlorotyrosine		X
21*	Monobromohistidine		X
22*	Monobromotyrosine		X
23*	Dichlorotyrosine		X

Table 1. *Cont.*

24	3-Monoiodotyrosine	X
25*	Monobromo-monochlorotyrosine	X
26	3,5-Dibromotyrosine	X
27*	Monochloro-monoiodotyrosine	X
28*	Monobromo-monoiodotyrosine	X
29	3,5-Diiodotyrosine	X

Figure 4. Gas chromatogram of the $Ba(OH)_2$ extract of the isolated *A. cavernicola* sponge skeletons before MeOH treatment. The relative retention time is related to the second peak of the internal standard. Components with * could not be verified with pure standards due to the lack of availability of these reference compounds.

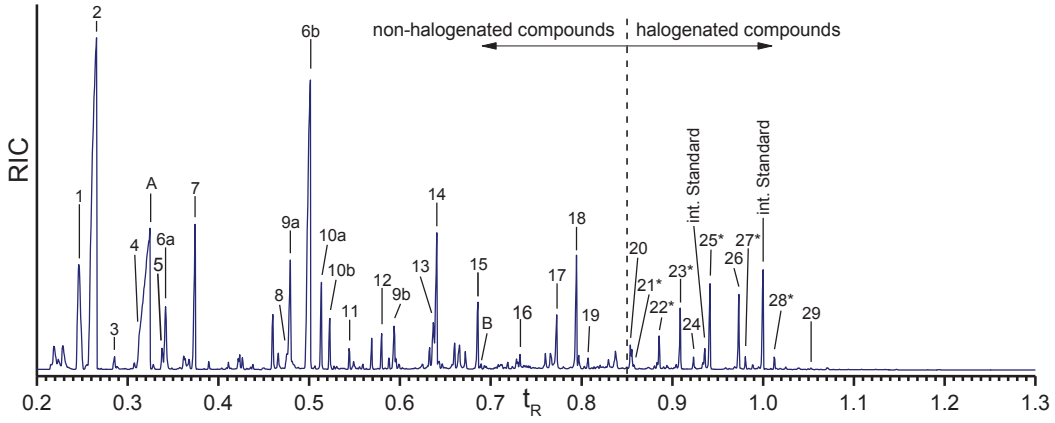

Nineteen different non-halogenated amino acids elute below a relative retention time of t_R = 0.85. Fifteen of them are proteinogenic amino acids. Several amino acids give rise to multiple peaks. Serine (peaks 6a, 6b) and hydroxyproline (peaks 9a, 9b) exhibit two signals due to different degrees of derivatization. Threonine (peaks 10a, 10b) yields two peaks for the same TBDMS derivative in the extracts as well as in the standard. Due to the existence of two stereocenters, threonine (peaks 10a, 10b) exhibits two different diastereomers [33] which can be separated by gas chromatography.

The largest peaks in the chromatogram are due to glycine (peak 2) and serine (peaks 6a, 6b). Moreover, proline (peak 7), threonine (peaks 10a, 10b), and tyrosine (peak 18) occur in larger quantities, while aspartic acid (peak 12), glutamic acid (peak 13), lysine (peak 15), and histidine (peak 17) occur in smaller amounts only. Leucine (peak 5), phenylalanine (peak 11), arginine (peak 16), and tryptophan (peak 19) exhibit the smallest concentrations. The amount of valine (peak 4) cannot be determined exactly due to the overlap with the urea peak. Nevertheless, an evaluation of specific ion tracks belonging to valine is possible and indicates a low concentration. Furthermore, the non-proteinogenic amino acids α-aminobutyric acid (peak 3), oxoproline (peak 8), hydroxyproline (peaks 10a, 10b), and ornithine (peak 14) can be identified. Measurements of the arginine standard treated with $Ba(OH)_2$ under the same conditions as the skeletons reveal that one part of arginine is cracked into urea (peak A) and ornithine by the alkaline treatment. This leads to the assumption that

the detected amount of urea in the $Ba(OH)_2$ extracts of the sponge skeletons may arise from the $Ba(OH)_2$ treatment of arginine. However, the comparison of the arginine/ornithine and arginine/urea ratios in the standard and the sample of the skeletons (see Table 2) reveal that the relative amounts of ornithine and urea related to arginine are larger in the $Ba(OH)_2$ extract of the sponge skeletons than in the standard. This leads to the assumption that urea and ornithine are indeed present in the sponge skeletons and are not just artefacts of the $Ba(OH)_2$ treatment.

Table 2. Comparison of the arginine/ornithine and arginine/urea ratios calculated for the standard and the skeleton sample before MeOH treatment.

Sample	Arginine/Ornithine Proportion	Arginine/Urea Proportion
Standard: arginine after Ba(OH)2	1:2.6	1:1.1
Ba(OH)2 extract of sponge skeletons before MeOH	1:8.8	1:9.1

Ten halogenated amino acids elute at relative retention times larger than 0.85. Interestingly, nine of them are tyrosine derivatives. Monohalogenated (e.g., monobromotyrosine (peak 22*)), dihalogenated (e.g., dichlorotyrosine (peak 23*)) as well as mixed halogenated (e.g., monobromo-monoiodotyrosine (peak 28*)) tyrosine occur. Only one halogenated derivative of another amino acid is identified, a monobrominated histidine (peak 21*). Dichlorotyrosine (peak 23*), monobromo-monochlorotyrosine (peak 25*), and 3,5-dibromotyrosine (peak 26) represent the most abundant halogenated amino acids. Monobromotyrosine (peak 22*) also occurs at relatively high concentration. The other halogenated amino acids occur only in small amounts.

Due to the lack of pure standard compounds, most of the halogenated amino acids were identified by their electon impact (EI) mass spectra. Figure 5 shows the EI mass spectra of the TBDMS derivatives of tyrosine and various halogenated tyrosines. The theoretical molecular weights of the expected compounds were calculated and compared with the experimentally observed fragmentation patterns in the mass spectra. Usually, the molecular ion peak is very weak or missing. The same is true for the (M-15) peak caused by the loss of a methyl group. Nevertheless, the spectra provide characteristic fragments. In particular, the (M-57) peak due to the loss of a *tert*-butyl group of the TBDMS group is intense in all spectra and can be used to determine the molecular weight of the respective compound. Furthermore, the peaks due to the loss of a *tert*-butyl group and a CO group (M-85) as well as of a CO-O-TBDMS group (M-159) are characteristic and intense. The base peak at *m/z* 302 is due to the $[TBDMS\text{-}NH\text{-}CH\text{-}CO\text{-}O\text{-}TBDMS]^+$-ion representing the backbone of each amino acid.

Brominated and chlorinated compounds could be easily identified by the characteristic isotope patterns due to the presence of two abundant isotopes. Bromine naturally occurs as ^{79}Br and ^{81}Br with relative abundances of approximately 1:1. Chlorine occurs as ^{35}Cl and ^{37}Cl with relative abundances of approximately 3:1. This results in characteristic isotope peaks with a mass difference of two mass units [34].

Measurements of a mixture of the standards tyrosine, 3-monoiodotyrosine, 3,5-diiodotyrosine and 3,5-dibromotyrosine treated with $Ba(OH)_2$ following the protocol as for the sponge skeletons reveal that the $Ba(OH)_2$ treatment has no influence on the structure of the halogenated tyrosines. The GC-MS

data show that the $Ba(OH)_2$ treatment did not cause any chemical transformation of the amino acids. It can, therefore, be assumed that all detected tyrosine derivatives occur in the native sponge skeletons.

Figure 5. Electron impact (EI)-MS data of TBDMS-derivatives of tyrosine (peak 18), monobromohistidine (peak 21*), monobromotyrosine (peak 22*), dichlorotyrosine (peak 23*), monobromo-monochlorotyrosine (peak 25*), 3,5-dibromotyrosine (peak 26), monochloro-monoiodotyrosine (peak 27*) and monobromo-monoiodotyrosine (peak 28*).

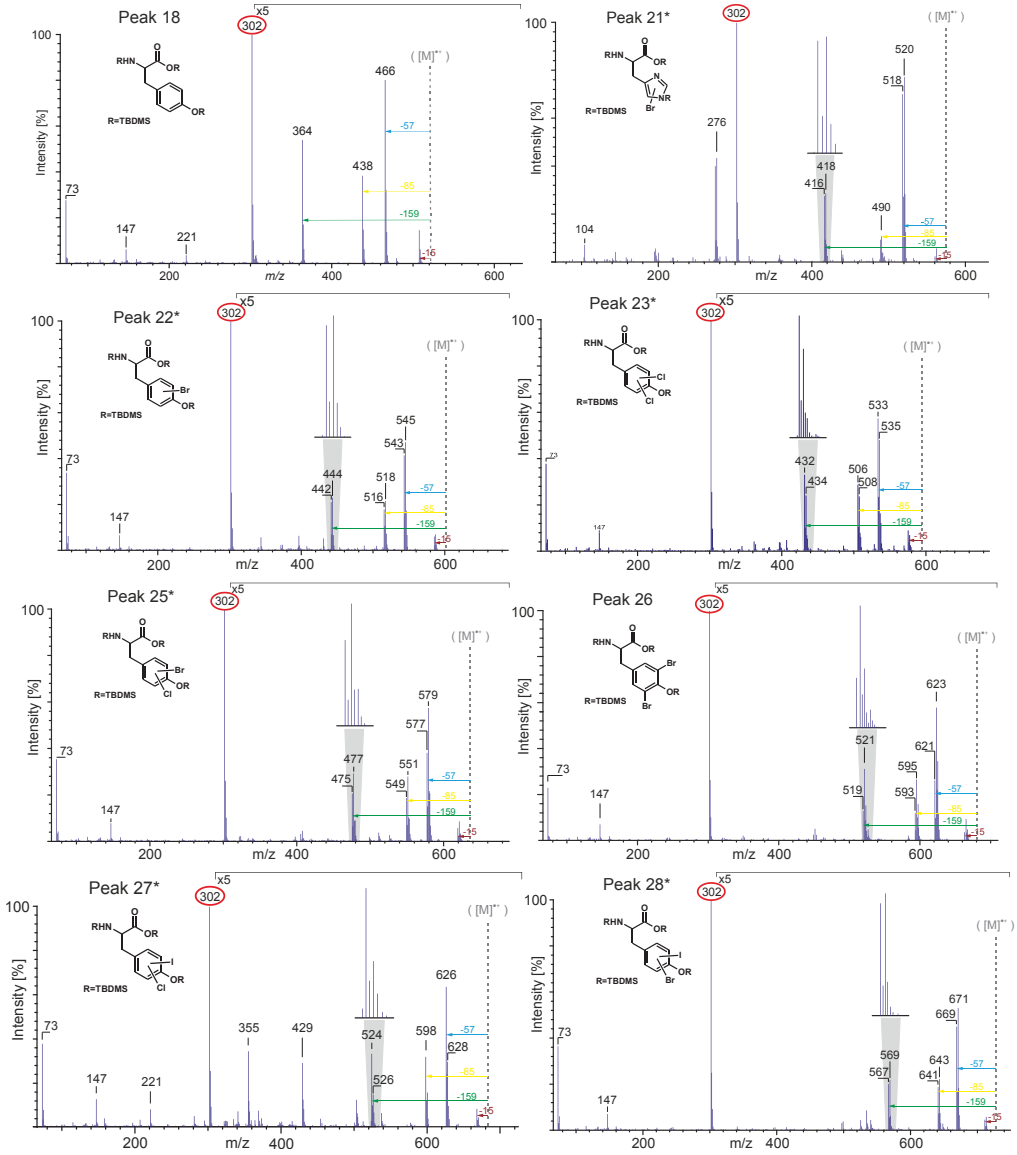

The comparison of the observed amino acid composition of *A. cavernicola* with the known amino acid compositions of different sponges shows a general agreement—but also some characteristic

differences. The results of these investigations are summarized in Table 3. The extraction of the amino acids from *Hippospongia equina* [29] and the bath sponge *Spongia officinalis obliqua* [30] was also based on an alkaline solution of $Ba(OH)_2$, *i.e.*, the data are well comparable. The observed differences in the amino acid compositions may be related to the fact that both, *H. equina* and the bath sponge, belong to the order Dictyoceratida. In contrast, *A. cavernicola* belongs to the order Verongida.

Table 3. Comparison of the found amino acids with the known amino acid composition of spongin from the literature.

Amino Acids (AAs)	Present Work	AAs in *Hippospongia equina* [29]	AAs in Spongia *Officinalis obliqua* [30]
α-Aminobutyric Acid (AABA)	X		X
γ-Aminobutyric Acid (GABA)		X	
Alanine	X	X	X
Arginine	X	X	
Aspartic Acid	X	X	X
Cystine		X	
Glutamic Acid	X	X	X
Glycine	X	X	X
Histidine	X	X	
Hydroxyproline	X	X	X
Leucine	X	X	X
Lysine	X	X	X
Methionine			X
Ornithine	X	X	
Oxoproline	X		
Phenylalanine	X	X	
Proline	X	X	X
Serine	X	X	
Threonine	X	X	
Tryptophan	X	X	X
Tyrosine	X	X	X
Valine	X	X	X
Monobromohistidine	X		
Monobromotyrosine	X		
3-Monochlorotyrosine	X		
3-Monoiodotyrosine	X		X
Monochloro-monoiodotyrosine	X		
Monobromo-monochlorotyrosine	X		
Monobromo-monoiodotyrosine	X		
Dichlorotyrosine	X		
3,5-Dibromotyrosine	X		X
3,5-Diiodotyrosine	X	X	X

The most striking difference between the amino acid composition of the *A. cavernicola* skeleton and the amino acid compositions described in the literature is the presence of various halogenated amino acids in the *A. cavernicola* sponge skeletons. In particular, the halogenated amino acids

monobromotyrosine (peak 22*), monobromo-monochlorotyrosine (peak 25*), 3-monochlorotyrosine (peak 20), dichlorotyrosine (peak 23*), monochloro-monoiodotyrosine (peak 27*), and monobromohistidine (peak 21*) do not occur in *H. equina* and *S. officinalis obliqua*. However, the naturally occurring amino acid monobromo-monochlorotyrosine could already be isolated from the gastropod mollusk *Buccinum undatum* [35]. In addition, the occurrence of AABA (peak 3) or GABA seems to depend on the taxonomy of the investigated sponges. Alanine (peak 1), aspartic acid (peak 12), glutamic acid (peak 13), glycine (peak 2), leucine (peak 5), lysine (peak 15), proline (peak 7), tryptophan (peak 19), tyrosine (peak 18), valine (peak 4) as well as the halogenated amino acid diiodotyrosine (peak 29) are found in both *A. cavernicola* skeletons and the dictyoceratid sponges *H. equina* and *S. officinalis obliqua*. The identified amino acids α-aminobutyric acid (peak 3), hydroxyproline (peaks 9a, 9b), oxoproline (peak 8), and ornithine (peak 14) were also detected previously in *H. equina* and *S. officinalis obliqua*. Both α-aminobutyric acid and hydroxyproline are present in the bath sponge *Spongia officinalis obliqua* [35]. Ornithine and oxoproline were found in *Aplysina aerophoba* [36].

Furthermore, the $Ba(OH)_2$ extract of the skeletons was examined with respect to the presence of aerothionin—one major bromotyrosine derivative found in the MeOH extracts of *A. cavernicola* skeletons [28]. Therefore, a standard of aerothionin was derivatized and measured by GC-MS. This measurement shows that aerothionin causes different GC peaks due to the decomposition into smaller fragments during GC injection. In comparison, only the degradation product at t_R = 0.69 (Peak B in Figure 4) can be found in the $Ba(OH)_2$ extract of the skeletons. The retention time, as well as the fragmentation pattern of peak B, are consistent with those of the aerothionin standard. The mass spectrum of this fragment of the standard is shown in the Supplementary Information (Figure S3). Based on the very small intensity of the peak and the lack of the other peaks observed in the standard it can be assumed that aerothionin only occurs in trace amounts. Since other aerothionin derivatives like homoaerothionin, 11-oxoaerothionin, or isofistularin-3 could cause the same fragment occurring at t_R = 0.69 due to their similar structure, it is not clear whether this peak represents aerothionin only. Its derivatives may also be present as minority components.

2.3.2. Skeletal Amino Acid Composition after MeOH Extraction

The relative amount of each amino acid after MeOH treatment was compared to the amount present before MeOH treatment.

Therefore, all intensities (peak heights) were normalized to the sample weight and the total intensity of both peaks of the internal standard. The comparison of the intensities of each amino acid before and after MeOH treatment enables the estimation of the decrease due to the MeOH extraction. The results are summarized in Table 4.

The comparison of the GC-MS data of the skeletons after MeOH extraction (Figure 6) with the GC-MS data of the skeletons before MeOH treatment reveals some differences. All amino acids found in the $Ba(OH)_2$ extract of the skeletons before MeOH extraction are present. However, their relative amounts have changed. That means, MeOH selectively reduces the amount of several amino acids. Interestingly, the largest decreases are observed for the proteinogenic amino acids. This leads to the assumption that either free amino acids or small proteins/peptides which are not tightly bound to the skeletons are removed by the MeOH extraction.

Table 4. Changes of the detected amounts of amino acids after MeOH extraction in comparison with the amounts before MeOH extraction. An average experimental error of approximately 15% is estimated (see Supplementary Information, Table S1).

TBDMS-Derivative	Decrease [1]
Alanine	+
Glycine	++
α-Aminobutyric Acid (AABA)	+++
Valine	+++
Leucine	+++
Serine (2 TBDMS)	−
Proline	++
Oxoproline	+
Hydroxyproline (2 TBDMS)	++
Serine (3 TBDMS)	++
Threonine (3 TBDMS)	++++
Threonine (3 TBDMS)	++++
Phenylalanine	+++
Aspartic Acid	+++
Hydroxyproline (3 TBDMS)	+++
Glutamic Acid	−
Ornithine	++
Lysine	++
Arginine	++
Histidine	+++
Tyrosine	+
Tryptophan	+
3-Monochlorotyrosine	–
Monobromohistidine	++
Monobromotyrosine	+
Dichlorotyrosine	–
3-Monoiodotyrosine	–
Monobromo-Monochlorotyrosine	–
3,5-Dibromotyrosine	–
Monochloro-Monoiodotyrosine	–
Monobromo-Monoiodotyrosine	–
3,5-Diiodotyrosine	–

[1] ++++ very strong decrease (residual content of 0%–25%); +++ strong decrease (residual content of 26%–50%); ++ medium decrease (residual content of 51%–75%); + weak decrease (residual content of more than 75%); − no decrease (residual 100% ± 15%).

In particular, the amount of threonine (peaks 10a, 10b) decreases very strongly. The amounts of AABA (peak 3), valine (peak 4), leucine (peak 5), phenylalanine (peak 11), aspartic acid (peak 12), and histidine (peak 17) also reduced considerably. For serine (peaks 6a, 6b), the decrease is different for the two TBDMS derivatives. The derivative with two TBDMS groups (incomplete derivatization) shows almost no decrease whereas the derivative with three TBDMS groups exhibits a medium decrease. This means, the total serine amount is slightly reduced. The same phenomenon is observed

for hydroxyproline (peaks 9a, 9b). The amount of the derivative with three TBDMS groups strongly decreases whereas the amount of the derivative with two TBDMS groups (incomplete derivatization) only shows a medium decrease.

Figure 6. Gas chromatogram of the amino acids in the isolated *A. cavernicola* sponge skeletons after MeOH treatment. Retention time is the relative retention time based on the second peak of the internal standard. Components with * could not be verified with standards. Numbering of the peaks is as in Table 1.

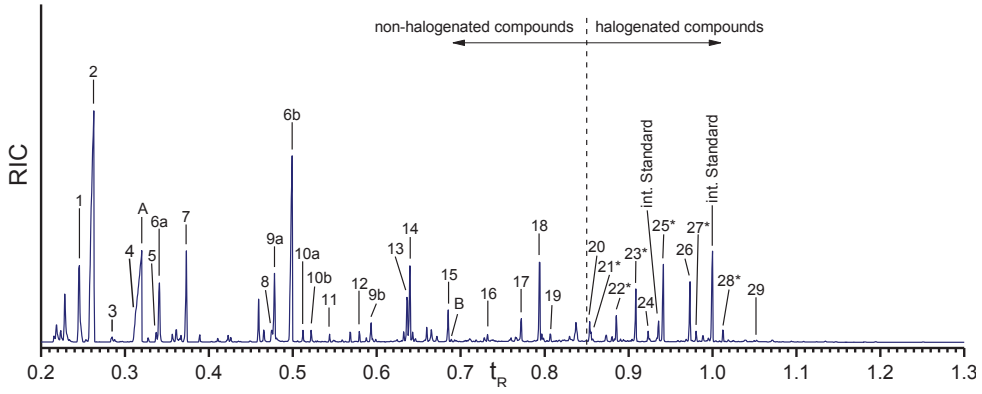

In contrast, the halogenated amino acids do not show a pronounced reduction, except for monobromohistidine (peak 21*). This observation leads to the conclusion that the halogenated tyrosines are strongly bound to the skeletons and confirms our hypothesis that halogenated molecules are tightly attached/covalently bound to the sponge skeleton.

Remarkably, traces of aerothionin or its derivatives can also be found in the skeletons after MeOH treatment. The identification was carried out as for the skeletons before MeOH treatment. This means, traces of such compounds are also incorporated into the skeletons of *A. cavernicola*. Also in this case, the retention time and the fragmentation pattern of peak B are consistent with those of the aerothionin standard.

2.3.3. Analysis of the MeOH Extract

In the MeOH extracts, different non-halogenated amino acids could be detected by GC-MS. The detected amino acids were: alanine, glycine, valine, leucine, proline, serine, tyrosine, and 3,5-diiodotyrosine. Interestingly, threonine which was effectively removed by MeOH extraction is not detected in the MeOH extract. That means, a significant amount of the extracted molecules must be present in the form of peptides or smaller proteins—which will not be detected by the applied analytical method. Furthermore, aerothionin or its derivatives can be found in the MeOH extract, which confirms our previous results [28]. The identification was carried out as in the skeletons before MeOH treatment. The retention time and the fragmentation pattern of the found aerothionin fragment are consistent with those of the aerothionin standard. The mass spectrum of the found Aerothionin fragment is shown in the Supplementary Information (Figure S4).

2.4. LC-MS Analysis of the Skeletal Amino Acid Composition

2.4.1. Skeletal Amino Acid Composition before MeOH Extraction

In addition to the GC-MS measurements, an on-line LC-ESI-MS analysis was performed with the skeleton extract resulting from the $Ba(OH)_2$ treatment. The focus of these measurements was placed on the verification of the presence of halogenated tyrosines. Since most of the other amino acids elute within the injection peak, they could not be determined via LC-MS. Apart from aliphatic hydroxyproline, ornithine, and arginine, the pseudo-molecular ions ($[M + H]^+$) of aromatic tryptophan, phenylalanine, and tyrosine were detected (data not shown). For tyrosine, different halogenated derivatives were identified within the (+)-ion trace as shown in Figure 7. For monobromo-, 3,5-dibromo-, 3-monoiodo-, and 3,5-diiodotyrosine the identity of the skeleton constituents was established via retention time and mass spectra comparison with native standards as demonstrated in Figure 8. In addition, the corresponding $[M + H]^+$-ions of mono- and dichloro-, as well as the mixed halogenated monobromo-monochloro-, monobromo-monoiodo- and monochloro-monoiodotyrosine were detected (spectra see Supplementary Information Figure S5).

Figure 7. (+)-Ion trace of LC-MS analysis of the $Ba(OH)_2$-extract prior MeOH extraction. Dark grey peaks correspond to halogenated tyrosines. Numbering refers to Table 1.

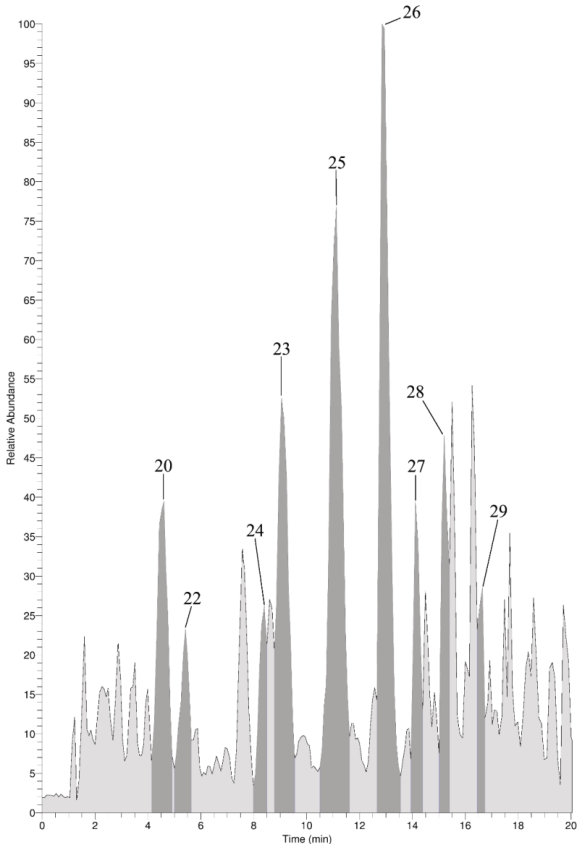

Figure 8. Structures and corresponding LC-ESI-MS spectra of brominated and iodinated tyrosine derivatives obtained from native standards and skeleton constituents of *A. cavernicola.*

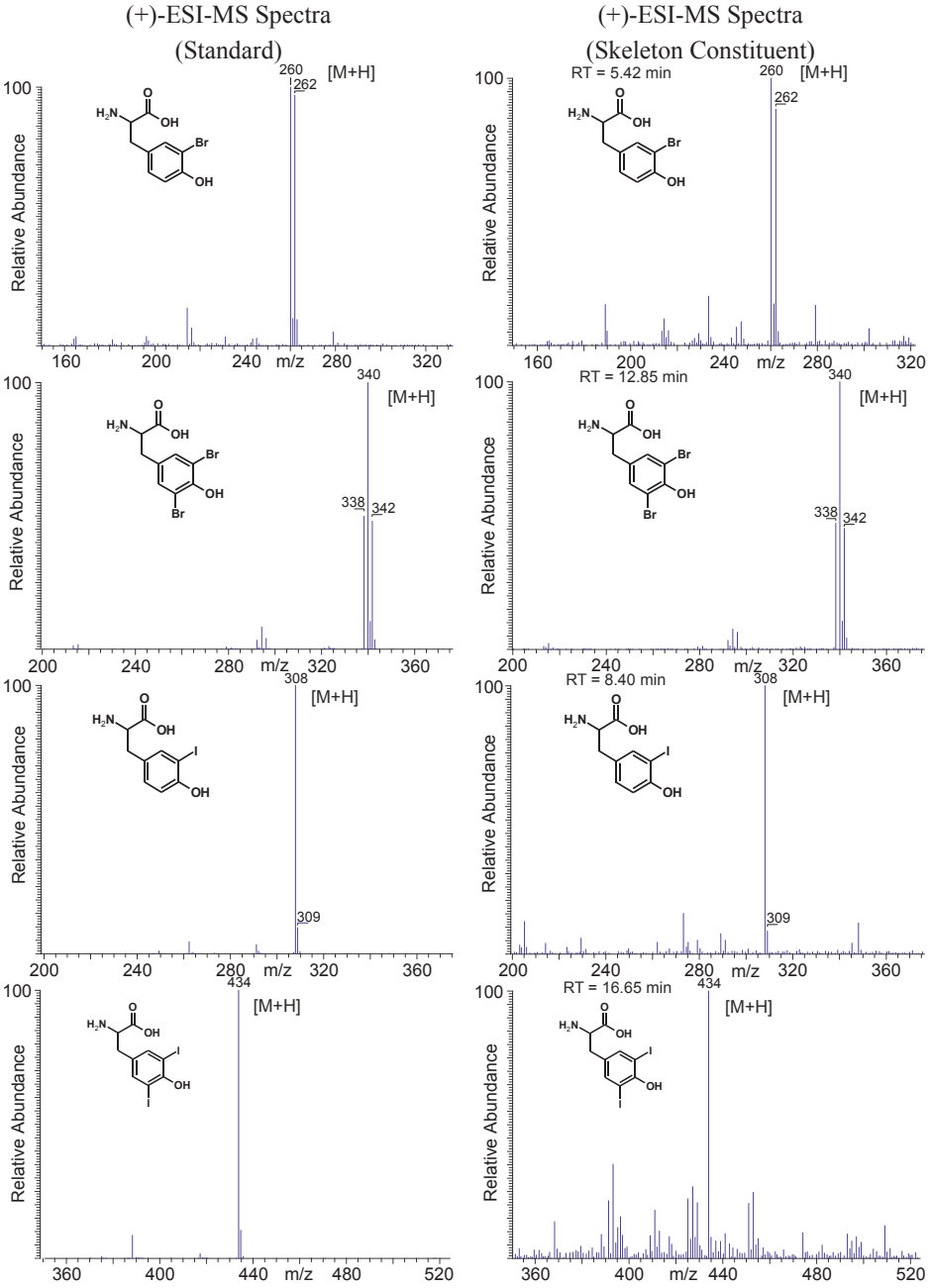

2.4.2. Skeletal Amino Acid Composition after MeOH Extraction

In analogy to 2.4.1, the $Ba(OH)_2$ extracts of the skeletons after MeOH treatment were also analyzed by LC-MS. The halogenated tyrosines found before MeOH treatment remained present after extraction with the organic solvent (spectra see Supplementary Information Figure S6). Moreover, the MeOH extract of the *A. cavernicola* skeleton was also analyzed via LC-MS. A specific search for the pseudo-molecular ions of all the halogenated amino acids found in the $Ba(OH)_2$ extracts was performed. None of the halogenated tyrosines identified in the $Ba(OH)_2$ extracts were detectable in the MeOH extract. These observations confirm the aforementioned results of GC-MS (Subsections 2.3.1 and 2.3.2) which demonstrated that the halogenated tyrosines are strongly attached or incorporated into the skeletons.

3. Experimental Sections

3.1. Sponge Samples

The *A. cavernicola* samples were collected in the Mediterranean Sea by the Hydra-Institute at Elba, Italy [37] and purchased from the Hydra Institut für Meereswissenschaften AG (Munich, Germany). After underwater collection the sponge samples were shock frozen. The samples were transported and stored on dry ice.

3.2. Extraction of the Skeletons

3.2.1. Isolation of the Skeleton

A. cavernicola skeletons were isolated from the sponge samples following the protocol described previously [28]. Approximately 10 g of the wet sponge were soaked in 40 mL of TE100 (10 mM Tris-HCl, 100 mM EDTA, pH 8). After two weeks, the remaining skeletons were washed in distilled water for 24 h under continuous shaking. The washing procedure was repeated six times.

3.2.2. MeOH Extraction of the Skeletons

The MeOH extraction of the purified skeletons was performed with methanol and acetonitrile as described previously [28]. The isolated skeletons were transferred into 200 mL methanol and sonicated for 1 min. After 24 h, the solvent was renewed and the samples were stirred for a further 24 h. Afterwards one extraction cycle was performed in 200 mL acetonitrile. The extracted skeletons were freeze-dried. The extracts were combined and dried under a gentle stream of nitrogen.

3.2.3. $Ba(OH)_2$ Extraction

Thirty mg of each dried isolated skeleton before and after MeOH extraction was treated with 15 mL of saturated $Ba(OH)_2$ solution containing 0.5 mg 5-bromotryptophan as internal standard at 37 °C for 6 days. Subsequently, the insoluble residue (chitin-fibers) was removed and the $Ba(OH)_2$ solution was neutralized with H_2SO_4 and centrifuged. The supernatant was removed and freeze dried.

3.3. Derivatization

3.3.1. Preparation of Standard Solutions

For the standard solutions, 12 mg of each amino acid was dissolved in a mixture of 5 mL H_2O and 1 mL 2.5 M HCl. The solutions were stored in a refrigerator until analysis. As an internal standard, a solution containing 5-bromotryptophan was prepared following the same procedure.

3.3.2. TBDMS-Derivatization of the Standard Solutions

Ten µL of the standard solution of the halogenated amino acids (alternatively 5 µL of the solution of the other amino acids) and 10 µL of the internal standard were mixed and dried under a gentle stream of nitrogen. The residue was soaked in 20 µL 2.5 M HCl and dried again. Subsequently, the residue was soaked twice in 40 µL EtOH and dried under nitrogen. 50 µL acetonitrile and 50 µL *N*-*tert*-butyldimethylsilyl-*N*-methylfluoroacetamide (MTBSTFA) with 1% *tert*-butyldimethylchlorosilane (TBDMSCl) were added to the dry residue. The mixture was sonicated for 30 s and then heated at 70 °C for 30 min. One µL of the resulting solution was injected into the GC-MS.

3.3.3. TBDMS-Derivatization of the Sponge Samples

One mg of the dried $Ba(OH)_2$ extract containing the internal standard was soaked in 20 µL 2.5 M HCl and dried under a gentle stream of nitrogen. Subsequently, the residue was soaked twice in 40 µL EtOH and dried under nitrogen. Fifty µL acetonitrile and 50 µL MTBSTFA were added to the dry residue. The mixture was sonicated for 30 s and then heated to 70 °C for 30 min. One µL of the resulting solution was injected into the GC-MS.

3.4. GC-MS Measurements

Analyses were carried out on a Varian 3400 gas chromatograph (Varian, Palo Alto, CA, USA) directly coupled to a Finnigan MAT 95 mass spectrometer (Finnigan/Thermo Fisher Scientific Inc., Waltham, MA, USA). The GC separations were performed on a SPB®-5 capillary GC column (Sigma-Aldrich, St. Louis, MO, USA). The flow of helium as carrier gas was 1 mL/min. The injector temperature was 300 °C. Split/Splitless injection was used (splitless time 1 min). The column temperature was programmed as followed: isothermal 115 °C for 3 min, then heating up to 300 °C at rate of 4K/min, then isothermal 300 °C for 30 min.

The ion source temperature was 250 °C and the transfer line temperature was 300 °C. The mass spectra were recorded with a scan cycle time of 1.284 s in the electron impact (EI) ionization mode at 70 eV, *m/z* range 70–850. The chromatograms were recorded after 3 min solvent delay. The retention time t_R was normalized to the second peak of the internal standard 5-bromotryptophan. The intensity was normalized to the weighted sample and the total intensity of both peaks of the internal standard.

3.5. Liquid Chromatography-Mass Spectrometry

3.5.1. Preparation of Standard Solutions

Amino acids were dissolved in MeOH/H_2O (10/1) to yield a sample concentration of 1 mg/mL.

3.5.2. Preparation of Sponge Extract Samples

Dried extracts resulting either from the $Ba(OH)_2$ treatment or the MeOH extraction of the *A. cavernicola* skeleton were dissolved in MeOH/H_2O (10/1) to yield a sample concentration of 1 mg/mL.

3.5.3. Measurement Conditions

All LC-MS analyses were performed on a Thermoquest Finnigan LCQDeca (Thermo Fisher Scientific Inc., Waltham, MA, USA) connected to an Agilent 1100 Series LC (Agilent, Santa Clara, CA, USA) with a Knauer Eurospher 100-3 C18, 100 × 2 mm column (Knauer, Berlin, Germany). As eluents 0.1% formic acid (Eluent A) and MeOH (Eluent B) were utilized and a gradient as shown in Table 5 was applied for all measurements. Electrospray ionization (ESI) mode was chosen for all analyzed samples.

Table 5. Eluent system utilized for LC-MS analyses.

t [min]	Eluent A [%]	Eluent B [%]
0	90	10
2	90	10
35	0	100
50	0	100
51	90	10
60	90	10

3.6. FTIR Spectroscopy

IR spectra were recorded using a Bruker FTIR spectrometer IFS 88 (Bruker, Karlsruhe, Germany). The samples were deposited on SPECAC Golden-Gate-ATR equipment (LOT-Oriel, Darmstadt, Germany). The spectra were measured in the range from 4000 to 650 cm^{-1} with a spectral resolution of 0.5 cm^{-1}. Each spectrum was recorded by the accumulation of 1000 scans. Subsequently, an ATR intensity correction was carried out. The spectra were baseline corrected and normalized to the most intensive band at about 1625 cm^{-1}.

3.7. Scanning Electron Microscopy (SEM) and Energy Dispersive X-ray Spectroscopy (EDX)

Some dried pieces of the skeletons were applied on a sample holder and coated with carbon. The SEM images were then recorded on a ZEISS DSM 982 GEMINI field emission scanning electron microscope (ZEISS, Oberkochen, Germany). Furthermore, EDX spectra were recorded. The spectra were measured with an acceleration voltage of 15 keV. The live time was 60 s.

3.8. Light Microscopy

Small pieces of the purified chitin-scaffolds after $Ba(OH)_2$ or NaOH were put on a sample holder. Microscopic studies were carried out on a Keyence BZ-8000K microscope (Keyence, Osaka, Japan). The images were acquired at 10-fold magnification.

4. Conclusions

The isolated skeletons of the marine demosponge *A. cavernicola* before and after the conventional MeOH extraction were analyzed with respect to the presence of halogenated amino acids. For this purpose, a $Ba(OH)_2$-based extraction method was applied which effectively removes all organic material from the remaining pure chitin. The $Ba(OH)_2$ extracts of the sponge skeletons of *A. cavernicola* were studied by GC-MS and LC-MS. These investigations revealed that the skeletons contain 10 halogenated amino acids. Nine of these 10 amino acids are halogenated tyrosines. These halogenated tyrosines are strongly attached to the skeletons since the conventional MeOH extraction method does not significantly reduce the amount of halogenated tyrosines in the skeletons. Furthermore, 19 different non-halogenated amino acids were identified. Among them are 15 proteinogenic amino acids. Glycine and serine exhibit the largest concentrations, while leucine, phenylalanine, arginine, and tryptophan are less abundant. In addition, trace amounts of aerothionin and/or its derivatives are present.

To summarize, it should be emphasized that the identified halogenated tyrosines are integral parts of the chitin-based skeletons of *A. cavernicola*. It is tempting to speculate that these compounds are covalently bound to the skeletons. In contrast, the amount of non-halogenated organic material is reduced during MeOH treatment. Investigations of the MeOH extracts suggest that these removed molecules are not only free amino acids but also peptides or small proteins.

Acknowledgments

The authors gratefully acknowledge financial support from the Deutsche Forschungsgemeinschaft (grant No. Br 1278/17-1, PE 348/27-1, PR 229/15-1).

Author Contributions

SU and SM designed the GC-MS experiments. SU performed the isolation of the sponge skeletons and the GC-MS experiments. SU and SM analyzed data resulting from GC-MS experiments. SU performed the FTIR experiments. PP and HN conceived and designed the LC-MS experiments. HN performed the LC-MS experiments. HN and PP analyzed data resulting from LC-MS experiments. EB supervised the scientific work. SU, SM, HN, PP and EB wrote this manuscript.

Conflicts of Interest

The authors declare no conflict of interest.

References

1. Müller, W.E.G. Origin of metazoa: Sponges as living fossils. *Naturwissenschaften* **1998**, *85*, 11–25.
2. Li, C.-W.; Chen, J.-Y.; Hua, T.-E. Precambrian sponges with cellular structures. *Science* **1998**, *279*, 879–882.
3. Proksch, P.; Putz, A.; Ortlepp, S.; Kjer, J.; Bayer, M. Bioactive natural products from marine sponges and fungal endophytes. *Phytochem. Rev.* **2010**, *9*, 475–489.
4. Thoms, C.; Wolff, M.; Padmakumar, K.; Ebel, R.; Proksch, P. Chemical defense of Mediterranean sponges *Aplysina cavernicola* and *Aplysina aerophoba*. *Z. Naturforsch. C* **2004**, *59*, 113–122.
5. Thoms, C.; Ebel, R.; Proksch, P. Activated chemical defense in *Aplysina.* sponges revisited. *J. Chem. Ecol.* **2006**, *32*, 97–123.
6. Paul, V.J.; Ritson-Williams, R.; Sharp, K. Marine chemical ecology in benthic environments. *Nat. Prod. Rep.* **2011**, *28*, 345–387.
7. Hickman, C.P.; Roberts, L.S.; Larson, A.; l'Anson, H.; Eisenhour, D.J. *Zoologie*, 13th ed.; Pearson Studium Verlag: München, Germany, 2008; pp. 375–387.
8. Harris, V.A. *Sessile Animals of the Sea Shore*; Chapman and Hall: London, UK, 1990; pp. 280–282.
9. Hill, M.S.; Hill, A.L. Morphological Plasticity in the Tropical Sponge *Anthosigmella. varians*: Responses to Predators and Wave Energy. *Biol. Bull.* **2002**, *202*, 86–95.
10. Hill, M.S.; Lopez, N.A.; Young, K.A. Anti-predator defenses in western North Atlantic sponges with evidence of enhanced defense through interactions between spicules and chemicals. *Mar. Ecol. Prog. Ser.* **2005**, *291*, 93–102.
11. Wehner, R.; Gehring, W.J. *Zoologie*; Georg Thieme Verlag: Stuttgart, Germany, 2007; pp. 698–699.
12. Bergquist, P.R.; Cook, S.D.C. Order Verongida Bergquist, 1978. In *Systema Porifera: A Guide to the Classification of Sponges*; Hooper, J.N.A., van Soest, R.W.M., Eds.; Kluwer Academic/Plenum Publishers: New York, NY, USA, 2002; Volume I, pp. 1081–1096.
13. Ehrlich, H.; Maldonado, M.; Spindler, K.-D.; Eckert, C.; Hanke, T.; Born, R.; Goebel, C.; Simon, P.; Heinemann, S.; Worch, H. First evidence of chitin as a component of the skeletal fibers of marine sponges. Part I. Verongidae (Demospongia: Porifera). *J. Exp. Zool. B Mol. Dev. Evol.* **2007**, *308*, 347–356.
14. Brunner, E.; Ehrlich, H.; Schupp, P.; Hedrich, R.; Hunoldt, S.; Kammer, M.; Machill, S.; Paasch, S.; Bazhenov, V.V.; Kurek, D.V.; *et al.* Chitin-Based scaffolds are an integral part of the skeleton of the marine demosponge *Ianthella basta*. *J. Struct. Biol.* **2009**, *168*, 539–547.
15. Uriz, M.-J.; Turon, X.; Becerro, M.A.; Agell, G. Siliceous spicules and skeleton frameworks in sponges: Origin, diversity, ultrastructural patterns, and biological functions. *Microsc. Res. Tech*. **2003**, *62*, 279–299.
16. Ehrlich, H. *Biological Materials of Marine Origin*, Biologically-Inspired Systems (Book 1); Springer Verlag: Dordrecht, The Netherlands, 2010; pp. 245–256.
17. Gross, J.; Sokal, Z.; Rougvie, M. Structural and chemical studies on the connective tissue of marine sponges. *J. Histochem. Cytochem.* **1956**, *4*, 227–246.

18. Junqua, S.; Robert, L.; Garrone, R.; Pavans de Ceccatty, M.; Vacelet, J. Biochemical and morphological studies on the collagens of Horny Sponges. Ircinia filaments compared to spongines. *Connect. Tiss. Res.* **1974**, *2*, 193–203.
19. Ehrlich, H.; Ilan, M.; Maldonado, M.; Muricy, G.; Bavestrello, G.; Kljajic, Z.; Carballo, J.L.; Shiaparelli, S.; Ereskovsky, A.V.; Schupp, P.; *et al.* Three-Dimensional chitin-based scaffolds from Verongida sponges (Demospongiae: Porifera). Part I. Isolation and identification of chitin. *Int. J. Biol. Macromol.* **2010**, *47*, 132–140.
20. Ehrlich, H.; Kaluzhnaya, O.V.; Brunner, E.; Tsurkan, M.V.; Ereskovsky, A.; Ilan, M.; Tabachnick, K.R.; Bazhenov, V.V.; Paasch, S.; Kammer, M.; *et al.* Identification and first insights into the structure and biosynthesis of chitin from the freshwater sponge *Spongilla lacustris*. *J. Struct. Biol*. **2013**, *183*, 474–483.
21. Ehrlich, H.; Keith Rigby, J.; Botting, J.P.; Tsurkan, M.V.; Werner, C.; Schwille, P.; Petrášek, Z.; Pisera, A.; Simon, P.; Sivkov, V.N.; *et al.* Discovery of 505-million-year old chitin in the basal demosponge *Vauxia gracilenta*. *Sci. Rep.* **2013**, *3*, 3497.
22. Hackman, R.H. Studies on chitin IV. The occurrence of complexes in which chitin and protein are covalently linked. *Aust. J. Biol. Sci.* **1960**, *13*, 568–577.
23. Blackwell, J.; Weih, M.A. Structure of chitin-protein complexes: Ovipositor of the ichneumon fly *Megarhyssa*. *J. Mol. Biol.* **1980**, *137*, 49–60.
24. Teeyapant, R.; Woerdenbag, H.; Kreis, P.; Hacker, J.; Wray, V.; Witte, L.; Proksch, P. Antibiotic and cytotoxic activity of brominated compounds from the marine sponge *Verongia aerophoba*. *Z. Naturforsch. C* **1993**, *48*, 939–945.
25. Faulkner, D.J. Marine pharmacology. *Antonie Van Leeuwenhoek* **2000**, *77*, 135–145.
26. Thomson, J.E.; Barrow, K.D.; Faulkner, D.J. Localization of two brominated metabolites, aerothionin and homoaerothionin, in spherulous cells of the marine sponge *Aplysina. fistularis* (=*Verongia thiona*). *Acta Zool.* **1981**, *64*, 199–210.
27. Turon, X.; Becerro, M.A.; Uriz, M.J. Distribution of brominated compounds within the sponge *Aplysina. aerophoba*: Coupling X-ray microanalysis with cryofixation techniques. *Cell Tissue Res.* **2000**, *301*, 311–322.
28. Kunze, K.; Niemann, H.; Ueberlein, S.; Schulze, R.; Ehrlich, H.; Brunner, E.; Proksch, P.; van Pée, K.-H. Brominated Skeletal Components of the Marine Demosponges, *Aplysina cavernicola* and *Ianthella basta*: Analytical and Biochemical Investigations. *Mar. Drugs* **2013**, *11*, 1271–1287.
29. Saper, J.; White, W.E. Amino-acid Composition of Sclero-protein of the Sponge *Hippospongia equina*. *Nature* **1958**, *181*, 285–286.
30. Low, E.M. Halogenated amino acids of the bath sponge. *J. Mar. Res.* **1951**, *10*, 239–245.
31. Ebada, S.S.; Edrada, R.A.; Lin, W.; Proksch, P. Methods of isolation, purification and structural elucidation of bioactive secondary metabolites from marine invertebrates. *Nat. Protoc.* **2008**, *3*, 1820–1831.
32. Sobolevsky, T.G.; Revelsky, A.I.; Miller, B.; Oriedo, V.; Chernetsova1, E.S.; Revelsky I.A. Comparison of silylation and esterification/acylation procedures in GC-MS analysis of amino acids. *J. Sep. Sci.* **2003**, *26*, 1474–1478.
33. North, M. *Principles and Applications of Stereochemistry*; CRC Press: Cheltenham, UK, 1998; pp. 75–77.

34. Reichenbächer, M.; Popp. J. *Strukturanalytik Organischer Und Anorganischer Verbindungen—Ein Übungsbuch*; Teubner Verlag: Wiesbaden, Germany, 2007.
35. Hunt, S.; Breuer, S.W. Isolation of a new naturally occuring halogenated amino acid: Monochloromonobromotyrosine. *Biochim. Biophys. Acta* **1971**, *252*, 401–404.
36. Čmelik, S. Über einen Farbstoff von Protein-Natur aus dem Schwamme *Aplysina aerophoba* Nardo. *Hoppe-Seyler's Z. Physiol. Chem.* **1952**, *289*, 218–220.
37. Institut für angewandte Hydrobiologie; HYDRA AG; HYDRA Institut für Meereswissenschaften AG; HYDRA Büro für Gewässerökologie Mürle & Ortlepp GbR; HYDRA Wiesloch—Dipl-Biol. Andreas Becker. Available online: http://www.hydra-institute.com (accessed on 17 March 2013).

Supplementary Information

Figure S1. EDX measurement of the isolated skeletons of *Aplysina cavernicola* before MeOH extraction.

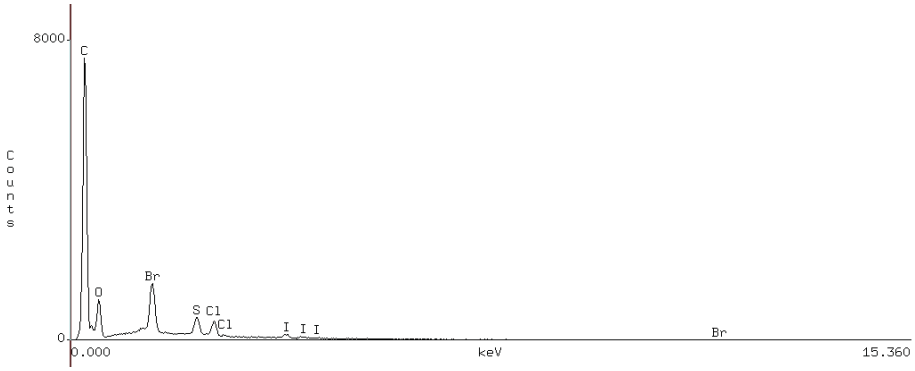

Figure S2. EDX measurement of the isolated skeletons of *A. cavernicola* after MeOH extraction.

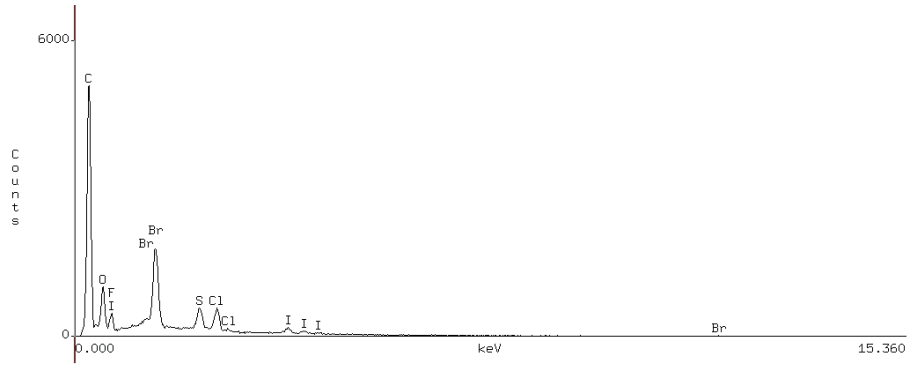

Figure S3. EI-MS data of TBDMS-derivative of the aerothionin standard.

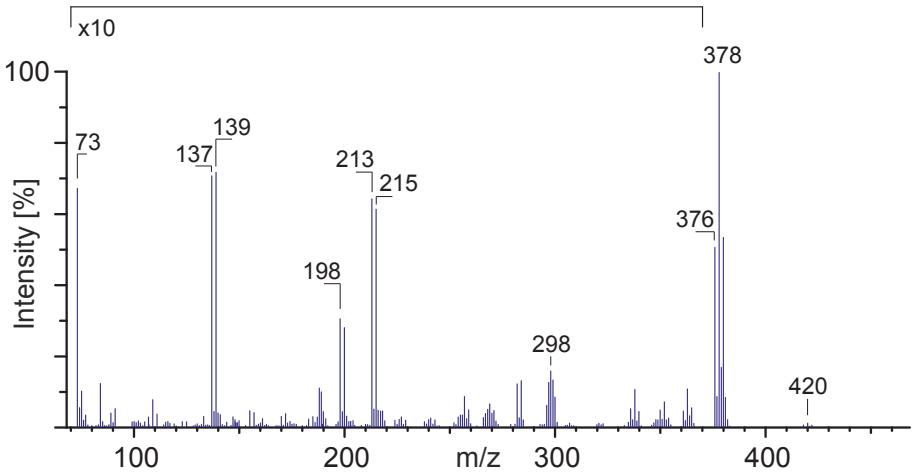

Figure S4. EI-MS data of TBDMS-derivative of the aerothionin fragment found in the MeOH extract.

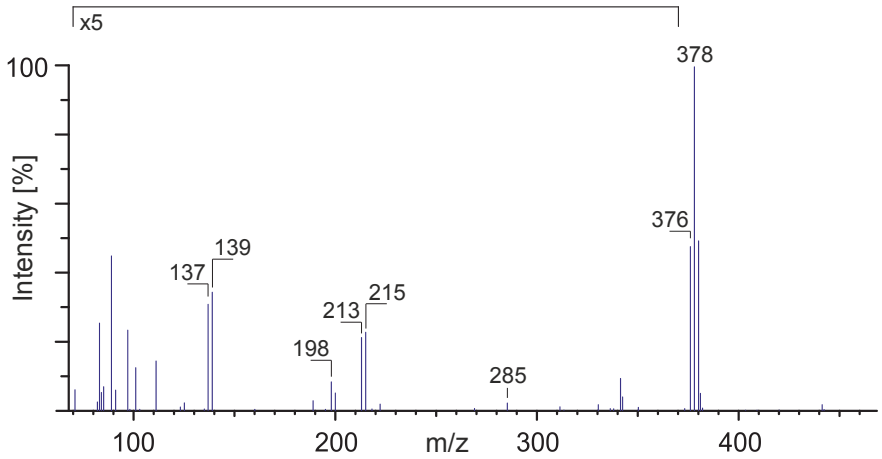

Table S1. Experimental Errors of six amino acids. ***** The experimental error is determined for these amino acids. For each amino acid, the experimental error is calculated from three measurements of the same sample. The average value is about 15%.

Amino Acid	Experimental Error *
Alanine (Peak 1)	4.8%
Phenylalanine (Peak 11)	23.8%
Aspartic Acid (Peak 12)	12.2%
Ornithine (Peak 14)	18.4%
Dichlorotyrosine (Peak 23*)	5.5%
Monobromo-Monochlorotyrosine (Peak 25*)	22.9%

Figure S5. LC-ESI-MS spectra of mono- and dichloro-, monobromo-monochloro-, monochloro-monoiodo- and monobromo-monoiodotyrosine detected in the $Ba(OH)_2$ skeleton extracts of *A. cavernicola*.

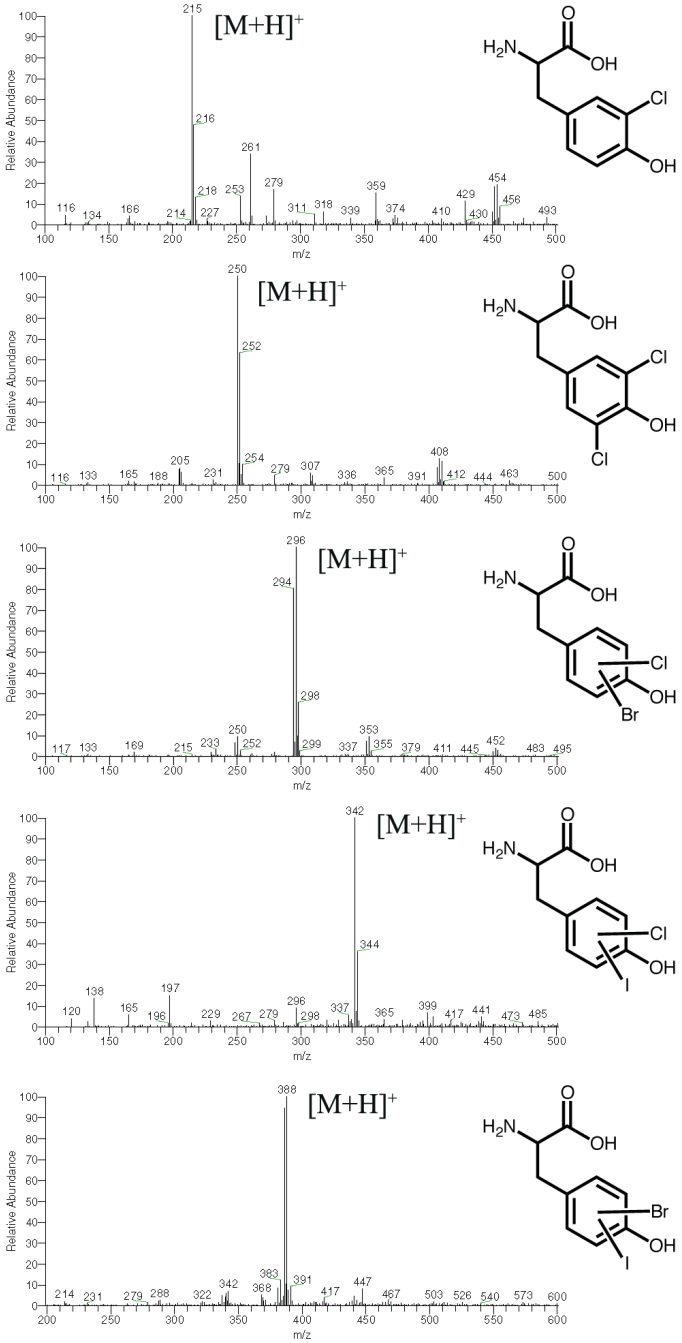

Figure S6. LC-ESI-MS spectra of halogenated tyrosines detected in the $Ba(OH)_2$ skeleton extract of *A*. *cavernicola* after MeOH extraction.

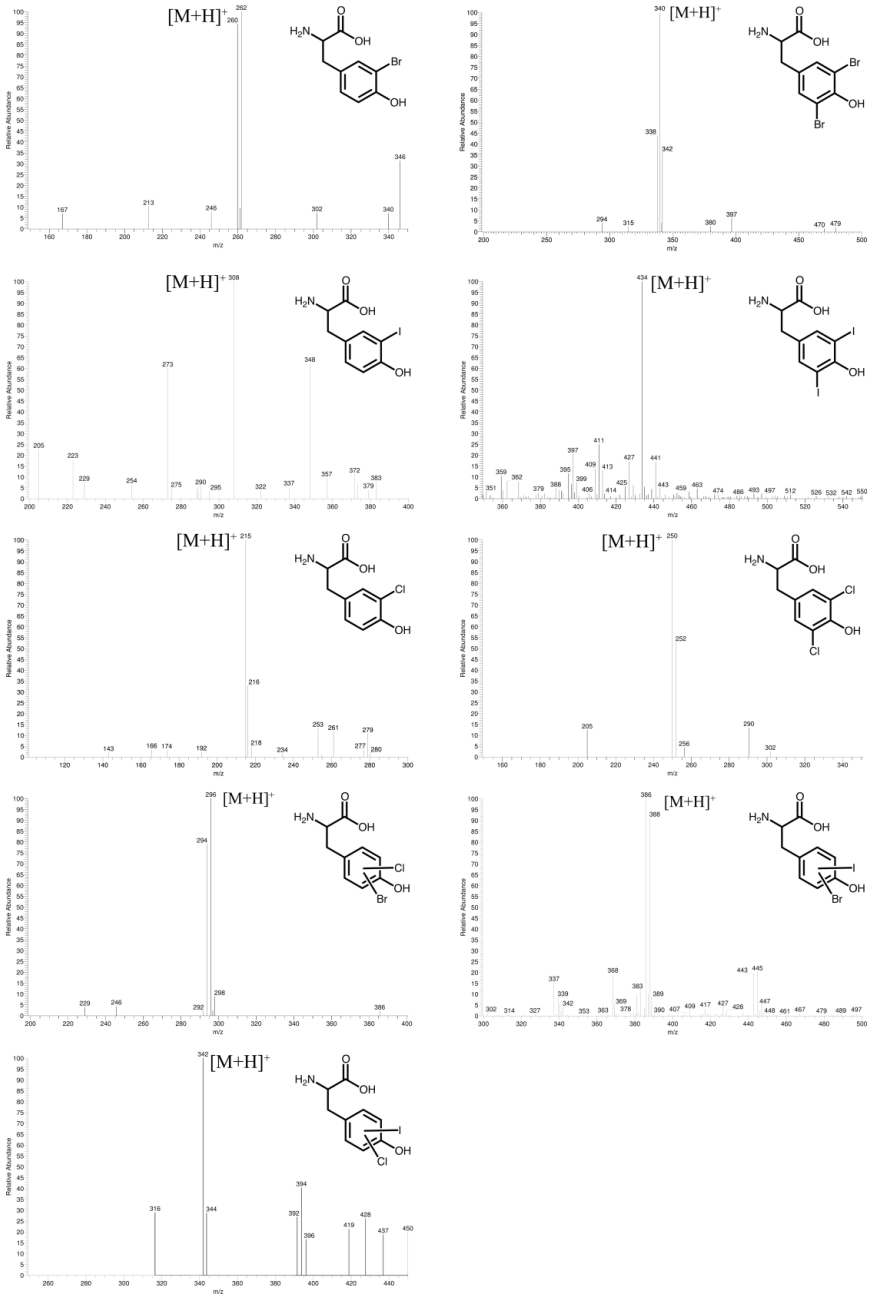

10 Discussion

10.1 Bastadins: Potential Anticancer Leads

Bastadins and their putative biogenetic building blocks, the hemibastadins, are oxime-bearing bromotyrosine derivatives, that are typically present in marine sponges of the order Verongida. Apart from their occurence in sponges bastadin-like lithothamnins have recently been isolated from red algae (Van Wyk *et al.*, 2011), rising the question of the true origin of these compounds. One plausible hypothesis might be that microbial symbionts, which can comprise as much as 40 % of the total sponge volume (Taylor *et al.*, 2007), are the producers of bastadins and closely related metabolites. It is well-known from sponge associated microorganisms such as bacteria, archaea, microalgae and fungi that these symbionts contribute significantly to host metabolism, e.g. via photosynthesis or nitrogen fixation (Taylor *et al.*, 2007). Therefore, a microbial involvement not only to processes of primary but also of secondary metabolism, such as bastadin biosynthesis is conceivable. One approach to answer this „chicken or egg debate“ is the metagenomic approach by identifying gen clusters leading to the respective secondary metabolites (Wang, 2006). The advancing interest to this question is demonstrated by the annual number of sponge derived 16S rRNA gene sequences recently deposited in GenBank, which has risen to more than 700 by 2005 (Taylor *et al.*, 2007). In publication 5 the genetic analyses of *A. cavernicola* and *I. basta* revealed that flavin-dependent halogenase genes originate from sponge symbionts, concluded from a high degree of analogy of investigated gene fragments to bacterial halogenase genes. One may therefore assume that bromotyrosine derivatives from these species and maybe also from other sponges originate from symbionts or are at least formed with the involvement of those.

So far, bastadins had only been reported as dimeric hemibastadin congeners. During this study the first trimeric congener, sesquibastadin 1, was isolated from *I. basta* (publication 2). With regard to its biosynthesis this compound was identified as a condensation product of the known structures bastadin 3 and hemibastadin 2, which are hypothetically coupled by a nucleophilic substitution forming a diaryl ether bond (figure 20). So far, the enzyme involved in this mechanism in respective sponge species has not been identified. Similar arylether bond formations are typically catalyzed by peroxidases like horseradish (*Armoracia rusticana*) peroxidase (HRP) (Sih and Malnar, 2000), so one might hypothesize that similar enzymes are also involved in this step of bastadin biosynthesis. Interestingly, HRP has served organic chemists as an enzymatic tool for the total synthesis of several bastadin congeners (Guo *et al.*, 1998).

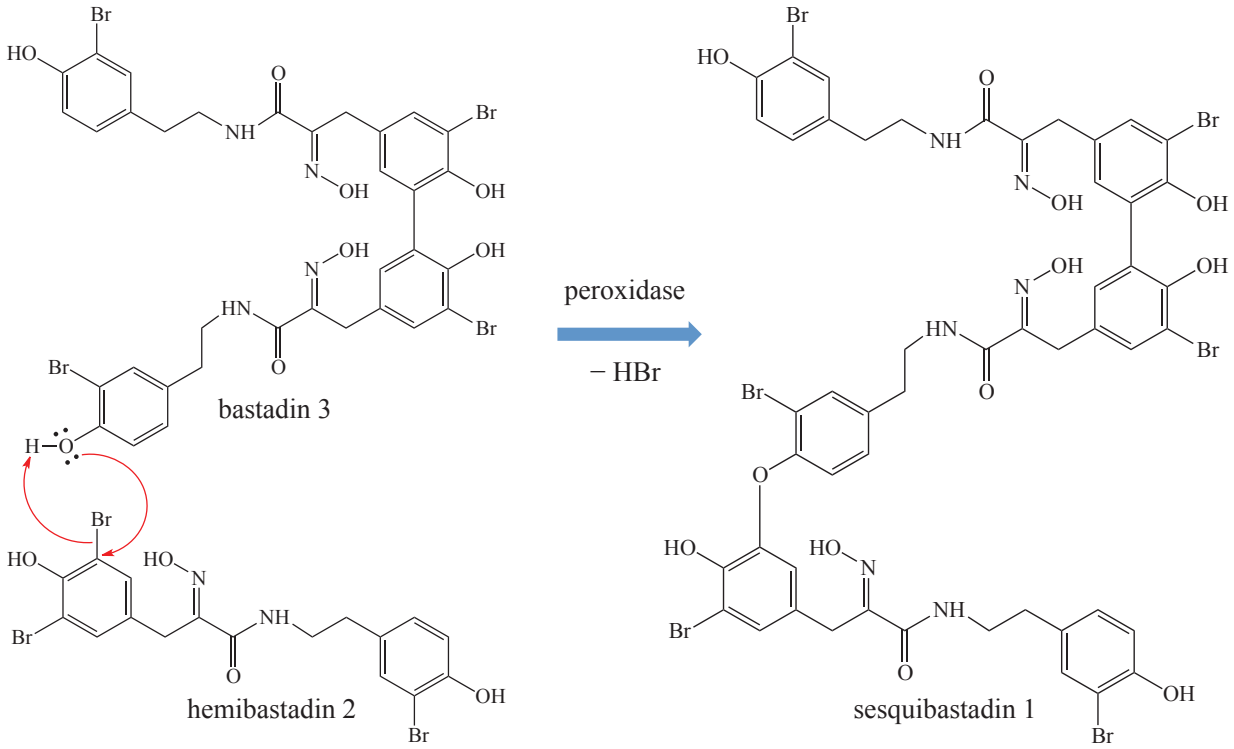

Figure 20. Final step of putative biosynthesis of trimeric sesquibastadin 1 by ether bond formation between the phenolic hydroxyl of bastadin 3 and the brominated aromatic carbon of hemibastadin 2 via nucleophilic substitution (red arrows) under catalysis of a peroxidase.

With regard to their clinical utilization bastadins and further halotyrosines have displayed an enormous potential. It is remarkable that bastadins demonstrate strong anticancer activities against various tumor cell lines and address several molecular tumor targets such as RyR-3 (Aoki *et al.*, 2006), IMPDH (Reddy *et al.*, 2006), topoisomerase II or dehydrofolate reductase (Carney *et al.*, 1993). These previously published studies are in agreement to the anticancer properties reported in publication 2 of this thesis, in which the inhibitory potential of isolated bastadin congeners against 22 protein kinases as well as the cytotoxicity against a murine lymphoma cell line (L5178Y) were investigated (figure 21). The fact that trimeric sesquibastadin 1 and its building unit bastadin 3 both showed strong protein kinase inhibition (IC_{50} values against all kinases ranging from 0.1~6.5 µM) suggests, that the addition of a third hemibastadin unit did not lead to a distinct change in the inhibitory potential. In detail, sesquibastadin 1 caused potent inhibitory activity against the receptor tyrosine kinases EGF-R (IC_{50} = 0.6 µM) and VEGF-R2 (IC_{50} = 0.6 µM), both being overexpressed in non-small-cell lung cancer cells (Herbst, 2004), and of the angiopoietin receptor TIE-2 (IC_{50} = 0.6 µM), which is involved in angiogenesis (Sato *et al.*, 1995). Inhibition of aurora A and B, both being serine/threonine kinases that regulate the cell cycle and are overregulated in breast cancer cells (Nouri *et al.*, 2014), was most pronounced for bastadin 3, with IC_{50} values of 0.1 µM against aurora A and of 0.5 µM against aurora B. Similar inhibition was shown for bastadin 3 against

TIE2 (IC_{50} = 0.8 µM). Due to this rather general inhibition of kinases a specificity of sesquibastadin 1 and bastadin 3 towards certain targets, which is highly favorable for new drug candidates, can not be stated. Surprisingly, both compounds lacked activity in the cellular assay, which might be explained by a hindered uptake of these linear bastadins by the investigated cell line. This was not the case for all investigated macrocyclic congeners, which demonstrated a considerably strong cytotoxic potential in the low micromolar range (1.5~5.3 µM). Looking ahead, further structure-activity-relationship studies by introducing semisynthetic alterations are necessary to elucidate whether a higher kinase specificity can be achieved for the linear bastadins. In order to clarify the discrepancy of strong protein kinase inhibition compared to the lack of cytotoxicity (bastadin 3 and sesquibastadin 1) future cellular uptake-studies could provide answers.

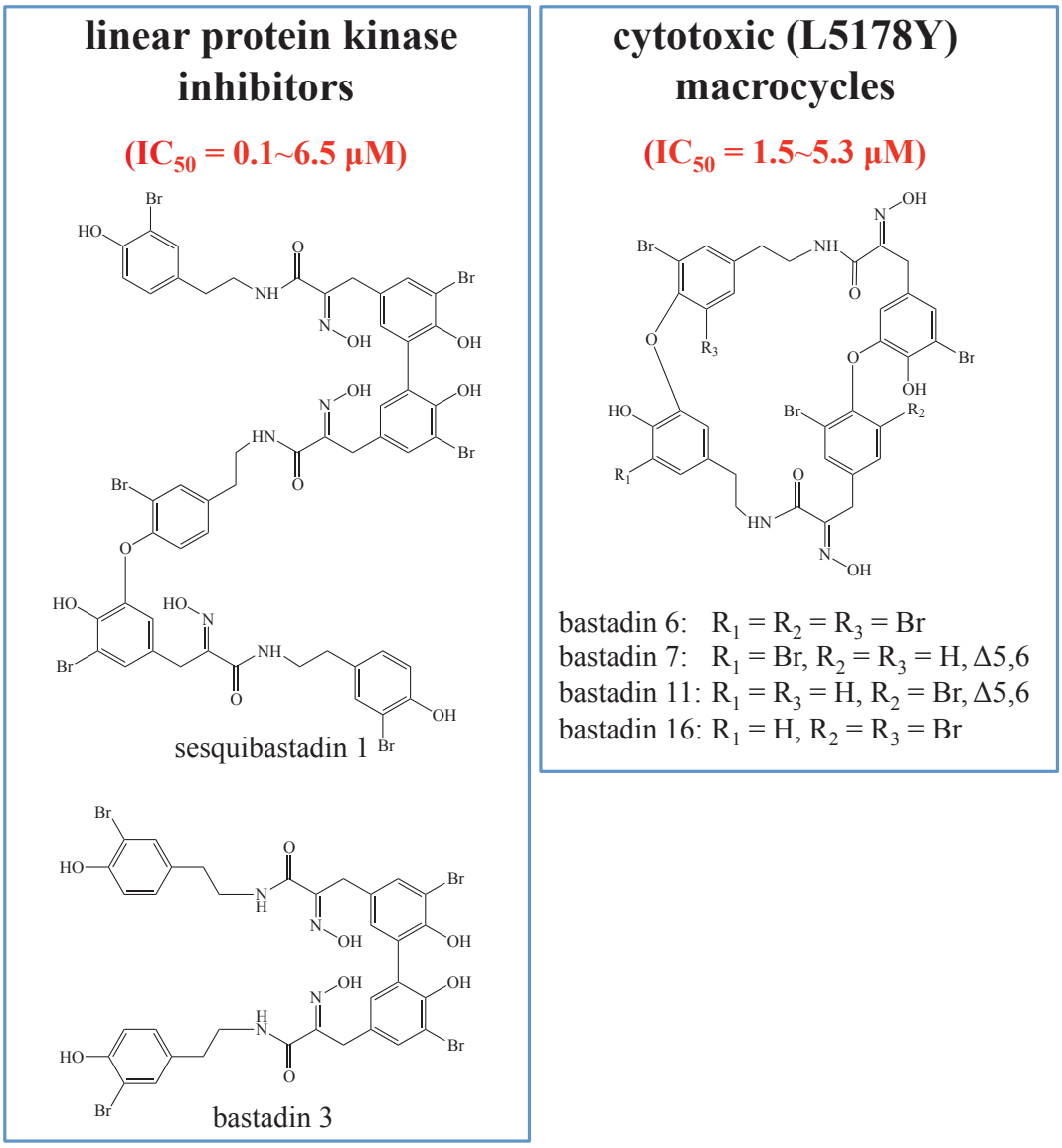

Figure 21. Contrasting activity profiles of linear and macrocyclic bastadins with regard to protein kinase inhibition and cytotoxicity against L5178Y cells.

Discussion

In accordance to publication 2 the macrocyclic bastadins 6, 9 and 16 (figure 22) demonstrated remarkable cytotoxic properties against further cancer cell lines (publication 3, table 1). The mean IC_{50} values, determined *in vitro* against human breast (MCF-7) and non-small-cell lung cancer cells (NSCLC), against oligodendro- (Hs683) and astroglioma (U373) and against the two melanoma cell lines B16F10 (murine) and SKMEL28 were found in the low micromolar range (4.0~7.0 μM).

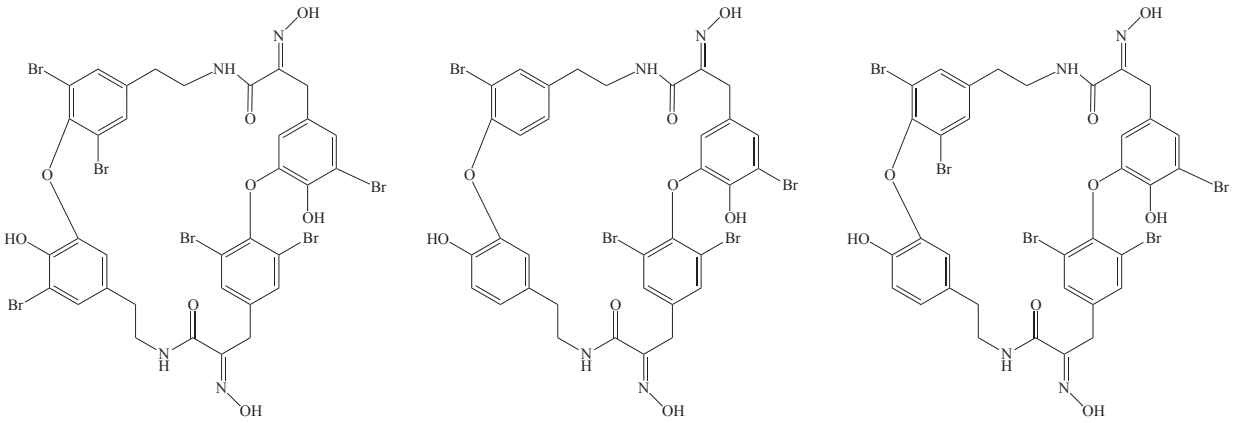

Figure 22. Structures of cytotoxic bastadins 6, 9 and 16 reported in publication 3.

Combining the results of both publications (2 and 3), macrocyclic bastadins appear to act with a general cytotoxic mode of action rather than addressing specific molecular targets. All cytotoxic results of bastadins found in this stduy are in good agreement with previously published data (Greve *et al.*, 2008; Miao *et al.*, 1990; Pettit *et al.*, 1996). Additionally, three synthetic hemibastadin congeners and two precursors were subject of the studies described in publication 3. Here, DBHB (figure 23) showed a tenfold decrease of *in vitro* cytoxicity (mean IC_{50} = 69 μM) towards the six investigated cell lines when compared to the dimeric macrocycles. In further experiments DBHB exhibited both anti-angiogenic effects against human umbilical vein endothelial cells (HUVEC) and anti-migratory effects in murine B16F10 melanoma cells. The anti-migratory effect that appeared at one-tenth of the IC_{50} *in vitro* growth inhibitory concentration was antagonized by addition of serum to the culture media of the B16F10 melanoma cells. Further experiments demonstrated that DBHB bound strongly to albumin.

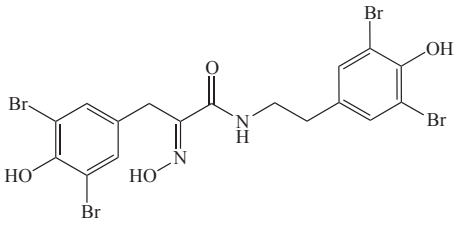

Figure 23. Structure of anti-angiogenic DBHB.

For bastadin 6 anti-angiogenic properties have been described by Aoki *et. al*., which were found to result from an induction of apoptotic cell death in HUVECs putatively caused by a modulation of cellular Ca^{2+} levels via an interaction of bastadin 6 with the ryanodine receptor-3 (RyR-3) (Aoki *et al.*, 2006). The results for DBHB shown in publication 3 suggest a mechanism of action that is anti-migratory but non-cytostatic and non-cytotoxic in HUVECs and therefore differs from that observed for bastadin 6 by Aoki *et al.* Eventually, also the strong copper chelating properties of (hemi)bastadins (Bayer *et al.*, 2011) might contribute to their anti-angiogenic potential as it is known that this transition metal acts as an important cofactor stimulating the proliferation and migration of endothelial cells and is required for the secretion of several angiogenic factors in tumor cells (Lowndes and Harris, 2005). The potential of copper chelators in anticancer therapy has just been discovered recently (Turski and Thiele, 2009). Ammonium tetrathiomolybdate (ATTM), a copper chelator first introduced as a treatment in Wilson's disease, a hereditary copper metabolism disorder, has recently reached clinical phase II for treatment of solid tumors and demonstrated efficacy with a favorable toxicity profile (Khan and Merajver, 2009). In conclusion, (hemi)bastadins such as DBHB might be further interesting candidates that could be included in screens of this new anticancer approach.

10.2 Antifouling Potential of Synthetic Hemibastadin Congeners

High general toxicity rates of past and current AF agents towards marine organisms have spiled the urge to find novel ecofriendly alternatives. The chemical arsenal of marine sponges might provide solutions to this challenging quest of modern bioprospecting. Hemibastadins constitute one class of compounds that is in focus of current AF investigations (Bayer *et al.*, 2011; Ortlepp *et al.*, 2007). During this PhD study synthetic endeavours leading to a set of structurally altered hemibastadin congeners were conducted and the potential of these compounds to inhibit blue mussel phenoloxidase, one specific molecular AF target, was evaluated (figure 24). Compounds from a previous SAR investigation (Bayer *et al.*, 2011) were tested in parallel and results were compared to draw a larger picture of the hemibastadin

enzyme interaction. The following discussion makes use of compound numbering that was chosen in publication 4 (figure 24). Fourfold brominated DBHB (**1**), which differs from naturally occurring hemibastadins only in the degree of bromination, was identified as the superior enzyme inhibitor among all tested derivatives. Interestingly, the type of halogen attached *ortho* to the phenolic hydroxyls seems to play a subordinated role, as iodinated (**4**) and chlorinated (**5**) congeners inhibited the enzyme with nearly identical IC_{50} values and only a negligible difference in comparison to **1** was observed. Nevertheless, the unhalogenated congener NBHB (**2**) was slightly less active than all halogenated derivatives indicating that bulky halogen substituents might lead to a better fit wihtin the active binding site of the enzyme. Additionally, the high electronegativity of such substituents leads to a slight increase in the acidity of the adjacent phenolic protons, which can be assumed from their chemical shifts in respective ^{1}H-NMR spectra. This effect may possibly further support the inhibitory potential of the respective compounds.

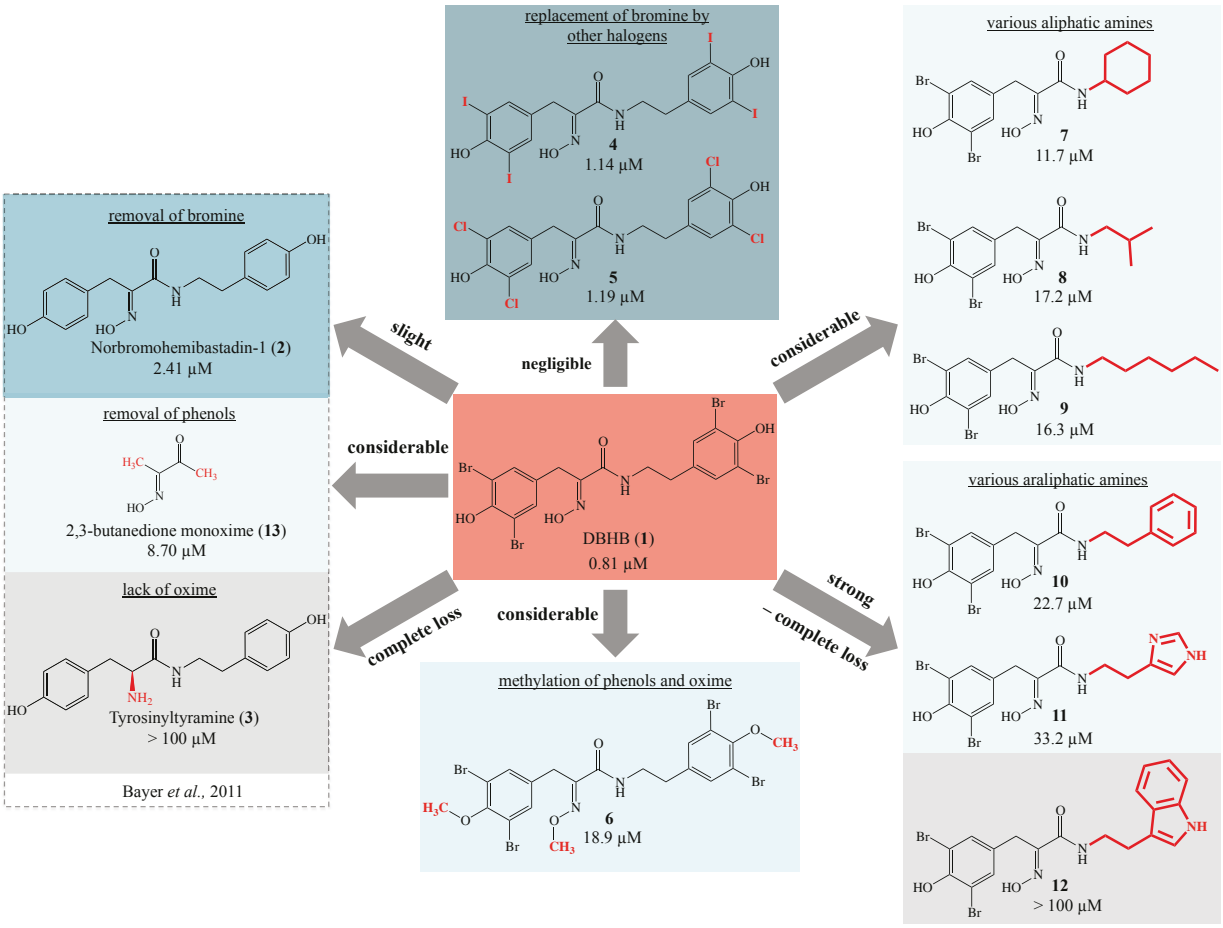

Figure 24. Inhibition of blue mussel phenoloxidase by DBHB and its analogues as indicated by their IC_{50} values.

A further central SAR finding was that the amine moiety might be involved in the stabilization of the enzyme inhibitor complex. An exchange in this part of the molecule led to a considerable loss in activity (**7**-**12**) as it was observed e.g. for a compound bearing a tryptamine unit (**12**). In this case the bulky and electron-rich indole moiety might lead to a hindered fit of the inhibitor into the active binding site of the phenoloxidase. The strong copper coordinating properties of the *α*-hydroxyimino-amide unit, which are probably responsible for phenoloxidase inhibition, are lost when the oxime is replaced by a primary amine group (**3**). In comparison, methylation (**6**) of this pharmacophoric core and terminal phenolic hydroxyl groups only leads to a considerable loss in inhibitory activity, but causes no total loss. The nature of the enzyme inhibitor complex still remains unclear as it is unknown whether a true copper coordination or just to a blockade of the active binding site leading to a hindered substrate supply take place. The latter-mentioned case was recently observed in a crystal structure of tropolone inhibiting *Agaricus bisporus* mushroom tyrosinase, where the specific inhibitor was found to form a pre-Michaelis complex with the enzyme near the binuclear copper-binding site (Ismaya *et al.*, 2011). Similar experiments as performed by Ismaya *et al*. could be objectives of further investigations of the hemibastadin phenoloxidase interaction.

In summary, evolutionary shaped DBHB (**1**) represents the strongest inhibitor of blue mussel phenoloxidase when compared to synthetically modified hemibastadins. In addition to its pronounced biological potency the rather simple and optimized synthesis protocol providing the compound in an overall yield of up to 45 % (publication 4) highlights this bromotyrosine as an interesting AF agent. Applications of DBHB in AF paints, embedded in a polymeric matrix, could be a conceivable biomimetic solution towards the biofouling issue.

10.3 Halotyrosines in Verongid Sponge Skeletons

The identification of bastadins 3, 4, 6, 7, 9 and 16 and the isoxazol-alkaloide aerothionin (figure 25) being associated to respective spongineous skeletons of *I. basta* and *A. cavernicola* was accomplished during this PhD thesis and reported in publication 5. The total quantity of identified bastadins in association with the examined skeleton sample was found to be nearly 300-fold less abundant when compared to fresh sponge tissue. The observation that bromotyrosines predominantly occurr within sponge cells and/or associated microbial symbionts is in line with the hypothesis that these compounds constitute a rapid chemical defence mechanism towards a variety of external cues, which is known for the *Aplysina* alkaloids (Thoms *et al.*, 2006).

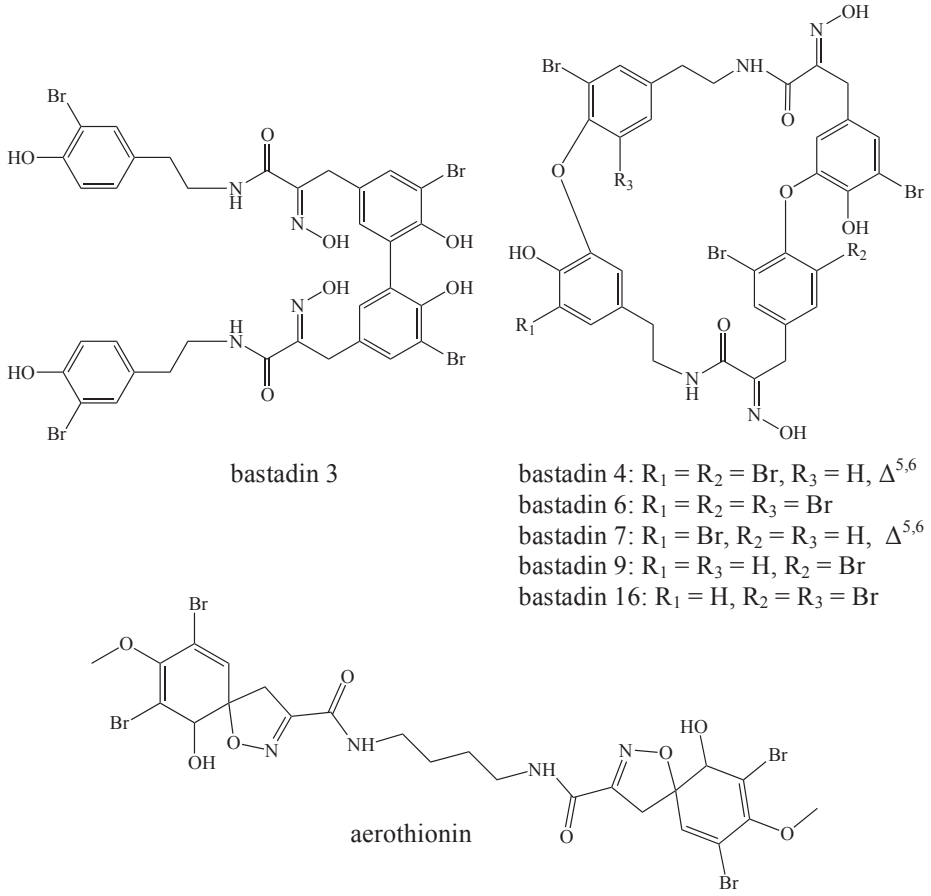

Figure 25. Structures of brominated tyrosines identified as associates to Verongid sponge skeletons.

Nevertheless, one may speculate that bromotyrosines also serve sponge skeletons, that have been demonstrated to consist of chitin-based scaffolds (Brunner *et al.*, 2009) as specific protecting agents. Formerly an inhibition of degrading chitinases (EC 3.2.1.14) was shown for the closely related *Aplysina* alkaloid psammaplin A (figure 26) (Tabudravu *et al.*, 2002). This observation that brominated secondary metabolites of sponges inhibit chitinases is not restricted to the class of tyrosine derivatives as several styloguanidine congeners such as 3-bromostyloguanidine (figure 26) from *Stylotella aurantium* demonstrated likewise an inhibition of these enzymes at a dose of 2.5 µg/mL, when investigated for their antimicrobial potential (Kato *et al.*, 1995). The proof of this hypothesis regarding the identified skeleton associates remains a subject of future studies.

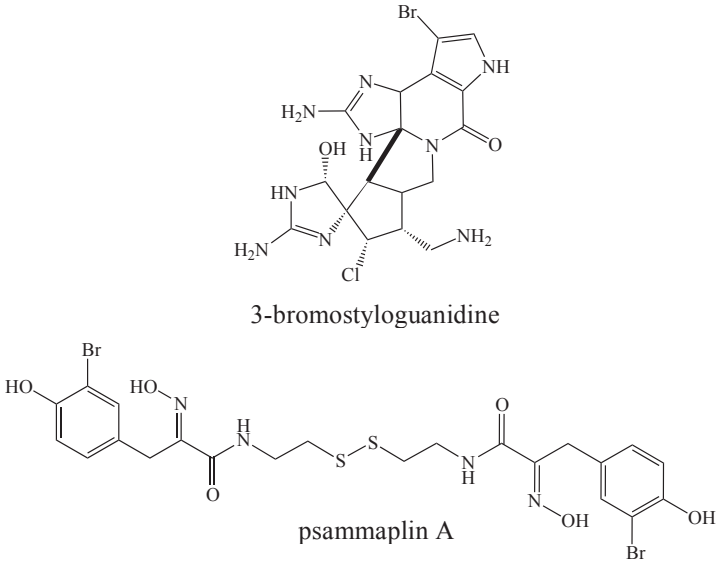

Figure 26. Structures of chitinase inhibiting sponge metabolites (Kato *et al.*, 1995; Tabudravu *et al.*, 2002).

As outlined in publication 5 only a minor fraction of the bromine content of sponge skeletons could be extracted by methanol, which led to the conclusion that brominated metabolites of unknown structure are primarily covalently bond to the sponge skeletons. In a subsequent study (publication 6) the amino acid composition of *A. cavernicola* skeletons was investigated after basic hydrolysis. Ten halogenated amino acids were identified unambigously within the hydrolysate by GC-MS and LC-MS analyses. Nine congeners were found to be halogenated tyrosines (figure 27). These results strongly suggest that halogenated tyrosines are obviously part of the spongineous protein fraction of *A. cavernicola* skeletons. These results are in accordance to the actual definition of spongin as being a halogenated protein (Ehrlich, 2010).

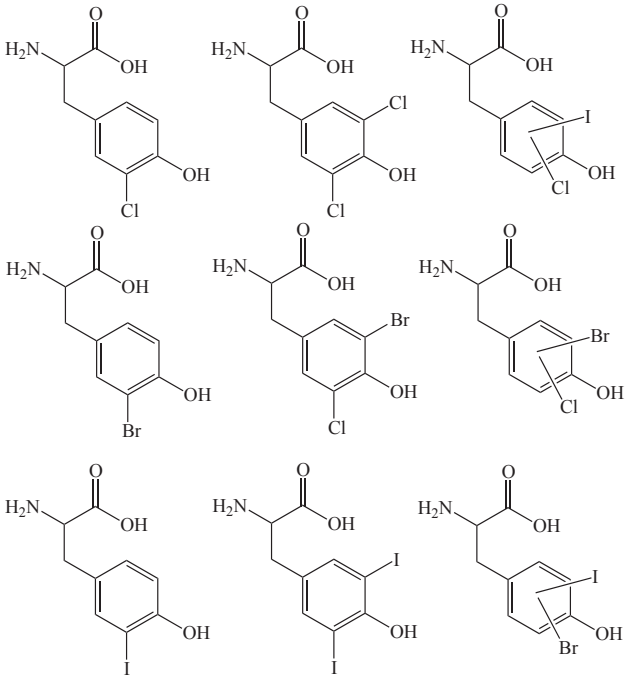

Figure 27. Structures of halogenated tyrosines identified via LC-ESI-MS in *A. cavernicola* skeleton hydrolysates.

The structural benefit of halogenation for the sponge organism has so far not been elucidated. One can hypothesize that the physico-chemical properties of the proteinous fraction are strongly influenced by halogenation, which might lead to an increased stability of these bioploymers. In analogy to the observations on sponge skeletons presented in this thesis Birkedahl *et al.* discovered halogenated amino acids and predominantly brominated and iodinated tyrosine congeners in the jaws of *Nereis*, a marine polychaete worm (Birkedal *et al.*, 2006). In the respective investigation the authors observed that the variations in modulus and hardness of the proteinous jaw material did not correlate with the distribution of bromine and iodine. The occurence of halogenated di- and trityrosines connected via C-C coupling led rather to the assumption that halogenation favors biaryl cross-linking. The authors conclude that a combination of cross-linking with halogen bonding should stabilize the jaw and render it insoluble and less susceptible to chemical and enzymatic attack. This hypothesis on the function of the proteinous fraction of *Nereis* jaws may also apply to skeletons of Verongid sponges, as such biaryl cross-links occur also in their secondary metabolism, e.g. the synthesis of bastadins such as bastadin 3 (figure 25). Future investigations might show, whether such di- or trimeric tyrosine congeners are present in Verongid skeleton hydrolysates to provide further proof for this hypothesis.

11 Further Scientific Achievements

Presentation of the following poster on the international conference BIOPROSP_15 in Tromsø, Norway on February 18-20th 2015:

SAR Studies of Hemibastadins Inhibiting Blue Mussel Phenoloxidase

Hendrik Niemann[1], Jens Hagenow[1], Mi-Young Chung[1], Claire Hellio[2,3], Horst Weber[1] and Peter Proksch[1]

[1]Institute of Pharmaceutical Biology and Biotechnology, Heinrich-Heine-University Düsseldorf, Universitätsstrasse 1, Geb. 26.23, Düsseldorf 40225, Germany; E-Mail: hendrik.niemann@hhu.de
[2]LEMAR UMR 6539 UBO CNRS Ifremer IRD, European Institute of Marine Studies (IUEM), Université de Bretagne Occidentale (UBO), European University of Brittany (UEB), Technopole Brest-Iroise, 29280 Plouzané, France
[3]Biodimar, Université de Bretagne Occidentale (UBO), European University of Brittany (UEB), 6 Avenue Victor Le Gorgeu, CS93837, 29238 Brest cedex 3, France

Introduction

Blue mussel (*Mytilus edulis*) phenoloxidase (PO) is a copper-depending enzyme, which plays a crucial role in the attachment of these macrofoulers to any submerged substrate. Previous studies [1] on synthetic analogues (**1-3**) of hemibastadins, typical metabolites of the pacific elephant ear sponge (*Ianthella basta*), revealed that the α-hydroxyimino-amide moiety represents the pharmacophoric core structure, which is responsible for the strong copper chelating and therefore PO inhibitory properties of these compounds. We have now introduced the following structural alterations into the hemibastadin molecule and evaluated their impact on PO inhibition:

- Replacement of bromine by further halogen atoms like chlorine and iodine (**4**, **5**),
- Methylation of phenolic hydroxyl groups as well as the oxime function (**6**),
- Substitution of the tyramine subunit by other ali-/araliphatic amine substituents (**7**–**12**).


© Simone Miljanovic

Methods and Results

Inhibition of blue mussel PO by DBHB (1) and its analogues as indicated by their IC_{50}-values:

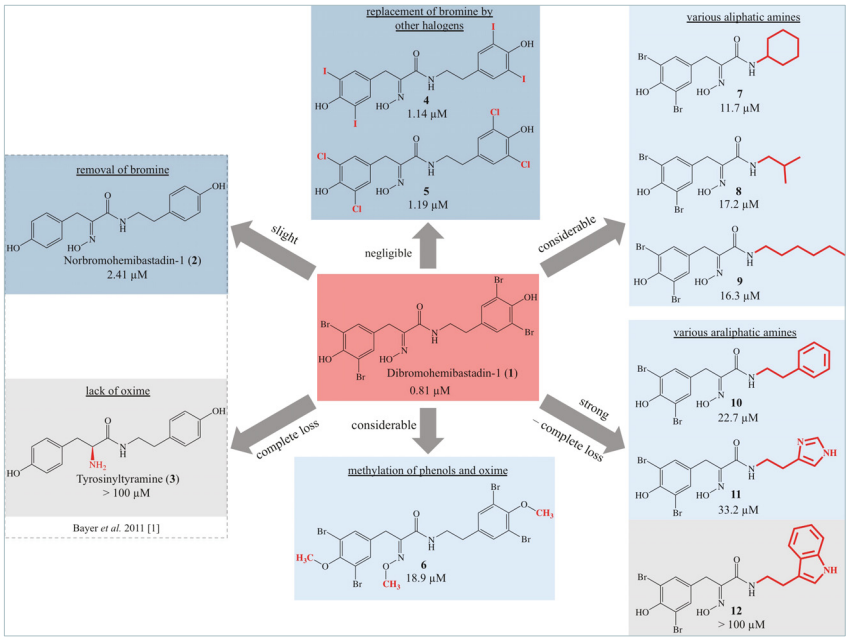

Central SAR statements:

- Halogenation in *ortho* to phenolic hydroxyl groups resulted in a slight increase in the inhibitory potential, but the difference between investigated bromine (**1**), chlorine (**4**) and iodine (**5**) substituents is negligible.
- Methylation of the oxime moiety and the phenolic hydroxyl groups (**6**) resulted in a considerable decrease in the inhibitory potential, but no total loss.
- Substitution with other ali-/araliphatic amines (**7-12**) leads to a decrease in the inhibitory properties in all cases.
- The presence of bulky and electron rich tryptamine (**12**) even resulted in a complete loss in activity.

Conclusions

- Evolutionary-shaped hemibastadins featuring all structural elements that are present in sponge-derived compounds revealed superior PO inhibitory properties.
- Methylation of both the oxime and the phenolic hydroxyl moieties (**6**) does not lead to a total loss in inhibition, suggesting that the pharmacophoric core structure was remained intact.
- The amine moiety is putatively involved in the stabilization of the enzyme-inhibitor-complex as a strong till complete loss in inhibitory activity of congeners bearing heterocyclic imidazole (**11**) and indole (**12**) suggests a missmatch with the PO active binding site.

Reference

1. Bayer M, Hellio C, Maréchal JP, Frank W, Lin WH, Weber H, Proksch P (2011) Antifouling bastadin congeners target mussel phenoloxidase and complex copper(II) ions. *Marine Biotechnology* **13**: 1148-58.

Acknowledgements

This study was supported from the Arbeitsgemeinschaft industrieller Forschungsvereinigungen Projekt GmbH (AiF, grant No. KF2388402AJ3).

12 Bibliography

Absalon, M.J., and Smith, F.O. (2009) Treatment strategies for pediatric acute myeloid leukemia. Expert Opinion on Pharmacotherapy **10**: 57-79.

Alzieu, C., Sanjuan, J., Deltreil, J., and Borel, M. (1986) Tin contamination in Arcachon Bay: effects on oyster shell anomalies. Marine Pollution Bulletin **17**: 494-498.

Aoki, S., Cho, S.-h., Ono, M., Kuwano, T., Nakao, S., Kuwano, M., Nakagawa, S., Gao, J.-Q., Mayumi, T., and Shibuya, M. (2006) Bastadin 6, a spongean brominated tyrosine derivative, inhibits tumor angiogenesis by inducing selective apoptosis to endothelial cells. Anti-Cancer Drugs **17**: 269-278.

Appeltans, W., Ahyong, Shane T., Anderson, G., Angel, Martin V., Artois, T., Bailly, N., Bamber, R., Barber, A., Bartsch, I., Berta, A.*, et al.* (2012) The magnitude of global marine species diversity. Current Biology **22**: 2189-2202.

Arrieta, J.M., Arnaud-Haond, S., and Duarte, C.M. (2010) What lies underneath: conserving the oceans' genetic resources. Proceedings of the National Academy of Sciences **107**: 18318-18324.

Bai, R., Paull, K., Herald, C., Malspeis, L., Pettit, G., and Hamel, E. (1991) Halichondrin B and homohalichondrin B, marine natural products binding in the vinca domain of tubulin. Discovery of tubulin-based mechanism of action by analysis of differential cytotoxicity data. Journal of Biological Chemistry **266**: 15882-15889.

Bayer, M., Hellio, C., Maréchal, J.-P., Frank, W., Lin, W., Weber, H., and Proksch, P. (2011) Antifouling bastadin congeners target mussel phenoloxidase and complex copper(II) ions. Marine Biotechnology **13**: 1148-1158.

Beaumont, A., and Newman, P. (1986) Low levels of tributyltin reduce growth of microalgae. Marine Pollution Bulletin **19**: 294-296.

Belarbi, E.H., Contreras Gómez, A., Chisti, Y., Camacho, F.G., and Grima, E.M. (2003) Producing drugs from marine sponges. Biotechnology Advances **21**: 585-598.

Bellas, J. (2006) Comparative toxicity of alternative antifouling biocides on embryos and larvae of marine invertebrates. Science of the Total Environment **367**: 573-585.

Bellas, J. (2007) Toxicity of the booster biocide Sea-Nine to the early developmental stages of the sea urchin *Paracentrotus lividus*. Aquatic Toxicology **83**: 52-61.

Bibliography

Bellas, J. (2008) Prediction and assessment of mixture toxicity of compounds in antifouling paints using the sea-urchin embryo-larval bioassay. Aquatic Toxicology **88**: 308-315.

Bergmann, W., and Feeney, R.J. (1951) Contributions to the study of marine products. XXXII. The nucleosides of sponges. I.1. The Journal of Organic Chemistry **16**: 981-987.

Bergquist, P. (1998) Porifera. Invertebrate Zoology: 10-27.

Birkedal, H., Khan, R.K., Slack, N., Broomell, C., Lichtenegger, H.C., Zok, F., Stucky, G.D., and Waite, J.H. (2006) Halogenated veneers: protein cross-linking and halogenation in the jaws of *Nereis*, a marine polychaete worm. ChemBioChem **7**: 1392-1399.

Brunner, E., Ehrlich, H., Schupp, P., Hedrich, R., Hunoldt, S., Kammer, M., Machill, S., Paasch, S., Bazhenov, V., and Kurek, D. (2009) Chitin-based scaffolds are an integral part of the skeleton of the marine demosponge *Ianthella basta*. Journal of Structural Biology **168**: 539-547.

Bryan, G., Gibbs, P., Burt, G., and Hummerstone, L. (1987) The effects of tributyltin (TBT) accumulation on adult dog-whelks, *Nucella lapillus*: long-term field and laboratory experiments. Journal of the Marine Biological Association of the United Kingdom **67**: 525-544.

Butler, M., Lim, T., Capon, R., and Hammond, L. (1991) The bastadins revisited: new chemistry from the Australian marine sponge *Ianthella basta*. Australian Journal of Chemistry **44**: 287-296.

Calcul, L., Inman, W.D., Morris, A.A., Tenney, K., Ratnam, J., McKerrow, J.H., Valeriote, F.A., and Crews, P. (2010) Additional insights on the bastadins: isolation of analogues from the sponge *Ianthella* cf. *reticulata* and exploration of the oxime configurations. Journal of Natural Products **73**: 365-372.

Callow, M.E., and Callow, J.A. (2002) Marine biofouling: a sticky problem. Biologist **49**: 1-5.

Carney, J.R., Scheuer, P.J., and Kelly-Borges, M. (1993) A new bastadin from the sponge *Psammaplysilla purpurea*. Journal of Natural Products **56**: 153-157.

Chen, L., Molinski, T.F., and Pessah, I.N. (1999) Bastadin 10 stabilizes the open conformation of the ryanodine-sensitive Ca^{2+} channel in an FKBP12-dependent manner. Journal of Biological Chemistry **274**: 32603-32612.

Bibliography

Ciminiello, P., Fattorusso, E., Forino, M., Magno, S., and Pansini, M. (1997) Chemistry of verongida sponges VIII[1]-bromocompounds from the mediterranean sponges *Aplysina aerophoba* and *Aplysina cavernicola*. Tetrahedron **53**: 6565-6572.

Coll, J.C., Kearns, P.S., Rideout, J.A., and Sankar, V. (2002) Bastadin 21, a novel isobastarane metabolite from the Great Barrier Reef marine sponge *Ianthella quadrangulata*. Journal of Natural Products **65**: 753-756.

Cresswell, T., Richards, J.P., Glegg, G.A., and Readman, J.W. (2006) The impact of legislation on the usage and environmental concentrations of Irgarol 1051 in UK coastal waters. Marine Pollution Bulletin **52**: 1169-1175.

D'Ambrosio, M., Guerriero, A., De Clauser, R., De Stanchina, G., and Pietra, F. (1983) Dichloroverongiaquinol, a new marine antibacterial compound from *Aplysina cavernicola*. Isolation and synthesis. Experientia **39**: 1091-1092.

D'Ambrosio, M., Guerriero, A., and Pietra, F. (1984) Novel, racemic or nearly-racemic antibacterial bromo- and chloroquinols and γ-lactams of the verongiaquinol and the cavernicolin type from the marine sponge *Aplysina* (= Verongia) *cavernicola*. Helvetica Chimica Acta **67**: 1484-1492.

Dabydeen, D.A., Burnett, J.C., Bai, R., Verdier-Pinard, P., Hickford, S.J., Pettit, G.R., Blunt, J.W., Munro, M.H., Gussio, R., and Hamel, E. (2006) Comparison of the activities of the truncated halichondrin B analog NSC 707389 (E7389) with those of the parent compound and a proposed binding site on tubulin. Molecular Pharmacology **70**: 1866-1875.

Danner, E.W., Kan, Y., Hammer, M.U., Israelachvili, J.N., and Waite, J.H. (2012) Adhesion of mussel foot protein Mefp-5 to mica: an underwater superglue. Biochemistry **51**: 6511-6518.

Davidson, I.C., Brown, C.W., Sytsma, M.D., and Ruiz, G.M. (2009) The role of containerships as transfer mechanisms of marine biofouling species. Biofouling **25**: 645-655.

De Vos, L., Rützler, K., Boury-Esnault, N., Donadey, C., and Vacelet, J. (1991) Atlas of sponge morphology. Smithsonian Institution Press, Washington & London: 117.

Diers, J.A., Pennaka, H.K., Peng, J., Bowling, J.J., Duke, S.O., and Hamann, M.T. (2004) Structural activity relationship studies of zebra mussel antifouling and antimicrobial agents from verongid sponges. Journal of Natural Products **67**: 2117-2120.

Drechsel, E. (1896) Contribution to the chemistry of a sea animal. Zeitschrift für Biologie **33**: 85-107.

Bibliography

Ebel, R., Brenzinger, M., Kunze, A., Gross, H.J., and Proksch, P. (1997) Wound activation of protoxins in marine sponge *Aplysina aerophoba*. Journal of Chemical Ecology **23**: 1451-1462.

Ehrlich, H. (2010). Biological materials of marine origin: invertebrates (biologically-inspired systems). Springer, Berlin.

Ehrlich, H., Maldonado, M., Spindler, K.d., Eckert, C., Hanke, T., Born, R., Goebel, C., Simon, P., Heinemann, S., and Worch, H. (2007) First evidence of chitin as a component of the skeletal fibers of marine sponges. Part I. Verongidae (Demospongia: Porifera). Journal of Experimental Zoology Part B: Molecular and Developmental Evolution **308**: 347-356.

Fattorusso, E., Minale, L., Sodano, G., Moody, K., and Thomson, R.H. (1970) Aerothionin, a tetrabromo-compound from *Aplysina aerophoba* and *Verongia thiona*. Journal of the Chemical Society D: Chemical Communications: 752-753.

Finnie, A.A., and Williams, D.N. (2010) Paint and coatings technology for the control of marine fouling. Biofouling **10**: 9781444315462.

Fishelson, L. (1981) Observations on the moving colonies of the genus *Tethya* (Demospongia, Porifera). Zoomorphology **98**: 89-99.

Franklin, M.A., Penn, S.G., Lebrilla, C.B., Lam, T.H., Pessah, I.N., and Molinski, T.F. (1996) Bastadin 20 and bastadin O-sulfate esters from *Ianthella basta*: novel modulators of the Ry1R FKBP12 receptor complex. Journal of Natural Products **59**: 1121-1127.

Galeano, E., Thomas, O.P., Robledo, S., Munoz, D., and Martinez, A. (2011) Antiparasitic bromotyrosine derivatives from the marine sponge *Verongula rigida*. Marine Drugs **9**: 1902-1913.

Gazave, E., Lapébie, P., Ereskovsky, A.V., Vacelet, J., Renard, E., Cárdenas, P., and Borchiellini, C. (2012) No longer Demospongiae: Homoscleromorpha formal nomination as a fourth class of Porifera. Hydrobiologia **687**: 3-10.

Gochfeld, D.J., Kamel, H.N., Olson, J.B., and Thacker, R.W. (2012) Trade-offs in defensive metabolite production but not ecological function in healthy and diseased sponges. Journal of Chemical Ecology **38**: 451-462.

Goldberg, E.D. (1986) TBT: an environmental dilemma. Environment: Science and Policy for Sustainable Development **28**: 17-44.

Bibliography

Gray, D. (1869). Note on *Ianthella*, a new genus of keratose sponges. Proceedings of the Zoological Society of London.

Greve, H., Kehraus, S., Krick, A., Kelter, G., Maier, A., Fiebig, H.-H., Wright, A.D., and König, G.M. (2008) Cytotoxic bastadin 24 from the Australian sponge *Ianthella quadrangulata* ⊥. Journal of Natural Products **71**: 309-312.

Gross, J., Sokal, Z., and Rougvie, M. (1956) Structural and chemical studies on the connective tissue of marine sponges. Journal of Histochemistry & Cytochemistry **4**: 227-246.

Guo, S., Lee, H.P., Teo, S.L.M., and Khoo, B.C. (2012) Inhibition of barnacle cyprid settlement using low frequency and intensity ultrasound. Biofouling **28**: 131-141.

Guo, S.F., Lee, H.P., Chaw, K.C., Miklas, J., Teo, S.L.M., Dickinson, G.H., Birch, W.R., and Khoo, B.C. (2011) Effect of ultrasound on cyprids and juvenile barnacles. Biofouling **27**: 185-192.

Guo, Z.-w., Machiya, K., Salamonczyk, G.M., and Sih, C.J. (1998) Total synthesis of Bastadins 2, 3, and 6. The Journal of Organic Chemistry **63**: 4269-4276.

Hackman, R. (1960) Studies on chitin IV. The occurrence of complexes in which chitin and protein are covalently linked. Australian Journal of Biological Sciences **13**: 568-577.

Hedner, E., Sjögren, M., Hodzic, S., Andersson, R., Göransson, U., Jonsson, P.R., and Bohlin, L. (2008) Antifouling activity of a dibrominated cyclopeptide from the marine sponge *Geodia barretti* ⊥. Journal of Natural Products **71**: 330-333.

Hellio, C., Bourgougnon, N., and Gal, Y.L. (2000) Phenoloxidase (EC 1.14. 18.1) from the byssus gland of *Mytilus edulis*: purification, partial characterization and application for screening products with potential antifouling activities. Biofouling **16**: 235-244.

Herbst, R.S. (2004) Review of epidermal growth factor receptor biology. International Journal of Radiation Oncology* Biology* Physics **59**: S21-S26.

Hertiani, T., Edrada-Ebel, R., Ortlepp, S., van Soest, R.W., de Voogd, N.J., Wray, V., Hentschel, U., Kozytska, S., Müller, W.E., and Proksch, P. (2010) From anti-fouling to biofilm inhibition: new cytotoxic secondary metabolites from two Indonesian *Agelas* sponges. Bioorganic & Medicinal Chemistry **18**: 1297-1311.

Bibliography

Hill, M.S., and Hill, A.L. (2002) Morphological plasticity in the tropical sponge *Anthosigmella varians*: responses to predators and wave energy. The Biological Bulletin **202**: 86-95.

Hill, M.S., Lopez, N.A., and Young, K.A. (2005) Anti-predator defenses in western North Atlantic sponges with evidence of enhanced defense through interactions between spicules and chemicals. Marine Ecology Progress Series **291**: 93-102.

Hirata, Y., and Uemura, D. (1986) Halichondrins-antitumor polyether macrolides from a marine sponge. Pure and Applied Chemistry **58**: 701-710.

Hogg, J. (1860). On the distinctions of a plant and an animal, and on a fourth kingdom of nature. The Edinburgh New Philosophical Journal.

Hooper, J.N., and Van Soest, R.W. (2002). Systema Porifera. A guide to the classification of sponges. Springer, 2nd edition, Berlin.

Huyck, T.K., Gradishar, W., Manuguid, F., and Kirkpatrick, P. (2011) Eribulin mesylate. Nature Reviews Drug Discovery **10**: 173-174.

IMO (2002): http://www.imo.org/OurWork/Environment/Anti-foulingSystems/Documents/FOULING2003.pdf

Inman, W., and Crews, P. (2011) Unraveling the bastarane and isobastarane oximo amide configurations and associated macrocycle conformations: implications of their influence on bioactivities. Journal of Natural Products **74**: 402-410.

Ismaya, W.T., Rozeboom, H.J., Weijn, A., Mes, J.J., Fusetti, F., Wichers, H.J., and Dijkstra, B.W. (2011) Crystal structure of *Agaricus bisporus* mushroom tyrosinase: identity of the tetramer subunits and interaction with tropolone. Biochemistry **50**: 5477-5486.

Kato, T., Shizuri, Y., Izumida, H., Yokoyama, A., and Endo, M. (1995) Styloguanidines, new chitinase inhibitors from the marine sponge *Stylotella aurantium*. Tetrahedron Letters **36**: 2133-2136.

Kazlauskas, R., Lidgard, R., Murphy, P., and Wells, R. (1980) Brominated tyrosine-derived metabolites from the sponge *Ianthella basta*. Tetrahedron Letters **21**: 2277-2280.

Kelly, J.R., Levine, S.N., Buttel, L.A., Carr, K.A., Rudnick, D.T., and Morton, R.D. (1990a) The effects of tributyltin within a *Thalassia* seagrass ecosystem. Estuaries **13**: 301-310.

Bibliography

Kelly, J.R., Rudnick, D.T., Morton, R.D., Buttel, L.A., Levine, S.N., and Carr, K.A. (1990b) Tributyltin and invertebrates of a seagrass ecosystem: exposure and response of different species. Marine Environmental Research **29**: 245-276.

Khan, G., and Merajver, S. (2009) Copper chelation in cancer therapy using tetrathiomolybdate: an evolving paradigm. Expert Opinion on Investigational Drugs **18**: 541-548.

King, D.H. (1988) History, pharmacokinetics, and pharmacology of acyclovir. Journal of the American Academy of Dermatology **18**: 176-179.

Konstantinou, I., and Albanis, T. (2004) Worldwide occurrence and effects of antifouling paint booster biocides in the aquatic environment: a review. Environment International **30**: 235-248.

Kotoku, N., Hiramatsu, A., Tsujita, H., Hirakawa, Y., Sanagawa, M., Aoki, S., and Kobayashi, M. (2008) Structure‐activity relationships study of bastadin 6, an anti‐angiogenic brominated‐tyrosine derived metabolite from marine sponge. Archiv der Pharmazie **341**: 568-577.

Koulman, A., Proksch, P., Ebel, R., Beekman, A.C., van Uden, W., Konings, A.W., Pedersen, J.A., Pras, N., and Woerdenbag, H.J. (1996) Cytoxicity and mode of action of aeroplysinin-1 and a related dienone from the sponge *Aplysina aerophoba*. Journal of Natural Products **59**: 591-594.

Kreuter, M.H., Robitzki, A., Chang, S., Steffen, R., Michaelis, M., Kljajić, Z., Bachmann, M., Schröder, H.C., and Müller, W.E. (1992) Production of the cytostatic agent aeroplysinin by the sponge *Verongia aerophoba* in *in vitro* culture. Comparative Biochemistry and Physiology Part C: Comparative Pharmacology **101**: 183-187.

Langston, W., Bryan, G., Burt, G., and Gibbs, P. (1990) Assessing the impact of tin and TBT in estuaries and coastal regions. Functional Ecology: 433-443.

Laport, M., Santos, O., and Muricy, G. (2009) Marine sponges: potential sources of new antimicrobial drugs. Current Pharmaceutical Biotechnology **10**: 86-105.

Lipowicz, B., Hanekop, N., Schmitt, L., and Proksch, P. (2013) An aeroplysinin-1 specific nitrile hydratase isolated from the marine sponge *Aplysina cavernicola*. Marine Drugs **11**: 3046-3067.

Loh, T.-L., and Pawlik, J.R. (2014) Chemical defenses and resource trade-offs structure sponge communities on Caribbean coral reefs. Proceedings of the National Academy of Sciences **111**: 4151-4156.

Bibliography

Löschau, M., and Krätke, R. (2005) Efficacy and toxicity of self-polishing biocide-free antifouling paints. Environmental Pollution **138**: 260-267.

Lowndes, S.A., and Harris, A.L. (2005) The role of copper in tumour angiogenesis. Journal of Mammary Gland Biology and Neoplasia **10**: 299-310.

Mack, M.M., Molinski, T.F., Buck, E.D., and Pessah, I.N. (1994) Novel modulators of skeletal muscle FKBP12/calcium channel complex from *Ianthella basta*. Role of FKBP12 in channel gating. Journal of Biological Chemistry **269**: 23236-23249.

Maldonado, M. (2009) Embryonic development of verongid demosponges supports the independent acquisition of spongin skeletons as an alternative to the siliceous skeleton of sponges. Biological Journal of the Linnean Society **97**: 427-447.

Manconi, R., Cadeddu, B., Ledda, F., and Pronzato, R. (2013) An overview of the Mediterranean cave-dwelling horny sponges (Porifera, Demospongiae). ZooKeys: 1.

Martinelli, E., Suffredini, M., Galli, G., Glisenti, A., Pettitt, M.E., Callow, M.E., Callow, J.A., Williams, D., and Lyall, G. (2011) Amphiphilic block copolymer/poly (dimethylsiloxane) (PDMS) blends and nanocomposites for improved fouling-release. Biofouling **27**: 529-541.

Martínez-Díez, M., Guillén-Navarro, M.J., Pera, B., Bouchet, B.P., Martínez-Leal, J.F., Barasoain, I., Cuevas, C., Andreu, J.M., García-Fernández, L.F., Díaz, J.F*., et al.* (2014) PM060184, a new tubulin binding agent with potent antitumor activity including P-glycoprotein over-expressing tumors. Biochemical Pharmacology **88**: 291-302.

Miao, S., Andersen, R.J., and Allen, T.M. (1990) Cytotoxic metabolites from the sponge *Lanthella basta* collected in Papua New Guinea. Journal of Natural Products **53**: 1441-1446.

Molinski, T.F., Dalisay, D.S., Lievens, S.L., and Saludes, J.P. (2008) Drug development from marine natural products. Nature Reviews Drug Discovery **8**: 69-85.

Montaser, R., and Luesch, H. (2011) Marine natural products: a new wave of drugs? Future Medicinal Chemistry **3**: 1475-1489.

Müller, W.E. (1998) Origin of Metazoa: sponges as living fossils. Naturwissenschaften **85**: 11-25.

Müller, W.E., Wang, X., Proksch, P., Perry, C.C., Osinga, R., Gardères, J., and Schröder, H.C. (2013) Principles of biofouling protection in marine sponges: a model for the design of novel

biomimetic and bio-inspired coatings in the marine environment? Marine Biotechnology **15**: 375-398.

Munoz, I., Bueno, M.J.M., Agüera, A., and Fernández-Alba, A.R. (2010) Environmental and human health risk assessment of organic micro-pollutants occurring in a Spanish marine fish farm. Environmental Pollution **158**: 1809-1816.

Nouri, M., Ratther, E., Stylianou, N., Nelson, C.C., Hollier, B.G., and Williams, E.D. (2014) Androgen-targeted therapy-induced epithelial mesenchymal plasticity and neuroendocrine transdifferentiation in prostate cancer: an opportunity for intervention. Frontiers in oncology **4**.

Omae, I. (2003) Organotin antifouling paints and their alternatives. Applied Organometallic Chemistry **17**: 81-105.

Ortlepp, S., Sjögren, M., Dahlström, M., Weber, H., Ebel, R., Edrada, R., Thoms, C., Schupp, P., Bohlin, L., and Proksch, P. (2007) Antifouling activity of bromotyrosine-derived sponge metabolites and synthetic analogues. Marine Biotechnology **9**: 776-785.

Pallas, P.A. (1766) Elenchus zoophytorum sistens generum adumbrationes generaliores et specierum cognitarium succinctas descriptiones cum selectis auctorum synonymis. Fransiscum Varrentrapp, Hagae: 451.

Pettit, G., Butler, M., Williams, M., Filiatrault, M., and Pettit, R. (1996) Isolation and structure of hemibastadinols 1−3 from the Papua New Guinea marine sponge *Ianthella basta*. Journal of Natural Products **59**: 927-934.

Philipp, E., and Abele, D. (2010) Masters of longevity? Lessons from long lived bivalves. Gerontology, DOI: 10.1159/000221004.

Pordesimo, E.O., and Schmitz, F.J. (1990) New bastadins from the sponge *Ianthella basta*. The Journal of Organic Chemistry **55**: 4704-4709.

Proksch, P. (1999) Chemical defence in marine ecosystems. Annual Plant Reviews **3**: 134-154.

Reddy, A.V., Ravinder, K., Narasimhulu, M., Sridevi, A., Satyanarayana, N., Kondapi, A.K., and Venkateswarlu, Y. (2006) New anticancer bastadin alkaloids from the sponge Dendrilla cactos. Bioorganic & Medicinal Chemistry **14**: 4452-4457.

Rieger, R. (2006) Spezielle Zoologie I. Einzeller und Wirbellose Tiere. Spektrum Akademischer Verlag, 2nd edition, Berlin.

Bibliography

Salta, M., Wharton, J.A., Stoodley, P., Dennington, S.P., Goodes, L.R., Werwinski, S., Mart, U., Wood, R.J., and Stokes, K.R. (2010) Designing biomimetic antifouling surfaces. Philosophical Transactions of the Royal Society A: Mathematical, Physical and Engineering Sciences **368**: 4729-4754.

Sato, T.N., Tozawa, Y., Deutsch, U., Wolburg-Buchholz, K., Fujiwara, Y., Gendron-Maguire, M., Gridley, T., Wolburg, H., Risau, W., and Qin, Y. (1995) Distinct roles of the receptor tyrosine kinases Tie-1 and Tie-2 in blood vessel formation. Nature **376**: 70-74.

Schultz, M., Bendick, J., Holm, E., and Hertel, W. (2011) Economic impact of biofouling on a naval surface ship. Biofouling **27**: 87-98.

Sih, C.J., and Malnar, I. (2000) Peroxidase-catalyzed oxidative phenolic coupling of some tripeptides containing tyrosine and hydroxyphenylglycine residues. Biocatalysis and Biotransformation **18**: 301-310.

Silverman, H.G., and Roberto, F.F. (2007) Understanding marine mussel adhesion. Marine Biotechnology **9**: 661-681.

Smith, J.A., Wilson, L., Azarenko, O., Zhu, X., Lewis, B.M., Littlefield, B.A., and Jordan, M.A. (2010) Eribulin binds at microtubule ends to a single site on tubulin to suppress dynamic instability. Biochemistry **49**: 1331-1337.

Storch, V., and Welsch, U. (2014). Kükenthal-Zoologisches Praktikum. Spinger Spektrum, 27th edition, Berlin.

Tabudravu, J.N., Tabudravu, V.G.H., Eijsink, G.W., Gooday, M., Jaspars, D., Komander, M., Legg, B., Synstad, D.M.F., and van, A. (2002) Psammaplin A, a chitinase inhibitor isolated from the fijian marine sponge *Aplysinella rhax*. Bioorganic & Medicinal Chemistry **10**: 1123-1128.

Taylor, M.W., Radax, R., Steger, D., and Wagner, M. (2007) Sponge-associated microorganisms: evolution, ecology, and biotechnological potential. Microbiology and Molecular Biology Reviews **71**: 295-347.

Teeyapant, R., Kreis, P., Wray, V., Witte, L., and Proksch, P. (1993) Brominated secondary compounds from the marine sponge *Verongia aerophoba* and the sponge feeding gastropod *Tylodina perversa*. Zeitschrift für Naturforschung C A Journal of Biosciences **48**: 640-644.

Thomas, K., and Brooks, S. (2010) The environmental fate and effects of antifouling paint biocides. Biofouling **26**: 73-88.

Bibliography

Thomas, X. (2009) Chemotherapy of acute leukemia in adults. Expert Opinion on Pharmacotherapy **10**: 221-237.

Thoms, C., Ebel, R., Hentschel, U., and Proksch, P. (2003) Sequestration of dietary alkaloids by the spongivorous marine mollusc *Tylodina perversa*. Zeitschrift für Naturforschung C **58**: 426-432.

Thoms, C., Ebel, R., and Proksch, P. (2006) Activated chemical defense in *Aplysina* sponges revisited. Journal of Chemical Ecology **32**: 97-123.

Thoms, C., Wolff, M., Padmakumar, K., Ebel, R., and Proksch, P. (2004) Chemical defense of Mediterranean sponges *Aplysina cavernicola* and *Aplysina aerophoba*. Zeitschrift für Naturforschung C **59**: 113-122.

Trepos, R., Pinori, E., Jonsson, P.R., Berglin, M., Svenson, J., Coutinho, R., Lausmaa, J., and Hellio, C. (2015) Innovative approaches for the development of new copper-free marine antifouling paints. Journal of Ocean Technology **in press**.

Turski, M.L., and Thiele, D.J. (2009) New roles for copper metabolism in cell proliferation, signaling, and disease. Journal of Biological Chemistry **284**: 717-721.

Uriz, M.J., Turon, X., Becerro, M.A., and Agell, G. (2003) Siliceous spicules and skeleton frameworks in sponges: origin, diversity, ultrastructural patterns, and biological functions. Microscopy Research and Technique **62**: 279-299.

Vacelet, J. (1959) Repartition generale des eponges et systematique des eponges cornees de la region de Marseille et de quelques stations mediterraneennes. Doctoral Dissertation.

Van Soest, R.W.M., Boury-Esnault, N., Vacelet, J., Dohrmann, M., Erpenbeck, D., De Voogd, N.J., Santodomingo, N., Vanhoorne, B., Kelly, M., and Hooper, J.N.A. (2012) Global diversity of sponges (Porifera). PLoS ONE **7**: e35105.

Van Wezel, A.P., and Van Vlaardingen, P. (2004) Environmental risk limits for antifouling substances. Aquatic Toxicology **66**: 427-444.

Van Wyk, A.W., Zuck, K.M., and McKee, T.C. (2011) Lithothamnin A, the first bastadin-like metabolite from the red alga *Lithothamnion fragilissimum*. Journal of Natural Products **74**: 1275-1280.

Bibliography

Voulvoulis, N. (2006). Antifouling paint booster biocides: occurrence and partitioning in water and sediments. Antifouling Paint Biocides, Springer, Berlin: 155-170.

Wang, G. (2006) Diversity and biotechnological potential of the sponge-associated microbial consortia. Journal of Industrial Microbiology and Biotechnology **33**: 545-551.

Weiss, B., Ebel, R., Elbrächter, M., Kirchner, M., and Proksch, P. (1996) Defense metabolites from the marine sponge *Verongia aerophoba*. Biochemical Systematics and Ecology **24**: 1-12.

Welinder, B.S. (1972) Halogenated tyrosines from the cuticle of *Limulus polyphemus* (L.). Biochimica et Biophysica Acta (BBA)-General Subjects **279**: 491-497.

Wester, P., Canton, J., Van Iersel, A., Krajnc, E., and Vaessen, H. (1990) The toxicity of bis (tri-n-butyltin) oxide (TBTO) and di-n-butyltindichloride (DBTC) in the small fish species *Oryzias latipes* (medaka) and *Poecilia reticulata* (guppy). Aquatic Toxicology **16**: 53-72.

WHOI (1952) The history of the prevention of fouling. Marine fouling and its prevention United States Department of the Navy, Bureau of Ships.

Wilkinson, C.R., and Vacelet, J. (1979) Transplantation of marine sponges to different conditions of light and current. Journal of Experimental Marine Biology and Ecology **37**: 91-104.

WoRMS (2015). http://www.marinespecies.org

Yebra, D.M., Kiil, S., and Dam-Johansen, K. (2004) Antifouling technology—past, present and future steps towards efficient and environmentally friendly antifouling coatings. Progress in Organic Coatings **50**: 75-104.

Zhou, X., Okamura, H., and Nagata, S. (2006) Remarkable synergistic effects in antifouling chemicals against *Vibrio fischeri* in a bioluminescent assay. Journal of Health Science **52**: 243-251.

Zieminska, E., Lazarewicz, J.W., Couladouros, E.A., Moutsos, V.I., and Pitsinos, E.N. (2008) Open-chain half-bastadins mimic the effects of cyclic bastadins on calcium homeostasis in cultured neurons. Bioorganic & Medicinal Chemistry Letters **18**: 5734-5737.

Zieminska, E., Stafiej, A., Pitsinos, E.N., Couladouros, E.A., Moutsos, V., Kozlowska, H., Toczylowska, B., and Lazarewicz, J.W. (2007) Synthetic bastadins modify the activity of ryanodine receptors in cultured cerebellar granule cells. Neurosignals **15**: 283-292.

13 Abbreviations

AF	Antifouling
ATR-FT-IR	Attenuated total reflection Fourier transformation infrared
Aur-A	Aurora kinase A
Aur-B	Auroroa kinase B
BC	Before Christ
2,3-BMO	2,3-Butandienone monoxime
^{13}C	Carbon
cm	Centimeter
COSY	Correlation spectroscopy
Cu	Copper
D	Dextro
d	Doublet
dd	Doublet of doublet
δ	Chemical shift
DBHB	5,5'-Dibromohemibastadin-1
DMSO-d_6	Deuterated dimethyl sulfoxide
DNA	Desoxyribonucleic acid
L-DOPA	L-3,4-dihydroxyphenylalanine
ε	Molar extinction coefficient
EGF-R	Endothelial growth factor receptor
EMA	European Medicines Agency
ESI	Electron spray ionisation
et al.	*et alii* (male) / *et aliae* (female) (and others)
EtOAc	Ethyl acetate
EU	European Union
FDA	Food and Drug Administration
GC-MS	Gas chromatography mass spectrometry
G_2-M phase	Pre-mitotic to mitotic phase in cell cycle
^{1}H	Proton
HMBC	Heteronuclear multiple bond connectivity
HMQC	Heteronuclear multiple quantum coherence
HPLC	High pressure liquid chromatography
HPLC-DAD	HPLC with diode array detector

Abbreviations

HRMS	High resolution mass spectrometry
HUVEC	Human umbilical vein endothelial cell
Hz	Hertz
IC_{50}	Half maximal inhibitory concentration
IMO	International Maritime Organization
IR	Infrared
J	Coupling constant
L	Levo
lat.	Latin
LC-MS	Liquid chromatography mass spectrometry
λ_{max}	Wavelength of absorbance maximum
M	Molar (mol/L)
m	Meter
m	Multiple signal
m/z	Mass to charge ratio
Mefp	*Mytilus edulis* foot protein
MeOH	Methanol
mg	Miligram
MHZ	Megahertz
min	Minute
µg	Microgram
µL	Microliter
µM	Micromolar
mL	Mililiter
mm	Milimeter
MS	Mass spectrometry
MTT	3-(4,5-Dimethylthiazol-2-yl)-2,5-diphenyltetrazolium bromide
MW	Molecular weight
NBHB	Norbromohemibastadin
nm	Nanometer
NMR	Nuclear magnetic resonance
ppm	Parts per million
ROESY	Rotating frame Overhauser enhancement spectroscopy

Abbreviations

RP18	Reversed phase C18
RyR	Ryanodine receptor
s	Singlet
SAR	Structure-activity relationships
SR	Sarcoplasmic reticulum
t	Triplet
TBT	Tributyltin
TT	Tyrosinyltyramine
UV	Ultraviolet
VEGF-R2	Vascular endothelial growth factor receptor 2
VLC	Vacuum liquid chromatography
WHO	World Healt Organization
WoRMS	World Register of Marine Species
X-ray	Electromagnetic radiation (λ 0.01-10 nm)

14 Declaration of Academic Honesty/Erklärung

Die vorliegende Dissertation habe ich eigenständig und ohne unerlaubte Hilfe angefertigt. Die meisten der für die Anfertigung dieser Arbeit erforderlichen Methoden wurden vom Autor selbständig durchgeführt. Folgende Methoden wurden in anderen Institutionen durchgeführt:

ATR-FTIR-Spektroskopie: Die Messungen wurden von Frau Susanne Überlein am Institut für Bioanalytische Chemie, TU Dresden, Dresden durchgeführt.

Festphasen-NMR-Spektroskopie: Die Messungen wurden von Frau Susanne Überlein am Institut für Bioanalytische Chemie, TU Dresden, Dresden durchgeführt.

GC-MS: Die Messungen wurden von Frau Susanne Überlein am Institut für Bioanalytische Chemie, TU Dresden, Dresden durchgeführt.

Genetische Analysen: Die Untersuchungen wurden von Kurt Kunze am Institut für Allgemeine Biochemie, TU Dresden, Dresden durchgeführt.

HR-ESI-Massenspektrometrie: Die Messungen wurden von Herrn Dr. Peter Tommes am HHU Center of Molecular and Structural Analytics (HHUCeMSA) mit einem UHR-QTOF maXis 4G Massenspektrometer der Firma Bruker Daltonics durchgeführt.

Identifikation des Schwammmaterials: Die taxonomische Identifikation der Schwammproben wurde von Frau Dr. Nicole de Voogd vom Naturalis Biodiversity Center, Leiden, Niederlande durchgeführt.

Isolation von Schwammskeletten: Die Schwammskelette wurden von Frau Susanne Überlein vom Institut für Bioanalytische Chemie, TU Dresden, Dresden isoliert.

Kinase-Inhibitionsassays: Die Kinase-Inhibitionsassays wurden durch Herrn Michael Kubbutat bei der Firma ProQinase GmbH in Freiburg durchgeführt.

NMR-Spektroskopie (^{1}H, ^{13}C, COSY, HMQC, HMBC, ROESY): Die NMR-spektroskopischen Messungen wurden am Institut für Anorganische Chemie der Heinrich-Heine Universität Düsseldorf durch Herrn Peter Behm an einem DRX 500 der Firma Bruker

und am Institut für Organische Chemie und Makromolekulare Chemie durch Frau Maria Beuer an einem Avance III 600 Bruker durchgeführt.

Phenoloxidaseinhibitionsassays: Die Untersuchungen zur Phenoloxidaseinhibition wurden durch Prof. Dr. Claire Hellio am LEMAR UMR 6539 UBO CNRS Ifremer IRD, European Institute of Marine Studies, Université de Bretagne Occidentale, European University of Brittany durchgeführt.

Potentiometrie: Die Messungen wurden von Frau Susanne Überlein am Institut für Bioanalytische Chemie, TU Dresden, Dresden durchgeführt.

Zytotoxizitätsassays: Die Untersuchungen auf zytotoxische Aktivität an der murinen Lymphomzelllinie (L5178Y) wurden durch Frau Renate Steffen am Institut für Physiologische Chemie der Johannes Gutenberg Universität Mainz durchgeführt. Die Untersuchungen auf Zytotoxizität gegenüber MCF-7, A549, Hs683, U373, B16F10 und SKMEL28 Zellen sowie Experimente zur Angiogenesehemmung wurden durch Véronique Mathieu im Laboratoire de Toxicologie, Faculté de Pharmacie, Université Libre de Bruxelles durchgeführt

Die Genehmigungen zur Veröffentlichung der Publikationen im Rahmen dieser Dissertation wurden von den entsprechenden Verlagen eingeholt. Hiermit erkläre ich ehrenwörtlich, dass ich die vorliegende Dissertation mit dem Titel „**Halogenated Tyrosines from Verongid Sponges – A Diverse Class of Marine Metabolites**“ (Halogenierte Tyrosine aus Verongiden Schwämmen – Eine diverse Klasse mariner Metaboliten) eigenständig angefertigt habe. Außer den angegebenen Quellen und Hilfsmitteln wurden dabei keine weiteren verwendet. Diese Dissertation wurde weder in dieser noch in ähnlicher Form in einem anderen Prüfungsverfahren vorgelegt. Ich erkläre außerdem, dass ich bisher keine erfolglosen Promotionsversuche unternommen habe.

Düsseldorf, den

(Hendrik Niemann)

15 Acknowledgements

This PhD study could not have been carried successfully without the support and acknowledgement of supervisors, colleagues, friends and my family. At this point I would like to express my gratitude with all my heart to the following persons that helped me during my PhD time:

- Prof. Dr. Peter Proksch for his supervision in this fascinating research field, his high interest in my work, critical discussions, for sending me for research stays to China and Egypt and the BIOPROSP conference in Norway and for the execellent work facilities in his labroratory in the Institute of Pharmaceutical Biology and Biotechnology at the Heinrich-Heine University, Düsseldorf.
- Prof. Dr. Matthias U. Kassack for evaluating my PhD thesis as second referee.
- Prof. Dr. Horst Weber for his enthusiastic mentorship in all organic synthesis work, his inspiring ideas regarding new hemibastadin congeners and putative target molecules and the wonderful discussion we had together.
- Prof. Dr. Bingui Wang (Laboratory of Experimental Marine Biology, Institute of Oceanology, Chinese Academy of Science) for his hospitality and supervision during my research stay in Qingdao, China in 2013.
- Prof. Dr. Wenhan Lin (National Research Laboratories of Natural and Biomimetic Drugs, Peking University, Health Science Center) for his hospitality during my visit in Beijing, China in 2013 and the chance to present my work in his group.
- Dr. Daowan Lai for his patience and extraordinary expertise with regard to NMR spectra interpretation and manuscript preparation.
- Dr. Cong-Dat Pham for providing the perfect start into marine bioprospecting during my first two months in summer 2011.
- Dr. Andreas Marmann for his continuous help in many situtations of practical lab life and after-work running sessions.
- Prof. Dr. Claus Paßreiter for his organizational help.
- Waltraud Schlag, Simone Miljanovic and Katja Friedrich for all their help in technical and practical issues and for many encouraging personal words. A special thanks to Simone Miljanovic for the extraordinary drawings of "*Ianthella basta*" that has been used for the title page of this dissertation and the "process of biofouling" (p. 32).
- Claudia Eckelskemper for being very helpful in all organizational matters.

Acknowledgements

- Mrs. Heike Goldbach-Gecke for performing antibacterial assays and for her help during PBI.
- Mrs. Eva Müller and Mr. Klaus Dieter Jansen for their help in PBII and PBIII.
- Ling-Hong Meng, Liu Yang and Li Xin for the amazing time I had during my research stay in Qingdao in summer 2013.
- Prof. Dr. Eike Brunner and Susanne Überlein (Bioanalytical Chemistry, TU Dresden, Dresden) for the good cooperation and the supply with sponge skeletons within the BMBF project.
- Prof. Dr. Claire Hellio for performing phenoloxidase inhibition assays.
- Professor Dr. Mohamed Abdel-Aziz (Microbial Chemistry Department, Genetic Engineering and Biotechnology Division, National Research Center, Dokki-Giza) and his co-workers for the exciting week in Cairo in November, 2012.
- Sven Reimann for the kind guidance and discussions on purification of blue mussel phenoloxidase.
- Dr. Rainer Kalscheuer and Nidja Rehberg for their help in performing antibacterial assays against marine microbes.
- Dr. Robert Bara, Dr. David Rönsberg and Mustapha El Amrani for great matches on the university tennis court.
- Robin Visse and his family for wonderful thursday evenings in spring 2015.
- The Deutsche Bahn AG for providing space and electricity for writing major parts of this dissertation.
- And all my former and recent colleagues at the HHU: Dr. Lena Hammerschmidt, Dr. Antonius Ola, Dr. Bartosz Lipowicz, Dr. Amal Hassan, Dr. Abdessamad Debbab, Dr. Weaam Ebrahim, Dr. Yaming Zhou, Mi-Young Chung, Catalina Peréz Hemphill, Marian Frank, Imke Form, Imran Malik, Amin Mokhlesi, Georgios Daletos, Moussa Al Tarabeen, Hervé Sergi Akone, Catherine Schumacher, Kirsten Famulla, Dr. Peter Sass, Dhana Thomy, Mohamed El-Naggar, Arta Kuci, Ingo Kolb, Liu Shuai, Huqin Chen, Yang Liu, Mariam Moussa, Hao Wang, Dr. Yanbo Zeng, Dr. Zhen Liu, Dr. Ramsay Kamdem, Catherine Bogner, Jens Hagenow, Stefanie Kaßel, Paula-Oxana Giesa and Kathrin Papadopoulos.
- The Deutsche Forschungsgemeinschaft (DFG) for financial support in the first two years of my PhD time.
- The European Union (EU) and the Deutsche Akademische Austauschdienst (DAAD) for financial support during my research stays in China and Egypt.

Acknowledgements

- Marie Simone Groppe for all her love.
- Jonathan Franz for energizing me in the final phase of writing.
- My mother and father, my sisters and friends for making me who I am.